

Durham E-Theses

Exploring the synthetic utility of HFO-1234yf

BEN JAMES MURRAY

How to cite:

MURRAY, BEN JAMES (2021) Exploring the synthetic utility of HFO-1234yf. Doctoral thesis, Durham University.

Use policy

The full-text may be used and/or reproduced, and given to third parties in any format or medium, without prior permission or charge, for personal research or study, educational, or not-for-profit purposes provided that:

- a full bibliographic reference is made to the original source
- a <https://etheses.durham.ac.uk/id/eprint/14247/> is made to the metadata record in Durham E-Theses
- the full-text is not changed in any way

The full-text must not be sold in any format or medium without the formal permission of the copyright holders.

Please consult the [full Durham E-Theses policy](#) for further details.



A thesis entitled

**Exploring the synthetic utility of
HFO-1234yf**

by

Ben James Murray

(Ustinov College)

A candidate for the degree of Doctor of Philosophy

Department of Chemistry, Durham University

2021

Abstract

The trifluoromethyl group is a common motif in pharmaceuticals, agrochemicals and organic materials due to its potential myriad beneficial effects on the properties of such molecules. However, the synthesis of compounds bearing a trifluoromethyl groups relies on the use of either a limited number of building blocks, notably trifluoroacetic acid and trifluorotoluene derivatives, or late stage trifluoromethylating reagents, which are often prohibitively costly on manufacturing scales. This thesis explores the utility of the low global warming potential refrigerant gas 2,3,3,3-tetrafluoropropene, also known as HFO-1234yf (**1**), as a new building block for the synthesis of pharmaceutically relevant trifluoromethylated compounds.

The reactivity of **1** towards nucleophiles was first investigated, using various mechanistic studies to resolve a discrepancy in previous literature and a range of differently substituted α -trifluoromethyl enol ethers and β -trifluoromethyl vinyl sulfides were then synthesised. Attempted reaction of **1** with carbon-centred nucleophiles led to the discovery of a rapid dehydrofluorination process to form 3,3,3-trifluoropropyne. Addition of this alkyne to aldehydes followed by oxidation afforded a range of trifluoromethyl ynones, which in turn reacted both as Michael acceptors with nucleophiles and as dienophiles in Diels-Alder reactions, both proving to be fast and efficient processes. Furthermore, reactions of trifluoromethyl ynones with dinucleophiles to give CF₃-substituted heterocycles were developed, exemplified by a novel synthesis of the anti-arthritis drug celecoxib.

Addition of the trifluoroalkynide formed *in situ* from **1** to ketones instead of aldehydes afforded tertiary alcohols that acted as building blocks for the synthesis of oxygen-rich trifluoromethylated heterocycles along with some promising initial results for use as bench-stable trifluoropropynylating reagents. 1,3-Dipolar cycloaddition of **1** with an azomethine ylide gave a new route to tetrafluorinated pyrrolidine systems. Finally, reactions with electrophiles were explored and, at room temperature, bromination of **1** was found to be facile. The resulting dibromoalkane underwent dehydrobromination followed by palladium-catalysed cross-coupling with aryl boronic acids and alkynes to afford tetrafluorinated styrenes and enynes, respectively.

Declaration

The copyright of this thesis rests with the author. No quotation from it should be published without prior written consent and information derived from it should be acknowledged.

The work described in this thesis was carried out by the author at Durham University between October 2017 and October 2021. This thesis is the work of the author, except where acknowledged by reference, and has not been submitted for any other degree.

Parts of this work have been the subject of the following publications:

- Ben J. Murray, Ellis D. Ball, Antal Harsanyi and Graham Sandford, *Eur. J. Org. Chem.*, 2019, 7666.
- Ben J. Murray, Tom G. F. Marsh, Dmitry S. Yufit, Mark A. Fox, Antal Harsanyi, Lee T. Boulton and Graham Sandford, *Eur J. Org Chem.*, 2020, 6236.
- Ben J. Murray, Lee T. Boulton and Graham Sandford, *J. Fluorine Chem.*, 2021, **245**, 109774.

This work has also been presented, in part, at:

- 19th RSC Fluorine Group Postgraduate Meeting, Online
10th - 11th June 2021 – Oral Presentation
- #RSCPoster Twitter Conference, Online
3rd March 2020 – Poster Presentation
- 19th European Symposium on Fluorine Chemistry, University of Warsaw
25th - 31st August 2019 – Poster & Flash Oral Presentations
- 2019 Durham Postgraduate Gala Research Symposium, Durham University
21st June 2019 – Poster Presentation
- 18th RSC Fluorine Group Postgraduate Meeting, University of Southampton
11th - 12th April 2019 – Poster Presentation

Acknowledgements

First and foremost, my thanks go to the award-winning Prof. Graham Sandford for his invaluable advice and support as my supervisor for the past five years, in this degree and the last. None of this high-quality work would have been possible without his help. Thanks also go to Dr. David Hodgson for kindly agreeing to take over as my supervisor for the final few months of this project following Graham's retirement, which we all hope is a long and happy one. Likewise, I am indebted to Dr. Antal (Tony) Harsanyi and Dr. Lee Boulton at GlaxoSmithKline for their guidance and input on the potentially useful industrial aspects of this effort. I thank GSK and the Engineering and Physical Sciences Council for providing the iCASE studentship funding that has facilitated this project.

This thesis contains contributions from a number of talented people at Durham to whom I am immensely grateful: Dr. Mark Fox who carried out all the DFT calculations discussed in this work; Dr. Dmitry Yufit who solved all the X-ray crystal structures in this thesis; and MChem students Ellis Ball, Thomas Marsh, Alessia Santambrogio, Jonathan Holland, and Matthew Grannan for performing supplementary synthetic work. I would also like to thank all of the analytical, technical, administrative, and support staff in Durham, in particular: Dr. Alan Kenwright, Dr. Juan Aguilar, Dr. Eric Hughes, and Catherine Heffernan for high-resolution and 2-D NMR spectroscopy; Dr. Jackie Mosely, Dr. David Parker, and Peter Stokes for mass spectrometry and accurate mass analysis; Malcolm Richardson and Aaron Brown for glassblowing; Annette Passmoor for her efficiency as storekeeper and from keeping the department from collapsing around us; Dave Hunter and Dr. Li Li for their management of the high pressure facilities; Emma Knighton, Kerry Strong, and Ashley Davenport for running our pandemic postal service; and Val, Ivan, Judith, Claire, and Alison for keeping the lab tidy and, much more significantly, the provision of a two doses of tea per day.

Finally, I would like to acknowledge the PhDreamers of CG115 who have made this endeavour bearable: Dr. Craig Fisher for welcoming me into the group on the very first day, expounding the benefits of classically trained acting, and passing on his knowledge of the deep lore of the lab; Dr. Darren Heeran for teaching me the ropes at the very beginning, refraining from argie-bargie during working hours, and being a top geezer; Dr. Etienne Lisse for his Gallic viewpoint on life, his renowned skill as a DJ, and smuggling

of the finest Parisian butter biscuits; Dr. Marcus Lancashire for his instruction in the use of autoclaves and the high pressure lab, our shared enjoyment of Fallout and Skyrim, and his political correctness; Dr. Josh Walton for his unerring positivity, his singing (especially at Christmas), and his barbeque; Dr. Alex Hampton for his quinuclidine, teaching me to play pool, and beginning my pathway to TV stardom on University Challenge; and last, but by absolutely no means least, Dr. Neshat Rozatian for noises with Jellis, brunch, and being the most magic of catstaceans. To all the other silly fourth years (Alex Melvin, Dan Cooper, Lawrence Tam, Sophie Martin, Rob Skelton, Jonny D.H. Hill, and Kiera Dodds), our neighbours in the Fox group (Dan von Emloh, Leon Devereux, Matt Hunt, Maranga Mokaya, Abi Riley, Ned Flanders, Amy Cook, and Tom McGurrell), our other neighbours in the O'Donoghue group (Dr. David Tucker, Hector Macrae, Dr. Kevin Maduka, Dr. Jiayun Zhu (Estelle), Isabelle Pickles, Emily Chin, Bechan Thomas, Yuan Gao (Lois), Dr. Markus Draskovits, Jacob Murray, Matthew Smith, James Mallyon, and Oliver Willis), and various visitors and assorted hangers-on (Anne Lückener, Dr. Mate Somlyay, Dr. Javier Ajenjo, Zahide Yilmaz, Sili Qiu (Bobby), Dr. Hachemi Kadri, Piotr Plaskota, Dr. Kalesh Karunakaran, Connor O'Leary, Ed Hall, Cameron Hunt, Dr. Alex Webster, and Dr. Laura Jennings), thank you for helping me to live the dream and keep chiselling over the past five years. Good-oh.

Abbreviations and nomenclature

Ac	acetyl
AI	atmospheric ionisation
Ar	aryl
atm	atmosphere
b.p.	boiling point
Bn	benzyl
Boc	<i>tert</i> -butyloxycarbonyl
Bpin	<i>bis</i> (pinacolato)boryl (pinacol = 2,3-dimethylbutane-2,3-diol)
Bz	benzoyl
cal	calories
CCDC	Cambridge Crystallographic Data Centre
COSY	correlation spectroscopy
Cy	cyclohexyl
D	debye
d	days
DABCO	1,4-diazabicyclo[2.2.2]octane
DAST	diethylaminosulfur trifluoride
dba	dibenzylideneacetone
DBM	dibenzoylmethane
DBU	1,8-diazabicyclo(5.4.0)undec-7-ene
DCE	1,2-dichloroethane
DCM	dichloromethane
DDQ	2,3-dichloro-5,6-dicyano-1,4-benzoquinone
DeoxoFluor [®]	<i>bis</i> (2-methoxyethyl)aminosulfur trifluoride
DEPT	distortionless enhancement by polarization transfer
DFT	density functional theory
dipp	2,6-diisopropylphenyl
DMA	<i>N,N</i> -dimethylacetamide
DMAP	4-dimethylaminopyridine
DME	1,2-dimethoxyethane
DMF	<i>N,N</i> -dimethylformamide

DMP	Dess-Martin periodinane
DMPU	<i>N,N'</i> -dimethylpropyleneurea
DMSO	dimethylsulfoxide
dppf	1,2- <i>bis</i> (diphenylphosphino)ethane
dppf	1,1'- <i>bis</i> (diphenylphosphino)ferrocene
E ⁺	electrophile
EI	electron ionisation
EPA	Environmental Protection Agency
eq.	equivalents
ESI	electrospray ionisation
Et	ethyl
FDA	Food & Drug Administration
GC-MS	gas chromatography-mass spectrometry
[H]	reducing agent
h	hours
HIV	human immunodeficiency virus
HMBC	heteronuclear multiple-bond correlation spectroscopy
HMPA	hexamethylphosphoramide
HOMO	highest occupied molecular orbital
HRMS	high resolution mass spectrometry
HSQC	heteronuclear single-quantum correlation spectroscopy
hν	irradiation with visible or ultraviolet light
ⁱ Pr	<i>iso</i> -propyl
IPr	1,3-diisopropylimidazolinylidene
LC-MS	liquid chromatography-mass spectrometry
lit.	literature
LUMO	lowest unoccupied molecular orbital
m.p.	melting point
mCPBA	<i>meta</i> -chloroperoxybenzoic acid
Me	methyl
MeTHF	2-methyltetrahydrofuran
min	minutes
Ms	methanesulfonyl
Naph	naphthyl

ⁿ Bu	<i>n</i> -butyl
NFSI	<i>N</i> -fluorodibenzenesulfonamide
NMP	<i>N</i> -methylpyrrolidine
NMR	nuclear magnetic resonance
NOESY	nuclear Overhauser effect spectroscopy
Nuc ⁻	nucleophile
[O]	oxidising agent
OMe	methoxy
Pd/C	palladium on carbon
Ph	phenyl
phen	1,10-phenanthroline
ppy	2-phenylpyridinato
PTFE	polytetrafluoroethylene (Teflon [®])
R _f	retention factor
R _F	perfluoroalkyl group
rt	room temperature (~20 °C)
s	seconds
SelectFluor TM	1-chloromethyl-4-fluoro-1,4-diazoniabicyclo[2.2.2]octane <i>bis</i> (tetrafluoroborate)
SET	single electron transfer
<i>T</i>	temperature
<i>t</i>	time
^t Bu	<i>tert</i> -butyl
TEMPO	(2,2,6,6-tetramethylpiperidin-1-yl)oxyl
Tf	trifluoromethanesulfonyl
THF	tetrahydrofuran
TLC	thin layer chromatography
TMS	trimethylsilyl
TON	turnover number
Ts	4-toluenesulfonyl
UV	ultraviolet
XPhos	2-dicyclohexylphosphino-2',4',6'-triisopropylbiphenyl
δ	chemical shift
Δ	heat

Table of Contents

Chapter 1: Introduction	1
1.1 Organofluorine chemistry	1
1.1.1 History of fluorine chemistry	1
1.1.2 Properties of the C-F bond	3
1.1.3 Biological role of fluorine in medicinal chemistry	7
1.1.4 Synthetic routes to organofluorine compounds	11
1.2 Significance of the trifluoromethyl group	15
1.2.1 CF ₃ groups in pharmaceuticals	15
1.2.2 Synthesis and applications of CF ₃ -containing building blocks	16
1.2.3 Late-stage trifluoromethylation strategies	20
1.3 HFO-1234yf	23
1.3.1 History and role of refrigerant gases	23
1.3.2 HFO-1234yf as a refrigerant	25
1.3.3 Manufacturing processes for HFO-1234yf	28
1.3.4 Uses of HFO-1234yf in organic synthesis	34
1.4 Conclusions	45
1.5 References for Chapter 1	46
Chapter 2: Aims and approach	55
2.1 Project objectives	55
2.2 Techniques for the reaction of HFO-1234yf	56
2.3 Characterisation of HFO-1234yf in solution	57
2.4 References for Chapter 2	61
Chapter 3: Nucleophilic substitution reactions of HFO-1234yf	62
3.1 Introduction	62
3.2 Results and discussion	65
3.2.1 Regioselectivity in the reactions of HFO-1234yf with nucleophiles	65
3.2.2 Reactions of HFO-1234yf with alkoxides	74

3.2.3	Reactions of α -trifluoromethyl enol ethers	79
3.2.4	Reactions of HFO-1234yf with thiolates	86
3.2.5	Reactions of HFO-1234yf with other nucleophiles	89
3.3	Conclusions	91
3.4	References for Chapter 3	92
Chapter 4: Synthesis and Michael addition reactions of trifluoromethyl ynones		95
4.1	Introduction	95
4.2	Results and discussion	99
4.2.1	Synthesis of trifluoromethyl ynones	99
4.2.2	Reactions of trifluoromethyl ynones with amines	108
4.2.3	Reactions of trifluoromethyl ynones with alcohols	112
4.2.4	Intramolecular cyclisation reactions of trifluoromethyl ynones	118
4.2.5	Reactions of trifluoromethyl ynones with dinucleophiles	120
4.3	Conclusions	125
4.4	References for Chapter 4	126
Chapter 5: Cycloaddition reactions of trifluoromethyl ynones		128
5.1	Introduction	128
5.2	Results and discussion	131
5.2.1	Initial reactivity studies of cycloaddition reactions	131
5.2.2	Deoxygenative aromatisation reactions	136
5.3	Conclusions	140
5.4	References for Chapter 5	140
Chapter 6: Towards a trifluoropropynylating reagent		143
6.1	Introduction	143
6.2	Results and discussion	145
6.2.1	Initial lithium 3,3,3-trifluoropropynide trapping attempts	145
6.2.2	Deacetonative Sonogashira coupling	147
6.2.3	Deacetonative nucleophilic substitution reactions	153

6.2.4	Other reactions of trifluoropropynyl tertiary alcohols	156
6.3	Conclusions	159
6.4	References for Chapter 6	160
Chapter 7: Miscellaneous reactions of HFO-1234yf		163
7.1	Cycloaddition reactions of HFO-1234yf	163
7.1.1	Diels-Alder reactions of HFO-1234yf	163
7.1.2	1,3-Dipolar cycloaddition reactions of HFO-1234yf	164
7.2	Electrophilic addition to HFO-1234yf	167
7.2.1	Bromination of HFO-1234yf	167
7.2.2	Reactivity of 1,2-dibromo-2,3,3,3-tetrafluoropropane	169
7.2.3	Other electrophilic addition reactions of HFO-1234yf	176
7.3	Conclusions	178
7.4	References for Chapter 7	179
Chapter 8: Conclusions and future work		182
Chapter 9: Experimental		187
9.1	General information	187
9.2	Experimental data for Chapter 2	188
9.3	Experimental data for Chapter 3	192
9.4	Experimental data for Chapter 4	199
9.5	Experimental data for Chapter 5	217
9.6	Experimental data for Chapter 6	220
9.7	Experimental data for Chapter 7	226
9.8	References for Chapter 9	233
Appendix I: X-ray crystallography data		235
Appendix II: DFT calculation data		239
Appendix III: Seminars and conferences attended		240

Chapter 1: Introduction

1.1 Organofluorine Chemistry

1.1.1 History of fluorine chemistry

Fluorine is the most electronegative of all the chemical elements.¹ The ultimate cosmological origins of fluorine are a subject of debate amongst astrophysicists² but it is, nevertheless, the 13th most abundant element in the Earth's crust, occurring mostly in the form of the minerals fluorite, also called fluorspar (CaF_2), and fluorapatite ($\text{Ca}_5(\text{PO}_4)_3\text{F}$).³ Fluorine is also found in the mineral cryolite (Na_3AlF_6), which has the unique distinction of being the only ore to ever be mined to commercial extinction as the only known natural deposit in Ivittuut, Greenland was depleted in 1987 and cryolite now has to be produced synthetically.⁴ Whilst fluorine is also present in several other minerals, such as the gemstone topaz ($\text{Al}_2\text{SiO}_4(\text{F},\text{OH})_2$), these are not commercially viable sources.

Fluorite has been used since the 16th Century as an additive to lower the melting point of iron ore during smelting.⁵ Indeed, the name of the element fluorine comes from the ore fluorite, which is in turn named from the Latin *fluores*, meaning 'flow', owing to this early use.⁶ Hydrofluoric acid (HF) was first prepared by acidification of fluorite in the 18th Century and it was from this that the existence of fluorine was first proposed by André-Marie Ampère in 1810,⁷ with Sir Humphry Davy suggesting the name. Efforts to isolate fluorine in its pure elemental form (F_2) occupied much attention through the 19th Century and several chemists were seriously injured, or even killed, in the pursuit of this elusive element.⁸ Following the efforts of these so-called 'fluorine martyrs', the first definitive proof of the isolation of F_2 was obtained by French chemist Henri Moissan in 1886 by the electrolysis of a mixture of potassium fluoride (KF) and HF.⁹ Moissan was awarded the Nobel Prize in Chemistry in 1906, the citation for which commended his work on "that savage beast among the elements". To this day, F_2 is still produced industrially from HF via a similar electrochemical process to Moissan's first reaction.¹⁰

However, C-F bonds are rare in nature and are known to be found in only around a dozen natural products despite the relatively high abundance of fluorine in minerals (Figure 1.1).¹¹ Sodium fluoroacetate (**2**) was the first naturally occurring organofluorine compound to be identified and is a highly toxic metabolite of the southern African plant

Dichapetalum cymosum, known locally as poison leaf.¹² Other examples have since been discovered including fluorocitric acid (**3**), which is found in very low levels in the tea plant *Thea sinensis*,¹³ and 4-fluorothreonine (**4**) from the bacterium *Streptomyces cattleya*,¹⁴ the fluorinase enzyme of which was subsequently identified and studied.¹⁵

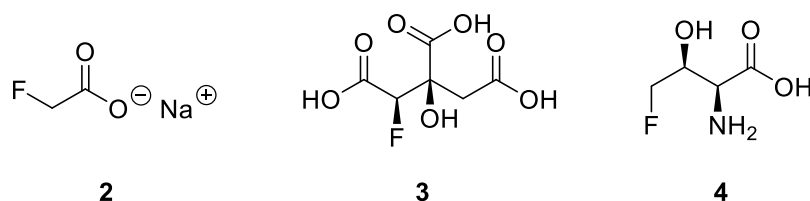


Figure 1.1. Examples of naturally occurring organofluorine compounds

Due to the scarcity of fluorine-containing natural products, organofluorine chemistry is almost entirely a synthetic field. The sources and industrial applications of fluorine are summarised in Figure 1.2. Nearly half of fluorite mined is still used in smelting with most of the rest used to make HF, from which all organofluorine compounds are ultimately derived.³ It has been estimated there are only 100 years of fluorite reserves left at the current rate of consumption so the recycling of fluorosilicic acid, a by-product from the consumption of fluorapatite by the fertilizer industry, is a developing area.

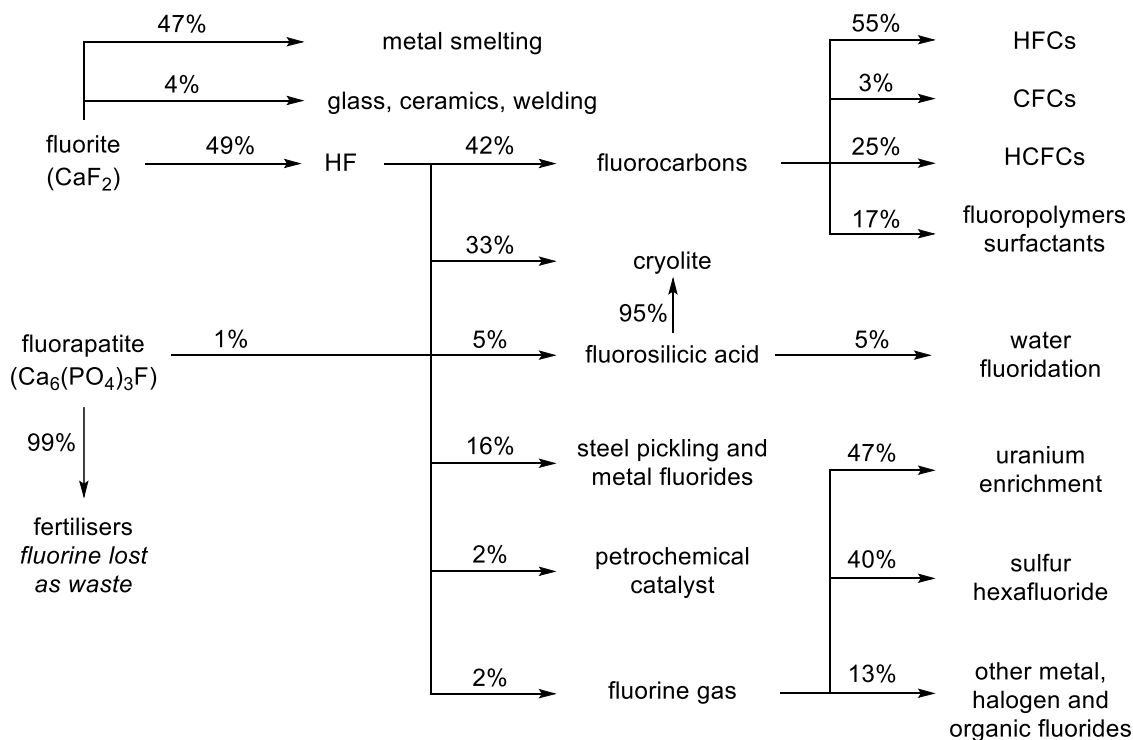


Figure 1.2. Overview of the industrial sources and uses of fluorine

Organofluorine chemistry was not carried out on a commercial scale until the 1920s when DuPont began to manufacture chlorofluorocarbon refrigerants.¹⁶ This work led to the serendipitous discovery of polytetrafluoroethylene (PTFE) in 1938 by Roy J. Plunkett and interest in perfluorinated polymers as chemically inert materials for a wide variety of applications continues to this day.¹⁷ Fluorine gas was first synthesised on a large scale during World War II for use in the Manhattan Project, where the diffusion of uranium hexafluoride (UF₆) was used to enrich samples in the fissile isotope ²³⁵U and the nuclear power industry continues to be the largest consumer of F₂. Another significant application of fluorine is in manufacturing sulfur hexafluoride (SF₆) for use as an inert gaseous dielectric medium to insulate high voltage electronic equipment.

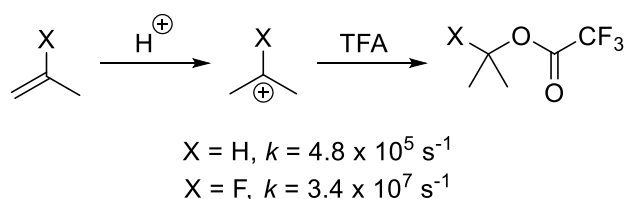
Whilst a relatively low percentage in terms of tonnage, bioactive small molecules containing fluorine are of great importance and worth many billions of dollars in the pharmaceutical and agrochemical sectors. Interest in the field began in the 1950s with the discovery of the biological activity of 9 α -fluorocorticosteroids¹⁸ and 5-fluorouracil¹⁹ and fluorinated drugs were widespread by the 1980s. Modern estimates for the number of therapeutic compounds containing fluorine are typically range from 20-30%.²⁰ Bioactive organofluorine compounds have remained highly relevant in recent years with 40% of FDA-approved new chemical entities in 2018,²¹ 34% in 2019²² and 37% in 2020²³ containing one or more fluorine atoms. Fluorinated pharmaceuticals, such as favipiravir and dexamethasone, have been amongst those trialed for the treatment of COVID-19 during the pandemic.²⁴ Other medicinal applications of fluorinated molecules include the use of ¹⁸F-labelled compounds as tracers for positron emission tomography (PET),²⁵ fragment-based drug discovery using ¹⁹F NMR spectroscopy,²⁶ and perfluoroalkyl compounds with high gas solubility used as artificial blood and for liquid breathing.²⁷

1.1.2 Properties of the C-F bond

The variety of uses for organofluorine compounds arises from the unique properties of the C-F bond.²⁸ Fluorine has the smallest atomic radius of any Period 2 element as atomic radii decrease across a period with increasing nuclear charge. Removal of an electron from fluorine to give F⁺ is highly endothermic (-1679 kJ mol⁻¹) as the electrons are very tightly held to the nucleus. In contrast, addition of an electron to give F⁻ is exothermic (328 kJ mol⁻¹) as the high nuclear charge acts to stabilise the closely held 2p valence

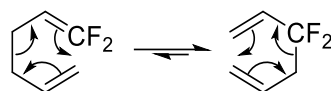
electrons. The carbon-fluorine bond is, therefore, amongst the strongest of all covalent bonds (average 441 kJ mol^{-1}) owing to the attractive forces between the partial charges of $\text{C}^{\delta+}$ and $\text{F}^{\delta-}$, giving the bond significant electrostatic character.

The significant electrostatic component of the C-F bond leads to a large dipole moment (1.85 D in fluoromethane).²⁹ Dipole-dipole and charge-dipole interactions can, therefore, have a significant effect on the preferred conformations adopted by organofluorine compounds. C-F moieties can coordinate metal ions, particularly the harder cations of Group 1 and 2 metals.³⁰ However, in spite of the high electron density of fluorine, C-F is not a good hydrogen bond acceptor due to the tightness with which fluorine's lone pairs are held to the nucleus and so typically only forms weak hydrogen bonds.³¹ The same argument can be applied to fluorine's ability to act as a π donor, i.e. the lone pairs on fluorine are tightly held and not readily donated. As an example of this phenomenon, whilst acyl fluorides have relatively high stability, they also show higher IR wavenumbers for the C=O bond than esters or amides.³² This suggests fluorine is not acting as a π donor, as oxygen and nitrogen do, and so the increased stability can be attributed to the strength of the C-F bond. However, there is some evidence of π donation by fluorine in positively charged systems. For example, in the addition of trifluoroacetic acid (TFA) to propene and 2-fluoropropene (Scheme 1.1), the vinyl fluoride reacts three orders of magnitude faster, which is likely due to some degree of fluorine π -donation.³³



Scheme 1.1. Reaction of trifluoroacetic acid with propene and 2-fluoropropene

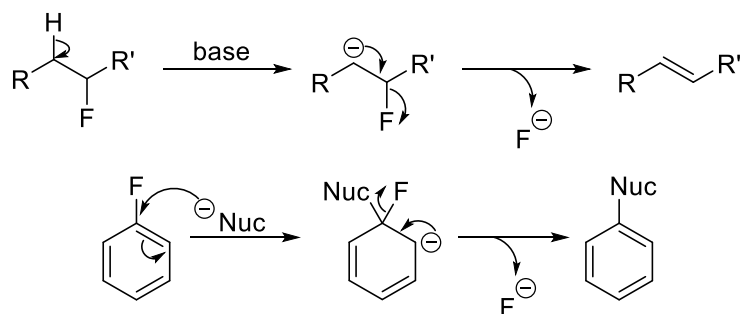
Given the tendency of fluorine to withdraw p-electron density, it would be expected to have an energetic preference to be bonded to sp^3 hybridised carbon centres over sp^2 . This is observed to be the case experimentally in, for example, the Cope rearrangement of 1,1-difluoro-1,5-hexadiene (Scheme 1.2), for which the $\text{sp}^3 \text{CF}_2$ moiety is preferred by 21 kJ mol^{-1} over the $\text{sp}^2 \text{CF}_2$.³⁴



Scheme 1.2. Cope rearrangement of 1,1-difluoro-1,5-hexadiene

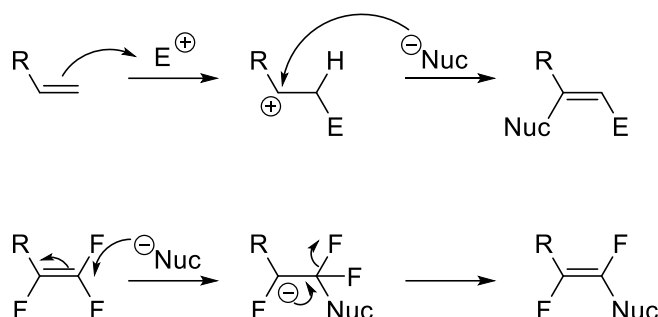
The highly polarised C-F bond leads to a low energy σ^* orbital, which is analogous to the C-O bond and so similar hyperconjugative effects can be observed. For example, an equivalent anomeric effect can be seen in the conformational preferences of fluorinated sugars.³⁵ 1,2-Difluoroalkanes are known to adopt *gauche* conformations, which has been attributed to σ C-H to σ^* C-F hyperconjugative stabilisation.³⁶ An alternative explanation is that the electron-rich C-C and C-H bonds are bent towards the highly polarised C-F bond and this overlap is optimal in the *gauche* conformation.³⁷ Similar arguments can rationalise the preferred all-*syn* conformation of 1,3-difluoroalkanes, which maximises hyperconjugation while minimising C-F repulsions.³⁸

However, fluoride is a relatively poor leaving group in spite of this n- σ^* overlap, once again owing to the strength of the C-F bond as, whilst population of σ^* weakens the covalent aspect of the C-F bond, it simultaneously strengthens the important ionic character of the bond.³⁹ Compared to other halogens, the fluoride ion is, therefore, a poor leaving group in substitution reactions due to this prohibitively high bond strength. Furthermore, the high electrostatic character of the C-F bond leads to poor polarisability and hence makes direct displacement of fluoride difficult.⁴⁰ However, the electron-withdrawing nature of fluorine allows it to inductively stabilise nearby carbanion sites and so it can promote E1cB elimination and S_NAr substitution reactions (Scheme 1.3).⁴¹



Scheme 1.3. Generic E1cB (top) and S_NAr (bottom) reactions promoted by fluorine

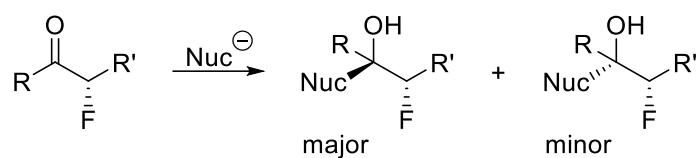
The ability of fluorine to stabilise carbanions leads to unique reactivity in highly fluorinated systems. Whilst hydrocarbon alkenes typically react by electrophilic addition processes, perfluoroalkenes instead react via nucleophilic substitution with inductively-stabilised carbanions in place of more traditional carbocation intermediates.⁴² Scheme 1.4 shows this difference in reactivity, which has led fluoroalkenes to be called ‘mirror images’ of hydrocarbon alkenes. These carbanion intermediates can be sufficiently stable as to be observable by NMR spectroscopy.⁴³ Perfluoroaromatic systems show similar carbanion intermediates in reactions with nucleophiles, which can be exploited to access a range of interesting structures that may otherwise be challenging to synthesise.⁴⁴



Scheme 1.4. Difference in reactivity between hydrocarbon alkenes (top) and perfluoroalkenes (bottom)

Where more than one reaction is possible, selectivity is dependent on the relative stability of intermediate carbanions. Fluorine directly bonded to a carbanion is stabilising by inductive withdrawal of electron density but destabilising by electronic repulsion between the lone pairs of fluorine and a carbanion. Fluorine β to a carbanion is still stabilising by induction but, in this case, there is no orbital destabilisation. The lowest energy transition state is, therefore, the one that maximises the stabilising inductive interactions whilst minimising destabilising orbital interactions. There will also be a thermodynamic preference to minimise the number of fluorine atoms at sp^2 sites, given the previously discussed preference of fluorine to be at sp^3 hybridised carbons.

The polarity of the C-F bond can also affect the facial selectivity in reactions of fluorinated unsaturated systems. For example, Scheme 1.5 shows that the major product of nucleophilic addition to an α -fluorinated carbonyl group is that which results from the nucleophile's trajectory approaching the opposite face to the fluorine atom.⁴⁵ This minimises electrostatic repulsion between the electron-rich nucleophile and the many lone pairs of the fluorine atom.



Scheme 1.5. Reactions of α -fluorocarbonyl derivatives with nucleophiles

With a van der Waals radius of 1.47 Å and an average C-F bond length of 1.35 Å, the fluorine atom is sufficiently small that it can be substituted for hydrogen atoms in organic molecules with minimal steric effects but a significant electrostatic effect.⁴⁶ Hydroxyl groups can be similarly replaced, albeit with a greater impact on intermolecular forces such as hydrogen bonding. Despite possessing little steric bulk, the presence of fluorine can lead to important geometric changes. Due to its electron-withdrawing nature, fluorine can pull electron density from carbon towards itself and so relax the repulsion between geminal bonds, allowing them to spread further apart.⁴⁷ An alternative explanation is that fluorine withdrawing electron density from the sp^3 orbital of carbon makes it more sp^2 -like and the geometry is altered accordingly. In either case, this effect can be seen in the H-C-H bond angle of the simplest organofluorine compounds, increasing from 109.5° in methane to 110.2° in fluoromethane and 113.8° in difluoromethane.⁴⁸

1.1.3 Biological role of fluorine in medicinal chemistry

The unique nature of the fluorine atom and the C-F bond lead to significant effects on many important physiochemical and conformational properties of molecules, hence why organofluorine compounds are commonplace in pharmaceuticals.⁴⁹ Notable examples, shown in Figure 1.3, include atorvastatin (Lipitor[®], **5**), which is used for lowering harmful cholesterol levels and was once the best-selling drug in the world, providing up to a quarter of Pfizer's total revenue.⁵⁰ Ciprofloxacin (**6**) is one example of the fluoroquinolones, a class of broad-spectrum antibiotics used to treat infections where other anti-bacterial drugs have failed.⁵¹

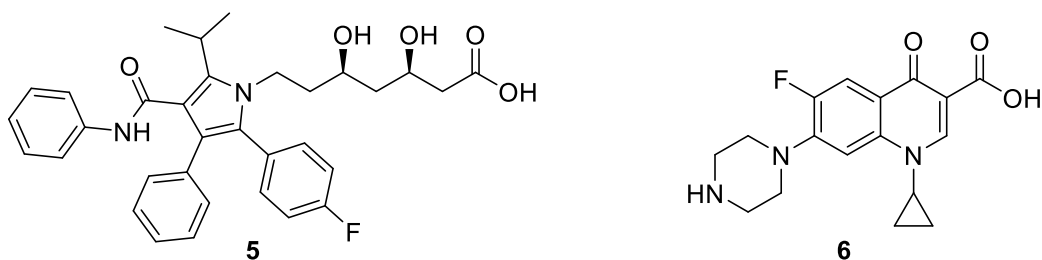


Figure 1.3. Notable examples of organofluorine pharmaceutical compounds

A key factor in the design of any drug molecule is pK_a , which contributes to the binding affinity of a compound and also determines bioavailability by affecting the absorption process.⁵² The presence of a fluorine atom acts to alter the pK_a of nearby functional groups. For example, a neighbouring fluorine would stabilise deprotonated carboxylate anions but would destabilise protonated ammonium cations. An example of this effect was shown in the synthesis of a fluorinated derivative of the potent opioid fentanyl (**7**).⁵³ Unsubstituted **7** is protonated at physiological pH whilst addition of a single fluorine atom, as shown in Figure 1.4, alters the pK_a such that the fluorinated analog (**8**) is not protonated at the same pH. This prevents **8** from binding to the opioid receptor except in areas of the body with unusually low pH, which are associated with inflammation. This allows the analgesic effect to be retained whilst reducing side effects.

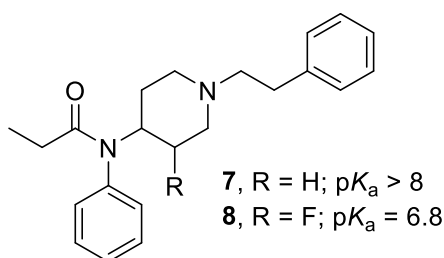


Figure 1.4. Fluorination of fentanyl alters pK_a and so reduces side effects

Fluorination also influences the lipophilicity of a molecule, which is measured by the partition coefficient ($\log P$) between *n*-octanol and water. Another important property is the distribution coefficient, $\log D$, which measures $\log P$ at different values of pH. In saturated alkyl groups, the introduction of a highly electronegative fluorine introduces a large dipole that increases polarity and so decreases lipophilicity.⁵⁴ However, fluorination near to a functional group will withdraw electron density and reduce the strength of intramolecular interactions such as hydrogen bonding, increasing lipophilicity. In addition, the introduction of fluorine to an aromatic ring or adjacent to a π -system will also increase lipophilicity owing to the low polarisability of the C-F bond. This effect was shown in the synthesis of fluorinated analogs of the neurotransmitter γ -aminobutyric acid (**9**, Figure 1.5).⁵⁵ Fluorinated mimic **10** showed greatly increased lipophilicity, allowing it to pass the blood-brain barrier, but was still able to bind to the intended γ -aminobutyric acid aminotransferase and so has potential as the basis for new anticonvulsant drugs.



Figure 1.5. Fluorinated mimic of γ -aminobutyric acid with increased lipophilicity

In addition to these physiochemical considerations, fluorination can also improve the metabolic stability of a compound.⁵⁶ A frequent problem in drug design is that the lead compound is metabolised before it can reach its target and have its desired effect. One common means of metabolism of drugs is oxidation by cytochrome P450, which decreases lipophilicity and allows the molecule to be more easily excreted. An example of lead optimisation to avoid such oxidation is the plasma cholesterol lowering drug ezetimib (Figure 1.6).⁵⁷ The lead compound **11** was doubly fluorinated to give the final compound **12**, with fluorine preventing oxidation of the pendant phenyl position.

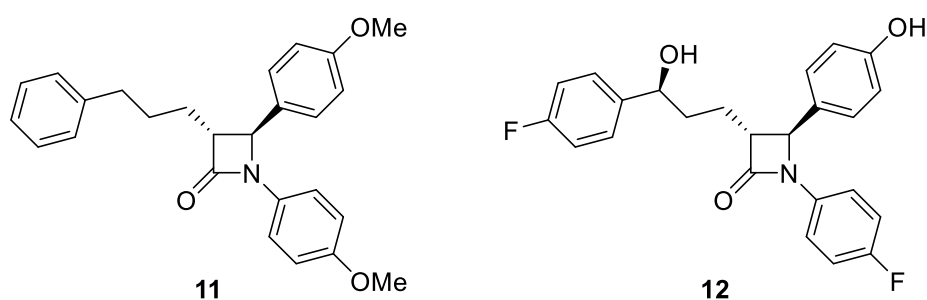


Figure 1.6. Lead optimisation of ezetimib by, in part, double fluorination

Infamously, the *R*-enantiomer of thalidomide is an effective treatment for morning sickness but the *S*-enantiomer is a potent teratogen and the two can interconvert *in vivo*.⁵⁸ Replacing the acidic hydrogen at the chiral centre with fluorine prevents epimerisation and so allows the therapeutic *R*-enantiomer (**13**, Figure 1.7) to be used for its originally intended effect, as well as a potential anti-cancer and anti-leprosy drug.⁵⁹

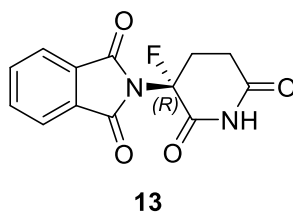


Figure 1.7. Structure of (3*R*)-fluorothalidomide, which does not interconvert *in vivo*

However, introduction of fluorine at labile sites can be deleterious as loss of fluoride would cause harmful side effects *in vivo*.⁶⁰ Intramolecular nucleophilic substitution within the drug molecule can lead to loss of fluoride. Some biological nucleophiles, such as glutathione or protein residues, can have the same effect so careful consideration of physiological pH, steric hindrance and conformation of the compound is required to avoid such effects. Defluorination can also occur for fluorine adjacent to lone pairs, such as in α -fluorocarbonyl or α -fluoroamine derivatives, so neighbouring group effects must also be considered. Even if neighbouring groups are not present in the drug molecule, they could be introduced via metabolism in the body. In some cases, it is even possible for cytochrome P450 enzymes to cause oxidative defluorination to form hydroxyl metabolites and release fluoride. In addition to the release of fluoride, structures capable of generating the highly toxic fluoroacetate moiety *in vivo* are also potentially problematic. In a recent example of this kind of phenomenon, workers at Merck identified a β -secretase 1 inhibitor for treatment of Alzheimer's disease where fluoropyrimidine **14** (Figure 1.8) was found to undergo epoxidation on the ring and elimination of fluoride.⁶¹ Dimethylation to give compound **15** prevented this metabolic defluorination and so improved stability and reduced side effects.

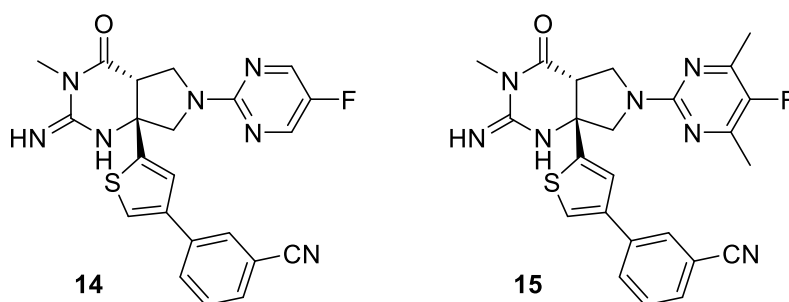


Figure 1.8. Example of a metabolically labile fluorine protected by dimethylation

As the introduction of fluorine does not usually cause significant geometric changes in organic systems, fluorinated compounds can often bind to active sites in the same way as their non-fluorinated analogues. However, the strength of the C-F bond can then prevent the usual activity of the protein and so the compound acts to inhibit the target. An example is shown in Figure 1.9, where steroid **16** can be converted by steroid C_{17 α} hydroxylase or lyase enzymes via its enol form to other steroids linked to prostate and breast cancers.⁶² Inhibition of these enzymes can be achieved by using the fluorinated analog **17**, which can bind to the enzyme as the fluoroalkene successfully mimics the carbonyl group but then cannot undergo the enolisation reaction and remains blocking the active site.⁶³

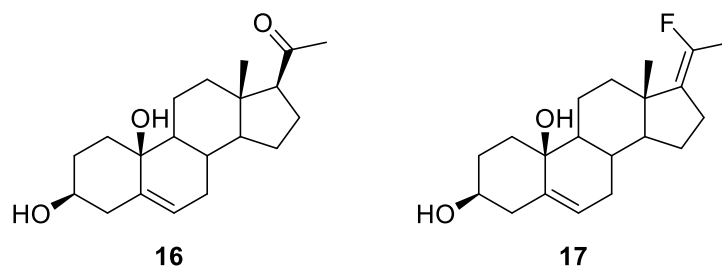


Figure 1.9. Fluorinated analog of steroid acts to inhibit enzymes linked to cancer

While fluorine can be substituted for a hydrogen or hydroxyl group with limited steric impact, there can be conformational effects as previously discussed. This can be used to alter the structure of a compound to better fit the target active site, hence improving the potency of the compound.⁶⁴ While hydrogen bonds involving fluorine are typically weak, they are possible and so can be important considerations in determining the preferred conformation and activity of a fluorinated molecule. An example of this effect was seen in Bruton's tyrosine kinase inhibitor **18** (Figure 1.10), an enzyme implicated in immunodeficiency, where fluorination led to a 400-fold increase in potency.⁶⁵ X-ray crystallography revealed that the fluorine was closely bound via hydrogen bonding to a lysine residue in the active site. The addition of a single fluorine atom to a complex molecule causing such a significant increase in efficacy is testament to the power of fluorination in pharmaceutical compounds.

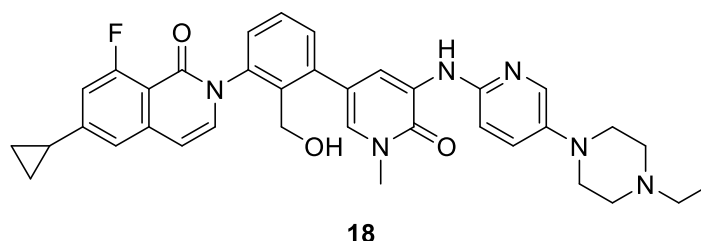


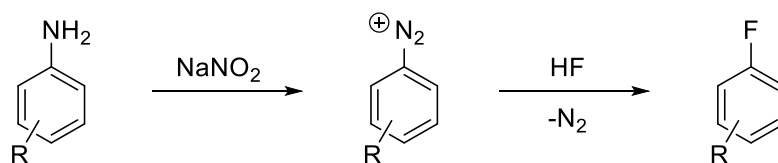
Figure 1.10. BTK inhibitor where fluorination improved potency 400-fold

1.1.4 Synthetic routes to organofluorine compounds

The electronegativity of fluorine imparts an extreme reactivity that can make the selective introduction of fluorine into complex, multifunctional bioactive compounds challenging. Fluorination reactions can be characterised by their mechanism of action. Nucleophilic fluorination involves the use of a fluoride anion source, such as potassium fluoride (KF) or tetrabutylammonium fluoride (TBAF), as nucleophiles in simple S_N1 , S_N2 or S_NAr reactions. Crown ethers can be used as phase transfer reagents to solubilise alkali metal

fluorides into organic solvents.⁶⁶ Industrially, anhydrous hydrogen fluoride (aHF) is commonly used as a cheap and effective nucleophilic fluorinating agent.⁶⁷ Nucleophilic fluorination reactions with aHF are often catalysed by metal fluorides, such as CrF_3 , and are particularly common in the synthesis of hydrofluorocarbons, displacing chlorine with fluorine.⁶⁸ More generally, the displacement with chlorine by fluorine by aHF is known as the Halex (halogen exchange) process and is also widely applied to the synthesis of aromatic fluorides.⁶⁹ However, the toxicity and corrosiveness of aHF, along with its low boiling point, are problematic and so amine-HF complexes such as Olah's reagent (70% pyridine, 30% HF)⁷⁰ or TREAT-HF ($\text{Et}_3\text{N}\cdot 3\text{HF}$)⁷¹ are more typically used on small scale.

A notable related process is the Balz-Schiemann reaction, in which aryl amines are converted to aryl fluorides via the corresponding diazonium species.⁷² Thermal or photochemical decomposition of diazonium tetrafluoroborate salts gives the aryl fluoride but, on industrial scales, direct treatment of the amine with aHF and sodium nitrite (NaNO_2) is preferred, as shown in Scheme 1.6. This, along with the Halex process, is how most aryl fluoride building blocks are synthesised.⁷³



Scheme 1.6. Generic Balz-Schiemann reaction of aryl amine to give an aryl fluoride

Deoxofluorination can be used to convert alcohols to fluorides, aldehydes and ketones to geminal difluorides and carboxylic acids to acyl fluorides or trifluoromethyl groups.⁷⁴ Such processes are carried out on large scale utilising gaseous sulfur tetrafluoride (SF_4), which is prepared by the reaction of sodium fluoride with elemental sulfur and chlorine.⁷⁵ As with aHF, SF_4 is corrosive and toxic so milder reagents such as DAST (**19**),⁷⁶ Deoxo-Fluor[®] (**20**)⁷⁷ and Ishikawa's reagent (**21**),⁷⁸ as shown in Figure 1.11, have been developed for deoxofluorination on smaller scales.

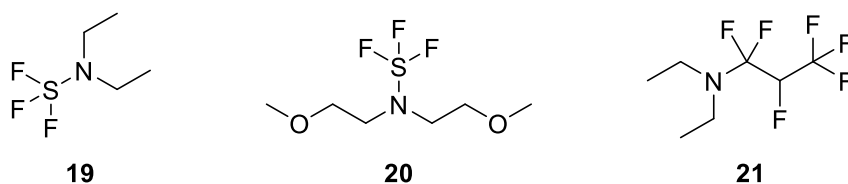
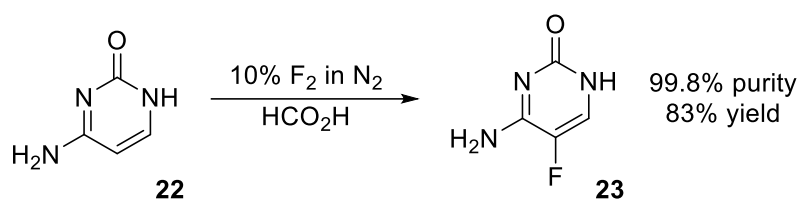


Figure 1.11. Notable deoxofluorination reagents

Electrophilic fluorination employs the opposite mechanism to nucleophilic, i.e. some equivalent of an F^+ cation is used. Fluorine gas (F_2) is analogous to aHF in that it is an inexpensive but dangerous and difficult to handle fluorinating reagent. However, with the appropriate apparatus and careful control of conditions, highly efficient and selective fluorinations of a wide range of aromatic⁷⁹ and dicarbonyl systems,⁸⁰ amongst others, can be carried out. This approach has recently been demonstrated in Durham with a new synthesis directly from cytosine (**22**) of antifungal drug flucytosine (**23**, Scheme 1.7), providing an efficient and lower cost route to this essential drug than previous methods.⁸¹



Scheme 1.7. Synthesis of flucytosine using F_2

Xenon difluoride (XeF_2)⁸² and O-F reagents such as acetyl hypofluorite (CH_3CO_2F)⁸³ have been used as somewhat milder alternatives to F_2 but both are still difficult to handle. A range of N-F reagents have been developed that are bench-stable, non-toxic and non-corrosive, albeit with greater cost and poorer atom economy than F_2 .⁸⁴ Amongst many examples, the most widely used of these reagents are SelectFluor™ (**24**),⁸⁵ NFSI (**25**)⁸⁶ and *N*-fluoropyridinium salts (**26**),⁸⁷ as shown in Figure 1.12. The mechanism of electrophilic fluorination continues to be debated between an S_N2 mechanism and a single electron transfer process, although recent kinetic studies suggest S_N2 is more likely.⁸⁸

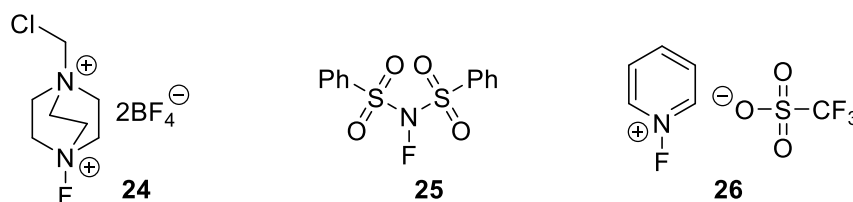


Figure 1.12. Common N-F electrophilic fluorinating reagents

In addition to their mechanism of action, fluorination strategies can also be roughly divided into early and late-stage processes depending on the point at which fluorine is incorporated into the molecule (Figure 1.13). Early-stage fluorinations introduce fluorine from the outset of a synthetic process and so eliminate potentially low-yielding

fluorination steps late in a synthesis. For this reason, early-stage fluorinations are often employed for large-scale manufacture with reagents such as aHF, F₂ and SF₄ but the availability of building blocks can limit the scope of subsequent chemistry that is possible. Fluorinations at a late stage can be precluded by harsh conditions not conducive to the synthesis of complex pharmaceutical molecules but great strides have been made in recent decades in the development of milder, bench-stable reagents for this purpose and are now commonplace for most small-scale applications, such as in academia and medicinal chemistry discovery programmes. However, this utility is often accompanied by an increase in cost and decrease in atom economy and so are typically limited to the discovery stage.⁸⁹ For example, Selectfluor™ contains only 6% by weight fluorine with the remainder typically lost as waste as such fluorinating reagents are difficult to recycle.

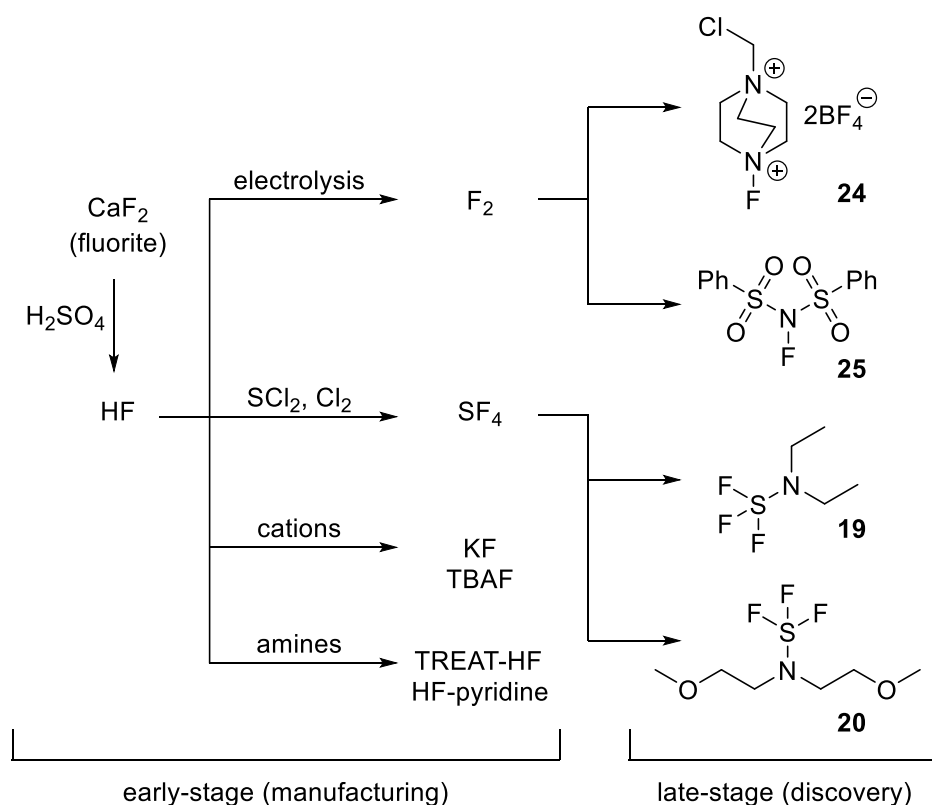


Figure 1.13. Overview of common early- and late-stage fluorinating reagents

1.2 Significance of the trifluoromethyl group

1.2.1 CF₃ groups in pharmaceuticals

An important sub-class of organofluorine compounds are those bearing a trifluoromethyl group. The electronegativity of a CF₃ group is similar to that of a nitrile group and its size between that of a methyl and an isopropyl group.⁹⁰ One of the very first widely-used drug compounds to contain fluorine was the anaesthetic halothane (**27**, Figure 1.14), first introduced in 1956.⁹¹ Many modern anaesthetics are also simple trifluoromethylated ethers, such as sevoflurane (**28**) and desflurane (**29**).⁹²

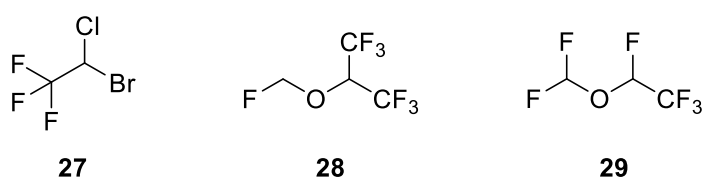


Figure 1.14. Structures of notable CF₃-substituted anaesthetics

The CF₃ group is now a common moiety in more complex therapeutic compounds. Recent estimates suggest that around 24% of approved fluorinated pharmaceuticals contain a trifluoromethyl group, with two thirds of those being on aryl rings, around 15% attached to alkyl groups, 12% on heteroaromatic systems and the remaining 6% being OCF₃ groups.⁹³ One notable example of a CF₃-containing pharmaceutical is fluoxetine (**30**, Figure 1.15). First developed by Eli Lilly and Company in 1972, and receiving FDA approval in 1987, it is perhaps better known by the trade name Prozac[®]. It was the first of many antidepressants of the selective serotonin reuptake inhibitor (SSRI) class and soon became the best-selling drug of its type, with sales reaching billions of dollars per year. The trifluoromethyl group acts to reduce serotonin reuptake six-fold compared to the non-fluorinated equivalent.⁹⁴ The difference is believed to arise from the CF₃ group altering the orientation of the phenoxy ring such that there are greater π -stacking interactions with aromatic residues in the serotonin transporter protein, increasing binding affinity.⁹⁵

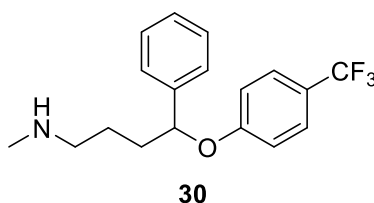


Figure 1.15. Structure of the antidepressant fluoxetine

Celecoxib (**31**, Figure 1.16), also known by trade name Celebrex[®] (Pfizer), is a non-steroidal anti-inflammatory (NSAID) used for the relief of pain, primarily for patients with arthritis. The presence of a trifluoromethyl group on the pyrazoyl ring was found to give the greatest selectivity for cyclooxygenase-2 (COX-2) over COX-1, the former being an inducible form of COX found in cells with inflammation whereas the latter is always present and so inhibition of COX-1 leads to unwanted side effects.⁹⁶

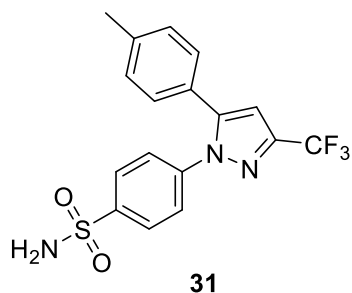


Figure 1.16. Structure of the anti-inflammatory drug celecoxib

Efavirenz (**32**, Figure 1.17), sold under the brand name Sustiva[®] (Bristol-Myers-Squibb) amongst others, is widely used in the treatment of HIV. It acts to inhibit a key reverse transcriptase of the virus via allosteric modification of the protein's active site. The role of the trifluoromethyl group is to lower the pK_a of the carbamate moiety and so strengthen hydrogen bonding interactions with the protein.⁹⁷

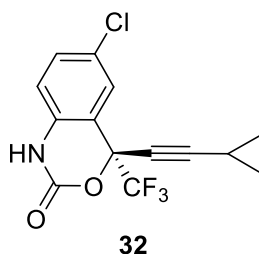
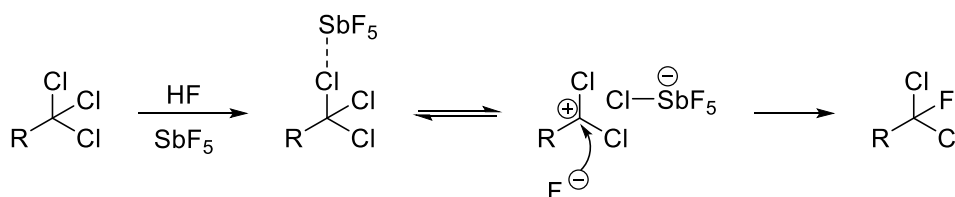


Figure 1.17. Structure of the anti-HIV drug efavirenz

1.2.2 Synthesis and applications of CF₃-containing building blocks

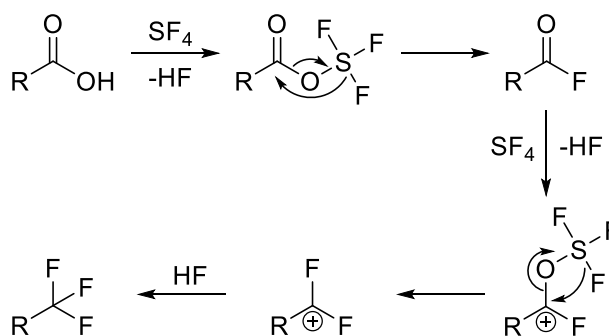
In the synthesis of most bioactive CF₃-substituted compounds, the trifluoromethyl group is present from the outset using a building block approach, i.e. an early-stage approach as described for monofluorination above. Industrially, aryl CF₃ groups are most commonly prepared by the exchange of chlorine for fluorine using aHF at elevated temperatures and pressures with Lewis acid catalysis, typically SbF₅. These are generally known as Swarts reactions after their inventor, Frédéric Swarts.⁹⁸ The organochlorine CCl₃-substituted

precursors can be prepared via various methods, most commonly from a CH_3 group by a radical process with chlorine and UV irradiation. The significantly higher strength of the C-F bond (485 kJ mol^{-1}) when compared to the C-Cl (327 kJ mol^{-1}) bond might suggest that halogen exchange should be facile. However, the electronegativity of fluorine makes each successive substitution more difficult as the chlorine atoms become worse donors to the catalyst, hence the need for high temperatures and pressures.⁹⁹ The mechanism for the first step is given in Scheme 1.8 and is simply repeated twice more to form the trifluoromethyl group. There are a wide range of commercially available aromatic and heterocyclic CF_3 building blocks that are synthesised via this method.¹⁰⁰



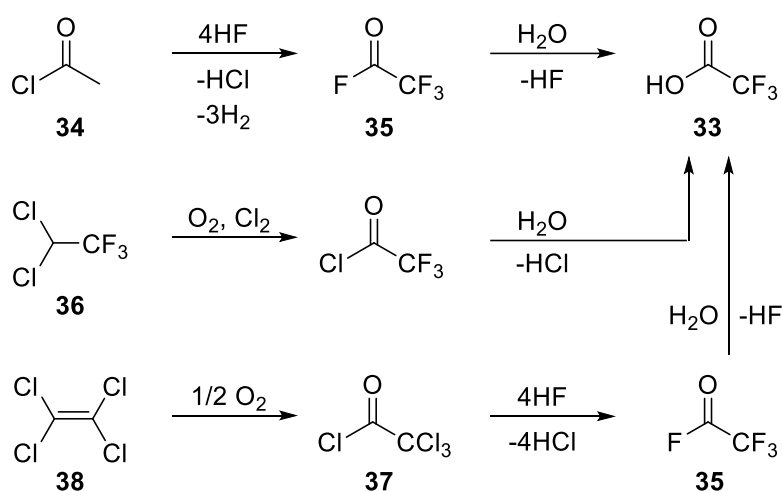
Scheme 1.8. Mechanism of Swarts halogen exchange reaction

An alternative approach is the deoxyfluorination of carboxylic acids with SF_4 and catalytic aHF, again performed at high temperatures and pressures. The mechanism is shown in Scheme 1.9, with the reaction initially proceeding via formation of the acid fluoride and then full deoxyfluorination gives the trifluoromethyl group.¹⁰¹ Milder reagents discussed earlier, such as DAST and DeoxoFluor, are insufficient for full conversion, reaching only the acid fluoride stage. In the case of both HF and SF_4 , the harsh reaction conditions are not well-suited to a laboratory setting or to late-stage trifluoromethylation of complex pharmaceutical molecules. Nevertheless, both aHF and SF_4 are still widely used for the synthesis of CF_3 -containing building blocks on the manufacturing scale.



Scheme 1.9. Prevailing mechanism for deoxyfluorination with SF_4

Amongst the most common trifluoromethyl building blocks is trifluoroacetic acid (TFA, **33**),¹⁰² which can be synthesised by electrofluorination of acetyl chloride (**34**) with aHF followed by hydrolysis of the resulting trifluoroacetyl fluoride (**35**) to give **33** (Scheme 1.10).¹⁰³ Other routes to **33** include chlorine-sensitised photooxidation of 2,2-dichloro-1,1,1-trifluoroethane (**36**, HCFC-123)¹⁰⁴ or via fluorination of trichloroacetyl chloride (**37**) derived from perchloroethene (**38**).¹⁰⁵ Further reactions of **33** such as esterification, decarboxylation, reduction and sulfonation give rise to a wide range of commercially available building blocks (Figure 1.18).^{106,107}



Scheme 1.10. Industrial routes to trifluoroacetic acid

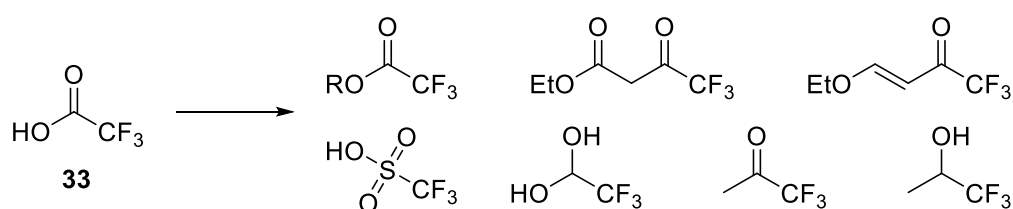
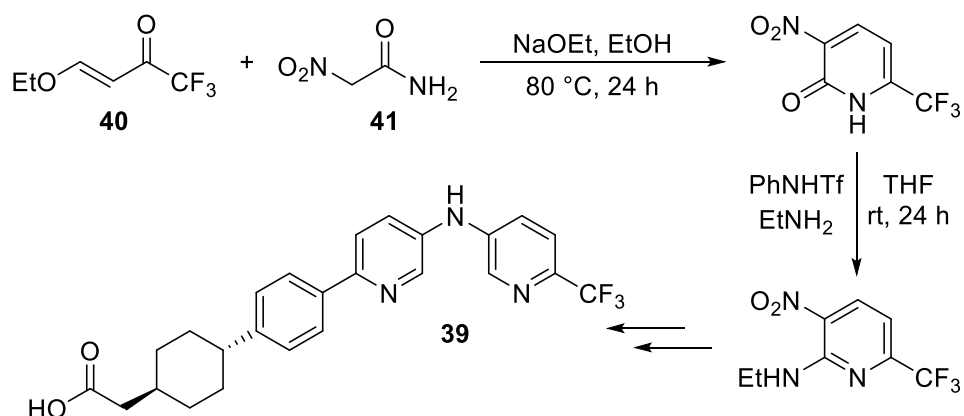


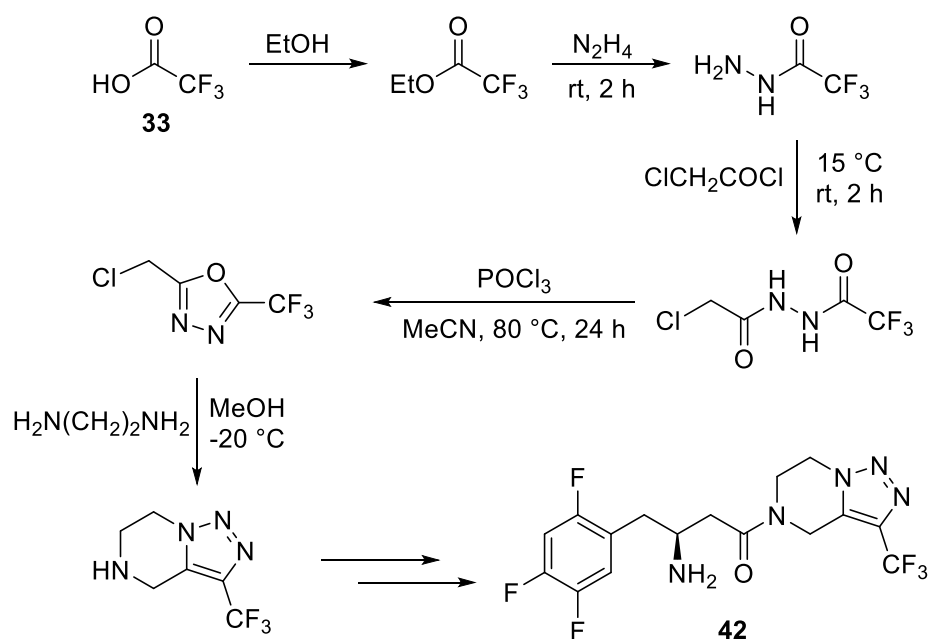
Figure 1.18. Commercially available building blocks derived from trifluoroacetic acid

One example of a pharmaceutical product manufactured from **33** is a potential treatment for non-alcoholic fatty liver disease, pradigastat (Novartis – **39**). The synthesis, shown in Scheme 1.11, involves the use of 4-ethoxy-1,1,1-trifluoro-3-buten-2-one (ETFBO, **40**) as the starting material to form a trifluoromethyl pyridine ring upon reaction with nitroacetamide (**41**).¹⁰⁸ **40** is derived from **33** by addition of the acid chloride to ethyl vinyl ether. An alternative synthesis from the pyridine carboxylic acid with SF₄ was considered but the route from **33** was ultimately preferred.



Scheme 1.11. Synthesis of pradigastat from trifluoroacetic acid

Another example is the diabetes medication sitagliptin (Januvia[®], Merck – **42**). In this case, shown in Scheme 1.12, the ethyl ester of **33** is converted to the hydrazine amide that is transformed to the CF₃-substituted heterocyclic core, which is linked to the rest of the compound via a simple amide bond forming reaction to give the final drug molecule.¹⁰⁹



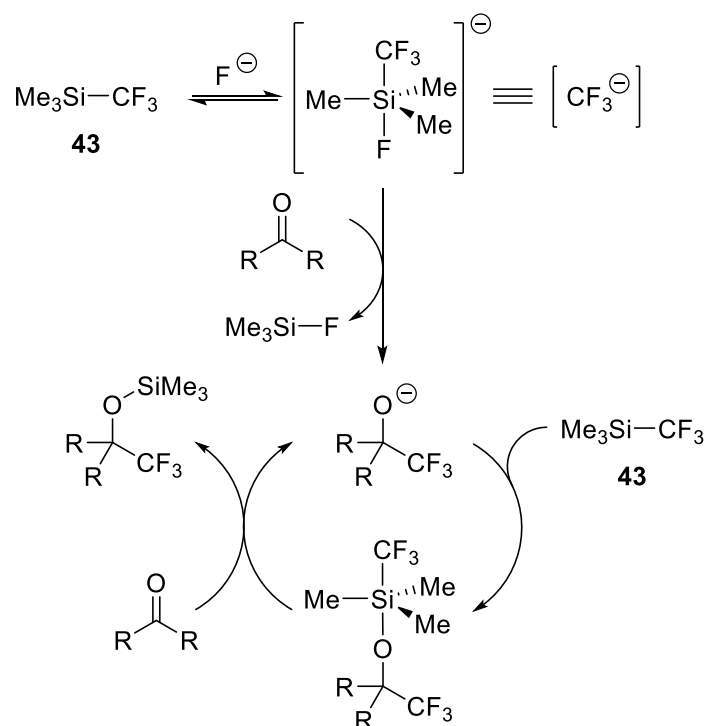
Scheme 1.12. Synthesis of sitagliptin from trifluoroacetic acid

Another potential building block is fluoroform, CHF₃, which is produced as a by-product in the manufacture of the ubiquitous polymer PTFE. Deprotonation of fluoroform with a strong base, such as potassium *tert*-butoxide, leads to *in situ* formation of a CF₃⁻ anion that can then act as a nucleophile.¹¹⁰ Alternatively, fluoroform can be used to generate

CuCF_3 , which can be made bench-stable by stabilisation with TREAT-HF.¹¹¹ This can then be used as either a nucleophilic or a radical source for introducing the CF_3 group. Whilst this method has yet to be applied on an industrial scale, the ready availability of fluoroform makes it potentially attractive for future use.

1.2.3 Late-stage trifluoromethylation strategies

Much like the monofluorination reactions described above, great advances have been made in recent decades in the development of selective and mild trifluoromethylation reagents for late-stage introduction of CF_3 groups into complex molecules. Perhaps the most well-known of these is trifluoromethyltrimethylsilane (**43**), otherwise known as the Ruppert-Prakash reagent.¹¹²⁻¹¹³ On activation by reaction with a fluoride anion, this acts as an equivalent of a CF_3^- anion for nucleophilic addition. The generally accepted mechanism is shown in Scheme 1.13.¹¹⁴ Typically, the electrophile is a carbonyl group but various different substrates have been used.¹¹⁵⁻¹¹⁶



Scheme 1.13. Mechanism of trifluoromethylation with the Ruppert-Prakash reagent

Decarboxylation of sodium trifluoroacetate (**44**),¹¹⁷ activation of CF_3I with *tetrakis*(dimethylamino)ethylene (**45**)¹¹⁸ and reaction of trifluoromethylphenylsulfone

(46) with *tert*-butoxide bases¹¹⁹ are alternative, albeit less commonplace, methods of generating CF_3^- *in situ* and their structures are given in Figure 1.19.

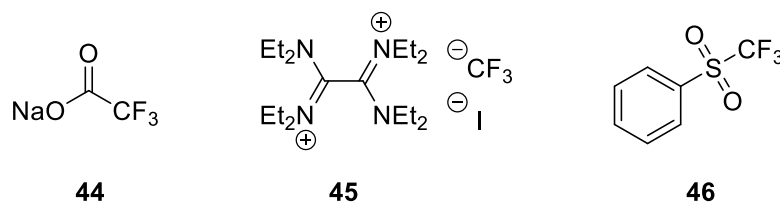


Figure 1.19. Structures of nucleophilic trifluoromethylating reagents

Electrophilic trifluoromethylation is made difficult by the high electronegativity of the CF_3 group but, nevertheless, reagents have been developed. Notable examples shown in Figure 1.20 include the use of dibenzothiophenium salts (47), the so-called Umemoto reagents,¹²⁰ and hypervalent iodine species (48), also known as Togni reagents.¹²¹

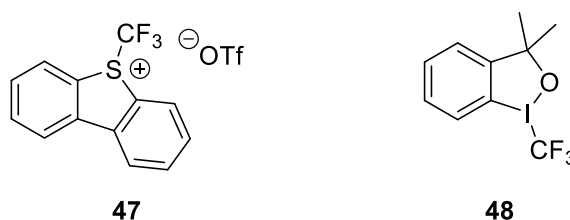
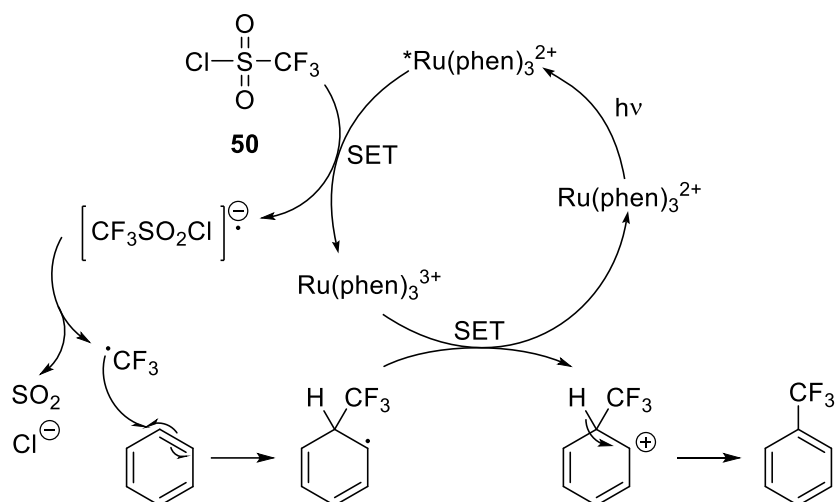


Figure 1.20. Representative examples of electrophilic trifluoromethylating reagents

One of the oldest known trifluoromethylation methods is radical addition of the CF_3 group, dating back to the photochemical reaction of CF_3I with alkenes reported by Haszeldine in 1949.¹²² The most widely used radical trifluoromethylating reagent in modern times is sodium trifluoromethanesulfinate, the Langlois reagent (49), in combination with an initiator such as *tert*-butyl hydroperoxide.¹²³ In a more recent example, Macmillan and co-workers demonstrated a metal-free photoredox catalysis process for C-H activation of arenes with triflyl chloride (50).¹²⁴ Figure 1.21 shows the structures of these radical trifluoromethylating reagents and Scheme 1.14 gives the mechanism of Macmillan's C-H activation methodology.



Figure 1.21. Notable examples of radical trifluoromethylating reagents



Scheme 1.14. Mechanism of photochemical C-H activation of arenes with triflyl chloride

Another older example of a trifluoromethylation is the McLoughlin-Thrower reaction of an aryl iodide with CF_3I via a radical mechanism catalysed by copper powder to give the aryl CF_3 product.¹²⁵ Cross-coupling reactions of aryl halides, boronic acids, diazonium salts and many other substrates with various sources of CF_3 have since been reported with copper, nickel and palladium catalysts.¹²⁶ Novel trifluoromethylation reactions are continually being developed and what is presented here is by no means an exhaustive list; the field has been extensively reviewed elsewhere.¹²⁷⁻¹³⁰ However, in all these cases, the selectivity and mild conditions come at the cost of relatively poor atom economy and high prices for the reagents or catalysts required. While aHF and SF_4 are toxic, corrosive and can be unselective, these reagents are inexpensive and widely available, which makes them well-suited to processes on an industrial scale where the milder trifluoromethylating reagents described above still struggle to compete economically.

1.3 HFO-1234yf

1.3.1 History and role of refrigerant gases

Approximately 80% by weight of organic fluorides produced industrially are small, simple molecules for use as refrigerant gases and polymer precursors with the refrigeration market is projected to grow to \$41.5 billion worldwide by 2024.¹³¹ Refrigerants are, therefore, relatively inexpensive and readily available and so could be ideal building blocks for the preparation of more complex fluorinated molecules, providing a possible alternative approach to the synthetic methods described above. Most modern refrigerators and air-conditioning units use these fluorinated gases in a process known as vapour-compression refrigeration.¹³² The basic design is shown in Figure 1.22 and involves a circulating gaseous refrigerant that is first compressed to a higher pressure and so a higher temperature.¹³³ This hot vapour is condensed further to a liquid by a condenser by being passed through a cooling coil, where heat is removed by a simple flow of air. The cooled refrigerant, still in liquid form, then enters a thermal expansion valve where the pressure is abruptly reduced. This leads to evaporation of the refrigerant back to the gas-phase and an accompanying reduction in temperature. The now cold refrigerant passes through an evaporation coil, where heat is transferred from the air in the compartment to be cooled to the refrigerant. At this stage, the refrigerant is a mix of liquid and vapour and the evaporation of remaining liquid serves to increase cooling. The refrigerant vapour is then returned to the compressor to repeat the cycle again.

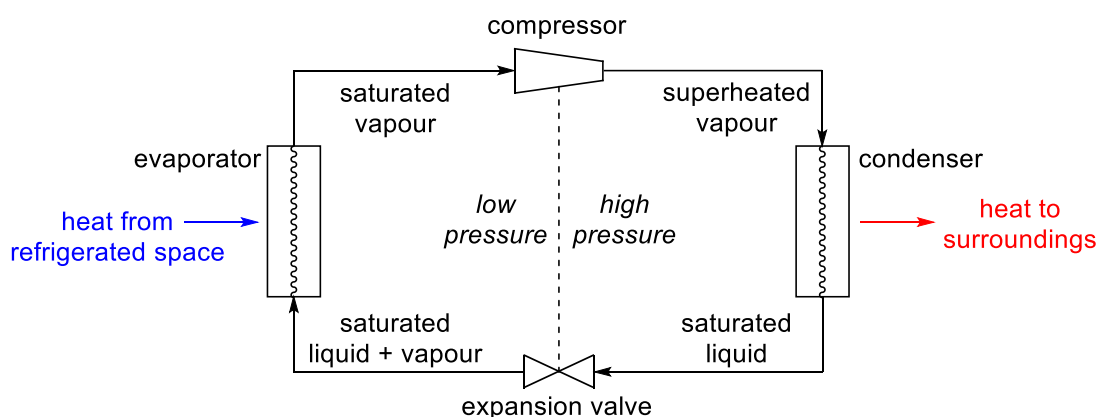


Figure 1.22. Schematic representation of a vapour-compression refrigeration system

Vapour-compression refrigeration was first proposed as a concept in 1805 by Oliver Evans.¹³⁴ The first-working prototype based on this design was constructed in 1835 by

Jacob Perkins but his design was a commercial failure. Several more attempts at such a device were attempted until the first practical machine was created by James Harrison in 1851, using diethyl ether, ammonia or ethanol in liquid form as the refrigerant. The first refrigerator to use gases was debuted by Ferdinand Carré in 1859 using gaseous ammonia. Carl von Linde's development of a method for the liquefaction of gases, patented in 1876, allowed for more widespread use of gases such as ammonia, sulfur dioxide and methyl chloride as refrigerants. Despite the toxicity of these compounds, they saw widespread use in refrigeration systems until the 1920s.

In the 1890s, Frédéric Swarts developed an efficient means for the synthesis of chlorofluorocarbons (CFCs) from carbon tetrachloride by halogen exchange.¹³⁵ This new class of compounds saw some use in fire suppression, owing to their low reactivity, but it was not until the 1920s that Thomas Midgely Jr. improved upon their synthesis and championed CFCs, such as CFCl_3 , as non-toxic and unreactive replacements for the gases then used in refrigeration.¹³⁶ CFCs, collectively known by the DuPont brand name Freon[®], became the dominant refrigerant gases until concerns were raised about their environmental impact in the 1970s. The pioneering work of Molina and Rowland showed that the relatively low reactivity of CFCs was problematic as they had atmospheric lifetimes of hundreds of years.¹³⁷ This provided sufficient time for CFC molecules to diffuse into the stratosphere where the increased intensity of UV radiation could lead to their decomposition into chlorine radicals. These radicals then catalyse the conversion of ozone to oxygen, particularly in the presence of crystalline ice surfaces. These fears were realised a decade later with the discovery of the ozone hole over Antarctica¹³⁸ and a smaller global decrease in stratospheric ozone levels.¹³⁹

These discoveries led to unprecedented global diplomatic action with the signing of the Montreal Protocol in 1987 calling for significant reductions in CFC production and use.¹⁴⁰ Further agreements and treaties in the following years have seen CFC usage decline and be replaced in many cases by hydrofluorocarbons (HFCs). The lack of a C-Cl bond in HFCs means they have no ozone-depleting potential. However, HFCs are potent greenhouse gases with significant atmospheric lifetimes owing to their lack of reactivity. In recent years, global efforts have been made to phase out HFCs in an analogous manner to CFCs, culminating in the 2016 Kigali Amendment to the original Montreal Protocol, which has now been signed and ratified by 108 nations and the European Union.¹⁴¹

Possible replacements for HFCs include hydrocarbons,¹⁴² supercritical carbon dioxide,¹⁴³ and hydrofluoroolefins (HFOs). Examples of each generation of fluorinated refrigerant are given in Figure 1.23, with the 1st generation represented by chloroform (**51**), the 2nd generation by CFC-113 (**52**) and the 3rd generation by HFC-134a (**53**). Finally, HFO-1234yf (**1**) is given as an example of the 4th and current generation of refrigerants and it is the chemistry of this molecule that is the focus of this thesis.

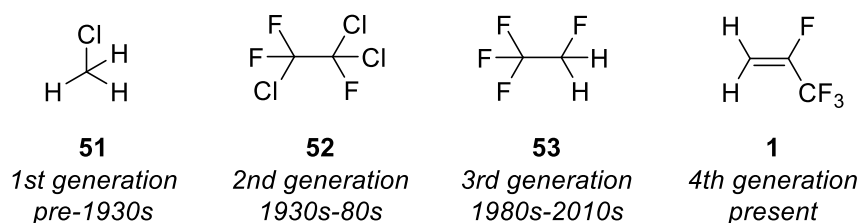


Figure 1.23. Example structures from each generation of refrigerants

Refrigerants are customarily referred to using nomenclature originally devised by the American Society of Heating, Refrigerating and Air-Conditioning Engineers (ASHRAE).¹⁴⁴ These consist of a series of up to four numbers, the first of which is simply the number of double bonds in the structure. If the molecule is entirely saturated, this number is omitted rather than including zero. The second number is equal to the number of carbon atoms in the structure minus one, the third number is equal to the number of hydrogen atoms plus one and the final number is equal to the number of fluorine atoms. For small molecules with few possible isomers, the most symmetrical isomer has no suffix and each subsequently less symmetrical isomer is labelled alphabetically. For molecules with three or more carbon atoms, the fragments attached to the first carbon atom have letters assigned. Thus, **1** is designated HFO-1234yf as it contains one double bond, three carbon atoms, two hydrogen atoms and four fluorine atoms with the ‘y’ representing the CF group and ‘f’ the CH₂ group.

1.3.2 HFO-1234yf as a refrigerant

2,3,3,3-Tetrafluoropropene, also known as HFO-1234yf (**1**), has emerged in recent years as the leading candidate to replace 1,1,1,2-tetrafluoroethane (HFC-134a, **53**) in automobile air conditioning units. Blends of **1** with other HFCs are also used in stationary refrigerant systems.¹⁴⁵ Refrigerants can be characterised by their coefficient of performance (COP), which is defined as the ratio of useful cooling provided to the input

of work required. Bench tests of **1** versus **53** show a decrease in COP of between 0.8% and 2.7%,¹⁴⁶ which broadly agrees with computational predictions.¹⁴⁷ The compressor discharge temperature was also determined, which gives an indirect measure of the refrigerant's stability and so dictates the system's useful lifetime. **1** was found to have a 6.4 °C to 6.7 °C lower compressor discharge temperature than **53**, suggesting systems based on **1** may be more reliable in the long-term. Finally, **1** has a reduced density when compared to **53** and so leaks are less likely.¹⁴⁸ This both increases the lifetime of the system and further reduces environmental impact. Overall, while **1** shows marginally worse performance than **53** in absolute terms, the higher reliability leads to increased performance when a full life-cycle analysis is carried out.

Given the commercial interest in **1**, the safety of this compound has been thoroughly investigated. Studies by the original developers of the compound, DuPont and Honeywell, have determined that the acute toxicity exposure limit of **1** is 101,000 ppm.¹⁴⁹ This compares very favourably with values of 50,000 ppm for **53** and 40,000 ppm for CO₂. **1** also shows no evidence of any mutagenic or carcinogenic activity. **53** causes cardiac sensitisation at 75,000 ppm whereas **1** displays no such behaviour. No environmental toxicity is observed below 100 mg L⁻¹, which passes EPA regulations. Studies of the metabolism of **1** in rats and rabbits show that the primary metabolite is cysteine derivative **54** (Figure 1.24), which is formed by oxidation of **1** to form an epoxide that then reacts with glutathione residues or is hydrolysed.¹⁵⁰ 90-95% of all **54** was excreted within 18 hours after exposure by inhalation.

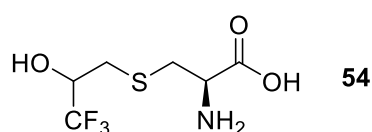


Figure 1.24. Major metabolite formed following inhalation of HFO-1234yf

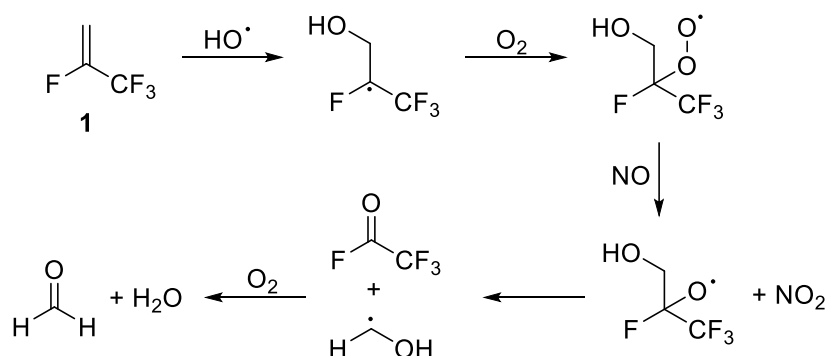
Experimental measurements of the maximum burning velocity of **1** gave a value of $1.2 \pm 0.3 \text{ cm s}^{-1}$, less than half that of HFC-32 (difluoromethane) and more than 30 times less flammable than propane.¹⁵¹ The lower flammability limit of **1** was determined to be 6.5% by volume, which is sufficient to be reached with a refrigerant gas leak caused by a large puncture, e.g. in a vehicle collision. Tests of potential ignition sources in a car's cabin or engine compartment showed no combustion was caused by a lit cigarette, 12-V battery sparks or hot manifold surfaces up to 900 °C.¹⁵² Weak ignition was observed in the

presence of a butane cigarette lighter or arc welder and full ignition only on the 900 °C surface in the presence of oil or with a fused nichrome wire filament. Based on these data, the estimated risk of injury from the ignition of **1** during a collision was calculated as only 2×10^{-11} per year, five orders of magnitude less likely than being struck by lightning. The flammability of **1** has possibly been exaggerated by automobile manufacturing companies to delay the potentially costly implementation of new refrigeration systems.

1 was developed as a more environmentally benign alternative to CFCs and HFCs. It has no ozone-depleting potential because it has no C-Cl bonds and so is incapable of generating the chlorine radicals responsible for the destruction of ozone caused by CFCs. **1** also has a significantly lower global warming potential (GWP) than **53**. The GWP value of a given gas is dependent on both its radiative forcing, a measure of how much heat a molecule absorbs, and its atmospheric lifetime. From computational predictions and experimental measurements of a molecule's infrared absorption cross-section, the radiative forcing of a compound can be calculated using a line-by-line radiative transfer model. Several different versions of these models exist, considering temperature, humidity, ozone levels and cloud properties at different latitudes to estimate the global impact. Using this approach, the radiative forcing of **1** was calculated as $0.24 \text{ W m}^{-2} \text{ ppb}^{-1}$,¹⁵³ relative to a value of $0.16 \text{ W m}^{-2} \text{ ppb}^{-1}$ found for **53**.¹⁵⁴

Given the higher radiative forcing of **1**, it might be expected that it would have a greater GWP than **53**. However, the atmospheric lifetime of a molecule must also be considered to calculate a GWP. For gases in the troposphere, the primary means of degradation is by reaction with hydroxyl radicals to give water-soluble compounds that are then washed out of the atmosphere via rainfall.¹⁵⁵ For molecules with slow rates of reaction with species in the atmosphere, there is sufficient time to diffuse into the stratosphere where the main degradation pathway becomes photolysis and reaction with various excited states of oxygen. In the case of **1**, reaction with HO• is rapid and so is the main route for degradation (Scheme 1.15).¹⁵⁶ This degradation pathway gives nitrogen dioxide, formaldehyde, water and trifluoroacetyl fluoride as the products. The major unnatural product of this degradation process, trifluoroacetyl fluoride, is hydrolysed in the atmosphere to TFA within an average time of ten days.¹⁵⁷ While toxic to aquatic organisms, estimates for the volume of TFA produced by the breakdown of **1**, assuming full replacement of **53**, place the highest annual mean concentration at 60 times lower

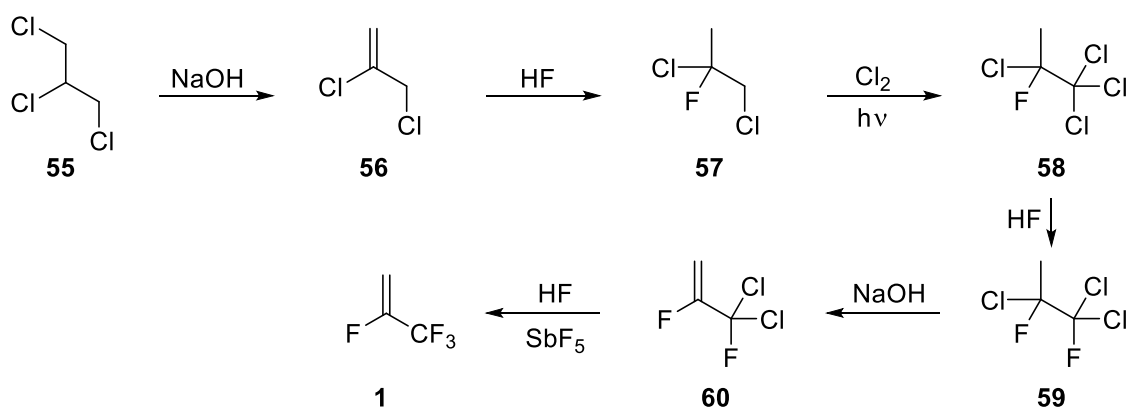
than minimum safe levels.¹⁵⁸ **1** can also be broken down by reaction with ozone, Cl^\bullet radicals and NO_3 but the concentrations of these species in the troposphere are much smaller than HO^\bullet and so the products of these other degradation pathways will have a negligible environmental impact.¹⁵⁹ Modelling atmospheric distributions and temperatures for these combined reaction pathways, the estimated atmospheric lifetime of **1** is only 11 days, which compares very favourably with a lifetime of 14 to 16 years for **53**.¹⁶⁰ Combining the radiative forcing and atmospheric lifetime contributions gives GWP values of 1300 for **53** and only 4 for **1**, a 99.7% reduction in GWP.¹⁶¹



Scheme 1.15. Mechanism of hydroxyl radical-mediated atmospheric degradation of HFO-1234yf

1.3.3 Manufacturing processes for HFO-1234yf

The synthesis of **1** was first reported by Henne and Waalkes in 1946 from 1,2,3-trichloropropane (**55**) long before there was any industrial use for **1** (Scheme 1.16).¹⁶²

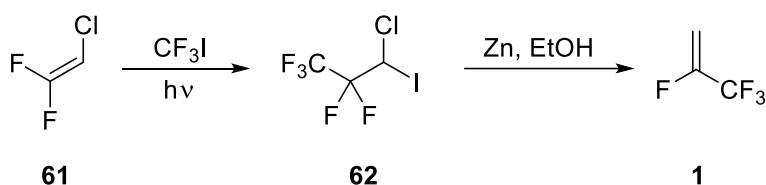


Scheme 1.16. Synthesis of HFO-1234yf via successive dehydrochlorination and fluorination reactions

Initial elimination of HCl using sodium hydroxide gives **56**, which is then fluorinated with HF to give **57**. Photochemical chlorination of **57** gives **58**, from which elimination

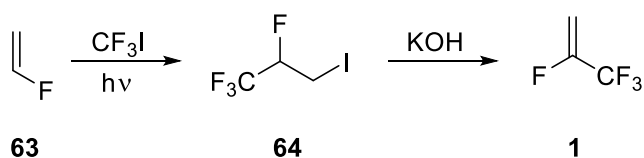
of HCl to give the corresponding trichloromethyl alkene was attempted but the product was too unstable towards hydrolysis. Partial fluorination of **58** with HF to give **59** is required before the second dehydrochlorination to form **60**, which is sufficiently stable to be isolated. Allylic fluorination with SbF_5 gives the final product **1**.

Haszeldine and Steele demonstrated radical addition of CF_3I across the double bond of difluorochloroethylene (**61**), initiated by irradiation with ultraviolet light in the 220-300 nm region (Scheme 1.17).¹⁶³ Addition of zinc in ethanol to the product **62** leads to successive eliminations of zinc iodide and zinc chloride to give a carbocation intermediate that loses fluoride to form **1**.



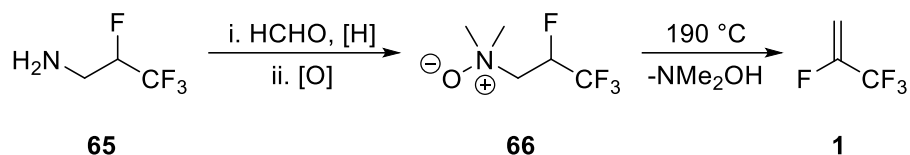
Scheme 1.17. Radical synthesis of a multi-halogenated species and dehalogenation to give HFO-1234yf

Haszeldine *et al.* later reported reaction of CF_3I with vinyl fluoride (**63**) to give a mixture of 1,1,1,2-tetrafluoro-3-iodopropane (**64**) and 1,1,1,3-tetrafluoro-2-iodopropane by a similar radical addition process (Scheme 1.18). Subsequent elimination of HI from **64** with potassium hydroxide gave **1**.¹⁶⁴



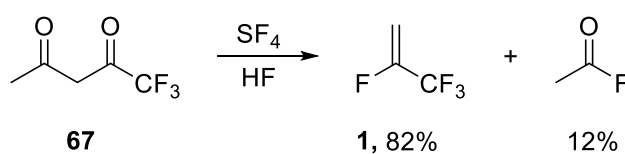
Scheme 1.18. Radical synthesis of an iodofluoropropane and dehydroiodination to give HFO-1234yf

Knunyants *et al.* reported deamination of polyfluorinated alkyl *N*-oxides and ammonium ions to give alkenes.¹⁶⁵ The synthesis of **1** was achieved by reductive amination of tetrafluoroalkane **65** followed by oxidation to *N*-oxide **66**, from which dimethylhydroxylamine is eliminated as a by-product as shown in Scheme 1.19. Specific details of the experimental conditions were not given. The amine starting material **65** was prepared by reaction of 1,1,2-trifluoroethene with HF and hexamethylenetetramine.



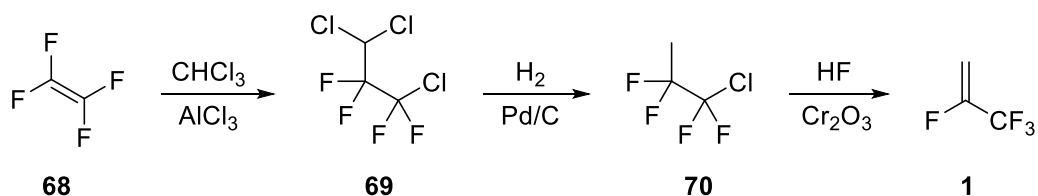
Scheme 1.19. Deamination route to synthesis of HFO-1234yf

Yagupolskii *et al.* reported the synthesis of **1** by the reaction of SF_4 with a range of trifluoromethyl carbonyl species.¹⁶⁶ The same reaction of trifluoroacetylacetone (**67**) with SF_4 was later reported by Banks *et al.* using HF as a catalyst/solvent to give an improved yield of **1** in a shorter time, as shown in Scheme 1.20.¹⁶⁷



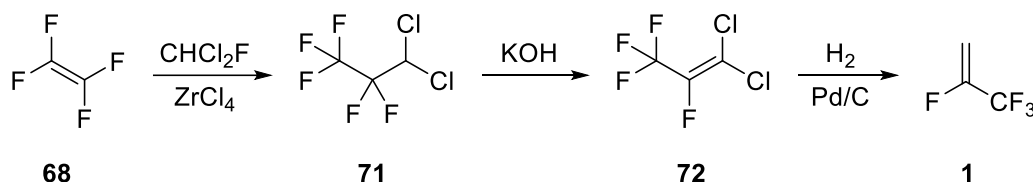
Scheme 1.20. Fluorination and cleavage of trifluoroacetylacetone with SF_4 to give HFO-1234yf

These early synthetic routes to **1** were developed before there was any particular use for the compound. As concerns about the impact of HFCs on climate change grow, the identification of HFOs as a potential replacement requires new processes more amenable to industrial scales. Tetrafluoroethylene (TFE, **68**) is used as a monomer in the synthesis of a wide variety of fluoropolymers, including the ubiquitous PTFE and is, therefore, available cheaply on huge scale. Three routes to make **1** from **68** have been developed. In the presence of AlCl_3 or aluminium chlorofluoride as a Lewis acid catalyst, **68** and chloroform (**51**) react to form chlorofluoroalkane **69** (Scheme 1.21).¹⁶⁸ Liquid-phase hydrogenation with palladium on carbon removes most of the chlorine atoms to form **70**. In the final step, the remaining chlorine atom is displaced by fluoride using aHF with simultaneous dehydrofluorination over a chromium oxide catalyst in the vapour-phase.¹⁶⁹



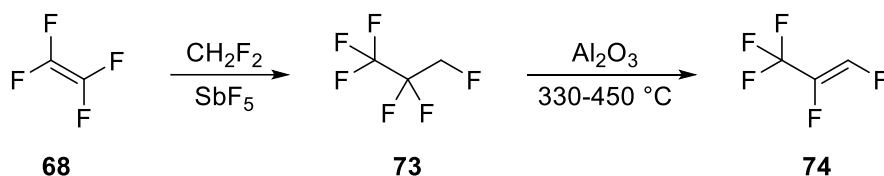
Scheme 1.21. Example of the TFE/chloroform route to HFO-1234yf

In the second route from **68** to **1**, fluorodichloromethane (HCFC-21) can be added to **68** using various Lewis acid catalysts, with $ZrCl_4$ and $HfCl_4$ giving the highest conversions to chlorofluoroalkane **71** (Scheme 1.22).¹⁷⁰ Several side products are formed in this reaction but these do not react with KOH in the next step to form chlorofluoroalkene **72** and so can be removed by distillation.¹⁷¹ Hydrogenation of **72** with palladium supported on Al_2O_3 , AlF_3 or activated carbon at 50-200 °C afforded **1**.¹⁷²



Scheme 1.22. Example of the TFE/HCFC-21 route to HFO-1234yf

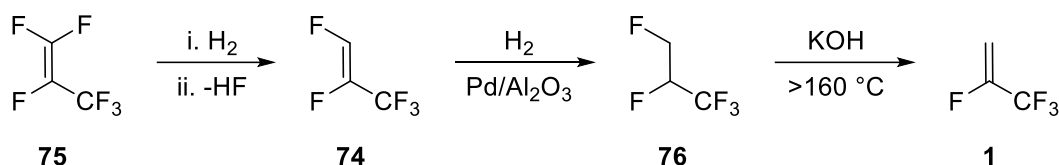
The third and final route from **68** to **1** begins with addition of difluoromethane (HFC-32), which can also be accomplished with various Lewis acid catalysts to form hexafluoropropane **73**, the best selectivity being achieved with SbF_5 (Scheme 1.23).¹⁷³ Subsequent dehydrofluorination is not facile and requires the use of fluorinated chromium or aluminium oxide catalysts at high temperatures to form HFO-1225yf (**74**) as an intermediate, which is a refrigerant in its own right.¹⁷⁴



Scheme 1.23. Example synthesis of HFO-1225yf from TFE

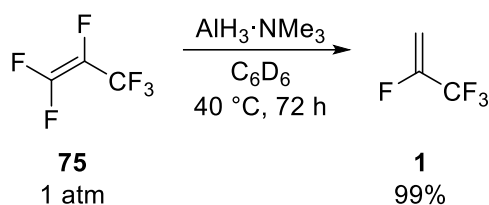
Alkene **74** can alternatively be prepared from hexafluoropropene (HFP, **75**) by hydrogenation followed by dehydrofluorination. **74** derived from either TFE or HFP is then converted to **1** via a second hydrogenation and dehydrofluorination step (Scheme 1.24). This method for the preparation of **1** was first reported by Knunyants *et al.* in 1960 through successive hydrogenation, with hydrogen and palladium on carbon, and dehydrofluorination, with potassium hydroxide, of HFP.¹⁷⁵ In modern procedures, hydrogenation is similarly carried out using palladium supported on carbon or alumina, with the latter being more stable and giving better selectivity for fluoroalkane **76**.¹⁷⁶ For the elimination step, low conversion was obtained for simple thermal pyrolysis so a range

of different catalysts have been employed.¹⁷⁷ These high temperature vapour-phase dehydrofluorination reactions have a maximum selectivity of 90%. By contrast, conducting the reaction in the liquid-phase with KOH melt gave selectivities of up to 99%.¹⁷⁸ However, precautions must be taken to deal with highly toxic fluoroacetate side products in the waste stream.



Scheme 1.24. Example synthesis of HFO-1234yf from hexafluoropropene

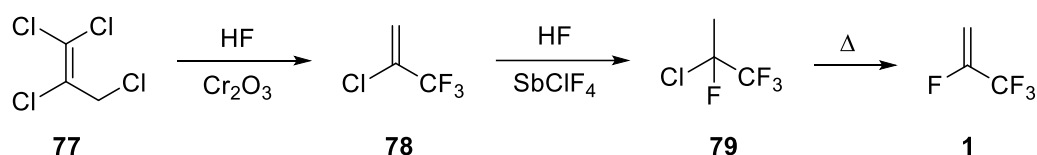
High temperature [2+2] cyclisation of **75** with ethene followed by pyrolysis of the resulting cyclobutene yields a mixture of **1** and 1,1-difluoroethene.¹⁷⁹ One-step dehydrofluorination of **75** has been demonstrated using tetramethyldisiloxane and Stryker's reagent, $[\text{CuH}(\text{PPh}_3)_4]_6$, as a catalyst.¹⁸⁰ More recently, Crimmin *et al.* reported that **75** could be directly hydrodefluorinated to **1** by $\text{AlH}_3 \cdot \text{NMe}_3$ (Scheme 1.25).¹⁸¹ DFT calculations suggest the reaction proceeds via a nucleophilic substitution mechanism, with hydride attacking **75** to form a stabilised carbanion that eliminates fluoride to form **74**, which then reacts with a second equivalent of hydride *in situ* to form **1**.



Scheme 1.25. Direct hydrodefluorination of hexafluoropropene to form HFO-1234yf

As of 2017, there were two plants in China using the HFP process with a total production of 13 kilotonnes per year. This accounted for approximately 50% of global production, with a single US plant producing 15 kilotonnes per year via a different process.¹⁸² The US route begins with the commercially available 1,1,2,3-tetrachloropropene (HCFC-1230xa, **77**), which is hydrofluorinated using aHF with a wide range of different possible Lewis acid catalysts (Scheme 1.26).¹⁸³ This reaction can be carried out in either the liquid or vapour-phase but yields are much lower in the former and so the vapour-phase is favoured. The initial chlorofluoroalkene product **78** is further hydrofluorinated using aHF

and a stronger Lewis acid catalyst, typically $\text{SbCl}_x\text{F}_{5-x}$, to form chlorofluoroalkane **79**.¹⁸⁴ This process can also be carried out in either the liquid or vapour-phase but the liquid-phase is preferred in this case as the side products that form in the vapour-phase are difficult to remove. **79** can be directly converted to **1** via a vapour-phase process with a range of metal oxide or Lewis acid catalysts but with fairly low selectivity.¹⁸⁵ Thermal pyrolysis of **79** is effective initially but selectivity decreases over time with fluorination of the walls of the reactor requiring careful control of aHF levels.¹⁸⁶ Dehydrochlorination to **1** can also be accomplished using KOH and a phase transfer catalyst, albeit with relatively low conversion.¹⁸⁷ Alternatively, the alkene intermediate **78** can be directly converted to **1** using either SbCl_5 on carbon or fluorinated Cr_2O_3 catalysts.¹⁸⁸ However, this process requires higher temperatures and is, therefore, less selective.



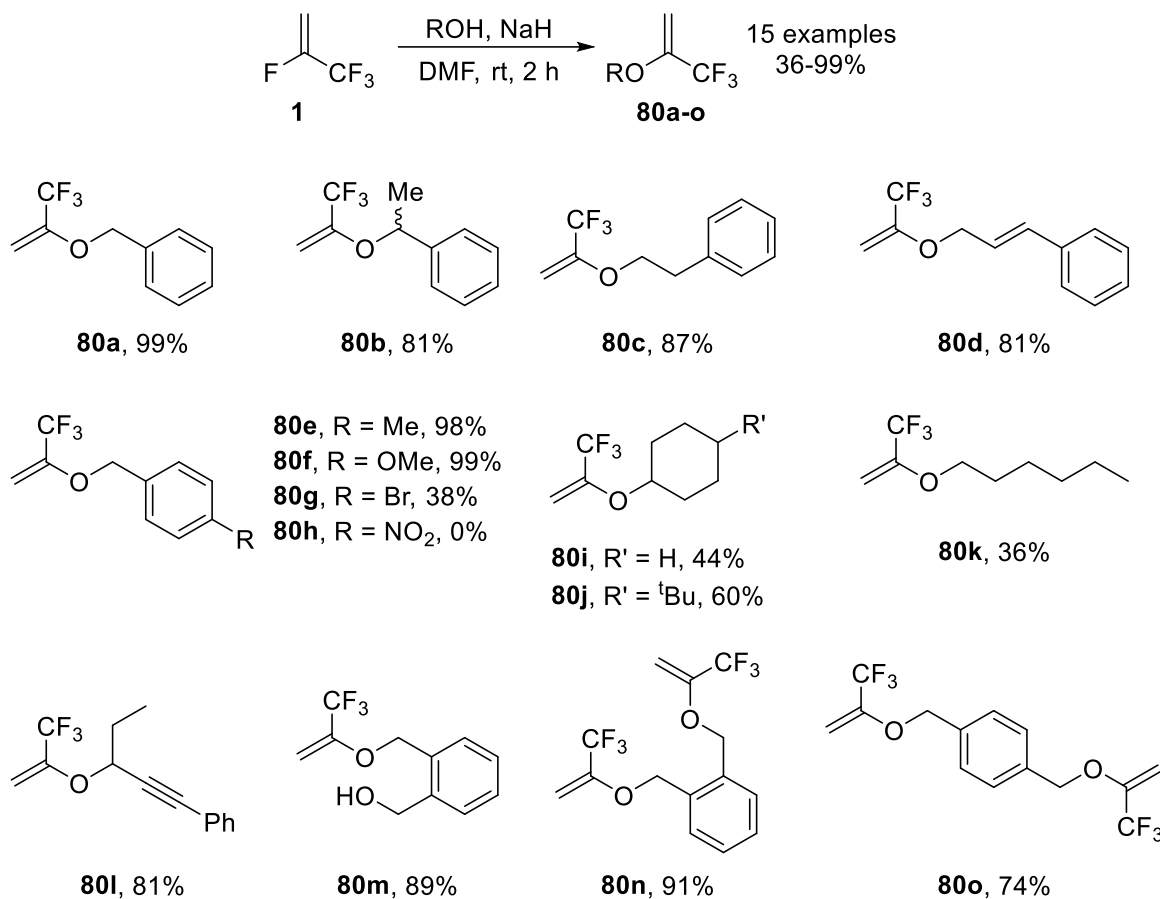
Scheme 1.26. Example of the HCFC-1230xa route to HFO-1234yf

There exists a vast array of patented routes to **1** via a variety of chlorocarbon intermediates and what is presented above is a brief overview of the commercially important manufacturing processes. Various other methods such as dehydration of appropriate tetrafluorinated propanols,¹⁸⁹ copper-catalysed addition of carbon tetrachloride to ethene followed by a series of fluorinations and dehydrochlorinations,¹⁹⁰ SbF_5 -catalysed Prins-type addition of fluoroform to trifluorochloroethene¹⁹¹ and pyrolysis of chloroform-hydrofluorocarbon mixtures¹⁹² have all been developed but few have yet seen widespread adoption. Ownership for the majority of industrially relevant patents lies with Honeywell and DuPont (now licensed to Chemours) and these two companies are currently the only major commercial suppliers of **1**. This is a significant contributing factor to the current wholesale price of **1**, which is far higher than **53** that it is intended to replace. However, this cost is expected to decrease in the near future as patents expire, allowing more suppliers to enter the market, and supply increases to match the increased demand for HFOs with the continuing legislative phase out of HFCs. At the time of writing, **1** could be purchased from BOC in 5 kg cylinders for the price of £0.07 per gram.¹⁹³

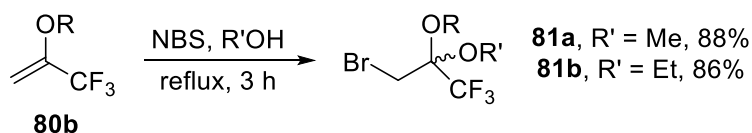
1.3.4 Uses of HFO-1234yf in organic synthesis

Despite the large-scale manufacture of **1**, there are few published examples of its use in synthesis beyond the manufacture of polyfluorinated polymers. Co-polymerisation reactions have been reported in the patent literature with 1,1-difluoroethene,¹⁹⁴ tetrafluoroethene,¹⁹⁵ ethene,¹⁹⁶ chlorotrifluoroethene,¹⁹⁷ hexafluoropropene,¹⁹⁸ ethyl vinyl ether,¹⁹⁹ other hydrofluoroolefins,²⁰⁰ β -pinene,²⁰¹ and acrylonitrile.²⁰²

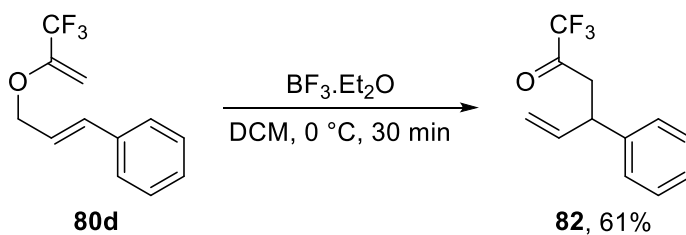
Yamazaki *et al.* reported reactions of **1** with alkoxides to give a range of α -trifluoromethyl enol ethers.²⁰³ Initial computational studies showed that the presence of a trifluoromethyl group would lead to a significant decrease in frontier orbital energy levels. The vinylic fluorine atom was also calculated to lead to a significant electropositive partial charge on the carbon atom to which it is bonded, mostly due to the inductive effect of the fluorine's electronegativity but also in part from p- π repulsion interactions. These two factors suggested that **1** might be reactive towards nucleophiles at this position. An initial screen of potential nucleophiles showed only benzyl alcohol underwent the desired addition-elimination reaction at room temperature, whereas no reaction was observed for benzylamine, phenol or thiophenol. Following optimisation of the reaction conditions, a range of enol ethers were prepared by the reaction of various alcohols with sodium hydride to give the corresponding alkoxide followed by addition to **1** with elimination of HF to give the products **80a-o** (Scheme 1.27). Synthesis of the aliphatic enol ethers **80i-k** required substitution of DMF as the solvent with 3:1 THF/DMF to ensure good solubility. Poor yields were obtained in cases where the product was volatile, e.g. **80i**, or where the alcohol had an electron-withdrawing substituent, e.g. **80g**. In the case of benzenedimethanol derivatives, good selectivity could be achieved for the 1,2-diol by controlling equivalents of the alcohol to give **80m** or **80n** but the 1,4-diol gave only the disubstituted product **80o** under all conditions attempted. **80b** was then reacted with *N*-bromosuccinimide (NBS) in an alcohol solvent to give brominated acetals **81a** and **81b** (Scheme 1.28). These brominated acetals are difficult to synthesise from trifluoroacetone due to the electrostatic effects of the CF₃ group. Finally, treatment of **80d** with boron trifluoride diethyl etherate led to a facile Claisen rearrangement to the corresponding ketone **82** (Scheme 1.29).



Scheme 1.27. Substitution reaction of HFO-1234yf with sodium alkoxides to give α -CF₃ enol ethers²⁰³



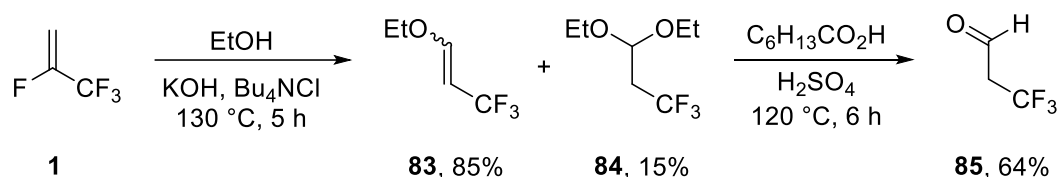
Scheme 1.28. Cofluorination of α -trifluoromethyl enol ether **80b**²⁰³



Scheme 1.29. Claisen rearrangement of α -trifluoromethyl enol ether **80d**²⁰³

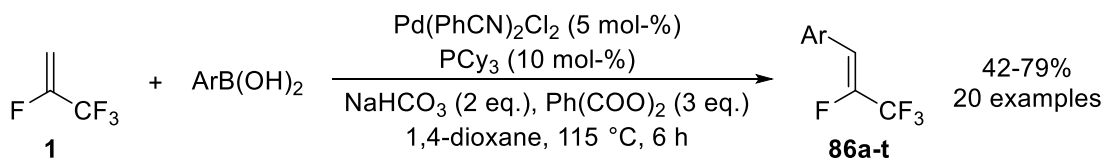
By contrast, Yagupolskii *et al.* reported the reaction of **1** with potassium hydroxide in ethanol with a phase transfer catalyst to give β -trifluoromethyl enol ether **83** along with some acetal **84**.²⁰⁴ The regioselectivity of the nucleophilic addition is opposite to that both predicted and observed by Yamazaki with sodium alkoxides and neither paper offers an

explanation for this discrepancy. Treatment of the crude reaction mixture with heptanoic acid and catalytic H₂SO₄ gave 3,3,3-trifluoropropanal (**85**) in an overall yield of 64% from **1** (Scheme 1.30).



*Scheme 1.30. Synthesis of 3,3,3-trifluoropropanal from HFO-1234yf*²⁰⁴

Li *et al.* demonstrated the use of **1** in an oxidative Heck coupling reaction to afford polyfluorinated styrenes **86a-t**, which are otherwise challenging to synthesise (Scheme 1.31).²⁰⁵ Optimised Heck reaction conditions were applied to a range of *ortho*, *meta* and *para*-substituted phenylboronic acids, with most around 70% isolated yield (Table 1.1). The reaction is highly selective for the *Z*-isomer, with *Z/E* ratios of between 93:7 and 99:1. This selectivity can be attributed to the steric repulsion between the aryl group and the phosphine ligands of the palladium complex in the intermediate formed following the migratory insertion step. Better yields were obtained for boronic acids with electron-donating substituents, suggesting that oxidative addition is the limiting step. These reactions were subsequently carried out using Pd/PdO@NGr-C, a nanoparticle catalyst derived from palladium acetate and 1,10-phenanthroline, with hydrogen peroxide as a more environmentally benign oxidant.²⁰⁶ A lower temperature of 80 °C was used but with a longer reaction time of 12 hours. This updated protocol used the same substrate scope of boronic acids and achieved higher yields (80-95%) with similar stereoselectivity. Additionally, the nanopalladium catalyst could be recycled up to five times with the yield remaining above 90%.

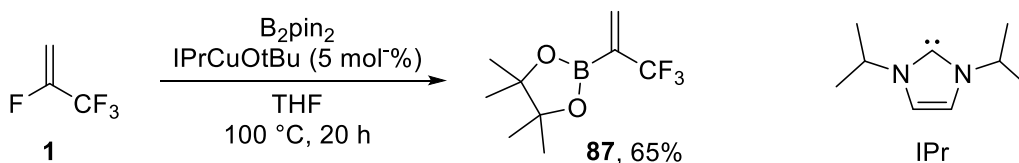


*Scheme 1.31. Oxidative Heck coupling of HFO-1234yf with aryl boronic acids to give Z-alkenes*²⁰⁵

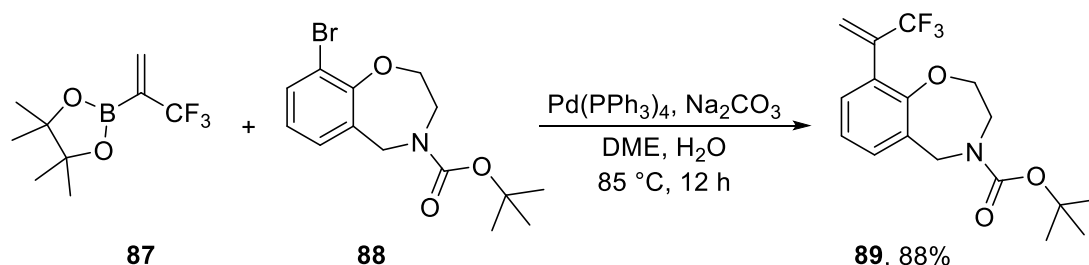
Table 1.1. Substrate scope for oxidative Heck coupling of HFO-1234yf²⁰⁵

Product	Substituent	% Isolated yield	Z:E
86a	4-OMe	79	99:1
86b	4-Me	78	96:4
86c	4-Et	75	97:3
86d	4- ⁿ Bu	69	97:3
86e	4- ⁱ Pr	62	97:3
86f	4- ^t Bu	42	97:3
86g	4-OBn	69	98:2
86h	4-CN	48	96:4
86i	4-CF ₃	60	97:3
86j	4-Cl	58	95:5
86k	2-OMe	61	93:7
86l	3-OMe	68	99:1
86m	3-CO ₂ Me	61	98:2
86n	3,4-OCH ₂ O	62	96:4
86o	3,5-diMe	50	96:4
86p	2,4-diMe	69	96:4
86q	3,4-diOMe	59	97:3
86r	2,4,6-triMe	52	97:3
86s	4-Ph	58	99:1
86t	4-carbazole	71	98:2

Ogoshi *et al.* demonstrated a highly regioselective defluoroborylation reaction of **1** to give the equivalent boronate ester **87** (Scheme 1.32).²⁰⁷ Based on mechanistic investigations with other fluorinated alkenes, the reaction is believed to proceed via formation of a Cu-Bpin complex *in situ* followed by addition across the double bond, then subsequent elimination of copper(I) fluoride to give the product.

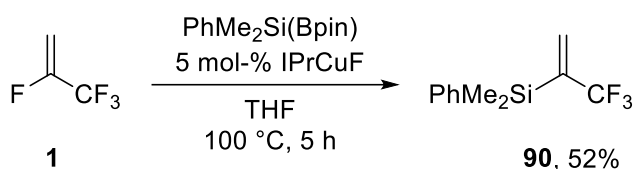
Scheme 1.32. Copper-catalysed defluoroborylation of HFO-1234yf to give a vinyl boronate ester²⁰⁷

No further reactions of **87** were explored in this paper. There is only one other reported use of **87**, which was in a Takeda Pharmaceuticals patent to convert aryl bromide **88** to α -trifluoromethyl alkene **89** via a Suzuki coupling reaction (Scheme 1.33). The resulting benzoxazepine derivative acts as an activator of the serotonin 5-HT_{2C} receptor and so can be used for treatment of lower pelvic prolapse.²⁰⁸



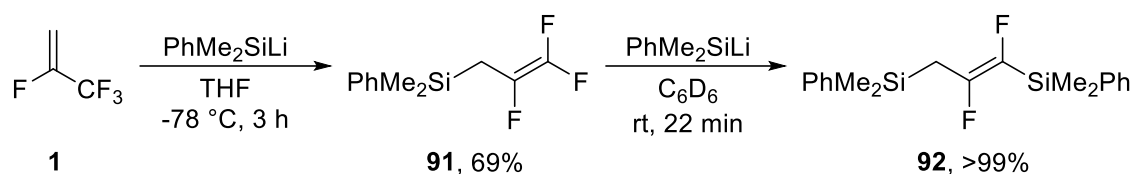
Scheme 1.33. Suzuki coupling of α -trifluoromethylvinyl boronic acid pinacol ester²⁰⁸

Ogoshi *et al.* separately reported an equivalent copper-catalysed defluorosilylation reaction with **1** to give vinyl silane **90** in 52% yield (Scheme 1.34), another potentially useful building block.²⁰⁹ The mechanism is again believed to involve formation of a copper complex *in situ*, in this case a copper-silane complex formed by transmetalation of the catalyst. This complex then adds across the carbon-carbon double bond, followed by elimination of copper fluoride to regenerate the catalyst. This elimination reaction is promoted by an F-Bpin species that is also formed *in situ*.



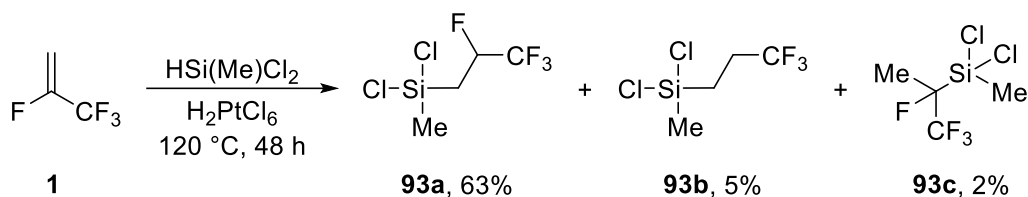
Scheme 1.34. Copper-catalysed defluorosilylation of HFO-1234yf to give a vinyl silane²⁰⁹

Crimmin *et al.* reported a different defluorosilylation reaction of **1**, in this case using a silyl lithium reagent (Scheme 1.35).²¹⁰ The use of a magnesium silyl reagent was attempted but was unsuccessful with **1** despite being reactive towards other fluoroolefins. The trifluorinated allylic silane product, **91**, undergoes a second defluorosilylation to form **92** if re-exposed to the same reaction conditions. DFT calculations suggest that the reaction proceeds via a concerted $\text{S}_{\text{N}}2'$ -type mechanism.



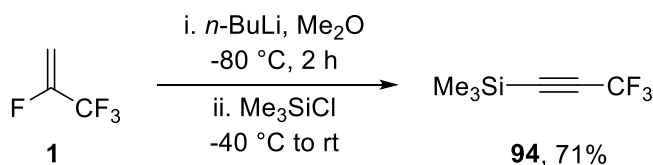
Scheme 1.35. Reaction of HFO-1234yf with a silyl lithium reagent²¹⁰

Contrasting with these defluorosilylation reactions, hydrosilylation of **1** with neat silanes was reported by Yagupolskii *et al.* (Scheme 1.36).²¹¹ Various silanes with different catalyst systems were trialled at varying temperatures and reaction times. With HSi(Me)Cl₂ and H₂PtCl₆ (Speier's Catalyst), the anti-Markovnikov addition product **93a** was favoured at 120 °C whereas the reduction product **93b** was preferred at 80 °C with small amounts of the Markovnikov product **93c** also formed. (Ph₃P)₃RhCl (Wilkinson's catalyst) gave exclusively **93b** whereas (Ph₃P)₂PdCl₂ gave very low conversion. Similar results were obtained with HSiCl₃ whilst HSiEt₃ favoured reduction over addition under all conditions.



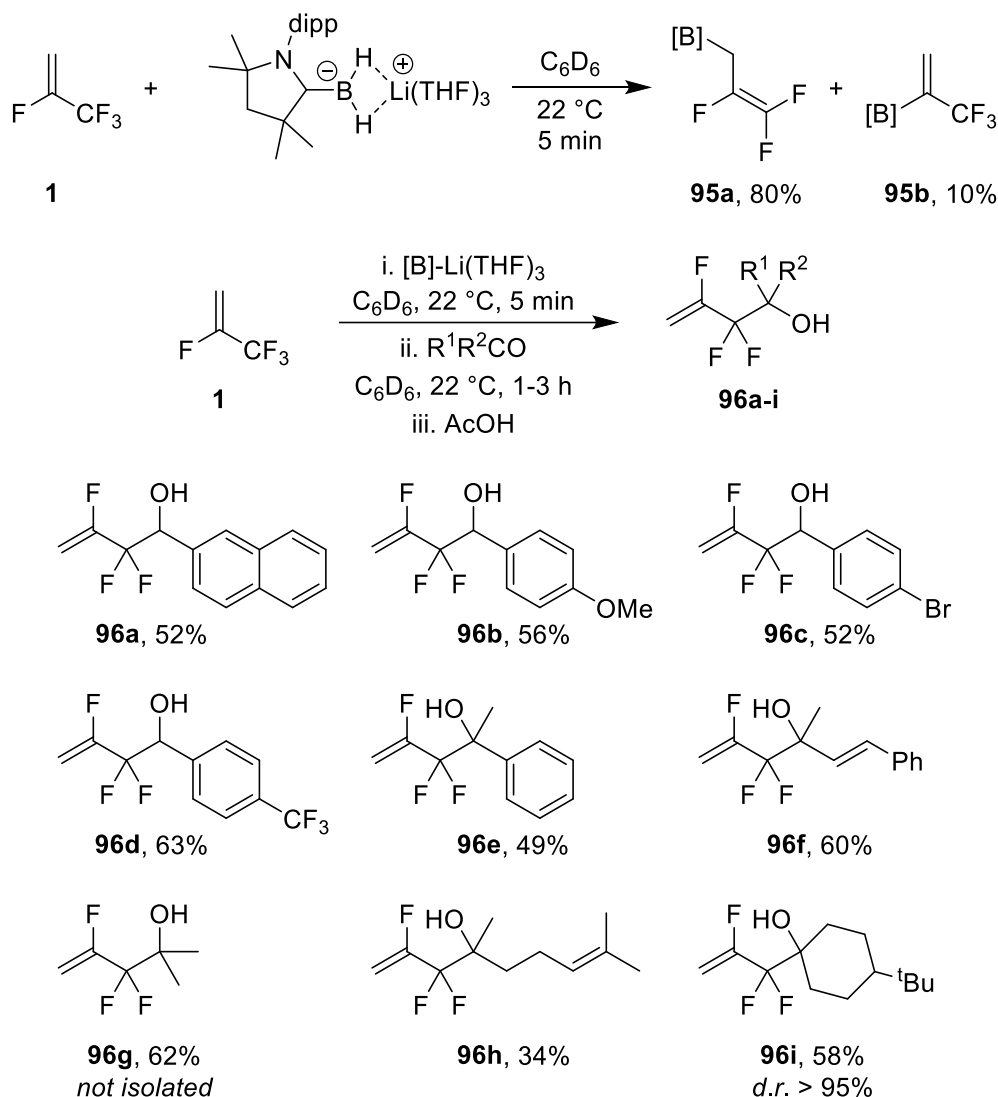
Scheme 1.36. Example hydrosilylation reaction of HFO-1234yf²¹¹

Hoge *et al.* reported another route from **1** to CF₃-substituted silanes beginning with dehydrofluorination of **1** using neat *n*-butyl lithium (Scheme 1.37).²¹² The resulting intermediate, lithium 3,3,3-trifluoropropynide, was trapped with trimethylsilylchloride and the product silane **94** isolated by distillation. Low temperature crystallographic studies demonstrated that the methyl group and the fluorine atoms were eclipsed, in contrast to CF₃SiMe₃ where they are staggered.



Scheme 1.37. Synthesis of trifluoropropynyl silane from HFO-1234yf²¹²

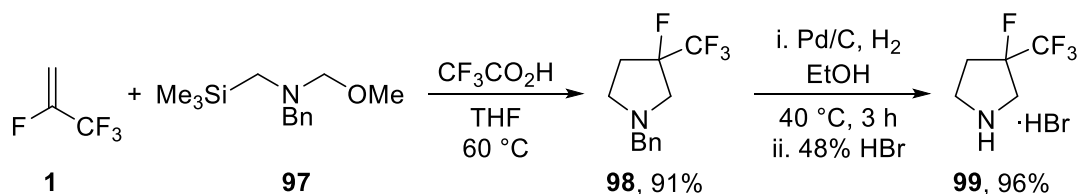
Reactions of **1** with a newly developed boron reagent were also described by Crimmin *et al.*²¹³ whereby the carbene-supported boron reagent initially attacks **1** by an S_N2' nucleophilic substitution process, as they previously reported with silicon-centered nucleophiles. The S_N2' product (**95a**) is favoured 9:1 versus the S_NV product (**95b**). The boron intermediate could not be isolated but was characterised by NMR spectroscopy and subsequently trapped with a range of different carbonyl electrophiles (**96a-i**).



Scheme 1.38. Reactivity of HFO-1234yf with a novel boron reagent²¹³

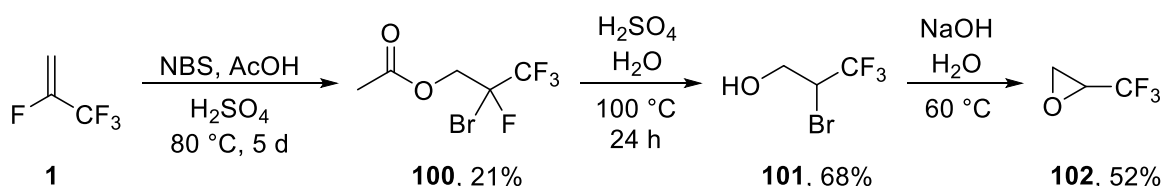
As part of a broader scope of trifluoromethyl-substituted alkenes, Meyer and El Qacemi demonstrated that **1** reacts with Achiwa's reagent (**97**) via a 1,3-dipolar cycloaddition process to form pyrrolidine **98**, which then underwent hydrogenation to the hydrobromide salt of the corresponding free amine **99** (Scheme 1.39).²¹⁴ The pK_a(H) of **98** was

determined to be 5.4, significantly lower than that of either *N*-benzylpyrrolidine ($pK_a(\text{H}) = 9.3$) or *N*-benzyl-3-trifluoromethylpyrrolidine ($pK_a(\text{H}) = 7.2$).



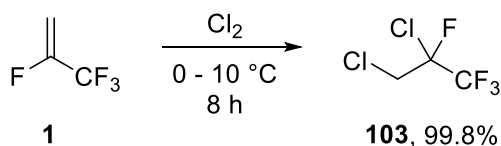
Scheme 1.39. Reaction of HFO-1234yf with Achiwa's reagent²¹⁴

A Mexichem patent described the cohalogenation of **1** with *N*-bromosuccinimide and acetic acid with sulfuric acid (Scheme 1.40).²¹⁵ The resulting ester **100** was then hydrolysed under acidic conditions to give alcohol **101**, which cyclised in the presence of strong base to give trifluoromethyl epoxide **102**. This epoxide was continuously distilled from the reaction mixture, in an overall yield of 7% from **1**. The regiochemistry of the cohalogenation observed suggests that the nucleophile adds to the least hindered carbon of the bromonium intermediate.



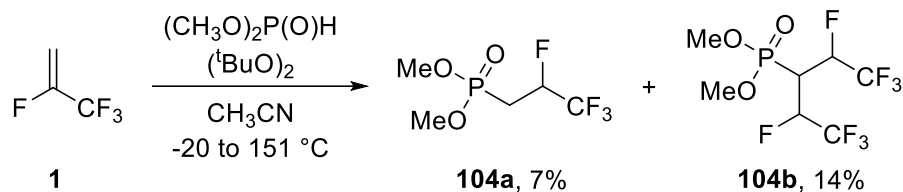
Scheme 1.40. Mexichem patented cohalogenation of HFO-1234yf leading to trifluoromethyl epoxide²¹⁵

An AGC patent reported the halogenation of **1** with elemental chlorine to give HCFC-234bb (**103**, Scheme 1.41).²¹⁶ The apparatus was irradiated with visible light and the formation of a small amount of trichlorinated side product suggests that this reaction proceeds via a radical mechanism rather than electrophilic addition.



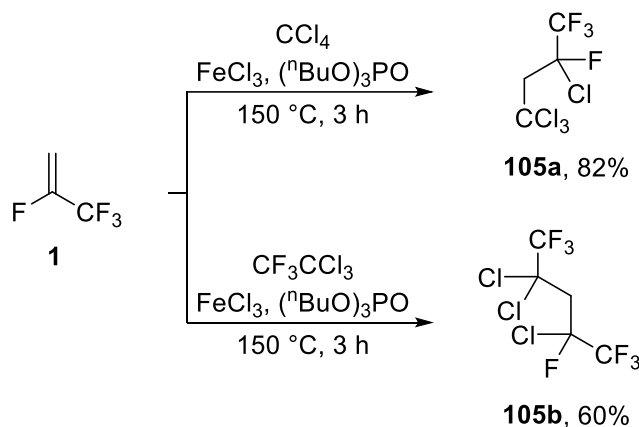
Scheme 1.41. AGC patented chlorination of HFO-1234yf²¹⁶

The French Alternative Energies and Atomic Energy Commission patented the use of **1** in a radical reaction with dimethyl phosphite, initiated by di-*tert*-butyl hydroperoxide, to give a mixture of phosphates **104a** and **104b** (Scheme 1.42).²¹⁷ The product fluoroalkyl phosphates are intended for use as additives to lithium ion batteries to prevent swelling.



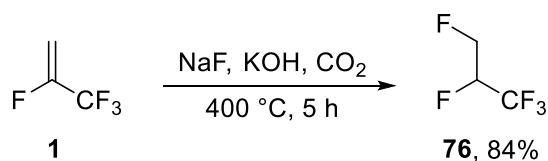
Scheme 1.42. Radical-mediated synthesis of fluorinated phosphites from HFO-1234yf²¹⁷

DuPont patented a different radical process in which iron(III) chloride and tributyl phosphate are used to synthesise CFCs **105a** and **105b** from **1** and carbon tetrachloride and trichlorotrifluoroethane (CFC-113a) respectively (Scheme 1.43).²¹⁸

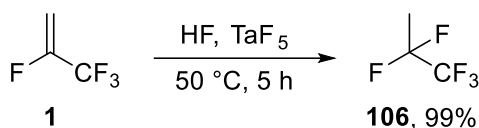


Scheme 1.43. Radical-mediated synthesis of CFCs from HFO-1234yf²¹⁸

AGC and Xi'an Modern Chemistry Research Institute patented two hydrofluorinations of **1** with differing regioselectivity. AGC used sodium fluoride at high temperatures with potassium hydroxide and carbon dioxide to give HFC-245eb (**76**, Scheme 1.44), which is an intermediate in the TFE/CHF₂ route for manufacturing **1**.²¹⁹ By contrast, Xi'an used aHF with a tantalum pentafluoride catalyst to give HFC-245cb (**106**, Scheme 1.45).²²⁰

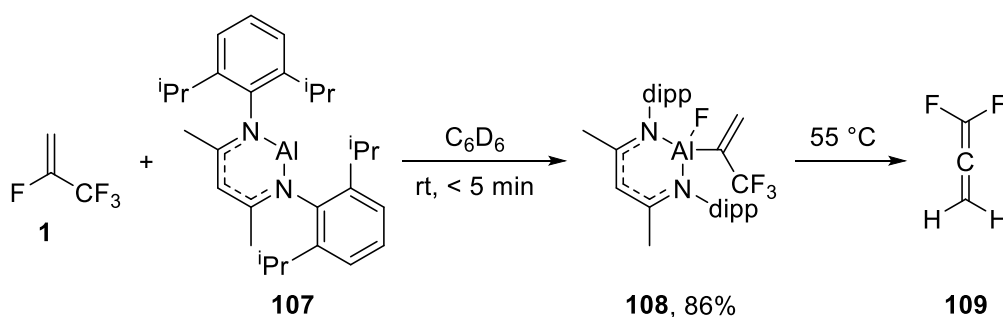


Scheme 1.44. Hydrofluorination of HFO-1234yf with sodium fluoride²¹⁹



Scheme 1.45. Hydrofluorination of HFO-1234yf with hydrogen fluoride ²²⁰

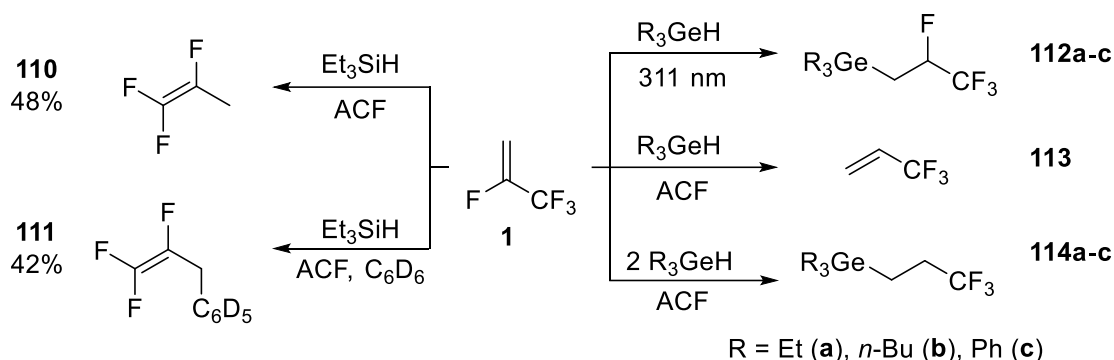
Crimmin *et al.* investigated reaction of **1** and other highly fluorinated alkenes with aluminium(I) complex **107**, shown in Scheme 1.46.²²¹ Activation of only the sp² C-F bond was observed, leading to rapid formation of fluorinated aluminium species **108** that was stable at room temperature. On heating, decomposition led to formation of 1,1-difluoroallene **109**.



Scheme 1.46. C-F activation of HFO-1234yf with an Al(I) complex and subsequent decomposition ²²¹

Braun *et al.* explored the activation of **1** by nanoscopic aluminium chlorofluoride (ACF) a high activity heterogeneous Lewis acid catalyst, an overview of which is given in Scheme 1.47 and Table 1.2.²²² Reaction of **1** and triethylsilane with ACF gives selective monodefluorination to form 1,1,2-trifluoropropene (**110**). The reaction is believed to proceed via activation of **1** to give a carbenium species with Et₃SiH then acting as a hydrogen source. With C₆D₆, a Friedel-Crafts reaction occurs following activation of the CF₃ group to give trifluoroallyl benzene **111**. No reaction was observed with Et₃GeH without photochemical activation but Et₃GeH, *n*-Bu₃GeH and Ph₃GeH were all successfully reacted under photolytic conditions to give the equivalent tetrafluoropropylgermanes **112a-c**. In the presence of ACF, these undergo an elimination reaction to form 3,3,3-trifluoropropene (**113**). However, with additional equivalents of germane, the trifluoropropylgermanes **114a-c** can then be formed by a second photochemical germylation reaction. These reactions are not observed under any conditions for the corresponding silanes and are believed to proceed via a radical pathway as no reaction occurred in the presence of radical scavenger TEMPO. Subsequently,

Braun *et al.* showed that **1** could be formed from pentafluoropropanes by either dehydrofluorination or hydrodefluorination reactions with ACF.²²³

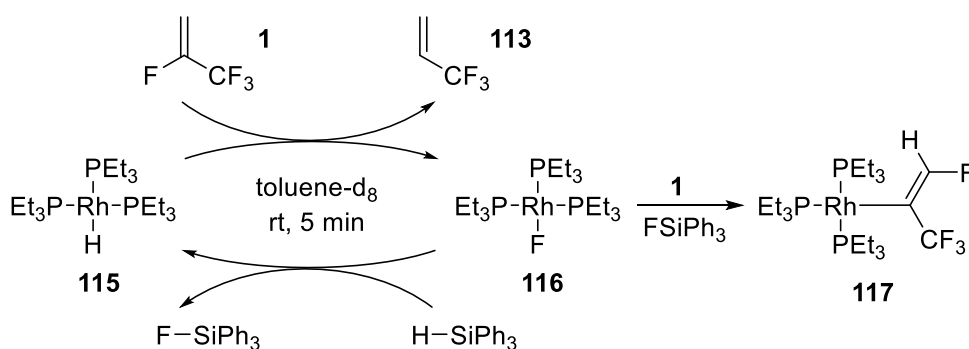


Scheme 1.47. Reactions of HFO-1234yf with triethylsilane and tertiary germanes²²²

Table 1.2. Product ratios for reactions of HFO-1234yf with tertiary germanes²²²

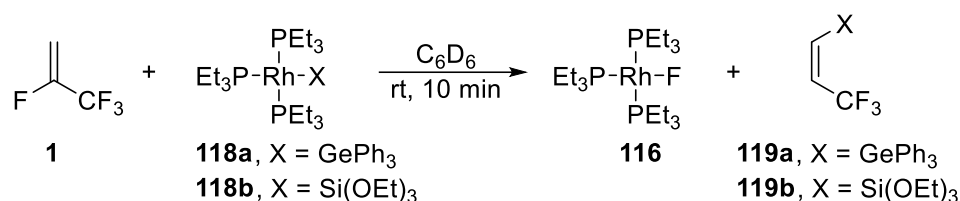
Hydride source	Equivalents R ₃ GeH	112:113:114	TON
Et ₃ GeH	1	1:20:3.5	34
Et ₃ GeH	2	1:5:86	37
ⁿ Bu ₃ GeH	1	1:4:0.8	13
ⁿ Bu ₃ GeH	2	1:0:1.6	9
Ph ₃ GeH	1	1:4:0.1	12
Ph ₃ GeH	2	1:0:3.5	11

Braun *et al.* later also reported that **1** reacts with rhodium hydride **115** at room temperature in toluene-*d*₈ to give quantitative conversion to 3,3,3-trifluoropropene (**113**) and rhodium fluoride **116**, as shown in Scheme 1.48.²²⁴ This hydrodefluorination becomes catalytic in the presence of HSiPh₃ and 5 mol-% of **115**. In the presence of FSiPh₃, C-H activation of **1** by **116** is observed with an unusual 1,2-shift of fluorine to give a polyfluorinated vinyl rhodium species **117**.



Scheme 1.48. Catalytic cycle for reaction of HFO-1234yf with Rh(H)(PEt₃)₃ (left) and structure of novel rhodium-fluoroalkene complex obtained with excess FSiPh₃ (right)²²⁴

Combining these two investigations, Braun *et al.* explored the reactivity of **1** with germyl rhodium complex **118a** (Scheme 1.49).²²⁵ This led to formation of **116** as before along with vinyl germane **119a** in exclusively the *cis* conformation. Reaction of **1** with silyl rhodium complex **118b** gave a mixture of **116** and vinyl silane **119b**, again as only the *cis* isomer. However, this mixture was unstable and **116** reacted with **119b** to form complex **117** after 18 hours. DFT calculations suggest the mechanism of these reactions proceed via coordination of **1** to the rhodium centre followed by insertion into the Rh-Ge or Rh-Si bond. Subsequent insertion and elimination of the β -hydride and β -fluoride give the stereoselectivity observed experimentally by NMR spectroscopy.



Scheme 1.49. Reaction of HFO-1234yf with germyl and silyl rhodium complexes²²⁵

1.4 Conclusions

Over the past century, organofluorine compounds have continued to grow in significance. As the most electronegative element, fluorine has a unique ability to stabilise carbanions and forms an exceptionally strong bond to carbon, leading to a range of distinctive reactivity. Introduction of fluorine into drug molecules can have a range of beneficial effects including improving bioavailability by modulating pK_a and increasing lipophilicity, blocking metabolically labile sites and altering conformational preferences to strengthen binding. Trifluoromethyl groups are a common fluorinated moiety in pharmaceuticals but the synthesis of such compounds requires either the use of CF₃-containing building blocks or late-stage trifluoromethylation by sometimes expensive and inefficient reagents. Industrially, CF₃-bearing building blocks are preferred due to their low cost and simplicity but these are generally limited to aryl CF₃ systems or trifluoroacetic acid derivatives.

One of the main uses of organofluorine compounds continues to be as refrigerants. With the phasing out of HFCs, the hydrofluoroolefins (HFOs) have emerged as the main class of 4th generation refrigerants. 2,3,3,3-Tetrafluoropropene (HFO-1234yf) is the leading

candidate to replace 1,1,1,2-tetrafluoroethane (HFC-134a) in air conditioning units, showing similar refrigerant performance and lack of toxicity or flammability but with a 99.7% reduction in global warming potential compared to HFC-134a. HFO-1234yf is now manufactured on a multi-tonne scale, with the majority being synthesised from either tetrafluoroethylene (TFE) or 1,1,2,3-tetrachloropropene (HCFC-1230xa). However, despite its increasing availability and decreasing cost, HFO-1234yf has yet to be employed as a building block in organic synthesis on any significant scale in academia or industry. Heck coupling, nucleophilic substitution, copper-catalysed borylation and silylation reactions and a range of organometallic chemistry have been reported but, so far, much synthetic chemistry of HFO-1234yf remains unexplored.

1.5 References for Chapter 1

- ¹ L. Pauling, *The Nature of the Chemical Bond and the Structure of Molecules and Crystals: An Introduction to Modern Structural Chemistry*, Cornell University Press, Ithaca, NY, 1939.
- ² C. Abia, K. Cunha, S. Cristallo and P. de Laverny, *Astron. Astrophys.*, 2015, **581**, A88.
- ³ A. Harsanyi and G. Sandford, *Green Chem.*, 2015, **17**, 2081.
- ⁴ J. Kolb, J. K. Keiding, A. Steinfeld, K. Secher, N. Keulen, D. Rosa and B. M. Stensgaard, *Ore Geol. Rev.*, 2016, **78**, 493.
- ⁵ G. Agricola, *De Re Metallica*, 1529, translated from Latin by H. Hoover and L. H. Hoover, The Mining Magazine, London, 1912.
- ⁶ N. N. Greenwood and A. Earnshaw, *Chemistry of the Elements*, Butterworth-Heinemann, Oxford, 2nd edition, 1988.
- ⁷ A.-M. Ampère, *Ann. Chim. Phys.*, 1816, **2**, 1.
- ⁸ R. E. Banks, *J. Fluorine Chem.*, 1986, **33**, 3.
- ⁹ H. Moissan, *C. R. Acad. Sci.*, 1886, **102**, 1543.
- ¹⁰ J. F. Ellis and G. F. May, *J. Fluorine Chem.*, 1986, **33**, 133.
- ¹¹ D. B. Harper and D. O'Hagan, *Nat. Prod. Rep.*, 1994, **11**, 123.
- ¹² J. C. S. Marais, *Onderstepoor J. Vet. Sci. Animal Ind.*, 1943, **18**, 230.
- ¹³ R. A. Peters and M. Shorthouse, *Phytochemistry*, 1972, **11**, 1337.
- ¹⁴ D. O'Hagan and D. B. Harper, *J. Fluorine Chem.*, 1999, **100**, 127.
- ¹⁵ D. O'Hagan, C. Schaffrath, S. L. Cobb, J. T. G. Hamilton and C. D. Murphy, *Nature*, 2002, **416**, 279.
- ¹⁶ P. Kirsch, *Modern fluoroorganic chemistry: synthesis, reactivity, applications*, Wiley-VCH, Weinheim, 2004.
- ¹⁷ T. Okazoe, *Proc. Jap. Acad. Ser. B*, 2009, **85**, 276.
- ¹⁸ J. Fried and E. F. Sabo, *J. Am. Chem. Soc.*, 1954, **76**, 1455.
- ¹⁹ C. Heidelberger, N. K. Chaudhuri, P. Danneberg, D. Mooren, L. Griesbach, R. Duschinsky and R. J. Schnitzer, *Nature*, 1957, **179**, 663.
- ²⁰ A. M. Thayer, *Chem. Eng. News*, 2009, **84**, 15.
- ²¹ H. Mei, J. Han, S. Fustero, M. Medio-Simon, D. M. Sedgwick, C. Santi, R. Ruzziconi and V. A. Soloshonok, *Chem. Eur. J.*, 2019, **25**, 11797.

- ²² H. Mei, A. M. Remete, Y. Zou, H. Moriwaki, S. Fustero, L. Kiss, V. A. Soloshonok and J. Han, *Chin. Chem. Lett.*, 2020, **31**, 2401.
- ²³ A. Mullard, *Nat. Rev. Drug. Discov.*, 2021, **20**, 85.
- ²⁴ S. Lam, A. Lombardi and A. Ouanounou, *Eur. J. Pharmacol.*, 2020, **886**, 173451.
- ²⁵ M. J. Welch and C. S. Redvanly, *Handbook of Radio-pharmaceuticals, Radiochemistry and Applications*, John Wiley and Sons Ltd, Hoboken, NJ, 2003.
- ²⁶ C. Dalvit, *Prog. Nucl. Magn. Reson. Spectrosc.*, 2007, **51**, 243.
- ²⁷ J. Gabriel, T. Miller, M. Wolfson and T. Shaffer, *ASAIJ*, 1996, **42**, 968.
- ²⁸ D. O'Hagan, *Chem. Soc. Rev.*, 2008, **37**, 308.
- ²⁹ K. B. Wiberg and P. R. Rablen, *J. Am. Chem. Soc.*, 1993, **115**, 614.
- ³⁰ H. Plenio, *ChemBioChem*, 2004, **5**, 650.
- ³¹ J. D. Dunitz and R. Taylor, *Chem. Eur. J.*, 1997, **3**, 89.
- ³² K. B. Wiberg and P. R. Rablen, *J. Org. Chem.*, 1998, **63**, 3722.
- ³³ T. X. Carroll, T. D. Thomas, H. Bergersen, K. J. Borge and L. J. Sæthre, *J. Org. Chem.*, 2006, **71**, 1961.
- ³⁴ W. R. Dolbier, A. C. Alty and O. Phansteil, *J. Am. Chem. Soc.*, 1987, **109**, 3046.
- ³⁵ M. L. Trapp, J. K. Watts, N. Weinberg and B. M. Pinto, *Can. J. Chem.*, 2006, **84**, 692.
- ³⁶ L. Goodman, H. Gu and V. Pophristic, *J. Phys. Chem. A*, 2005, **109**, 1223.
- ³⁷ K. B. Wiberg, M. A. Murcko, K. E. Laidig and P. J. MacDougall, *J. Phys. Chem.*, 1990, **94**, 6956.
- ³⁸ D. Wu, A. Tian and H. Sun, *J. Phys. Chem. A*, 1998, **102**, 9901.
- ³⁹ D. J. Tozer, *Chem. Phys. Lett.*, 1999, **308**, 160.
- ⁴⁰ G. Sandford, *Phil. Trans. R. Soc. Lond. A*, 2000, **358**, 455.
- ⁴¹ J. Clayden, N. Greeves and S. Warren, *Organic Chemistry*, OUP, Oxford, 2nd edition, 2012.
- ⁴² R. D. Chambers, *Fluorine in Organic Chemistry*, Blackwell Publishing, Oxford, 2004.
- ⁴³ D. A. Dixon, T. Fukunaga and B. E. Smart, *J. Am. Chem. Soc.*, 1986, **108**, 4027.
- ⁴⁴ M. W. Cartwright, E. L. Parks, G. Pattison, R. Slater, G. Sandford, I. Wilson, D. S. Yufit, J. A. K. Howard, J. A. Christopher and D. D. Miller, *Tetrahedron*, 2010, **66**, 3222.
- ⁴⁵ (a) N. T. Anh and O. Eisenstein, *Nouv. J. Chim.*, 1977, **1**, 61; (b) R. E. Rosenberg, R. L. Abel, M. D. Drake, D. J. Fox, A. K. Ignatz, D. M. Kwiat, K. M. Schaal and P. R. Virkler, *J. Org. Chem.*, 2001, **66**, 1694.
- ⁴⁶ A. Bondi, *J. Phys. Chem.*, 1964, **68**, 441.
- ⁴⁷ P.-Y. Lien, R.-M. You and W.-P. Hu, *J. Phys. Chem. A*, 2001, **105**, 2391.
- ⁴⁸ R. J. Gillespie and E. A. Robinson, *Chem. Soc. Rev.*, 2005, **34**, 396.
- ⁴⁹ K. Müller, C. Faeh and F. Diederich, *Science*, 2007, **317**, 1881.
- ⁵⁰ Crain's New York Business, *Lipitor becomes world's top-selling drug*, 2011, Associated Press, New York, NY.
- ⁵¹ M. I. Anderson and A. P. MacGowan, *J. Antimicrob. Chemother.*, 2003, **51**, 1.
- ⁵² D. A. Smith, H. van de Waterbeemd and D. K. Walker, *Methods and Principles in Medicinal Chemistry, vol. 31: Pharmacokinetics and Metabolism in Drug Design*, 2006, Wiley-VCH, Weinheim.
- ⁵³ V. Spahn, G. Del Vecchio, D. Labuz, A. Rodriguez-Gaztelumendi, N. Massaly, J. Temp, V. Durmaz, P. Sabri, M. Reidelbach, H. Machelska, M. Weber and C. Stein, *Science*, 2017, **355**, 966.
- ⁵⁴ B. E. Smart, *J. Fluorine Chem.*, 2001, **109**, 3.
- ⁵⁵ J. Qiu, S. H. Stevenson, M. J. O'Beirn and R. B. Silverman, *J. Med. Chem.*, 1999, **42**, 329.

- ⁵⁶ S. Purser, P. R. Moore, S. Swallow and V. Gouverneur, *Chem. Soc. Rev.*, 2008, **37**, 320.
- ⁵⁷ S. B. Rosenblum, T. Huynh, A. Afonso, H. R. Davis, Jr., N. Yumibe, J. W. Clader and D. A. Burnett, *J. Med. Chem.*, 1998, **41**, 973.
- ⁵⁸ S. K. Teo, W. A. Colburn, W. G. Tracewell, K. A. Kook, D. I. Stirling, M. S. Jaworsky, M. A. Scheffler, S. D. Thomas and O. L. Laskin, *Clin Pharmacokinet.*, 2004, **43**, 311.
- ⁵⁹ Y. Takeuchi, T. Shiragami, K. Kimura, E. Suzuki and N. Shibata, *Org. Lett.*, 1999, **1**, 1571.
- ⁶⁰ Y. Pan, *ACS Med. Chem. Lett.*, 2019, **10**, 1016.
- ⁶¹ M. Mandal, K. Mitra, D. Grotz, X. Lin, J. Palamanda, P. Kumari, A. Buevich, J. P. Caldwell, X. Chen, K. Cox, L. Favreau, L. Hyde, M. E. Kennedy, R. Kuvelkar, X. Liu, R. D. Mazzola, E. Parker, D. Rindgen, E. Sherer, H. Wang, Z. Zhu, A. W. Stamford and J. N. Cumming, *J. Med. Chem.*, 2018, **61**, 10700.
- ⁶² D. L. Corina, S. L. Miller, J. N Wright and M. Akhtar, *J. Chem. Soc. Chem. Commun.*, 1991, 782.
- ⁶³ J. P. Burkhardt, P. M. Weintraub, C. A. Gates, R. J. Resvick, R. J. Vaz, D. Friedrich, M. R. Angelastro, P. Bey and N. P. Peet, *Bioor. Med. Chem.*, 2002, **10**, 929.
- ⁶⁴ N. A. Meanwell, *J. Med. Chem.*, 2018, **61**, 5822.
- ⁶⁵ Y. Lou, X. H. A. Kuglstatler, R. K. Kondru, Z. K. Sweeney, M. Soth, J. McIntosh, R. Litman, J. Suh, B. Kocer, D. Davis, J. Park, S. Frauchiger, N. Dewdney, H. Zecic, J. P. Taygerly, K. Sarma, J. Hong, R. J. Hill, T. Gabriel, D. M. Goldstein and T. D. Owens, *J. Med. Chem.*, 2015, **58**, 512.
- ⁶⁶ D. Badone, G. Jommi, R. Pagliarin and P. Tavecchia, *Synthesis-Stuttgart*, 1987, **10**, 920.
- ⁶⁷ J. A. Wilkinson, *Chem. Rev.*, 1992, **92**, 505.
- ⁶⁸ W. R. Dolbier, *J. Fluorine Chem.*, 2005, **126**, 157.
- ⁶⁹ B. Langlois, L. Gilbert and G. Forat, *Ind. Chem. Libr.*, 1992, **8**, 244.
- ⁷⁰ G. A. Olah, J. T. Welch, Y. D. Vankar, M. Nojima, I. Kerekes and J. A. Olah, *J. Org. Chem.*, 1972, **44**, 3872.
- ⁷¹ R. Franz, *J. Fluorine Chem.*, 1980, **15**, 423.
- ⁷² G. Balz and G. Schiemann, *Chem. Ber.*, 1927, **5**, 1186.
- ⁷³ G. Sandford, *Fluoroarenes in Science of Synthesis, Houben-Weyl Methods of Molecular Transformations, Volume 31a: Compounds with Two Carbon-Heteroatom Bonds*, ed. C. A. Ramsden, Thieme, Stuttgart, 2007.
- ⁷⁴ K. Uneyama, *Organofluorine Chemistry*, 2006, Blackwell Publishing Ltd., Oxford.
- ⁷⁵ C. W. Tullock, F. S. Fawcett, W. C. Smith and D. D. Coffman, *J. Am. Chem. Soc.*, 1960, **82**, 539.
- ⁷⁶ W. J. Middleton, *J. Org. Chem.*, 1975, **40**, 574.
- ⁷⁷ G. S. Lal, G. P. Pez, R. J. Pesaresi, F. M. Prozonc and H. Cheng, *J. Org. Chem.*, 1999, **64**, 7048.
- ⁷⁸ A. Takaoka, H. Iwakiri and N. Ishikawa, *Bull. Chem. Soc. Japan*, 1979, **52**, 3377.
- ⁷⁹ R. D. Chambers, G. Sandford, J. Trmcic and T. Okazoe, *Org. Process Res. Dev.*, 2008, **12**, 339.
- ⁸⁰ A. Harsanyi and G. Sandford, *Green Chem.*, 2015, **17**, 3000.
- ⁸¹ A. Harsanyi, A. Conte, L. Pichon, A. Rabion, S. Grenier and G. Sandford, *Org. Process Res. Dev.*, 2017, **21**, 273.
- ⁸² M. A. Tius, *Tetrahedron*, 1995, **51**, 6605.
- ⁸³ S. Rozen, O. Lerman, M. Kol, *J. Chem. Soc. Chem. Commun.*, 1981, **10**, 443.

- ⁸⁴ J. Badoux and D. Cahard, *Org. React.* 2007, **69**, 347.
- ⁸⁵ R. E. Banks, S. N. Mohialdin-Khaffaf, G. S. Lal, I. Sharif and R. G. Syvret, *J. Chem. Soc. Chem. Commun.*, 1992, **8**, 595.
- ⁸⁶ E. Differding and H. Ofner, *Synlett*, 1991, **3**, 187.
- ⁸⁷ T. Umemoto and K. Tomita, *Tetrahedron Lett.*, 1986, **27**, 3271.
- ⁸⁸ N. Rozatian, I. W. Ashworth, G. Sandford and D. R. W. Hodgson, *Chem. Sci.*, 2018, **9**, 8692.
- ⁸⁹ S. Caron, *Org. Proc. Res. Dev.*, 2020, **24**, 470.
- ⁹⁰ J. E. True, T. Darrah Thomas, R. W. Winter and G. L. Gard, *Inorg. Chem.*, 2003, **42**, 4437.
- ⁹¹ S. R. Walker, *Trends and Changes in Drug Research and Development*, Springer Science and Business Media, Berlin, 2012.
- ⁹² E. M. Sakai, L. A. Connolly and J. A. Klauck, *Pharmacotherapy*, 2005, **25**, 1773.
- ⁹³ M. Inoue, Y. Sumii and N. Shibata, *ACS Omega*, 2020, **5**, 10633.
- ⁹⁴ D. T. Wong, F. P. Bymaster and E. A. Engleman, *Life Sci.*, 1995, **57**, 411.
- ⁹⁵ D. L. Roman, C. C. Walline, G. J. Rodriguez and E. L. Barker, *Eur. J. Pharmacol.*, 2003, **479**, 53.
- ⁹⁶ T. D. Penning, J. J. Talley, S. R. Bertenshaw, J. S. Carter, P. W. Collins, S. Docter, M. J. Graneto, L. F. Lee, J. W. Malecha, J. M. Miyashiro, R. S. Rogers, D. J. Rogier, S. S. Yu, G. D. Anderson, E. G. Burton, J. N. Cogburn, S. A. Gregory, C. M. Koboldt, W. E. Perkins, K. Seibert, A. W. Veenhuizen, Y. Y. Zhang and P. C. Isakso, *J. Med. Chem.*, 1997, **40**, 1347.
- ⁹⁷ S. R. Rabel, S. Sun and M. B. Maurin, *AAPS PharmSci*, 2001, **3**, 1.
- ⁹⁸ F. J. E. Swarts, *Acad. Roy. Belg.*, 1892, **3**, 474.
- ⁹⁹ R. E. Banks, *Organofluorine Chemicals and their Industrial Applications*, 1979, Ellis Horwood Ltd., Chichester.
- ¹⁰⁰ M. Schlosser, *Angew. Chem. Int. Ed.*, 2006, **45**, 5432.
- ¹⁰¹ W. Dmowski and A. Kolinski, *Pol. J. Chem.*, 1978, **52**, 547.
- ¹⁰² S. E. López and J. Salazar, *J. Fluorine Chem.*, 2013, **156**, 73.
- ¹⁰³ G. Siegemund, W. Schwertfeger, A. Feiring, B. Smart, F. Behr, H. Vogel and B. McKusick, *Fluorine Compounds, Organic in Ullmann's Encyclopedia of Industrial Chemistry*, ed. B. Elvers, 2005, Wiley-VCH, Weinheim.
- ¹⁰⁴ M. Braun, W. Rudolph and K. Eichholz, EP 659729, 1995.
- ¹⁰⁵ H. S. Tung and R. S. Wedinger, WO 0206194, 2002.
- ¹⁰⁶ M. Braun and J. Eicher, *The Fluorine Atom in Health Care and Agrochemical Applications: A Contribution to Life Science*, in *Modern Synthesis Processes and Reactivity of Fluorinated Compounds*, eds. H. Groult, F. Leroux and A. Tressaud, Elsevier, Amsterdam, 2016.
- ¹⁰⁷ V. Dambrin and D. Revelant, US201908492A1, 2019.
- ¹⁰⁸ B. Simoneau, US 028807, 2002.
- ¹⁰⁹ Y. Xiao, J. D. Armstrong III, S. W. Krska, E. Njolito, N. R. Rivera, Y. Sun and T. Rosner, EP1606243A1, 2008.
- ¹¹⁰ B. Folléas, I. Marek, J.-F. Normant and L. S. Jalmes, *Tetrahedron Lett.*, 1998, **39**, 2973.
- ¹¹¹ A. Zanardi, M. A. Novikov, E. Martin, J. Benet-Buchholz and V. V. Grushin, *J. Am. Chem. Soc.*, 2011, **133**, 20901.
- ¹¹² I. Ruppert, K. Schlich and W. Volbach, *Tetrahedron Lett.*, 1984, **25**, 2195.
- ¹¹³ P. Ramaiah, R. Krishnamurti and G. K. S. Prakash, *Org. Synth.*, 1995, **72**, 232.

- ¹¹⁴ A. Kolomeitsev, E. Rusanov, G. Bissky, E. Lork, G.-V. Röschenhaler and P. Kirsch, *Chem. Commun.*, 1999, 1017.
- ¹¹⁵ G. K. S. Prakash and A. K. Yedin, 1997, *Chem. Rev.*, **97**, 757.
- ¹¹⁶ X. Liu, C. Xu, M. Wang and Q. Liu, *Chem. Rev.*, 2015, **115**, 683.
- ¹¹⁷ Y. Qiao, L. Zhu, B. R. Ambler and Ryan A. Altman, *Curr. Top. Med. Chem.*, 2014, **14**, 966.
- ¹¹⁸ W. Xu and W. R. Dolbier, *J. Org. Chem.*, 2005, **70**, 4741.
- ¹¹⁹ G. K. S. Prakash, J. Hu and G. A. Olah, *Org. Lett.*, 2003, **5**, 3253.
- ¹²⁰ T. Umemoto, *Chem. Rev.*, 1996, **96**, 1757.
- ¹²¹ P. Eisenberger, S. Gischig and A. Togni, *Chem - Eur. J.*, 2006, **12**, 2579.
- ¹²² R. N. Haszeldine, *J. Chem. Soc.*, 1949, 2856.
- ¹²³ B. R. Langlois, E. Laurent and N. Roidot, *Tetrahedron Lett.*, 1991, **32**, 7525.
- ¹²⁴ D. A. Nagib and D. W. C. MacMillan, *Nature*, 2011, **480**, 224.
- ¹²⁵ V. C. R. McLoughlin and J. Thrower, *Tetrahedron*, 1969, **25**, 5921.
- ¹²⁶ O. A. Tomashenko and V. V. Grushin, *Chem. Rev.*, 2011, **111**, 4475.
- ¹²⁷ J.-A. Ma and D. Cahard, *J. Fluorine Chem.*, 2007, **128**, 975.
- ¹²⁸ T. Liang, C. N. Neumann and T. Ritter, *Angew. Chem. Int. Ed.*, 2013, **52**, 8214.
- ¹²⁹ W. Zhu, J. Wang, S. Wang, Z. Gu, J. L. Aceña, K. Izawa, H. Liu and V. A. Soloshonok, *J. Fluorine Chem.*, 2014, **167**, 37.
- ¹³⁰ C. Alonso, E. M. de Martigorta, G. Rubiales and F. Palacios, *Chem. Rev.*, 2015, **115**, 1847.
- ¹³¹ A. J. Sicard and R. T. Baker, *Chem. Rev.*, 2020, **120**, 9164.
- ¹³² I. Dincer, *Refrigeration Systems and Applications*, John Wiley and Sons Ltd., Hoboken, NJ, 2003.
- ¹³³ S. Turns, *Thermodynamics: Concepts and Applications*, Cambridge University Press, Cambridge, 2006.
- ¹³⁴ R. Stokes, *Building Upon Air: A History of the International Industrial Gases Industry from the 19th to the 21st Centuries*, Cambridge University Press, Cambridge, 2015.
- ¹³⁵ G. B. Kauffman, *J. Chem. Educ.*, 1955, **32**, 301.
- ¹³⁶ T. Midgley and A. L. Henne, *Ind. Eng. Chem.*, 1930, **22**, 542.
- ¹³⁷ M. J. Molina and F. S. Rowland, *Nature*, 1974, **249**, 810.
- ¹³⁸ J. C. Farman, B. G. Gardiner and J. D. Shanklin, *Nature*, 1985, **315**, 207.
- ¹³⁹ R. Stolarski, R. Bojkov, L. Bishop, C. Zerefos, J. Staehelin and J. Zawodny, *Science*, 1992, **256**, 342.
- ¹⁴⁰ E. Parson, *Protecting the Ozone Layer: Science and Strategy*, Oxford University Press, Oxford, 2003.
- ¹⁴¹ Official Journal of the European Union, Directive 200640EC of the European Parliament and of the Council, 2006.
- ¹⁴² E. Granryd, *Int. J. Refrig.*, 2001, **24**, 15.
- ¹⁴³ D. Sánchez, J. Patiño, C. Sanz-Kock, R. Llopis, R. Cabello and E. Torrell, *Appl. Therm. Eng.*, 2014, **66**, 227.
- ¹⁴⁴ U. K. Deiters, *Fluid Phase Equilib.*, 1997, **132**, 265.
- ¹⁴⁵ *Industrial Syntheses of Hydrohaloolefins and Related Products*, M. Nappa, S. Peng and X. Sun, in *Modern Synthesis Processes and Reactivity of Fluorinated Compounds*, eds. H. Groult, F. Leroux and A. Tressaud, Elsevier, Amsterdam, 2016.
- ¹⁴⁶ Y. Lee and D. Jung, *Appl. Therm. Eng.*, 2012, **35**, 240.

- ¹⁴⁷ C. Zilio, S. S. Brown and A. Cavallini, presented in part at the 3rd Conference on Thermophysical Properties and Transfer Processes of Refrigeration, Boulder, CO, June 2009.
- ¹⁴⁸ B. H. Minor and M. Spatz, presented in part at the International Refrigeration and Air Conditioning Conference, Purdue, IN, July 2008.
- ¹⁴⁹ M. Spatz and B. H. Minor, presented in part at the SAE World Congress, Detroit, MI, April 2008.
- ¹⁵⁰ (a) P. Schuster, R. Bertermann, T. A. Snow, X. Han, G. M. Rusch, G. W. Jepson and W. Dekant, *Toxicol. Appl. Pharmacol.*, 2008, **233**, 323; (b) P. Schuster, R. Bertermann, G. M. Rusch and W. Dekant, *Toxicol. Appl. Pharmacol.*, 2020, **244**, 247; (c) T. Schmidt, R. Bertermann, G. M. Rusch, G. M. Hoffman and W. Dekant, *Toxicol. Appl. Pharmacol.*, 2012 **263**, 32.
- ¹⁵¹ K. Takizawa, K. Tokuhashi and S. Kondo, *J. Hazard. Mater.*, 2009, **172**, 1329.
- ¹⁵² B. H. Minor, D. Herrmann and R. Gravell, *Process Saf. Prog.*, **29**, 2010.
- ¹⁵³ V. C. Papadimitriou, R. K. Talukdar, R. W. Portmann, A. R. Ravishankar and J. B. Burkholder, *Phys. Chem. Chem. Phys.*, 2008, **10**, 808.
- ¹⁵⁴ P. M. de F. Forster, J.B. Burkholder, C. Clerbaux, P.F. Coheur, M. Dutta, L.K. Gohar, M.D. Hurley, G. Myhre, R.W. Portmann, K.P. Shine, T.J. Wallington and D. Wuebbles, *J. Quant. Spectrosc. Radiat. Transfer*, 2005, **93**, 447.
- ¹⁵⁵ M.D. Hurley, T.J. Wallington, M.S. Javadi and O.J. Nielsen, *Chem. Phys. Lett.*, 2008, **450**, 263.
- ¹⁵⁶ O. J. Nielsen, M. S. Javadi, M. P. Sulbaek Andersen, M. D. Hurley, T. J. Wallington and R. Singh, *Chem. Phys. Lett.*, 2007, **439**, 18.
- ¹⁵⁷ T.J. Wallington, W.F. Schneider, D.R. Worsnop, O.J. Nielsen, J. Sehested, W. DeBruyn and J.A. Shorter, *Environ. Sci. Technol.*, 1998, **28**, 320.
- ¹⁵⁸ S. Henne, D. E. Shallcross, S. Reimann, P. Xiao, D. Brunner, S. O'Doherty and B. Buchmann, *Environ. Sci. Technol.*, 2012, **46**, 1650.
- ¹⁵⁹ V. C. Papadimitriou, Y. G. Lazarou, R.K. Talukdar and J. B. Burkholder, *J. Phys. Chem. A*, 2011, **115**, 167.
- ¹⁶⁰ World Meteorological Organization, *Scientific Assessment of Ozone Depletion: 2010, Global Ozone Research and Monitoring Project – Report No. 50*, 2011, Geneva, Switzerland.
- ¹⁶¹ Ø. Hodnebrog, M. Etminan, J. S. Fuglestedt, G. Marston, G. Myhre, C. J. Nielsen, K. P. Shine and T. J. Wallington, *Rev. Geophys.*, 2013, **51**, 300.
- ¹⁶² A. L. Henne and T. P. Waalkes, *J. Am. Chem. Soc.*, 1946, **68**, 496.
- ¹⁶³ R. N. Haszeldine and B. R. Steele, *J. Chem. Soc.*, 1957, 2193.
- ¹⁶⁴ R. N. Haszeldine, D. W. Keene and A. E. Tipping, *J. Chem. Soc.*, 1970, 414.
- ¹⁶⁵ L. S. German, A. V. Podolskii and I. L. Knunyants, *Doklady Akademii Nauk SSSR*, 1967, **173**, 1328.
- ¹⁶⁶ I. V. Stepanov, A. I. Burmakov, B. V. Kunshenko, L. A. Alekseeva and L. M. Yagupolskii, *Zhurnal Organicheskoi Khimii*, 1983, **19**, 273.
- ¹⁶⁷ R. E. Banks, M. G. Barlow and M. Nickkho-Amiry, *J. Fluorine Chem.*, 1997, **82**, 171.
- ¹⁶⁸ (a) M. R. Joyce Jr., US 2462402, 1946; (b) D. D. Coffman, R. Cramer and G. W. Rigby, *J. Am. Chem. Soc.*, 1949, **71**, 979; (c) S. Morikawa, S. Samejima, K. Ohnishi, H. Okamoto, Y. Ohmori and T. Tanuma, WO 9101287, 1991.
- ¹⁶⁹ (a) M. Nose, D. Karube, A. Sugiyama, T. Shibanuma and T. Chaki, WO 2010013795, 2010; (b) Y. Shiotani, K. Hanabusa, T. Chaki and K. Takahashi, WO 2011122157, 2011.

- ¹⁷⁰ (a) M. R. Joyce Jr., US 2462402, 1949; (b) K. Ohnishi, H. Okamoto, T. Tanuma, K. Yanase, T. Kawasaki and R. Takei, WO 9108183, 1991; (c) H. Aoyama, T. Yasuhara, S. Kono, S. Koyama and S. Ueda, EP 492527, 1992; (d) T. Tanuma, H. Okamoto, K. Ohnishi and S. Morikawa, *Appl. Catal. A General*, 2008, **348**, 236.
- ¹⁷¹ H. Okamoto and Y. Sasao, WO20100742545 A1, 2010.
- ¹⁷² V. N. M. Rao and A. C. Sievert, WO2008060614 A2, 2008.
- ¹⁷³ G. G. Belen'kii, V. A. Petrov and P. R. Resnick, *J. Fluorine Chem.*, 2001, **108**, 15.
- ¹⁷⁴ A. C. Sievert, M. J. Nappa and B. A. Mahler, WO2008030441 A1, 2008.
- ¹⁷⁵ I. L. Knunyants, M. P. Krasuskaya and E. I. Mysov, *Bull. Acad. Sci. USSR, Div. Chem. Sci.*, 1960, **9**, 1312.
- ¹⁷⁶ V. N. M. Rao, A. C. Sievert and M. J. Nappa, WO2008030440 A2, 2008.
- ¹⁷⁷ S. Mukhopadhyay, H. K. Nair, H. S. Tung, M. van der Puy, D. C. Merkel, R. K. Dubey and J. J. Ma, US20070112230, 2007.
- ¹⁷⁸ G. R. Cook, H. Kopkalli, S. Cottrell, Y. Chiu, P. Scheidle and D. C. Merkel, US20110269999 A1, 2011.
- ¹⁷⁹ R. Banavali, H. K. Nair and Y. Zhai, US 9790151 B2, 2017.
- ¹⁸⁰ (a) N. O. Andrella, N. Xu, B. M. Gabidullin, C. Ehm and R. T. Baker, *J. Am. Chem. Soc.*, 2019, **141**, 11506; (b) R. T. Baker and N. O. Andrella, WO 2018039794 A1, 2018.
- ¹⁸¹ (a) N. A. Phillips, A. J. P. White and M. R. Crimmin, *Adv. Synth. Catal.*, 2019, **361**, 3351; (b) M. R. Crimmin and N. A. Phillips, WO2020002932 A1, 2020.
- ¹⁸² D. Sherry, M. Nolan, S. Seidel and S. O. Andersen, *HFO-1234yf: An Examination of Projected Long-Term Costs of Production*, 2017, Centre for Climate and Energy Solutions, Arlington, VA.
- ¹⁸³ D. C. Merkel and H. S. Tung, WO2009015317 A1, 2009.
- ¹⁸⁴ M. J. Nappa, A. Jackson and D. C. Merkel, WO2013071024 A1, 2013.
- ¹⁸⁵ W. Mao, Y. Bai, W. Wang, B. Wang, Q. Xu, L. Shi, C. Li and J. Lu, *ChemCatChem*, 2017, **9** (5), 824-832.
- ¹⁸⁶ M. J. Nappa, US20120232317, 2012.
- ¹⁸⁷ S. Bektesevic, H. S. Wang, H. Wang, D. C. Merkel and R. C. Johnson, WO2011139646 A2, 2011.
- ¹⁸⁸ A. Suzuki, M. Nose and T. Yamashita, WO2010123154 A2, 2010.
- ¹⁸⁹ (a) K. Ihara, F. Yamaguchi and S. Yamane, US4900874, 1989; (b) M. J. Nappa, X. Sun, L. M. Yagupolskii, A. A. Filatov, V. N. Boiko and Y. L. Yagupolskii, WO2009067571 A1, 2009.
- ¹⁹⁰ A. P. Sharratt, C. N. Rees, C. E. McGuinness, M. Doran and C. J. Cronshaw, WO2016128763 A1, 2016.
- ¹⁹¹ H. S. Tung, S. Mukhopadhyay, M. van der Puy, D. C. Merkel, J. J. Ma, C. L. Bortz, B. A. Light, S. D. Phillips and R. K. Dubey, US8084653 B2, 2007.
- ¹⁹² D. M. Marquis, US2931840, 195.
- ¹⁹³ R1234yf refrigerant cylinder, www.boconline.co.uk/shop/en/uk/gas/refrigerant-gas/r1234yf-170249 (accessed 30.09.21)
- ¹⁹⁴ (a) C.-Q. Lu, A. J. Poss and R. R. Singh, WO2014186138, 2014; (b) C.-Q. Lu, A. J. Poss, R. R. Singh, D. Nalewajek and C. Cantlon, WO2014099508, 2014; (c) T. Morikawa, K. Washino, S. Morita, S. Fukuoka, M. Doi, S. Yokokotani, T. Furuya and J. Terada, JP2013216915, 2013; (d) Y. Patil, A. Alaaeddine, T. Ono and B. Ameduri, *Macromolecules*, 2013, **46**, 3092; (e) A. Bonnet, C. Mathieu, B. Ramfel and A. Reyna-Valencia, WO2015028765, 2015.

- ¹⁹⁵ M. Takahashi, K. Ueno, K. Kurashima, K. Ishikawa, K. Watanabe and H. Yamamoto, JP2012092164, 2012.
- ¹⁹⁶ K. Keng, A. J. Poss, J. Liu, Y. Lin and R. R. Singh, WO2014046908, 2014.
- ¹⁹⁷ G. J. Samuels, G. J. Shafer, T. Li, C. A. Threlfall, N. Iwamoto and E. J. Rainal, WO2008079986, 2008.
- ¹⁹⁸ (a) R. Amin-Sanayei, C.-P. Lin, C. Airaud, J. Schmidhauser and S. Gaboury, WO2012112840, 2012; (b) G. J. Samuels and G. J. Shafer, US20080153977, 2008.
- ¹⁹⁹ (a) Y. Imahori and K. Imoto, WO2011125740, 2011; (b) W. Jiang, R. R. Singh, G. Xu, S. Zhang and Y. Lin, WO 2016040525, 2016.
- ²⁰⁰ G. Xu, S. Zhang, W. Jiang, L. Duan and Z. Ding, WO2017087764, 2010.
- ²⁰¹ (a) S. J. Teerstra, P. Nguyen, J. Watson and G. Arsenault, WO2015164963, 2015; (b) P. Nguyen, J. Watson and G. Arsenault, WO2015164964, 2015; (c) P. Nguyen, J. Watson and G. Arsenault, WO2015164965, 2015.
- ²⁰² S. Feng, A. J. Poss, R. R. Singh and Y. Lin, WO2014179946, 2014.
- ²⁰³ (a) Y. Hiraoka, T. Kawasaki-Takasuka, Y. Morizawa and T. Yamazaki, *J. Fluorine Chem.*, 2015, **179**, 71; (b) T. Yamazaki and Y. Morisawa, JP2015168650 A, 2015.
- ²⁰⁴ Y. L. Yagupolskii, N. V. Pavlenko, S. V. Shelyazhenko, A. A. Filatov, M. M. Kremlev, A. I. Mushta, I. I. Gerus, S. Peng, V. A. Petrov and M. Nappa, *J. Fluorine Chem.*, 2015, **179**, 134.
- ²⁰⁵ Y. Li, D.-H. Tu, Y.-J. Gu, B. Wang, Y.-Y. Wang, Z.-T. Liu, Z.-W. Liu and J. Lu, *Eur. J. Org. Chem.*, 2015, **20**, 4340.
- ²⁰⁶ Y. Li, N. Sun, M. Hao, C.-L. Zhang, H. Li and W.-Q. Zhu, *Catal. Lett.* 2021, **151**, 764.
- ²⁰⁷ H. Sakaguchi, Y. Uetake, M. Ohashi, T. Niwa, S. Ogoshi and T. Hosoya, *J. Am. Chem. Soc.*, 2017, **139**, 12855.
- ²⁰⁸ S. Junya, M. Takahiro and K. Izumi, WO2018108445 A1, 2008.
- ²⁰⁹ H. Sakaguchi, M. Ohashi and S. Ogoshi, *Angew. Chem. Int. Ed.*, 2018, **57**, 328.
- ²¹⁰ G. Coates, H. Y. Tan, C. Kalff, A. J. P. White and M. R. Crimmin, *Angew. Chem. Int. Ed.*, 2019, **58**, 12514.
- ²¹¹ N. V. Pavlenko, S. Peng, V. Petrov, A. Jackson, X. Sun, L. Sprague and Y. L. Yagupolskii, *Eur. J. Org. Chem.*, 2020, **33**, 5425.
- ²¹² M. Keßler, S. Porath, H.-G. Stammer and B. Hoge, *Eur. J. Inorg. Chem.*, 2020, 907.
- ²¹³ N. A. Phillips, G. J. Coates, A. J. P. White and M. R. Crimmin, *Chem. Eur. J.*, 2020, **26**, 5365.
- ²¹⁴ D. Meyer and M. El Qacemi, *Org. Lett.*, 2020, **22**, 3479.
- ²¹⁵ J. H. Murray and A. P. Sharratt, WO2018197897 A1, 2018.
- ²¹⁶ T. Taniguchi, S. Furuta and H. Shiota, US2018297918 A1, 2018.
- ²¹⁷ H. Galiano, S. Cadra, N. Pierre, B. Ameduri and A. Alaaeddine, US2016200748 A1, 2016.
- ²¹⁸ (a) M. J. Nappa, E. N. Swearingen and S. R. Sterlin, WO201267865 A1, 2012; (b) M. J. Nappa, E. N. Swearingen and S. R. Sterlin, WO201267870 A1, 2012.
- ²¹⁹ Y. Tomiyori and M. Nakamura, US201837524 A1, 2018.
- ²²⁰ J. Lyu, J. Zeng, X. Tang, S. Han, W. Zhang, J. Kang, B. Wang, Z. Hao, Z. Yang and F. Li, CN105439805 A, 2016.
- ²²¹ C. Bakewell, A. J. P. White and M. R. Crimmin, *Angew. Chem. Int. Ed.*, 2018, **57**, 6638.
- ²²² G. Meißner, K. Kretschmar, T. Braun and E. Kemnitz, *Angew. Chem. Int. Ed.*, 2017, **56**, 16338.

²²³ M.-C. Kervarec, T. Braun, M. Ahrens and E. Kemnitz, *Beilstein J. Org. Chem.*, 2020, **16**, 2623.

²²⁴ M. Talavera, C. N. von Hahmann, R. Müller, M. Ahrens, M. Kaupp and T. Braun, *Angew. Chem. Int. Ed.*, 2019, **58**, 10688.

²²⁵ M. Talavera, R. Müller, T. Ahrens, C. N. von Hahmann, B. Braun-Cula, M. Kaupp and T. Braun, *Faraday Discuss.*, 2019, **220**, 328.

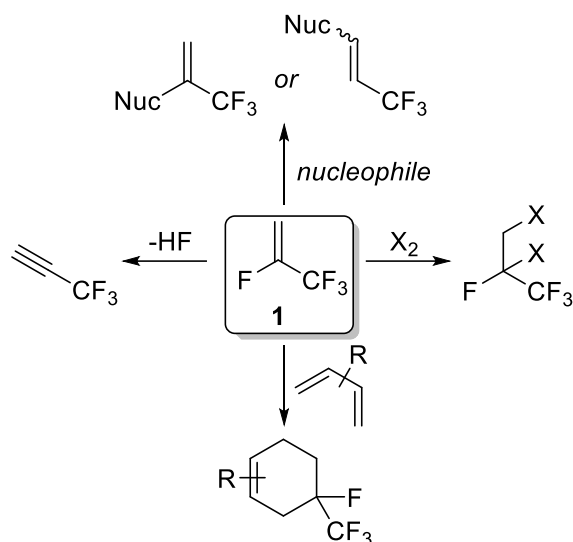
Chapter 2: Aims and approach

2.1 Project objectives

The aim of this project is to explore the synthetic utility of 2,3,3,3-tetrafluoropropene (HFO-1234yf, **1**) as a building block to access pharmaceutically relevant trifluoromethylated systems. As discussed in Chapter 1, **1** is an inexpensive and readily available refrigerant gas and so could provide a cost-effective feedstock for the synthesis of more complex trifluoromethylated compounds of relevance to drug discovery and manufacturing programmes. Given that most CF₃-substituted compounds synthesised at scale have to be derived from simple CF₃-aromatic or trifluoroacetic acid building blocks, the use of **1** has the potential to allow for the synthesis of systems that might not otherwise be facile to create without the use of late-stage trifluoromethylating reagents, the cost of which would be prohibitive on the process scale.

As reviewed in Chapter 1, there has been relatively little published work on the organic chemistry of **1** and much of what has been described uses conditions not ideal for larger scale applications, i.e. expensive and air-sensitive transition metal catalysis. Many textbook reactions of alkenes, such as halogenation, lithiation and cycloaddition, have not been extensively explored where **1** is the substrate. In order to effectively utilise **1** as a building block, the research explored in this thesis aims to gain more fundamental information about how **1** behaves in reactions with nucleophiles, electrophiles and dienes. Through these studies, opportunities to apply the chemistry of **1** to the synthesis of desired pharmaceutically relevant systems may be established.

To that end, Chapter 3 of this thesis explores the reactivity of **1** with nucleophiles and work in Chapter 4 focuses on elimination of lithium fluoride from **1** to form 3,3,3-trifluoropropyne and the subsequent reactivity of trifluoropropynyl systems. Chapter 5 expands upon reactions of the CF₃-ynones formed from these reactions whilst Chapter 6 details the use of compounds derived from **1** as bench-stable building blocks for further trifluoropropynylation reactions. Finally, Chapter 7 describes how **1** reacts with electrophiles and through cycloaddition processes. Scheme 2.1 illustrates these planned reactions of **1**.



Scheme 2.1. Initially planned potential reactions of HFO-1234yf explored in this work

2.2 Techniques for the reactions of HFO-1234yf

1 has a boiling point of $-28\text{ }^{\circ}\text{C}^1$ and so developing its organic chemistry requires special consideration. The use of gaseous reagents has declined in recent years in academic and life science discovery settings despite their great utility, largely owing to safety concerns. Stable, solid gas surrogates have been developed in many cases that perform the same transformations but such reagents have poor atom economy compared to small, efficient gas molecules and so are often too expensive for industrial scales.

The simplest approach to using gases in synthesis is simply to use a balloon filled with the gas. While this is not feasible for toxic or corrosive gases, it can be successfully used for small scale reactions with non-toxic and inert gases such as **1**. Simple balloons are not viable for scales above a few hundred milligrams, but a similar strategy can be employed using a medical grade gas bladder. These larger, thick-walled rubber vessels can be fitted with a tap adapter for use with any standard ground-glass jointed glassware and so are much less prone to leakage than balloons as well as being able to hold significantly larger quantities of gas. Figure 2.1 shows a reaction set-up using a gas bladder, with the reservoir of gas connected to a 100 mL two-necked round bottomed flask. In this case, the other neck is connected via tubing to a Schlenk line to easily facilitate reactions under anhydrous and anaerobic conditions. The majority of reactions of **1** described in this work use this gas bladder set-up.



Figure 2.1. Typical gas bladder reaction set-up

In order to reach reflux temperatures and handle larger scale reactions, more specialist techniques were required as heating the typical gas bladder set-up leads to a reduction of the amount of gas in solution. For this purpose, glass Carius tubes or, for even higher temperatures and pressures, a Hastelloy autoclave were employed. Further information on the set-up and use of this equipment is given in the experimental chapter of this thesis. However, as most reactions of **1** investigated through this work could be conducted at ambient temperature, more specialist high pressure equipment was rarely required.

2.3 Characterisation of 2,3,3,3-tetrafluoropropene in solution

To aid the investigation of the reactions of **1** throughout this project, the ^{19}F NMR spectrum of the dissolved gas was analysed (Figure 2.2). The ratio of the integrals of the two peaks is 3:1, which is consistent with **1**, and, in terms of coupling, the CF_3 group appearing as a doublet of doublets (dd) and the vinyl fluoride as a doublet of doublets of quartets (ddq). The trifluoromethyl group shows a three bond F-F coupling to the vinyl fluoride and a four bond H-F coupling to the *trans* proton. Coupling of the CF_3 fluorine atoms to the *cis* proton is not observed. The vinyl fluoride shows the same three bond F-F coupling along with two three bond H-F couplings. The coupling to the *trans* proton is larger than that of the *cis*. The spectrum is also consistent with previous literature reports for the ^{19}F NMR spectrum of **1**.²

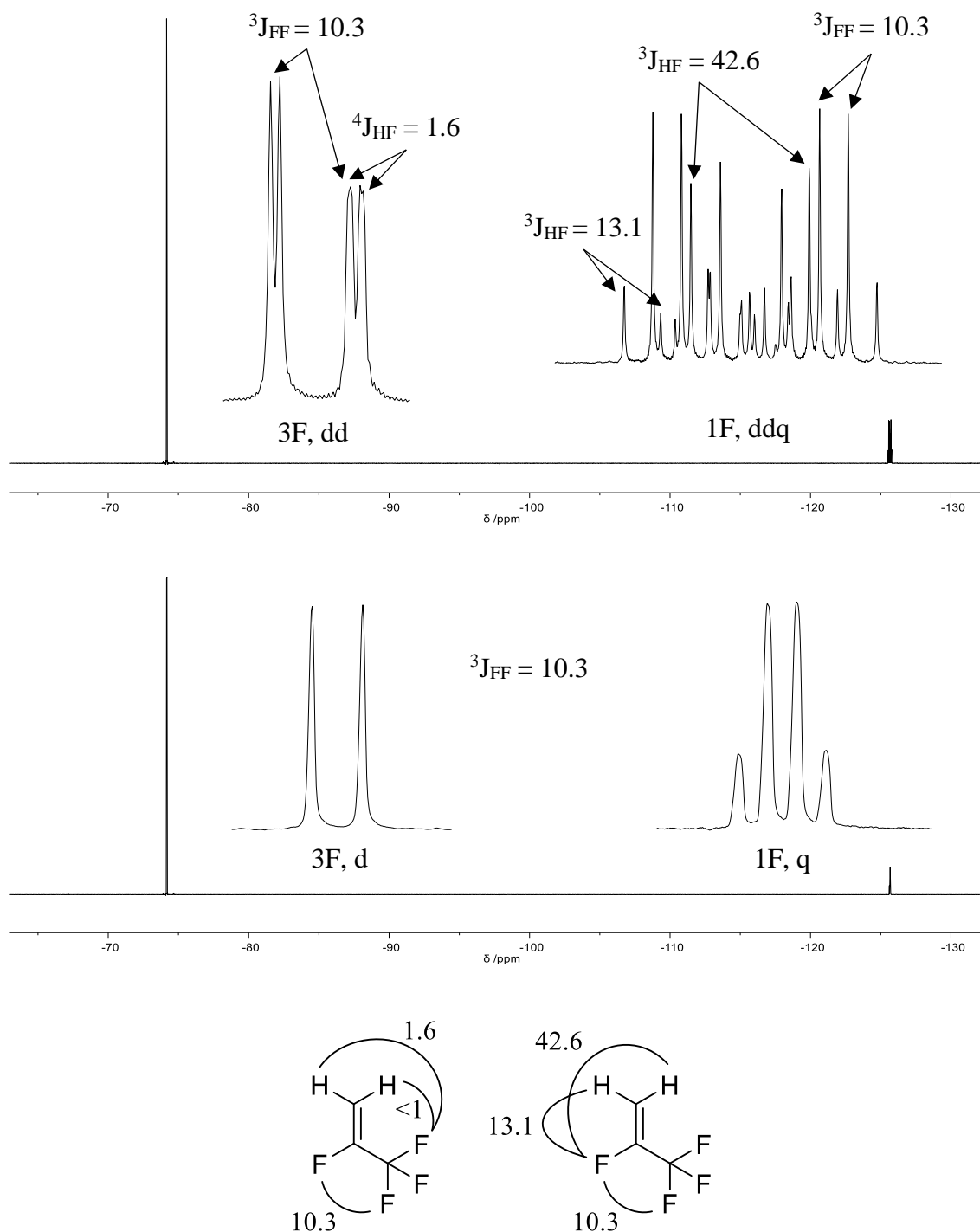


Figure 2.2. ^{19}F NMR spectrum of **1** (top); $^{19}\text{F}\{^1\text{H}\}$ NMR spectrum of **1** (middle); assignment of CF_3 (left) and CF (right) couplings (bottom), coupling constants in Hz; NMR recorded in $\text{CD}_3\text{CO}_2\text{D}$ at 376 MHz

1 must be, therefore, at least somewhat soluble in some organic solvents and this raised the possibility that a stock solution might be prepared for use in laboratory experiments, based on the precedent of using stock solutions of CF_3I in DMF or DMSO.³ To inform the design of future reactions, a screen of eighteen solvents were initially selected,

covering a wide range of polarities and functional groups. Consideration was also given to the environmental impact of each solvent choice with a number of environmentally benign alternatives included along with more commonplace solvents.⁴ Screening was carried out by stirring a sealed microwave vial containing each solvent at room temperature under an atmosphere of **1** provided by a balloon. After one hour, the concentration of **1** in each solvent was measured by comparing the integrals in the ¹⁹F NMR spectra to an internal standard of fluorobenzene (Table 2.1), or 2,2,2-trifluoroethanol for solvents immiscible with fluorobenzene.

Table 2.1. Concentration of 1 in various solvents

Solvent	Concentration of 1 /mmol dm ⁻³	Solvent	Concentration of 1 /mmol dm ⁻³
Water	0.01	Dichloromethane	14.5
Ethanol	7.72	Ethyl acetate	23.5
2-Butanol	2.31	MeTHF	11.1
Acetic acid	26.1	MTBE	13.0
Acetonitrile	8.47	Toluene	8.32
DMSO	14.5	<i>p</i> -Cymene	4.60
Sulfolane	4.18	Triethylamine	7.02
DMF	5.42	Perfluorohexane	15.8
Acetone	12.5	Cyclohexane	6.12

Plotting concentration against the relative permittivity, dipole moment or E_T^N (an empirical measure of polarity derived from transition energies)⁵ gave no clear correlations. It may be that the absolute values of concentration calculated in this case are not accurate enough given the difficulties in dispensing precise volumes of gases and, therefore, in ensuring that exactly the same conditions were used for the screening of each solvent. However, **1** can be seen, at least qualitatively, to be reasonably soluble in all solvents, except water, with polar aprotic solvents being the most effective. The solutions with the highest concentrations were left to stand in NMR tubes open to air for 48 hours then for a further 7 days. The concentrations of **1** were measured after each period of time to determine stability with respect to degassing (Table 2.2).

Table 2.2. Stability of solutions of **1**

Solvent	Concentration of 1 after 48 hours /mmol dm ⁻³	Concentration of 1 after 7 days /mmol dm ⁻³
Acetic acid	16.5	0.08
DMSO	12.3	3.00
Acetone	13.0	-
Dichloromethane	9.34	-
Ethyl acetate	22.8	5.33
MeTHF	13.4	2.80
MTBE	12.1	-
Perfluorohexane	0.00	-

1 still had measurable concentrations in all solvents chosen except perfluorohexane after 48 hours open to the air. For acetone and MTBE, the concentration was observed to increase, which indicates that the evaporation of these solvents is faster than degassing of **1** from them. After one week, the more volatile solvents had evaporated and so the concentration of **1** could no longer be determined. In the four solvents that remained in sufficient volume for NMR spectroscopy, all still contained measurable amounts of dissolved **1**. To provide further evidence of the stability of solutions of **1**, the concentration of **1** in a solution of DMF in a sealed NMR tube was measured at more frequent intervals over a period of around six days (Figure 2.3).

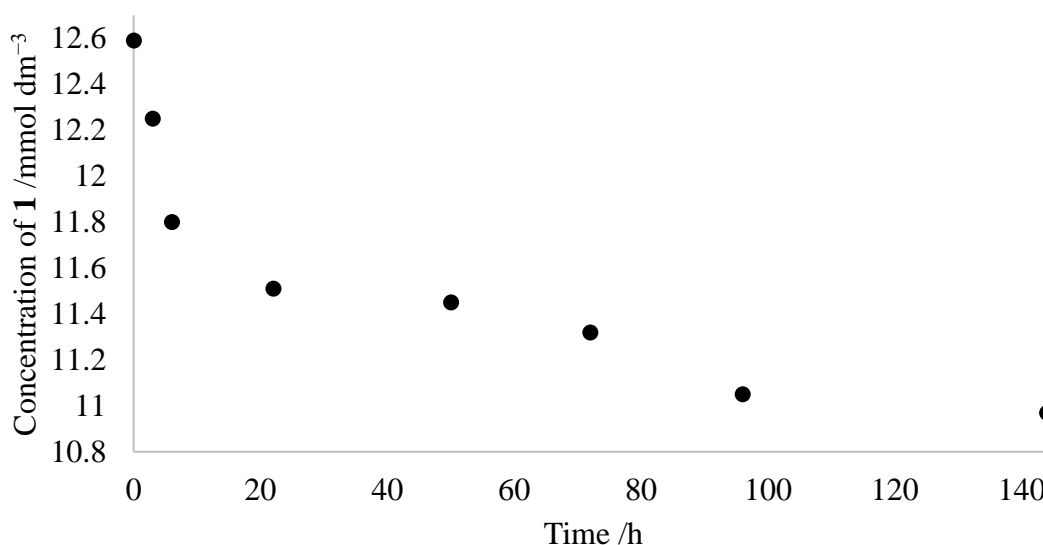


Figure 2.3. Concentration of HFO-1234yf in DMF solution over time as determined by ¹⁹F NMR spectroscopy (376 MHz; unlocked)

After an initial sharp decrease, the concentration becomes relatively stable after around four days. The concentration was measured again 14 days after the first measurement and found to be $10.70 \text{ mmol dm}^{-3}$, a decrease of only $0.27 \text{ mmol dm}^{-3}$ in the final eight days. Based on these data, it seems reasonable that stock solutions of **1** could be prepared and used over relatively long periods of time, especially if kept in well-sealed vessels at low temperatures. These results also suggest that **1** would be amenable to reactions in flow with a variety of solvents if good mixing can easily be achieved even at atmospheric pressure. The use of flow chemistry for the safer and more efficient reaction of a variety of gases is a well-established technique⁶ and, whilst not employed in this work, could be of use for carrying out reactions described in upcoming chapters on an increased scale.

2.4 References for Chapter 2

¹ A. L. Henne and T. P. Waalkes, *J. Am. Chem. Soc.*, 1948, **68**, 496.

² (a) R. S. Dickson and G. D. Sutcliffe, *Aust. J. Chem.*, 1972, **25**, 761; (b) V. Montanari and D. D. DesMarteau, *J. Org. Chem.*, **57**, 5018; (c) R. E. Banks, M. G. Barlow and M. Nickkho-Amiry, *J. Fluorine Chem.*, 1997, **82**, 171.

³ A. Harsanyi, E. Dorko, A. Csapo, T. Bako, C. Peltz and J. Rabai, *J. Fluorine Chem.*, 2011, **132**, 1241.

⁴ R. K. Henderson, C. Jiménez-González, D. J. C. Constable, S. R. Alston, G. G. A. Inglis, G. Fisher, J. Sherwood, S. P. Binks and A. D. Curzon, *Green Chem.*, 2011, **13**, 854.

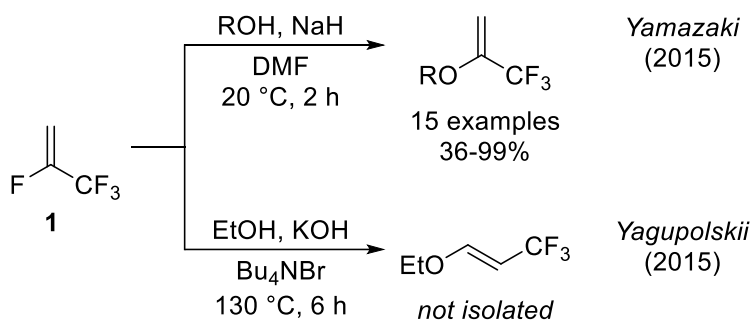
⁵ C. Reichart and T. Welton, *Solvents and Solvent Effects in Organic Chemistry*, Wiley-VCH, Weinheim, 2010, pp. 550-553.

⁶ C. J. Mallia and I. R. Baxendale, *Org. Process Res. Dev.*, 2016, **20**, 327.

Chapter 3: Nucleophilic substitution reactions of HFO-1234yf

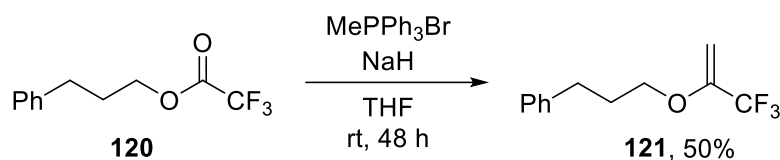
3.1 Introduction

Since there is extensive literature concerning reactions of poly- and per-fluoroalkenes with nucleophiles,¹ our first studies on the synthetic utility of 2,3,3,3-tetrafluoropropene (**1**) as a CF₃-containing building block in organic synthesis began with nucleophilic substitution reactions. Although there is little literature precedent for the use of **1** in synthetic applications, there have been two independent reports of the reaction of **1** with alkoxides.^{2,3} Even more intriguing is that the two publications claim opposite regioselectivity is obtained under the different conditions used, as shown in Scheme 3.1.



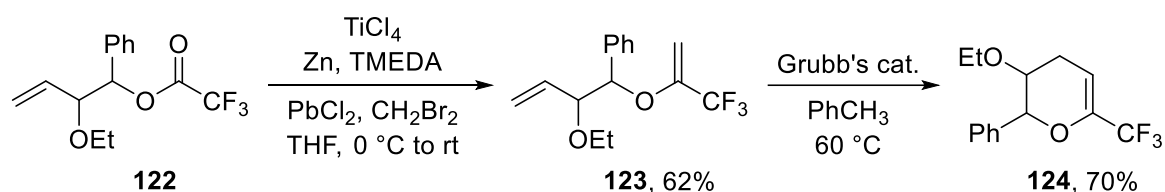
Scheme 3.1. Conflicting reports for the reaction of HFO-1234yf with alkoxides^{2,3}

In this chapter, both of these literature reaction conditions were repeated to verify that the reported regioselectivities were accurate. The mechanism of these reactions was then investigated before expanding the scope of the alkoxides that could be used in the reaction as well as exploring the reactions of other classes of nucleophiles with **1**. The two major classes of compound synthesised were trifluoromethyl enol ethers and trifluoromethyl vinyl sulfides and so literature routes to these systems not involving **1** as the starting material are briefly outlined below by way of comparison. One such method is by Wittig olefination of simple trifluoromethyl esters such as **120**, which are derived from trifluoroacetic acid, to form enol ethers (**121**) as reported by Bégué *et al.* (Scheme 3.2).⁴ Epoxidation and bromination reactions of these systems were then described, with the resulting brominated compounds reacting further via lithium-halogen exchange and subsequent addition to carbonyl electrophiles⁵ or Suzuki cross-coupling reactions.⁶



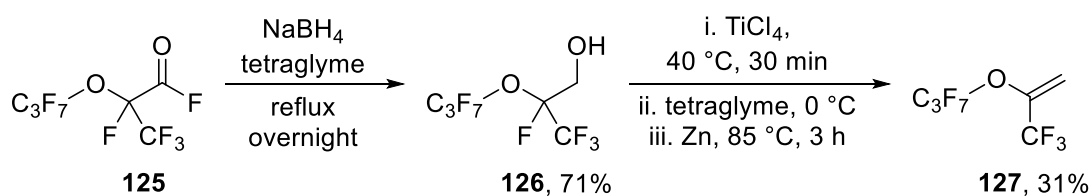
Scheme 3.2. Example synthesis of CF_3 -enol ether via Wittig reaction ⁴

An alternative to the Wittig reaction is the Takai-Nozaki olefination. Gajewski *et al.* demonstrated the synthesis of allylic $\alpha\text{-CF}_3$ enol ethers with this approach, using titanium(IV) chloride, tetramethylethylenediamine (TMEDA), zinc and dibromomethane.⁷ Subsequent Cope reactions of these allylic enol ethers were carried out and the presence of a CF_3 group was found to lead to an increase in reaction rate by a factor of 73 over the non-fluorinated parent compound. Donohoe *et al.* later used the same olefination reaction but with an improved yield by using lead(II) chloride as a catalyst (Scheme 3.3) converting ester **122** to enol ether **123**, which was then used in metathesis reactions to form the corresponding dihydropyran (**124**).⁸



Scheme 3.3. Example synthesis of CF_3 -enol ether via Takai-Nozaki olefination reaction ⁸

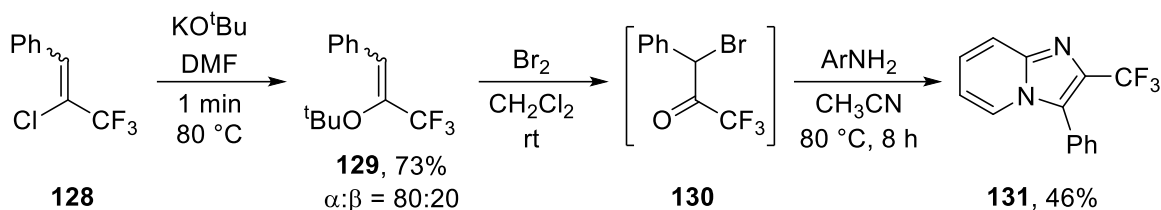
The synthesis of a wide variety of perfluorinated enol ethers was described by Smith *et al.* in a recent patent for use as working fluids for heat transfer, solvent cleaning, deposition coating solvents and electrolyte solvents and additives (Scheme 3.4).⁹ Firstly, the acid fluoride **125** is reduced to the corresponding alcohol **126**. This is followed by dehydration and elimination of HF to give the enol ether **127**.



Scheme 3.4. Example synthesis of perfluorinated enol ethers ⁹

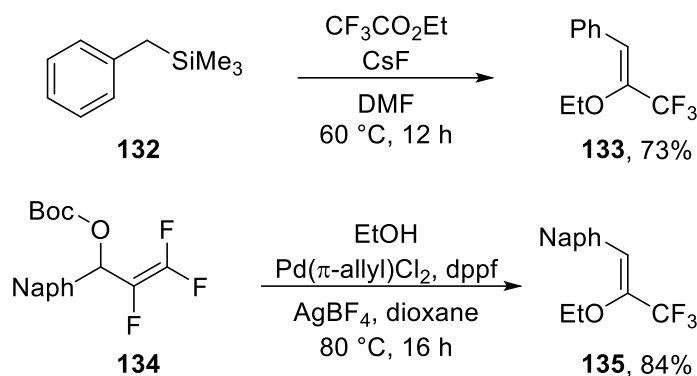
1-Aryl-2-chloro-3,3,3-trifluopropenes (**128**) were shown by Haufe *et al.* to react with *t*-butoxide to give a mixture of α - and $\beta\text{-CF}_3$ enol ethers (**129**, Scheme 3.5).¹⁰ Bromination

gave trifluoromethyl ketones such as **130**, which were then immediately reacted with 2-aminopyridines to form imidazopyridine heterocycles like **131**.



*Scheme 3.5. Example synthesis of CF_3 -enol ether from a chloroalkene precursor*¹⁰

More recent synthetic methods reported include addition of benzyl-TMS carbanions (**132**) to CF_3 -esters to give enol ether **133**¹¹ and palladium-catalysed rearrangement of 2,3,3-trifluoroallylic carbonates (**134**) to form the enol ether **135** (Scheme 3.6).¹²



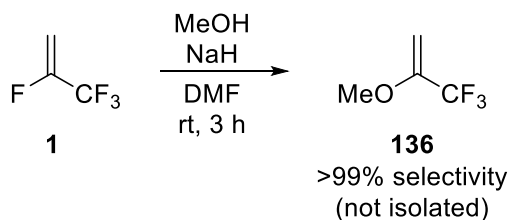
Scheme 3.6. Recently developed examples of CF_3 -enol ether syntheses^{11,12}

Similarly to α -trifluoromethyl enol ethers, β -trifluoromethyl vinyl sulfides can be synthesised by Wittig olefination of the corresponding trifluoromethyl thioester¹³ or by addition of thiolates to trifluoromethylalkynes¹⁴ and either fluoro-,¹⁵ chloro-¹⁶ or bromo-trifluoromethylalkenes.¹⁷ More recently, copper-catalysed addition of TMS- CF_3 to unsubstituted vinyl sulfides has been reported.¹⁸ Bromination¹⁹ and epoxidation²⁰ of these CF_3 -vinyl sulfides has been described in the literature along with direct lithiation followed by addition to electrophiles,²¹ as ylide precursors for [3+2] cycloaddition reactions²² and directly as dienophiles for Diels-Alder reactions.²³ β - CF_3 vinyl sulfides have even more synthetic utility as they can be converted to the corresponding sulfone²⁴ or sulfonium salt,²⁵ both of which have seen some limited usage as CF_3 -containing building blocks.

3.2 Results and discussion

3.2.1 Regioselectivity in the reactions of HFO-1234yf with nucleophiles

Given the discrepancy in the literature, we first sought to confirm these reports. Firstly, the reaction of **1** with methanol was carried out as described by Yamazaki *et al.*² using sodium hydride in DMF with **1** provided via the gas bladder technique as described in Chapter 2 (Scheme 3.7). Clean conversion to a single product was observed by ¹⁹F NMR spectroscopy (Figure 3.1), which was consistent with formation of α -trifluoromethyl enol ether **136**. Whilst Yamazaki reported no splitting in the ¹⁹F NMR spectrum of such products, a small doublet ($^4J_{\text{HF}} = 2.0$ Hz) was observed for the CF₃ resonance but this difference is likely simply due to using a higher resolution spectrometer (376 MHz versus 283 MHz). This assignment was corroborated by an identical splitting for one of the two vinyl protons in the ¹H NMR spectrum (Figure 3.2). **136** was not isolated due to its volatility but these NMR spectra suggest Yamazaki's description of an entirely selective reaction for the α -regioisomer under these conditions is accurate.



Scheme 3.7. Reaction of HFO-1234yf with methanol under Yamazaki's conditions

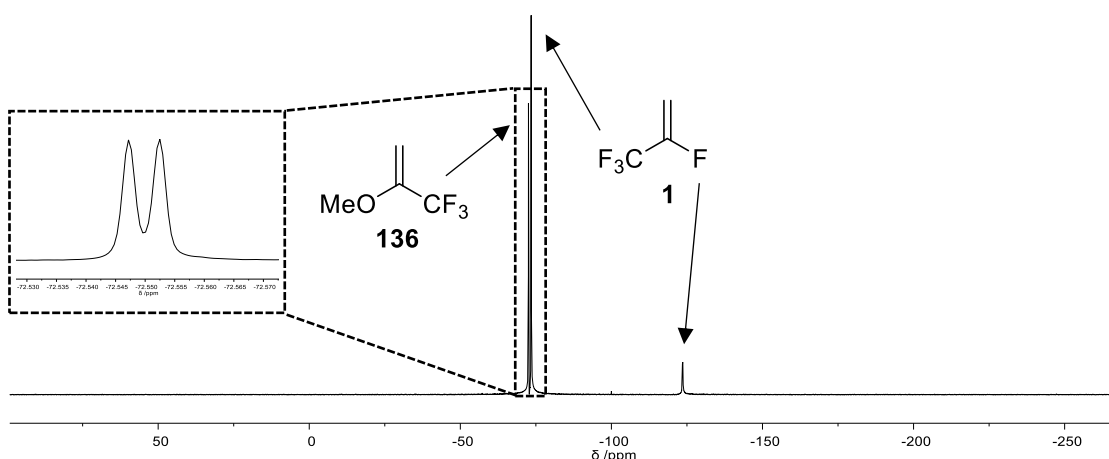


Figure 3.1. ¹⁹F NMR spectrum of 136

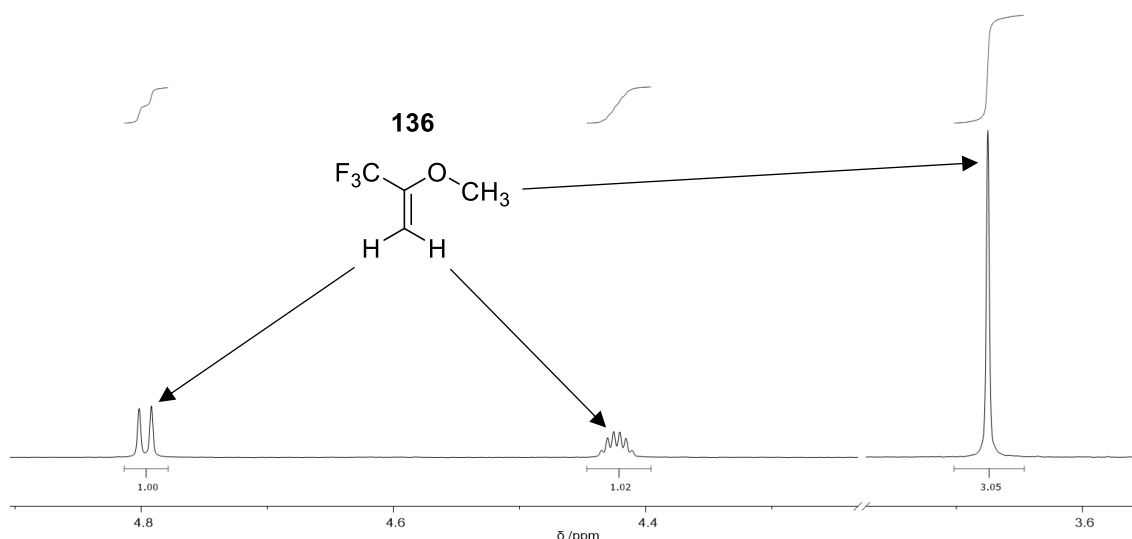
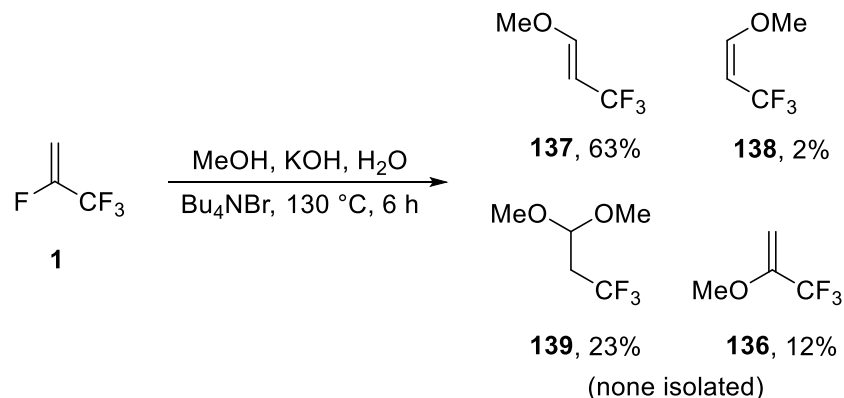


Figure 3.2. ^1H NMR spectrum of **136**

1 was then reacted with methanol under Yagupolskii's conditions,³ using potassium hydroxide and a phase transfer catalyst (Bu_4NBr) in a Carius tube (Scheme 3.8). The contents of the reaction mixture were analysed by ^{19}F NMR spectroscopy (Figure 3.3) because the products were, again, too volatile to be isolated. There were several unidentified polymerisation and decomposition minor products that complicated the ^1H NMR spectrum (Figure 3.4), making unequivocal assignments difficult. However, the major product appeared to be the β -regioisomer **137**. This was assigned on the basis of a three-bond coupling ($^3J_{\text{HF}} = 8.2$ Hz) of the CF_3 fluorine to the geminal proton. There is no coupling to the vicinal proton, suggesting that the major product **137** is the *E*-stereoisomer as *trans* coupling is typically larger than *cis*.²⁶ Some of the *Z*-stereoisomer (**138**) was also formed, with both three- and four-bond couplings observed ($^3J_{\text{HF}} = 6.4$ and $^4J_{\text{HF}} = 2.0$ Hz respectively). Overall, 97% of the β -regioisomer that formed was the *E*-stereoisomer **137**. Some acetal (**139**) was also formed, as was reported by Yagupolskii.

In addition to these three products, some α -regioisomer **136** was also observed. The ^1H and ^{19}F NMR splitting patterns for **136** were identical to those obtained under Yamazaki's conditions. Overall, a nearly 1:3 ratio of α : β regioisomers was obtained. While there was no reported synthesis of the α -regioisomer in the Yagupolskii's paper, the crude reaction mixture was directly subjected to acid hydrolysis to form 3,3,3-trifluoropropanal from **137**, **138** and **139**. Under these conditions, **136** would be converted to the highly volatile 1,1,1-trifluoroacetone and so could have been lost during purification of the aldehyde

without being detected. Yagupolskii *et al.* did not report any spectral data for this reaction but our results are generally consistent with their reports. These data demonstrate that both of the originally reported regioselectivities in the literature are accurate, although neither paper discusses the different results obtained or any possible mechanisms.



Scheme 3.8. Reaction of HFO-1234yf with methanol under Yagupolskii's conditions

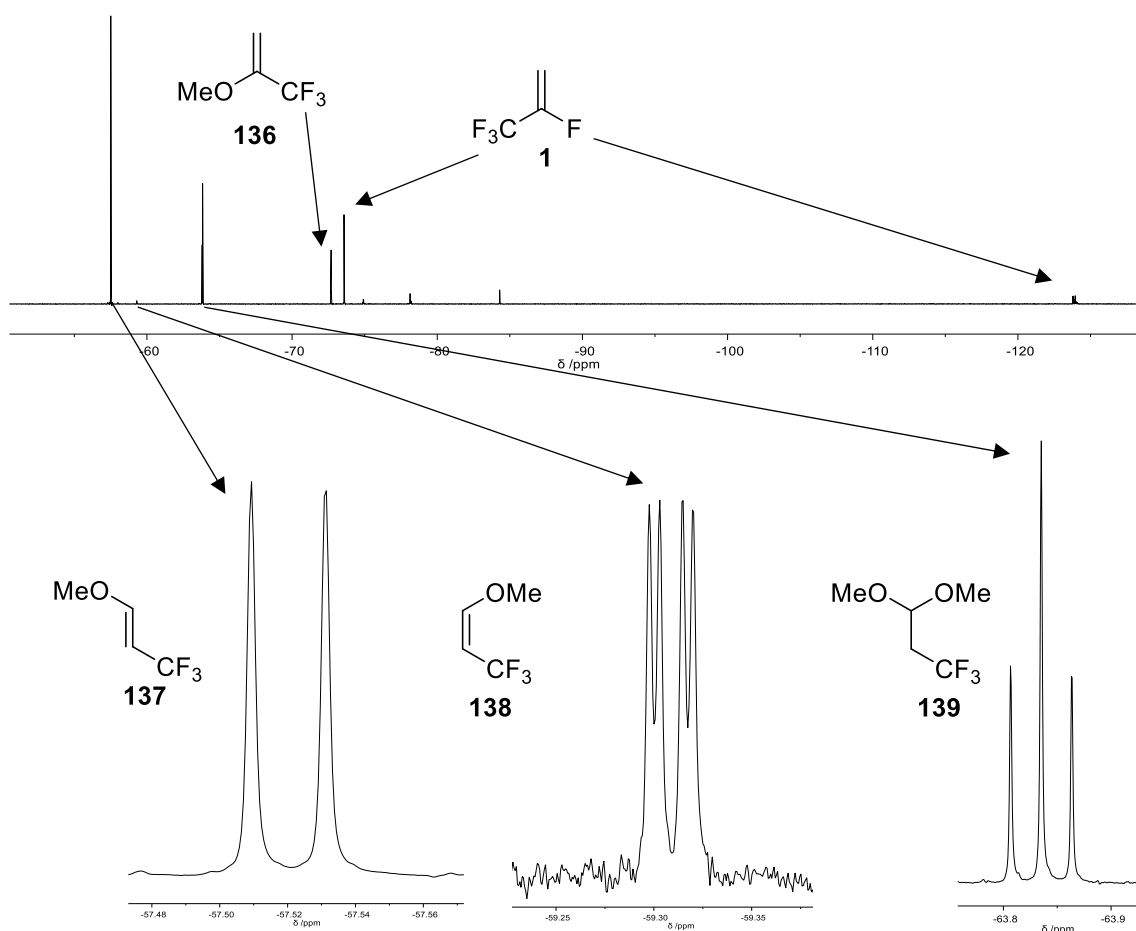


Figure 3.3. ¹⁹F NMR spectrum from reaction under Yagupolskii's conditions

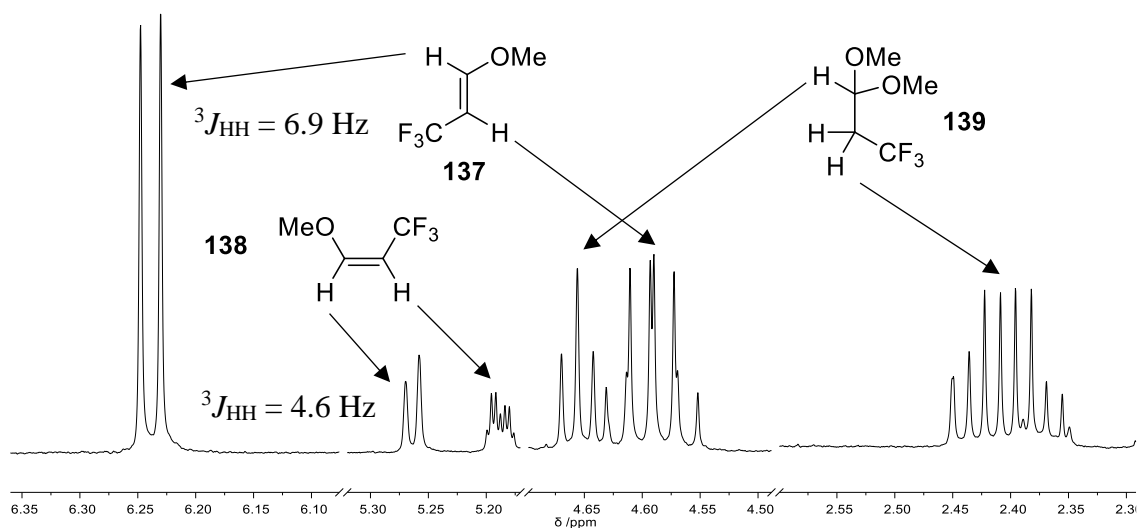


Figure 3.4. ^1H NMR spectrum from reaction under Yagupolskii's conditions

The differing regioselectivities likely arise from the mechanism of these reactions under different conditions. We propose that these reactions proceed via an addition-elimination nucleophilic vinylic substitution process similar to those that are well established for reactions of other CF_3 -substituted alkenes.²⁷ Nucleophilic attack can occur at one of two positions, leading to formation of two possible carbanions. From our calculated LUMO of **1**, there is no major difference between the two alkenyl carbon atoms and, therefore, attack of a nucleophile at either site should be possible with no significant orbital control of selectivity (Figure 3.5). However, the atomic charges reveal that C^2 (C-F) is more electropositive (0.315) than C^1 (CH_2 , -0.412) and should, therefore, be the favoured site of reaction with nucleophiles.

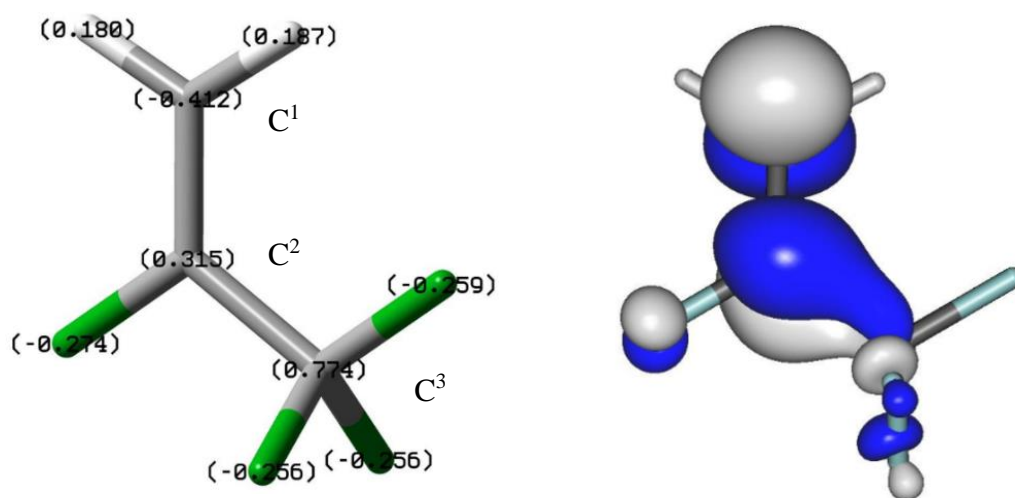
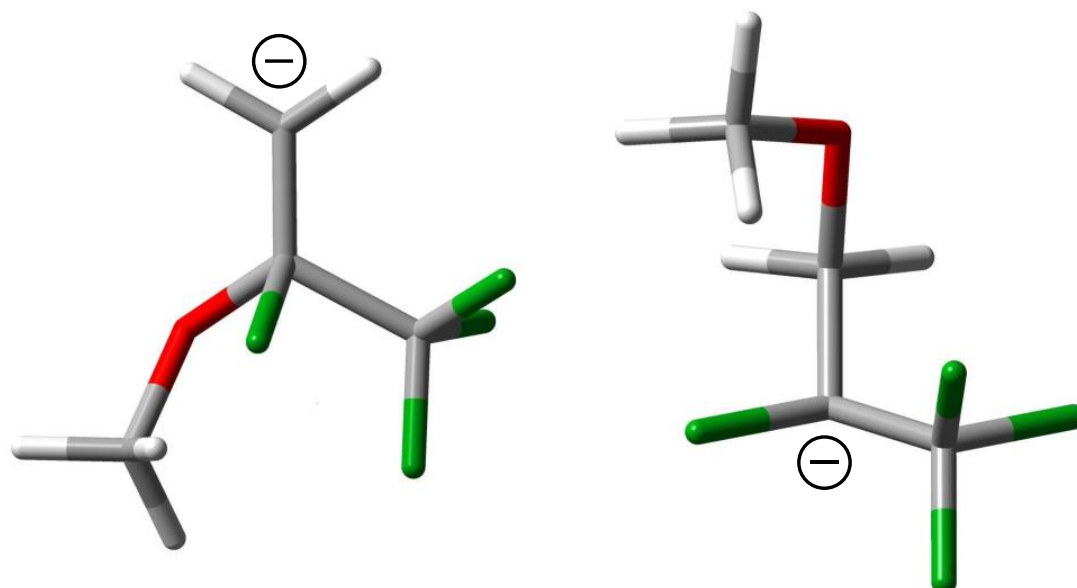


Figure 3.5. Calculated atomic charges (left) and LUMO (right) of HFO-1234yf; calculations carried out by Dr. Mark Fox (Durham University)

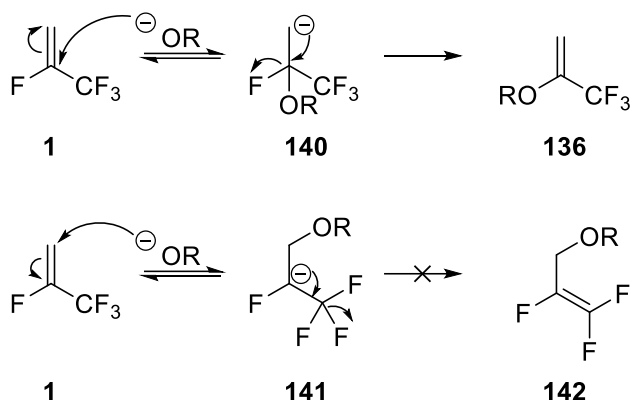
The optimised geometries of the proposed carbanion intermediates were then calculated for the reaction of **1** with methoxide (Figure 3.6). The C-F bond is elongated from 1.344 Å in **1** to 2.076 Å for intermediate **140** and 1.462 Å for intermediate **141**. This implies the bond is weakened and so the fluorine is more likely to act as a leaving group. The C-F bond is significantly longer for **140** and, therefore, the likelihood of elimination is higher, driving the reaction forward. **141** was calculated to be 1.5 kcal mol⁻¹ less stable than **140**, which is not a significant difference in energy and so both intermediates should be able to form. While the negative charge is closer to the CF₃ group for **141** and hence the inductive stabilising effect is stronger, the carbanion is adjacent to the fluorine atom. This leads to destabilisation by repulsion between the lone pairs of the carbanion and those of the fluorine atom.



*Figure 3.6. Optimised geometries of possible carbanion intermediates **140** (left) and **141** (right); calculations carried out by Dr. Mark Fox (Durham University)*

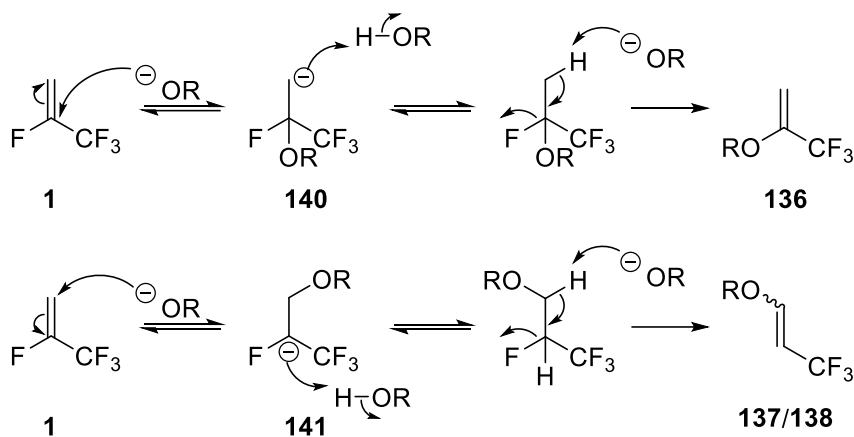
Under Yamazaki's aprotic conditions, direct elimination of fluoride can occur from **140** to give either the α -trifluoromethyl enol ether, such as **136** (Scheme 3.9), which is an S_NV process. Whilst **141** could also hypothetically eliminate fluoride from the CF₃ group to form an allylic ether product (**142**) via an S_N2' process, the DFT calculations (Figure 3.6) show no C-F bond elongation in the CF₃ group and so these fluorine atoms are unlikely to compete as leaving groups. Furthermore, formation of **142** would also give three fluorine atoms at sp² hybridised centres and so this product would be relatively thermodynamically disfavoured compared to no sp² C-F bonds in **136**. Indeed, we never observed any signals matching **142** by ¹⁹F or ¹H NMR spectroscopy. This contrasts with

the selectivity reported by Crimmin *et al.* who found that silicon nucleophiles give 100% S_N2' reactivity whilst boron nucleophiles are 90% selective for S_N2' over S_NV .



Scheme 3.9. Proposed mechanism for reaction of HFO-1234yf with alkoxides under aprotic conditions

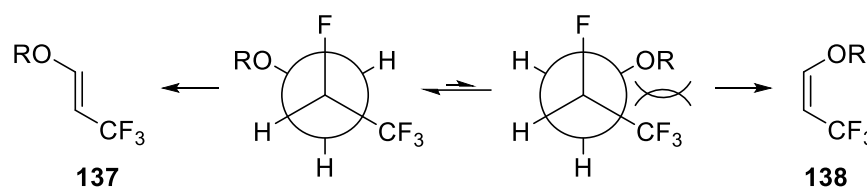
Yagupolskii's conditions give opposing regiochemistry to Yamazaki's but we propose that a similar mechanism is followed. However, under protic conditions, either intermediate **140** or **141** can be rapidly protonated (Scheme 3.10). This is then followed by elimination of HF to give either the α (**136**) or β -regioisomer (**137/138**) of the enol ether and so both products are observed.



Scheme 3.10. Proposed mechanism for reaction of HFO-1234yf with methoxide under protic conditions

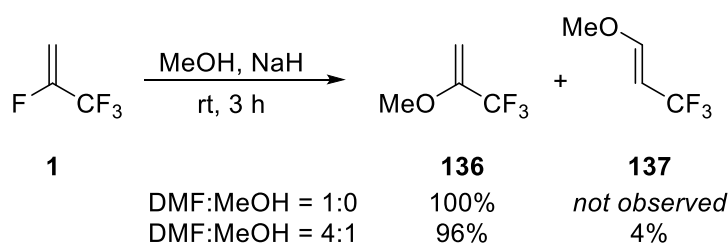
The β -trifluoromethyl enol ether product can exist as either the *E*- and *Z*-stereoisomers, with the stereochemistry of the product determined by the conformation of the protonated intermediates (Scheme 3.11). The intermediate that would lead to the *Z*-isomer involves steric clash between the CF_3 and OR groups whereas there is less hindrance in the conformation that gives the *E*-isomer and so this would most likely be favoured. This matches the stereoselectivity observed experimentally between **137** and **138**. By contrast, selective formation of the *Z*-stereoisomer was reported when reacting 2-bromo²⁸ and 2-

chloro-3,3,3-trifluoropropene^{29,30} with alkoxides. In these cases, the reaction instead proceeds via elimination of HBr or HCl to give an alkyne intermediate with which the alkoxide reacts by a conjugate addition. Reaction of isolated 3,3,3-trifluoropropyne with nucleophiles gives the *Z*-stereoisomer and β -regioisomer, confirming this hypothesis.³¹ The different stereochemistry, with selectivity for the *E*-stereoisomer, under Yagupolskii's conditions suggests an alkyne intermediate is not formed from **1**, which follows given the significantly higher strength of the C-F bond compared to C-Cl or C-Br.³²



Scheme 3.11. Origin of stereoselectivity in synthesis of β -trifluoromethyl enol ethers

If the mechanism proposed is correct then solvent composition would be likely to alter the regioselectivity of the reaction. To support this theory, the reaction of **1** with methanol and sodium hydride was carried out with a mixture of 1:4 ratio of methanol to DMF used as the solvent system. Selectivity decreased from 100% for **136** with fully deprotonated methanol to 96% under these conditions, with the remaining 4% being **137** (Scheme 3.12). There was no reaction at all with greater proportions of methanol in the solvent mixture, likely due to the lower solubility of **1** in methanol compared to DMF.

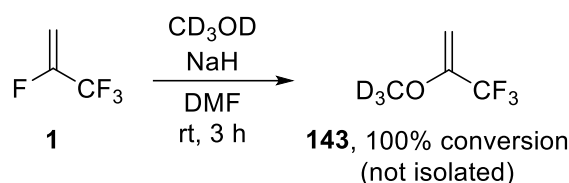


Scheme 3.12. Change in regioselectivity with solvent composition

Given that Yamazaki *et al.* reported quantitative yields without rigorous exclusion of oxygen, a radical mechanism seems unlikely. However, to rule out single electron transfer processes, the reaction of **1** with methanol and sodium hydride to give **136** was repeated in the presence of an equimolar amount of TEMPO radical. Clean conversion to **136** was again obtained with no evidence of any adduct formation between TEMPO and radical intermediates observed by ¹⁹F or ¹H NMR spectroscopy or by LC-MS analysis. The lack

of any such radical trapping would strongly suggest that this reaction does not proceed via a single electron transfer process.

Trapping of the proposed carbanion intermediates **140** and **141** was then attempted. Reaction of **1** with methanol- d_4 and sodium hydride, i.e. Yamazaki's conditions, gave complete conversion to α -trifluoromethyl enol ether **143** (Scheme 3.13). No deuterium incorporation was observed at the vinylic positions, which is consistent with our proposed mechanism for formation of intermediate **140** followed by immediate elimination of fluoride. This was evidenced by the retention of splitting in the ^{19}F NMR resonances and only the methoxy protons disappearing from the ^1H NMR spectrum (Figure 3.7).



Scheme 3.13. Reaction of HFO-1234yf and methanol- d_4 with sodium hydride

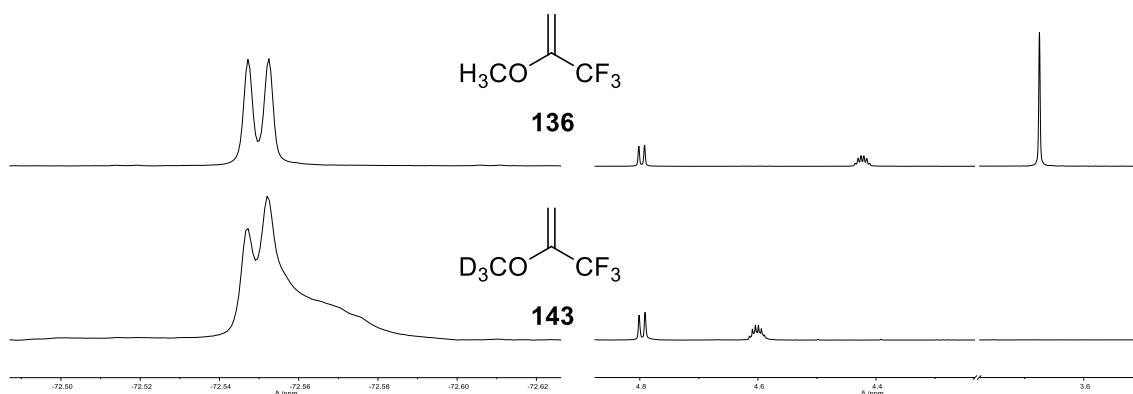
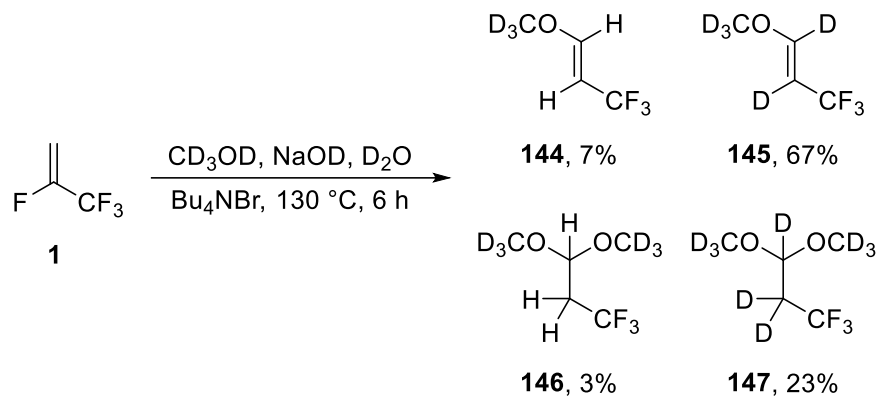


Figure 3.7. ^{19}F (left) and ^1H (right) NMR spectra of **136** and **143**

Under Yagupolskii's conditions, **1** with methanol- d_4 and sodium deuterioxide gave a mixture of deuterated and undeuterated products (Scheme 3.14). As before, the *E*-stereoisomer of the β -regioisomer, in this case **144**, is the major product under these conditions. The ^{19}F NMR peak observed for this product using methanol- d_4 is a singlet rather than the doublet seen for **137** (Figure 3.8), implying that the α -proton has been replaced by deuterium to give **145**. A small signal arising from formation of **136** was also observed but was too small to establish the extent of deuterium incorporation. Acetal formation was again observed to give **146**, but the major peak for this product was also a singlet, unlike the triplet of **139**, again suggesting replacement of hydrogen by deuterium

to give **147**. The ^1H NMR spectrum (Figure 3.9) shows no peaks in the 4-6 ppm region except for HDO, with the resonances of the $(n\text{-Bu})_4\text{NBr}$ phase transfer catalyst being used as a standard for comparison. In the reaction of **1** with undeuterated methanol a range of peaks from different compounds was observed. This strongly implies that no protons were present in the major product observed by ^{19}F NMR spectroscopy, i.e. deuterium was incorporated both α and β to the trifluoromethyl group. This is consistent with reversible formation of a carbanion as proposed above (Scheme 3.15).



Scheme 3.14. Reaction of HFO-1234yf and methanol- d_4 with sodium deuteroxide

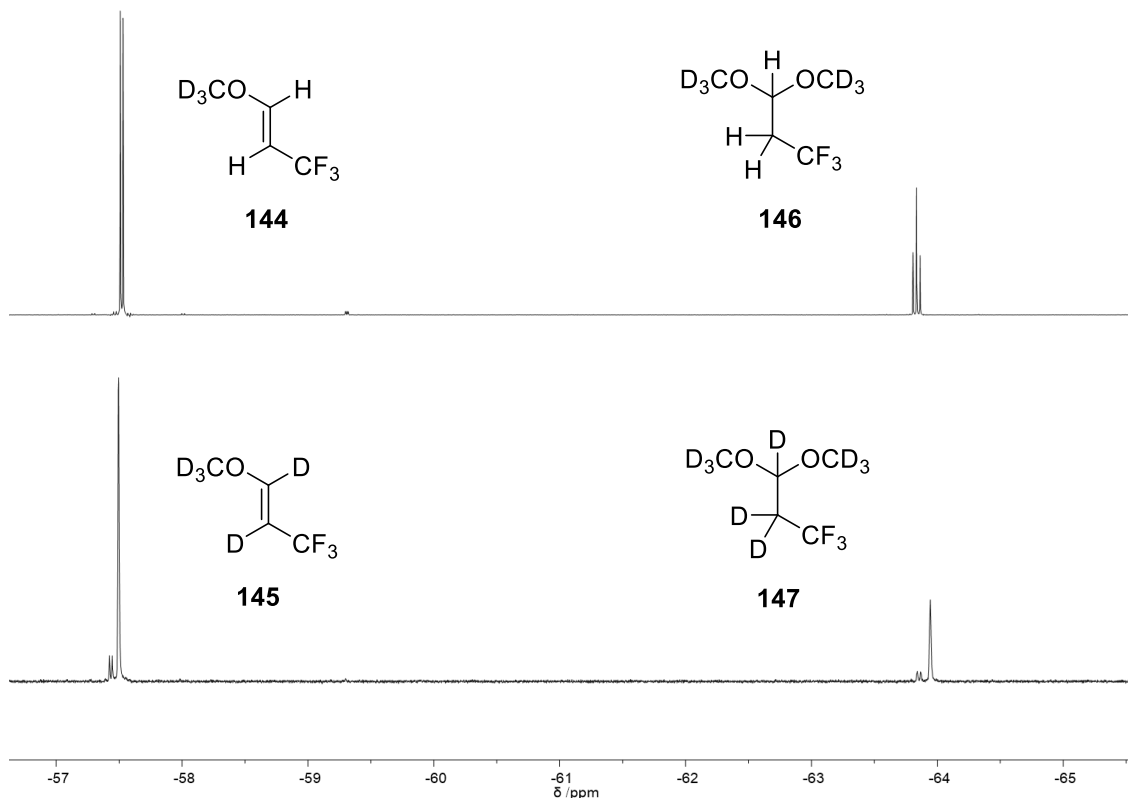


Figure 3.8. ^{19}F NMR spectrum from reaction of HFO-1234yf with $\text{CH}_3\text{OH}/\text{KOH}/\text{H}_2\text{O}/\text{Bu}_4\text{NBr}$ (top) and $\text{CD}_3\text{OD}/\text{NaOD}/\text{D}_2\text{O}/\text{Bu}_4\text{NBr}$ (bottom) at 130 °C for 6 hours

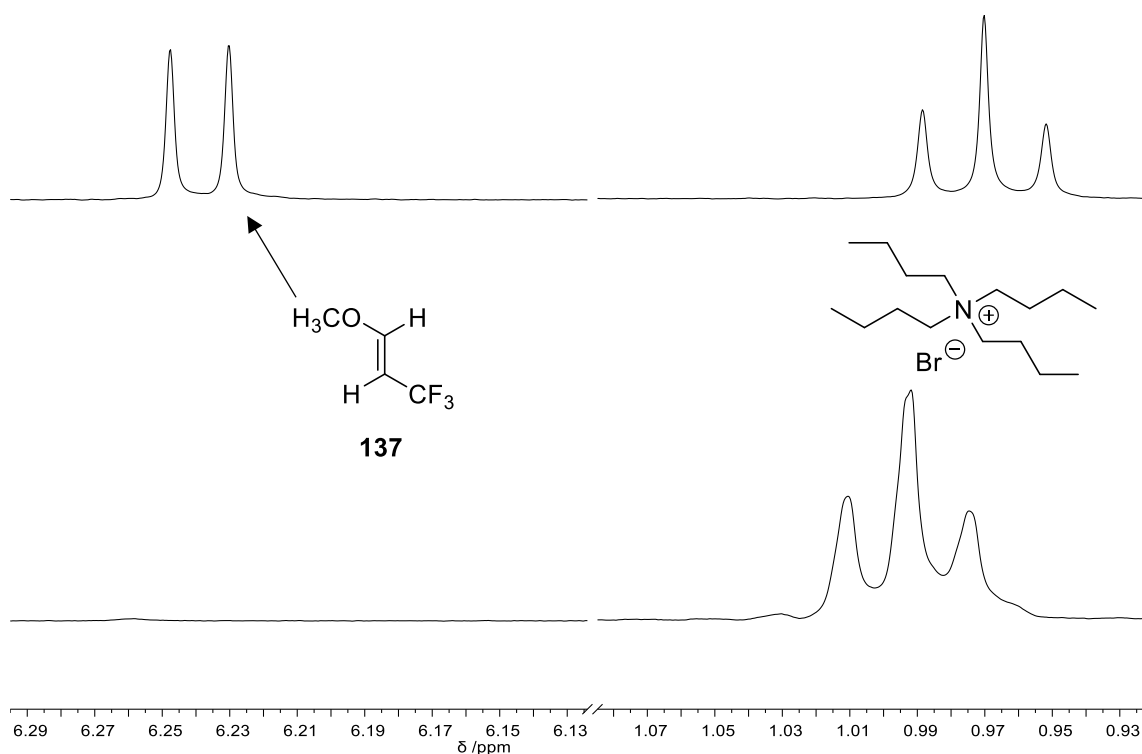
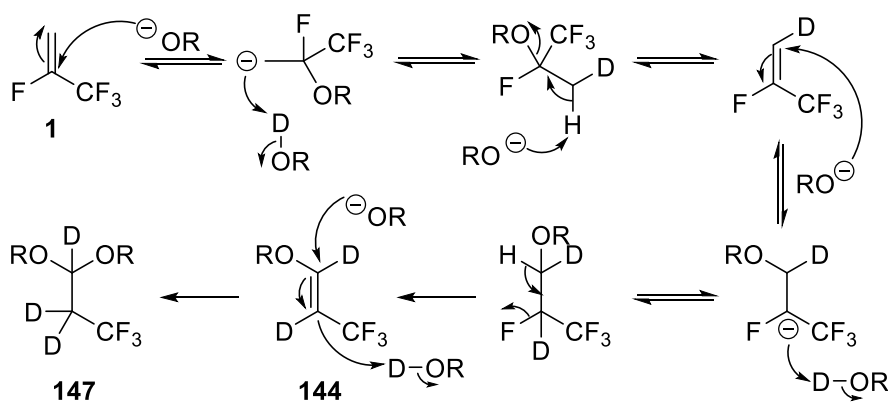


Figure 3.9. ^1H NMR spectrum from reaction of HFO-1234yf with $\text{CH}_3\text{OH}/\text{KOH}/\text{H}_2\text{O}/\text{Bu}_4\text{NBr}$ (top) and $\text{CD}_3\text{OD}/\text{NaOD}/\text{D}_2\text{O}/\text{Bu}_4\text{NBr}$ (bottom) at $130\text{ }^\circ\text{C}$ for 6 hours

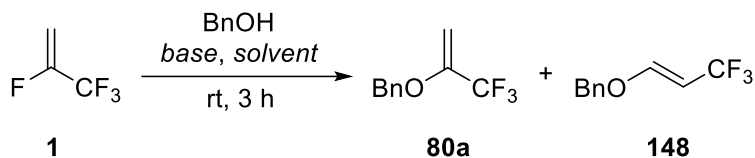


Scheme 3.15. Proposed mechanism for incorporation of deuterium into **145** and **147**

3.2.2 Reactions of HFO-1234yf with alkoxides

Having established a plausible mechanism for the nucleophilic substitution reaction of **1**, optimised conditions were sought for the synthesis of α -trifluoromethyl enol ethers using the operationally simple gas bladder approach. Yamazaki *et al.* obtained 2-benzyloxy-3,3,3-trifluoroprop-1-ene, **80a**, in quantitative yield using sodium hydride as the base and DMF as the solvent. However, the pyrophoricity of NaH and toxicity of DMF make them

less desirable choices, particularly if the reaction were to be scaled up. A range of alternative bases and solvents were tested and the conversion from BnOH to **80a** was measured (Scheme 3.16). Conversion of **1** to the products was determined by comparison of the signals for the respective benzylic protons in the ^1H NMR spectra (Table 3.1). Formation of β -regioisomer **148** was also observed under some conditions.



Scheme 3.16. Reaction of 1 with benzyl alcohol for screening of conditions

Table 3.1. Screening of conditions for reaction of 1 with benzyl alcohol

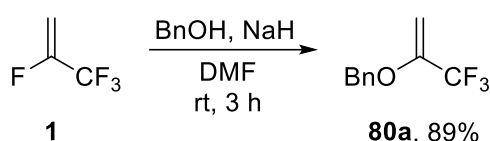
Base	Solvent	% 80a ^[a]	% 148 ^[a]
KO ^t Bu		29	10
NaO ^t Bu	DMF	19	3
NaHMDS		80	0
Cs ₂ CO ₃		0	0
		THF	42
	MeTHF	13	0
	DMA	100	0
NaH	NMP	98	0
	DMSO	100	0
	Acetonitrile	97	3
	Propylene carbonate	39	0

^[a] determined by ^{19}F NMR spectroscopy

The relatively poor solubility of **1** in THF and MeTHF is believed to be the reason for the lower conversions in these solvents. Polar aprotic solvents are generally the best options with DMA and DMSO both showing complete conversion to the desired product **80a**. Some **148** was formed in acetonitrile, likely the result of incomplete drying of the solvent as this would provide a proton source and so allow the intermediate carbanions to be protonated and so give access to the β -regioisomer. Propylene carbonate caused significant transesterification and, therefore, was not a viable solvent. Of all the bases trialled, only sodium hexamethyldisilazane (NaHMDS) was found to be a viable

alternative to NaH. For the *tert*-butoxide bases, decomposition on storage to form the equivalent alcohol and KOH or NaOH is probably responsible for the formation of **148**.

Overall, Yamazaki's original conditions using DMF and NaH gave one of the highest conversions and were more convenient on a lab scale than using DMSO so were used for further reactions. The synthesis of **80a** was successfully repeated on an increased scale of using a simple rubber gas bladder set-up to produce approximately twenty grams of **80a** (Scheme 3.17). The reaction remained entirely regioselective for the α -regioisomer. By using **1** in a large excess with respect to benzyl alcohol, **80a** could be isolated in excellent yield with simple filtration through Celite and aqueous workup needed for purification.



Scheme 3.17. Optimised conditions for reaction of HFO-1234yf with sodium benzyloxide

The products **80a** and **148** showed identical H-F coupling patterns with very similar coupling constants to those seen for **136** and **137** respectively. For **80a**, further information was obtained through ^1H - ^1H NOESY spectroscopy, which revealed a through-space correlation between the vinylic proton that is coupled to the CF_3 group and the benzylic protons (Figure 3.10). This demonstrates that it is the vinylic proton *trans* to the CF_3 group that shows H-F coupling whereas the vinylic proton *cis* to the CF_3 group shows no H-F coupling, which confirms our earlier assignments of stereochemistry.

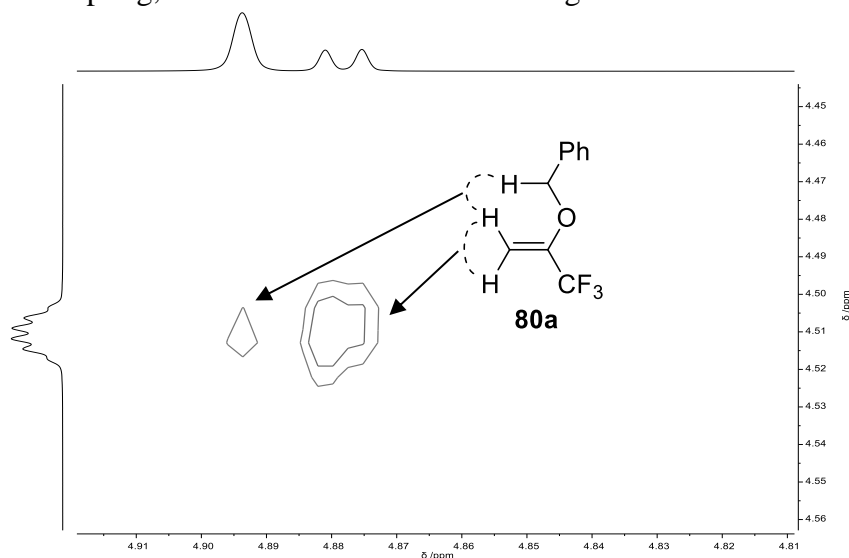
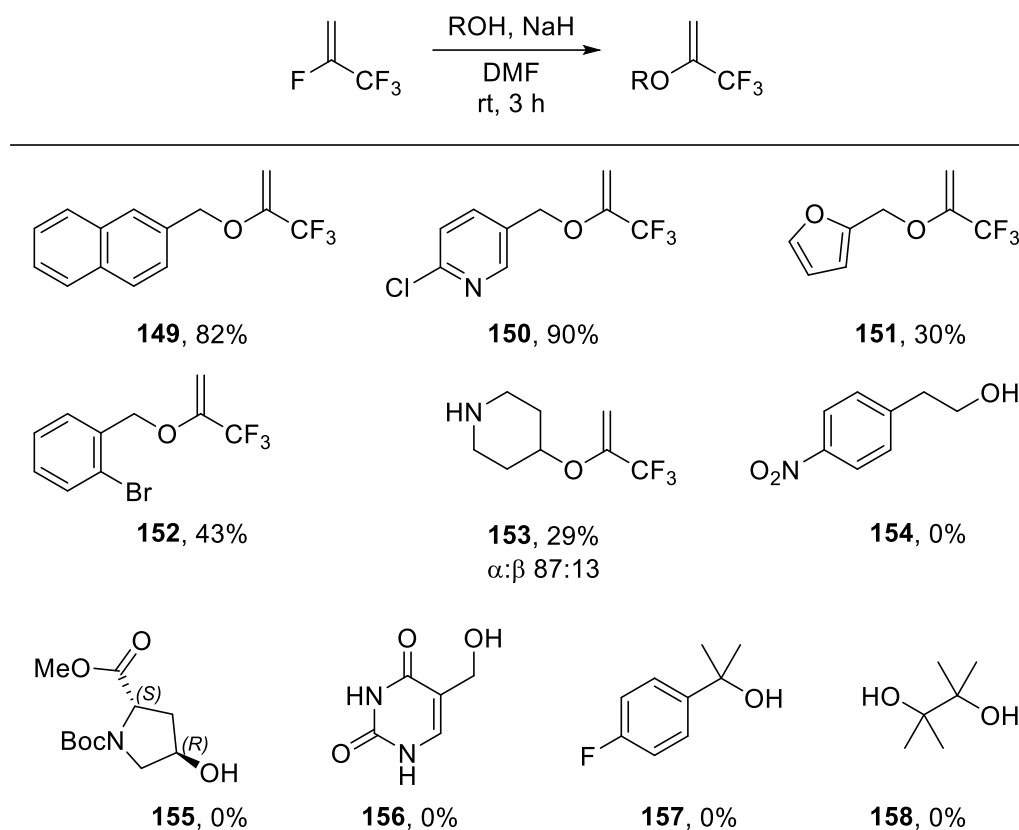


*Figure 3.10. ^1H - ^1H NOESY spectrum of **80a** with key coupling highlighted*

The scope and limitations of this α -trifluoromethyl enol ether synthesis were then explored, focusing on pharmaceutically relevant sp^3 -rich and heterocyclic substrates (Scheme 3.18). As before, the only purification needed in most cases was a simple filtration followed by aqueous workup. Naphthyl (**149**), pyridinyl (**150**) and furanyl (**151**) cyclic systems were well tolerated, with the lower yield for **151** attributed to the volatility of the product rather than any chemical incompatibility. The presence of an activated chloride functionality had no detrimental impact on the yield of **150**. 2-Bromobenzyl alcohol (**152**) gave a similar yield to that obtained by Yamazaki with 4-bromobenzyl alcohol, suggesting that there is no significant impact of steric hindrance on the reaction.



Scheme 3.18. Substrate scope for synthesis of α -trifluoromethyl enol ethers

Free amines were tolerated but gave significantly reduced yield of piperidinyl enol ether **153** as a mixture of α - and β -regioisomers was obtained as the free amine acted as a proton source. 4-Nitrobenzyl alcohol was reported to be unreactive by Yamazaki and we found that 4-nitrophenethyl alcohol (**154**) was similarly unreactive, suggesting some reactions involving sodium hydride and the nitro group are to blame rather than the nitro group simply being too electron-withdrawing. Amide (**155** and **156**) substrates were unsuccessful as the corresponding alkoxides had poor solubility in DMF and so negligible

conversion was obtained in all four cases. Tertiary alcohols (**157** and **158**) were likewise completely unreactive. **149** was a crystalline solid and so allowed for unequivocal confirmation of regioselectivity by X-ray crystallography (Figure 3.11).

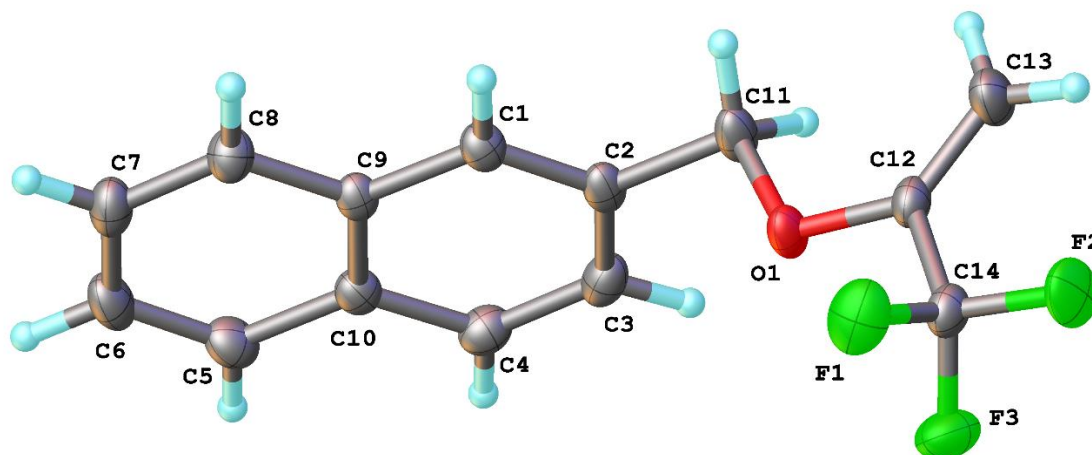
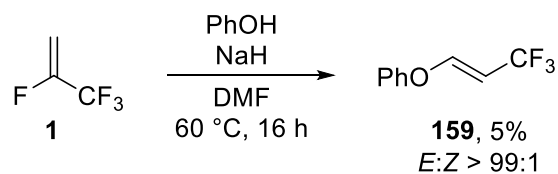


Figure 3.11. Molecular structure of **149** as determined by X-ray crystallography

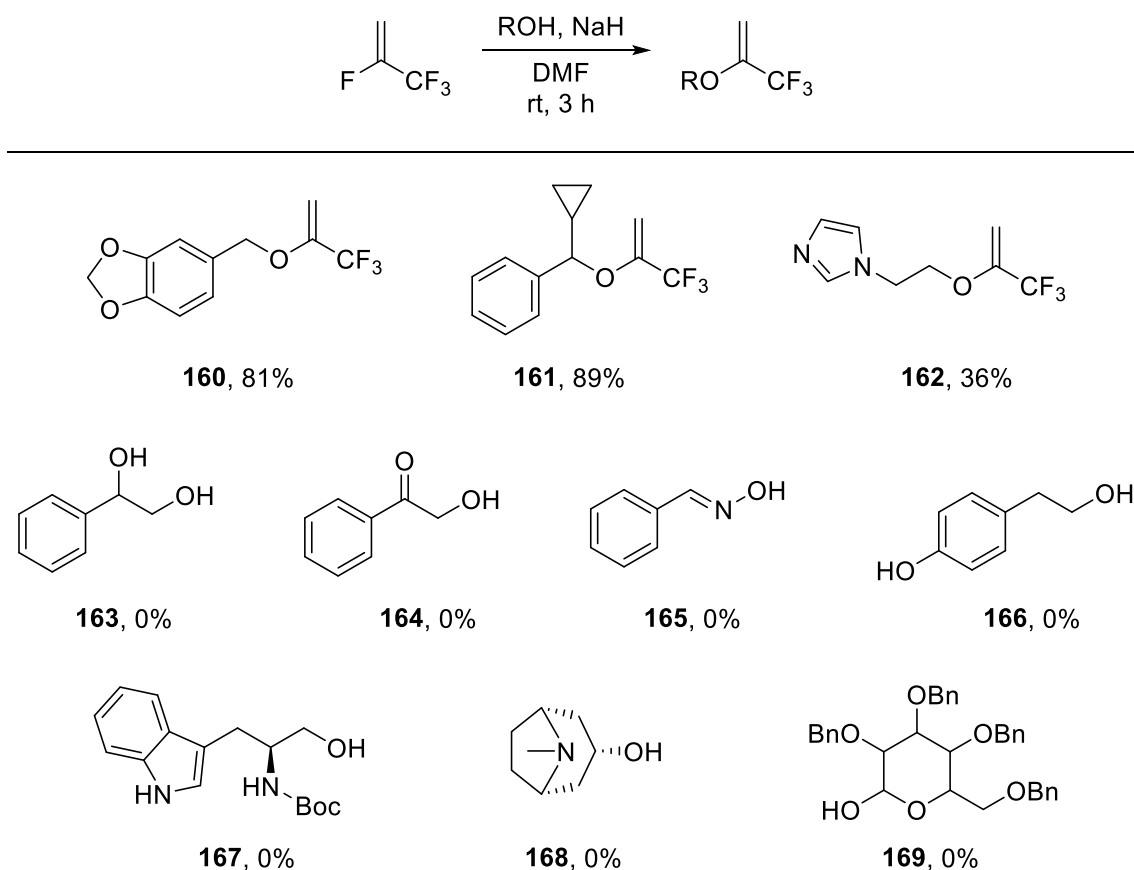
Phenols were reported by Yamazaki *et al.* to be unreactive with **1** at room temperature. However, at 60 °C, we found that **1** and 2-naphthol reacted in DMF with sodium hydride, albeit giving very low conversion to enol ether **159** (Scheme 3.19). Only the *E*-stereoisomer of the β -regioisomer was obtained, which is consistent with our mechanistic proposal. The low yield can be attributed to a lack of any proton source besides residual water in the reaction. No α -regioisomer formation was detected, possibly because the phenol is too bulky to attack adjacent to the trifluoromethyl group.



Scheme 3.19. Reaction of HFO-1234yf with sodium phenoxide

Some further examples of α -CF₃ enol ether syntheses from **1** were carried out by MChem student Ellis Ball at Durham and are included below in Scheme 3.20 for completeness. The presence of piperonyl (**160**), cyclopropyl (**161**) and imidazolyl (**162**) systems were all well-tolerated, with the lack of side reactions for the cyclopropyl derivative providing further evidence for a lack of radical intermediate formation in the mechanism of these reactions. Diol **163** reacted with **1** successfully but formed a mixture of mono- and di-

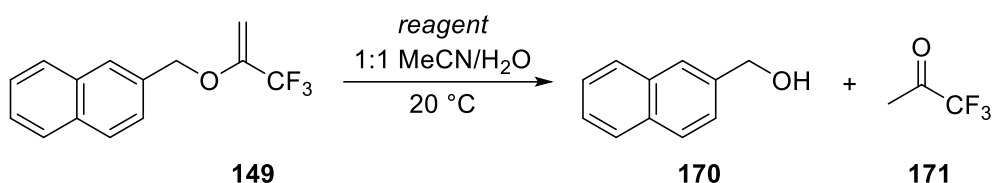
substituted products that could not be readily separated. Acetophenone derivative **164** formed a complex mixture of products, likely due to interfering enolisation processes. Oxime **165**, tyrosol **166** and amino alcohols **167** and **168** were all completely unreactive with **1**, likely due to the solubility issues discussed above. Finally, under these conditions, debenzoylation of protected sugar **169** was observed leading to clean formation of benzylic enol ether **80a** from reaction of the benzyl alcohol formed *in situ* with **1**.



Scheme 3.20. Reactions of HFO-1234yf with alcohols carried out by MChem student Ellis Ball

3.2.3 Reactions of α -trifluoromethyl enol ethers

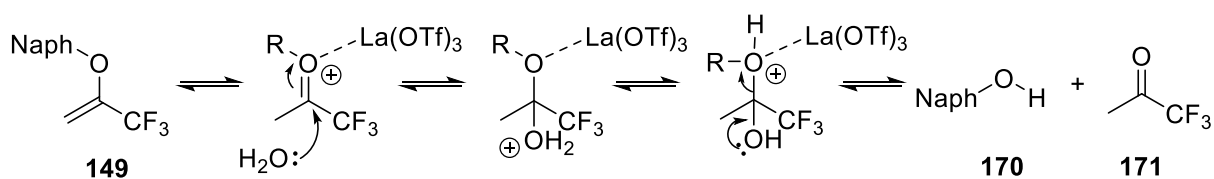
The stability of α -trifluoromethyl enol ethers under various conditions was investigated to establish their potential utility as building blocks to access more complex CF_3 -substituted systems. Conditions were sought (listed in Table 3.2) that could hydrolyse naphthyl enol ether **149** to 2-naphthalenemethanol (**170**) and the highly volatile 1,1,1-trifluoroacetone (**171**), as shown in Scheme 3.21.

Scheme 3.21. Hydrolysis of **149** to give **170** and **171**Table 3.2. Screening of hydrolysis conditions for **149**

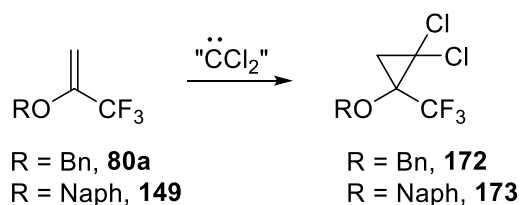
Reagent	Reaction time /h	% Conversion ^[a]
HCl (37%)	48	0
HBr (48%)	4	0
HI (55%)	4	0
(CO ₂ H) ₂	48	0
TsOH	16	0
La(OTf) ₃	4	83
(NH ₄) ₂ Ce(NO ₃) ₆	16	0
Cs ₂ CO ₃	48	0
NaOH	48	0
Et ₃ N	48	0
DBU	48	0

^[a] determined by ¹⁹F NMR analysis of crude reaction mixture

149 proved remarkably resilient to hydrolysis by Brønsted acids and bases including oxalic acid, which is commonly used for deprotection of benzylic enol ethers.³³ Even acids such as HI with nucleophilic anions were tolerated. Likewise, radical deprotection conditions using cerium(IV) ammonium nitrate (CAN) were unsuccessful. Lanthanum(III) triflate was trialled as a mild Lewis acid and showed good conversion, with a ¹⁹F NMR signal consistent with **171** detected.³⁴ Using boron trifluoride diethyl etherate with anhydrous dichloromethane as the solvent gave only 13% conversion, which would suggest the presence of water is significant (Scheme 3.22).

Scheme 3.22. Proposed mechanism for Lewis acid-catalysed hydrolysis of **149**

CF₃-substituted cyclopropane rings (TFCPs) have been proposed as metabolically stable bioisosteres for *tert*-butyl groups³⁵ and are, therefore, interesting structures in medicinal chemistry. Cyclopropanation of enol ethers derived from **1** would, in principle, provide a route to TFCPs in just two steps from an inexpensive building block. Attempted addition of dichlorocarbene (Scheme 3.23) via various methods was attempted but the highest conversion obtained was only 20% (Table 3.3). The product *gem*-dichlorocyclopropanes (**172** and **173**) are very similar in polarity to the parent enol ether and so isolation by column chromatography was not possible. Attempted hydrolysis of the enol ether to aid separation led to decomposition of the cyclopropyl ring.



Scheme 3.23. General *gem*-dichlorocyclopropanation of α -CF₃ enol ethers

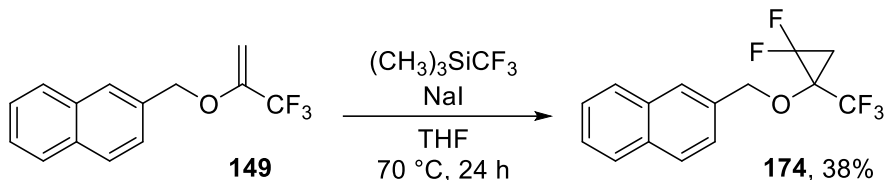
Table 3.3. Conditions attempted for *gem*-dichlorocyclopropanation of α -CF₃ enol ethers

R	Base	CCl ₂ source	PTC	Solvent	T / °C	% ^[a]
Bn	KOH	CHCl ₃	Bu ₄ NBr	CH ₂ Cl ₂	40	8
	KOH	CHCl ₃	Bu ₄ NBr	CH ₂ Cl ₂	40	0
	KO ^t Bu	CHCl ₃	-	THF ^[b]	20	0
	NaOMe	CCl ₃ CO ₂ Et	-	THF ^[b]	0-20	0
	KOH	CHCl ₃	Bu ₄ NBr	CH ₂ Cl ₂ ^[b]	40	0
	NaOH	CHCl ₃	BnEt ₃ NCl	-	20	6
Naph	KOH	CHCl ₃	BnEt ₃ NCl	CH ₂ Cl ₂	20	5
	NaOH	CHCl ₃	BnEt ₃ NCl	CH ₂ Cl ₂	20	0 ^[d]
	KOH	CHCl ₃	BnEt ₃ NCl	CH ₂ Cl ₂	20	0 ^[d]
	KOH	CHCl ₃	BnEt ₃ NCl	-	40	5 ^[d]
	KOH	CHCl ₃	BnEt ₃ NCl & Et ₃ N	-	40	0 ^[d]
	KOH	CHCl ₃	BnEt ₃ NCl	-	20	5
	KOH	CHCl ₃ ^[c]	BnEt ₃ NCl	-	20	20
	KOH	CHCl ₃	BnEt ₃ NCl	-	60	5
	NaOH	CHCl ₃	BnEt ₃ NCl & NaCl	-	50	3 ^[d]

[a] % conversion determined by ¹⁹F NMR spectroscopy after overnight reaction [b] dry solvent was used;

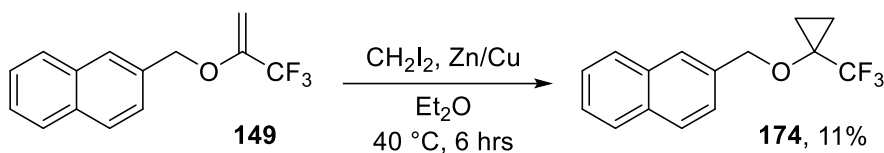
[c] CHCl₃ was degassed; [d] syringe pump was used

Better conversion was obtained using Prakash's method of generating difluorocarbene from TMS-CF₃,³⁶ using the slow addition protocol developed by Grygorenko,³⁷ forming *gem*-difluorocyclopropane **174** with reasonable conversion (Scheme 3.24). However, isolation was again not possible as above due to the similar polarities of **149** and **174**.



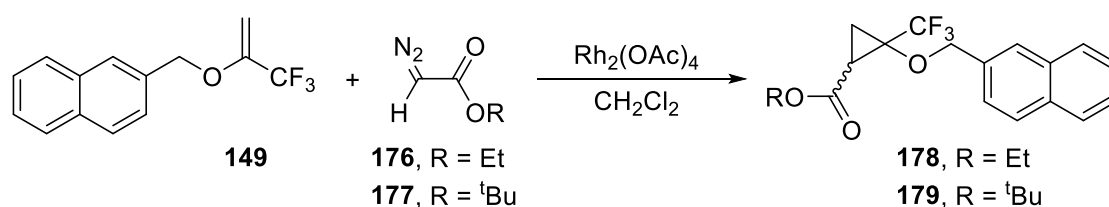
Scheme 3.24. gem-Difluorocyclopropanation of 149 (not isolated)

Attempted Simmons-Smith reaction to give the unsubstituted cyclopropane **175** was also unsuccessful, giving very low conversion (Scheme 3.25) and attempted synthesis of **175** via the Corey-Johnson-Chaykovsky reaction using trimethylsulfoxonium iodide and sodium hydride also proved unsuccessful. Cyr *et al.* recently reported the cyclopropanation of CF₃-substituted styrenes using methyl(diphenyl)sulfonium tetrafluoroborate and sodium hexamethyldisilazane in THF.³⁸ However, using their conditions, no reaction was observed by ¹⁹F NMR spectroscopy after one hour at room temperature nor on microwave heating to 80 °C for one hour.



Scheme 3.25. Cyclopropanation of 149 to give 175 (not isolated)

The reaction of diazoacetates **176** and **177** with **149** was attempted using rhodium(II) acetate as a catalyst (Scheme 3.26), which has previously been used for the cyclopropanation of α -CF₃ silyl enol ethers.³⁹ As shown in Table 3.4, increasing reaction time led to the greatest improvement in conversion whereas heating and increasing catalyst loading gave little or no improvement. As with previous examples, the isolation of the product cyclopropanes **178** and **179** proved too difficult. Attempted direct cyclopropanation of **1** with ethyl diazoacetate under these conditions to give the equivalent tetrafluorinated cyclopropane was also unsuccessful, showing no reaction by ¹⁹F NMR spectroscopy.



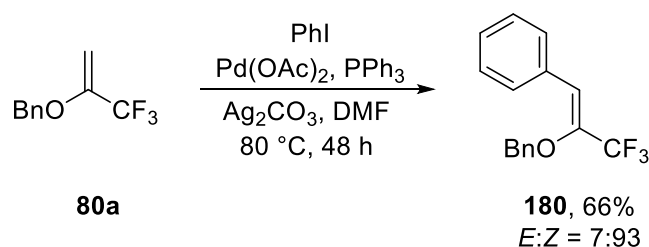
Scheme 3.26. Rhodium-catalysed cyclopropanation of **149** with diazoacetates

Table 3.4. Screening of reaction conditions for rhodium-catalysed cyclopropanation of **149**

R	<i>t</i> /hrs	<i>T</i> /°C	Catalyst /mol-%	% Conversion ^[a]	<i>d.r.</i> ^[a]
Et	1	20	2.5	35	51:49
Et	5	20	2.5	42	53:47
Et	6	30	2.5	49	55:45
^t Bu	6	20	5	44	64:36

^[a]determined by ¹⁹F NMR spectroscopy

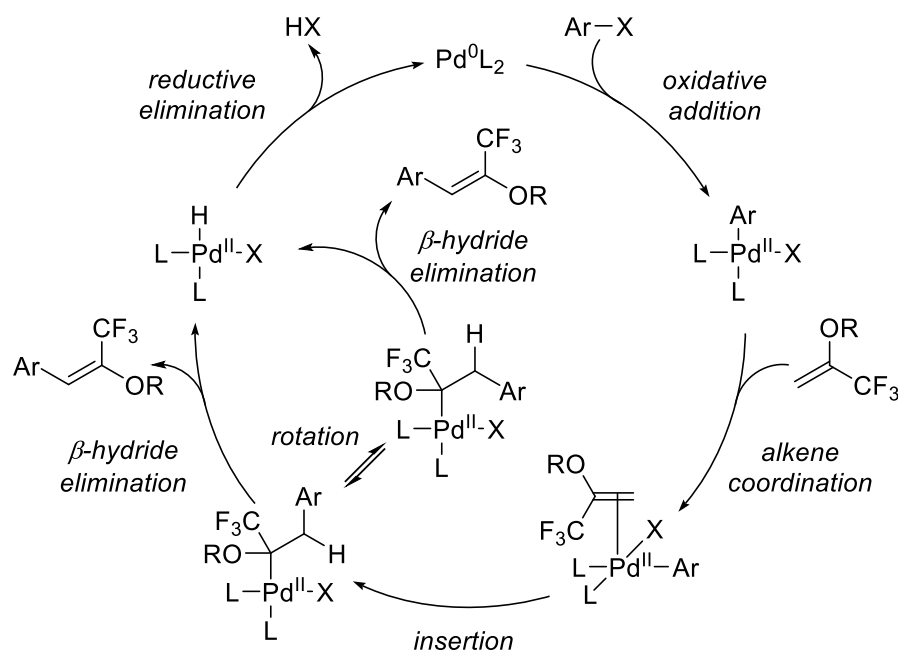
Heck coupling reactions are another well-established means of functionalising alkenes to form new C-C bonds. However, no Heck couplings have previously been reported for α -trifluoromethyl enol ethers. Using the conditions described by Shi *et al.* for coupling of the β -regioisomers,⁴⁰ **80a** was reacted with iodobenzene using palladium acetate and triphenylphosphine as the catalyst system, with silver carbonate acting as a base and iodide ion scavenger (Scheme 3.27).



Scheme 3.27. Heck coupling of **80a** with iodobenzene to give **180** (not isolated)

Conversion to aryl enol ether **180** reached 66% after 22 hours as determined by ¹⁹F NMR spectroscopy and there was no further reaction after a further 26 hours and the product was not isolated. However, as with the cyclopropyl derivatives described above, isolation of the products proved difficult due to their similar polarity to the starting material. The product mixture was found, again by ¹⁹F NMR spectroscopy, to contain a 93:7 ratio of the *Z*- and *E*-stereoisomers respectively. The stereoisomers could be identified by NMR spectroscopy as the *Z*-stereoisomer shows no H-F coupling as the alkenyl proton is *cis* to the CF₃ group whereas the *E*-stereoisomer, where the alkenyl proton is *trans*, displays a

small H-F coupling of 0.7 Hz. Stereoselectivity in Heck coupling reactions is determined by the relative steric clash in the intermediate palladium complex prior to β -hydride elimination (Scheme 3.28). In this case, the Ar-CF₃ interaction is more disfavoured than Ar-OBn and so the Z-stereoisomer is the major product. Smaller alkoxy groups would presumably increase this stereoselectivity by decreasing the Ar-OR interaction.



Scheme 3.28. Mechanism for Heck coupling reaction of an α -trifluoromethyl enol ether

After these initial results, optimised conditions for the Heck coupling reaction were sought. Iodobenzene was replaced with bromobenzene due to the problematic nature of handling hazardous iodinated waste and a microwave reactor was used to allow for higher temperatures. A range of catalysts and bases were screened and the conversion from **80a** to **180** was determined by ¹⁹F NMR spectroscopy (Table 3.5).

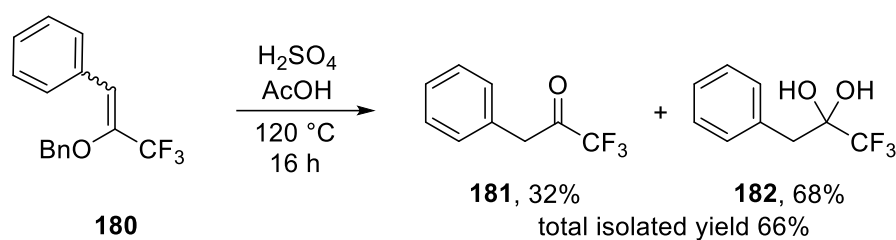
Table 3.5. Catalyst and base screening for Heck coupling of **80a** (DMF, 150 °C, 30 min)

Catalyst	Base	% Conversion ^[a]
$\text{Pd}(\text{OAc})_2/\text{PPh}_3$	Ag_2CO_3	17
$\text{Pd}(\text{dppf})\text{Cl}_2$	Et_3N	0 ^[b]
$\text{Pd}(\text{dppf})\text{Cl}_2/\text{PPh}_3$	K_3PO_4	2
$\text{Pd}(\text{dba})_2$	K_3PO_4	0
$\text{Pd}(\text{PPh}_3)_4$	K_3PO_4	6

^[a] determined by ¹⁹F NMR spectroscopy; ^[b]3 hrs at 80 °C (non-microwave)

Poor conversion was obtained using bromobenzene in spite of the use of a significantly higher temperature. Other catalyst and base systems used in the literature for Heck reactions, shown in Table 3.5, gave worse conversion than our original conditions.

Yagupolskii *et al.* showed that the β -trifluoromethyl enol ether could be hydrolysed to give 3,3,3-trifluoropropanal.³ While the α -regioisomer should be able undergo the same reaction, this would yield the highly volatile and already readily-available 1,1,1-trifluoroacetone so would be of little synthetic use. However, hydrolysis of the substituted enol ethers obtained by Heck coupling would provide access to α -trifluoromethyl- β -aryl ketones that otherwise might be challenging to synthesise. The crude reaction mixture for the initial synthesis of **180** from **80a** and iodobenzene was hydrolysed under acidic conditions to give ketone **181** (Scheme 3.29). The reaction mixture was found by ¹⁹F NMR spectroscopy to contain some of the desired ketone but more of the equivalent hydrate **182**. After stirring this mixture with phosphorus pentoxide at room temperature for an hour, the ketone to hydrate ratio became approximately 1:1.



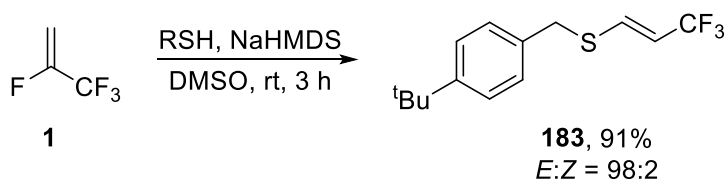
Scheme 3.29. Hydrolysis of 180 to give a mixture of ketone 181 and its hydrate

Subsequently, MChem student Ellis Ball carried out several more reactions of **80a**, which are reported here for completeness. The Heck coupling product **180** was isolated in 67% yield with an *E:Z* ratio of 11:89 using the conditions shown in Scheme 3.27 after rigorous purification via column chromatography. However, attempted reactions with 4-iodoanisole and 4-iodonitrobenzene gave low conversion of 15% and 13% respectively, as determined by ¹⁹F NMR spectroscopy. Further screening of other catalyst systems, notably $\text{Pd}(\text{CF}_3\text{CO}_2)_2$ and AgOTf , as used in the Heck coupling of CF_3 -acrylates,⁴¹ did not lead to improved conversion. Intramolecular Heck coupling of *ortho*-bromobenzyl enol ether **152** was also attempted to form the corresponding isochromene but was unsuccessful due to polymerisation of the product through further Heck coupling reactions. Finally, epoxidation and bromination of **80a** using mCPBA and Br_2 respectively gave clean conversion and isolated yields of 78% and 80%.

3.2.4 Reactions of HFO-1234yf with thiolates

Having established the reactivity of alkoxides with **1**, thiolates were anticipated to follow a similar pattern of regioselectivity. Consequently, the reaction of **1** with 4-(*tert*-butyl)benzyl mercaptan, an odourless alternative to benzyl mercaptan,⁴² and NaH at atmospheric pressure and room temperature via the gas bladder approach was first attempted. However, under these conditions, an intractable complex mixture of products was obtained. The major products appear to be the expected vinyl ether along with its regioisomer and a range of thioacetals, sulfoxides and sulfones. Acetal formation was never observed for the equivalent alcohol reaction and so thioacetal formation is likely due to the increased nucleophilicity of thiols compared to alkoxides.

This reaction was repeated using NaHMDS and DMSO as the base and solvent respectively and this led to varying mixtures, with the product composition strongly dependent on the equivalents of NaHMDS used. Two equivalents of NaHMDS gave the cleanest conversion, forming β -trifluoromethyl vinyl sulfide **183** (Scheme 3.30) in good yield and high purity without needing column chromatography. The large value of the $^3J_{\text{HF}}$ coupling (Figure 3.12) suggests the β -regioisomer whereas the small value of the $^4J_{\text{HF}}$ coupling suggests the *E* stereoisomer. The *Z*-stereoisomer was also seen as a minor side product, which had a larger $^4J_{\text{HF}}$ coupling constant



Scheme 3.30. Reaction of HFO-1234yf and 4-(*tert*-butyl)benzyl mercaptan with NaHMDS

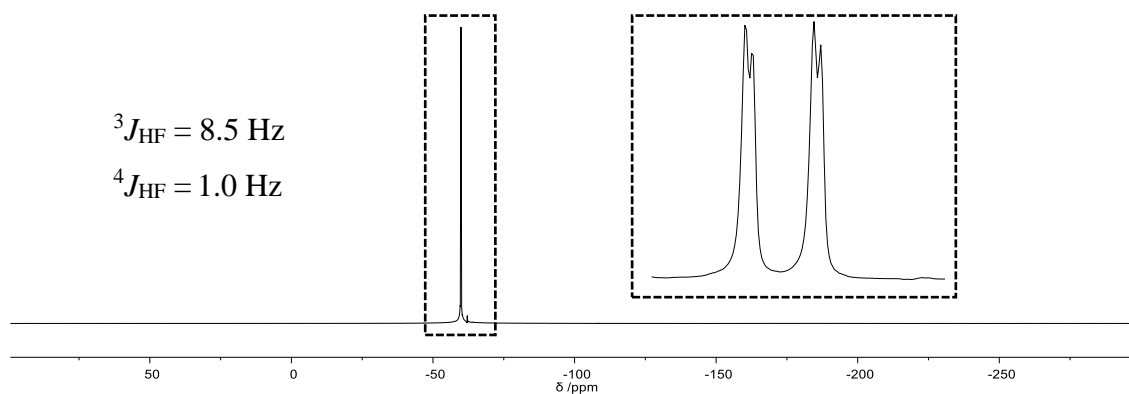
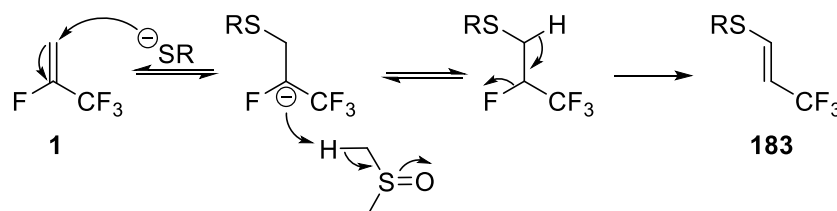


Figure 3.12. ^{19}F NMR spectrum (376 MHz; CDCl_3) of **183**

This change in regioselectivity could be due to steric hindrance, with the increased size of the thiolate compared to an alkoxide making approach to the CF₃-substituted carbon more hindered. An alternative, complementary explanation is that the softer nature of the sulfur-centered nucleophile favours attack at the opposite end of the molecule due to more favourable orbital overlap. The stereochemical assignment was made based on the fact vicinal alkene protons typically have lower coupling constants for *cis* protons.²⁶ Selectivity for the *E*-stereoisomer is also supported by our proposed mechanism for the reaction of **1** with nucleophiles. Initially, the sodium thiolate adds to **1** to form a carbanion intermediate stabilised by the highly electron-withdrawing nature of the adjacent fluorine atoms (Scheme 3.31). This carbanion is then protonated and eliminates HF to give the vinyl sulfide product. Via an E2 elimination mechanism, the *E*-stereoisomer would be expected to be the major product due to there being less steric clash in the conformation of the protonated intermediate leading to this product and this is what is observed in the synthesis of **183**, with very little *Z*-stereoisomer detected.

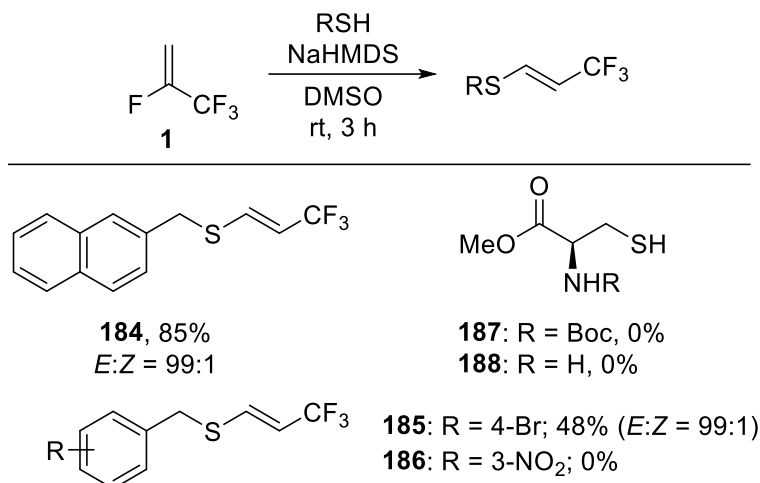


Scheme 3.31. Proposed mechanism for formation of 183

Using this mechanistic information, formation of the β -trifluoromethyl regioisomer requires a proton source. Using DMSO as the solvent provides a possible proton source, although the pK_a of DMSO is 35⁴³ while NaHMDS is only approximately 26.⁴⁴ It could be that the intermediate carbanion is more basic and so is able to deprotonate DMSO.

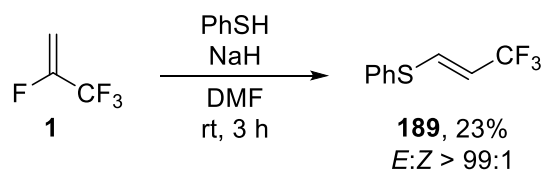
A brief substrate scope (Scheme 3.32) for the reaction of **1** with different thiolates was then carried out. Naphthyl and bromobenzyl thiols were used successfully to form vinyl sulfides **184** and **185** whereas 3-nitrobenzyl mercaptan was unsuccessful in forming **186**. The 2-naphthyl thiol starting material for the synthesis of **184** was not commercially available and so was prepared by reaction of 2-bromonaphthalene with thiourea followed by alkaline hydrolysis in an overall isolated yield of 44% over two steps. The use of L-cysteine methyl ester, both as the *N*-Boc amide (**187**) and the free amine (**188**), led to formation of complex mixtures, possibly due to side reactions with the ester group or

disulfide formation. Changing solvent to DMF did not improve selectivity, suggesting any potential redox activity of DMSO is not at fault in this case. This matches the functional group tolerance observed for reactions of **1** with alkoxides and suggests that the same range of substrates could be used for the equivalent reaction with thiolates.



Scheme 3.32. Substrate scope for reactions of HFO-1234yf with thiolates

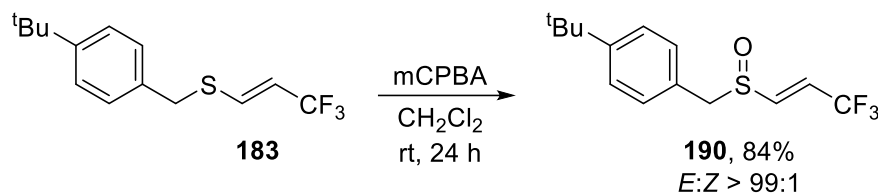
Thiophenol was also successfully used as a nucleophile at room temperature, returning to sodium hydride as a base, to form **189** (Scheme 3.33). Whilst **189** was obtained in low yield, the reaction of **1** with a phenoxide to form enol ether **159** required heating and gave an isolated yield of only 5%. This difference is likely simply due to the relatively higher nucleophilicity of thiolates when compared to alkoxides.



Scheme 3.33. Reaction of HFO-1234yf with sodium thiophenolate

Oxidation of **183** to give the corresponding sulfone was attempted as such an electron-poor alkene would be a highly reactive building block in, for example, Diels-Alder reactions. However, the use of Oxone[®], mCPBA and hydrogen peroxide gave only sulfoxide **190**, as evidenced by mass spectrometry, without any loss of stereoselectivity. Stronger oxidising reagents, such as potassium permanganate, gave intractable complex mixtures of products. Nevertheless, **190** was obtained in a high yield using mCPBA (Scheme 3.34) and could be a useful building block in its own right, with similar CF₃-

vinyl sulfoxides having previously been used as Michael acceptors⁴⁵ and reacting via aryne σ -bond insertion into the S–O-bond.⁴⁶



Scheme 3.34. Oxidation of vinyl sulfide **183** to give sulfoxide **190**; R = 4-(*tert*-butyl)benzyl

3.2.5 Reactions of HFO-1244yf with other nucleophiles

Hexafluoropropene (**75**) reacts rapidly with diethylamine at 0 °C to give Ishikawa's reagent (**21**).⁴⁷ This precedent suggested **1** may also react with amines and so addition of benzylamine was used as a model reaction and attempted under a range of different conditions (Table 3.6) but in no case was any reaction observed by ¹⁹F NMR spectroscopy after stirring and heating overnight.

Table 3.6. Screening of conditions for the reaction of **1** with benzylamine

Solvent	Base	<i>T</i> / °C	<i>t</i> / h	Result
MeCN	-	75	16	no reaction
MeCN	Et ₃ N	75	16	no reaction
Et ₃ N	-	75	16	no reaction
DMF	DMAP	80	18	no reaction
DMF	K ₃ PO ₄	80	16	no reaction
DMF	Cs ₂ CO ₃	80	16	no reaction

Likewise, the reaction of **1** with imidazole was attempted with sodium hydride in DMF. However, there was again no observable reaction. This is in spite of the imidazolyl anion being approximately 10⁵ times more nucleophilic than the methoxide anion.⁴⁸ This suggests that steric hindrance plays a significant role in determining the reactivity of **1** with nucleophiles. Indeed, this is consistent with tertiary alkoxides being wholly unreactive with **1** and the complete change in regioselectivity between benzyloxide and phenoxide nucleophiles reported earlier.

An alternative approach to reacting **1** with amines was then attempted using *N*-methylbenzylamine and *n*-butyl lithium to form the corresponding lithium amide. This showed some reaction but not to the intended trifluoromethyl enamine product. Instead, elimination of HF from **1** was observed to form 3,3,3-trifluoropropyne. The same reaction was observed between **1** and sodium amide or, moving to carbon-centered nucleophiles, with **1** and *n*-butyl lithium, *n*-Bu₂CuLi (Gilman reagent), phenyl lithium or lithium phenylacetylide. Chapter 4 details our investigations of the synthetic utility of this lithiation-elimination procedure.

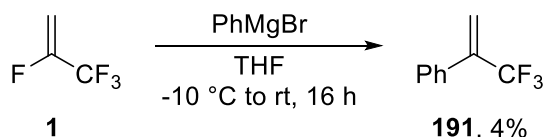
The reaction of **1** with a wide range of other carbon-centered nucleophiles was also attempted but in no case was any reaction observed. A number of different enolates were generated with various different bases (Table 3.7) but all were unreactive towards **1** under all conditions trialled.

Table 3.7. Screening of conditions for the reaction of **1** with enolates

Ketone	Base	Solvent	<i>T</i> / °C	<i>t</i> / h	Result
Dimethyl malonate	NaH	DMF	20	16	no reaction
	NaH	DMF	60	3	no reaction
	NaH	DMF	60	16	no reaction
	NaOMe	THF	60	16	no reaction
	NaH	DMSO	20	48	no reaction
	NaH	DMSO	60	3	no reaction
Dibenzoyl methane	NaH	DMSO	20	16	no reaction
	NaH	DMSO	60	16	no reaction
	KO ^t Bu	DMSO	20	16	no reaction
	KO ^t Bu	DMSO	60	3	no reaction
Acetophenone	NaH	DMF	20	1	no reaction
Cyclohexane-1,3-dione	Cs ₂ CO ₃	DMF	60	16	no reaction
	NaHMDS	DMF	60	16	no reaction
	NaH	DMF	60	16	no reaction

Similarly, deprotonation of nitromethane with sodium hydride in DMF to give the corresponding carbanion was carried out but the anion did not act as a nucleophile

towards **1**. The reaction of **1** and Grignard reagent phenylmagnesium bromide gave very low conversion, observed by ^{19}F NMR spectroscopy, to a peak that could correspond to α -trifluoromethylstyrene (**191**), as shown in Scheme 3.35. However, all attempts to improve this conversion failed, including the use of CuI or $\text{NiCl}_2(\text{dppe})$ catalysts. **1** was also unreactive towards sodium azide or ammonium thiocyanate in DMF at room temperature and with *in situ* generated cyanide⁴⁹ and CF_3^- anions.⁵⁰



Scheme 3.35. Reaction of HFO-1234yf with Grignard phenylmagnesium bromide (not isolated)

3.3 Conclusions

Beginning from a discrepancy observed in the reported reactivity of 2,3,3,3-tetrafluoropropene (HFO-1234yf, **1**) with alkoxide nucleophiles, the literature conditions were repeated and found to both be accurate. Through computational and reactive intermediate trapping studies, this differing regioselectivity was found to result from a difference in mechanism under protic and aprotic conditions. In the absence of any proton source, i.e. Yamazaki's conditions using sodium hydride in DMF, the intermediate carbanion formed reacts by direct elimination of fluoride to form the α -trifluoromethyl enol ether product. By contrast, if a proton source is present, i.e. Yagupolskii's conditions with hydroxide in ethanol, lead to protonation of the intermediate carbanion and subsequent elimination of HF to form a mixture of α - and β -trifluoromethyl enol ethers.

With a better understanding of the reactivity of **1** established, the synthesis of α - CF_3 enol ethers was optimised and a substrate scope explored. The original literature conditions of sodium hydride in DMF proved the most effective but NaHMDS in DMSO could be a viable alternative. Various synthetically useful functional groups, such as activated heteroaryl chlorides, aryl bromides and free amines, were tolerated to varying extents under the reaction conditions although amide-bearing systems and tertiary alcohols were unreactive. These reactions require only a simple aqueous workup and filtration, making them highly scalable. X-ray crystallography was used to unequivocally confirm the structure of the naphthyl derivative synthesised in this process. These enol ethers were

found to be resistant to hydrolysis under most conditions except using La(OTf)₃ as a mild Lewis acid. Various cyclopropanation and Heck coupling reactions were attempted but no products could be isolated in any case due to generally poor conversions and the similarity in polarity between the starting materials and products.

Reaction of **1** with thiols gave rise to complex mixtures using the same conditions as alcohols but NaHMDS in DMSO gave clean reaction to form β-trifluoromethyl vinyl sulfides. This opposing regioselectivity can be explained by the fact thiolates are softer and larger nucleophiles than alkoxides and so prefer to attack the softer and less crowded CH₂ vinylic carbon. Similar reactivity was also seen when 2-naphthol was used as the substrate, a softer and more hindered oxygen nucleophile than the others used previously. Both α-trifluoromethyl enol ethers and β-trifluoromethyl vinyl sulfides have the potential to be useful building blocks for a wide range of reactions to access more complex, pharmaceutically relevant CF₃-substituted systems and both classes of compound can be synthesised from the inexpensive and readily available refrigerant gas **1** in just one step under relatively mild conditions with minimal purification required.

Attempted reaction of **1** with various carbon- and nitrogen-centred nucleophiles either gave no reaction, as in the case of amines, azides, enolates, Grignard reagents and cyanides, or elimination of lithium fluoride to give 3,3,3-trifluoropropyne, which was seen with various organolithium reagents. This is in contrast to the high reactivity of perfluoroalkenes towards such nucleophiles reported in the literature and so suggests, despite its four fluorine atoms, **1** is a less-electron poor alkene than might initially be predicted. Further details and applications of the lithiation-elimination reaction are discussed in the next chapter.

3.4 References for Chapter 3

¹ R. D. Chambers, *Fluorine in Organic Chemistry*, 2004, Blackwell Publishing Ltd., Oxford and references cited therein.

² (a) Y. Hiraoka, T. Kawasaki-Takasuka, Y. Morizawa and T. Yamazaki, *J. Fluorine Chem.*, 2015, **179**, 71; (b) T. Yamazaki and Y. Morisawa, JP 168650, 2015.

³ Y. L. Yagupolskii, N. V. Pavlenko, S. V. Shelyazhenko, A. A. Filatov, M. M. Kremlev, A. I. Mushta, I. I. Gerus, S. Peng, V. A. Petrov and M. Nappa, *J. Fluorine Chem.*, 2015, **179**, 134.

- ⁴ J.-P. Bégué, D. Bonnet-Delpon and A. Kornilov, *Synth. Comm.*, 1996, **26**, 1057.
- ⁵ D. Bonnet-Delpon, D. Bouvet, M. Ourévitch and M. H. Rock, *Synthesis*, 1998, **3**, 288.
- ⁶ L. Allain, Lydie, J.-P. Bégué, D. Bonnet-Delpon and D. Bouvet, *Synthesis*, 1998, **6**, 847.
- ⁷ J. J. Gajewski, K. R. Gee and J. Jurayj, *J. Org. Chem.*, 1999, **55**, 1813-.
- ⁸ T. J. Donohoe, L. P. Fishlock, A. R. Lacy and P. A. Procopiu, *Org. Lett.*, 2007, **9**, 953.
- ⁹ S. M. Smith, W. M. Lamanna, M. G. Costello and M. J. Bulinski, WO2017/195070.
- ¹⁰ V. M. Muzalevskiya, V. G. Nenajdenko, A. V. Shastin, E. S. Balenkova and G. Haufe, *Synthesis*, 2009, **13**, 2249.
- ¹¹ M. Das and D. F. O'Shea, *Tetrahedron*, 2013, **69**, 6448.
- ¹² Y. Hosino, K. Isa, T. Hanakawa, H. Tsuji and M. Kawatsura, *Tetrahedron*, 2018, **74**, 1555.
- ¹³ C. Hager, R. Miethchen and H. Reinke, *J. Fluorine Chem.*, 2000, **104**, 135.
- ¹⁴ N. P. Stepanova, N. Ya. Kuzmina, E. S. Tubanova and M. L. Petrov, *J. Org. Chem. USSR (Engl. Transl.)*, 1986, **22**, 1667.
- ¹⁵ M. S. Kim and I. H. Jeong, *Tetrahedron Lett.*, 2005, **46**, 3545.
- ¹⁶ T. Taguchi, G. Tomizawa, M. Nakajima and Yoshiro Kobayashi, *Chem. Pharm. Bull.*, 1985, **33**, 4077.
- ¹⁷ T. Hanamoto, R. Anno, K. Yamada and K. Ryu, *Tetrahedron Lett.*, 2007, **48**, 3727.
- ¹⁸ Z. Mao, F. Huang, H. Yu, J. Chen, Z. Yu and Z. Xu, *Chem. Eur. J.*, 2014, **20**, 3439.
- ¹⁹ Y. Fukuda, T. Kikumura, S. Sakoda, G. Ikeda, Y. Nakamura, M. Dojyo, Y. Yamada and T. Hanamoto, *Synlett*, 2019, **30**, 837.
- ²⁰ F. Laduron, Z. Janousek and H. G. Viehe, *J. Fluorine Chem.*, 1995, **73**, 83.
- ²¹ T. Hanamoto, R. Anno, K. Yamada and K. Ryu, *Tetrahedron Lett.*, 2007, **48**, 3727.
- ²² Y. Li, C. Mück-Lichtenfeld and A. Studer, *Angew. Chem. Int. Ed.*, 2016, **55**, 14435.
- ²³ C.-M. Hu, F. Hong, B. Jiang and Y. Xu, *J. Fluorine Chem.*, 1994, **66**, 215.
- ²⁴ T. Taguchi, G. Tomizawa, A. Kawara, M. Nakajima and Y. Kobayashi, *J. Fluorine Chem.*, 1998, **40**, 171.
- ²⁵ R. Maeda, K. Ooyama, R. Anno, M. Shiosaki, T. Azema and T. Hanamoto, *Org. Lett.*, 2010, **12**, 2548.
- ²⁶ U. Vogeli and W. von Philipsborn, *Org. Magn. Reson.*, 1975, **7**, 617.
- ²⁷ e.g. (a) J.-P. Bégué, D. Bonnet-Delpon and M. H. Rock, *Synlett*, 1995, 659; (b) J. Ichikawa, H. Fukui and Y. J. Ishibashi, *J. Org. Chem.*, 2003, **68**, 7800.
- ²⁸ F. Hong and C.-M. Hu, *Chem. Commun.*, 1996, 57.
- ²⁹ K. Dai, K. Wang, Y. Li, J.-G. Chen, Z.-W. Liu, J. Lu and Z.-T. Liu, *J. Org. Chem.*, 2017, **82**, 4721.
- ³⁰ D. Meyer and M. El Qacemi, *Org. Lett.*, 2020, **22**, 3479.
- ³¹ (a) A. L. Henne and R. Nager, *J. Am. Chem. Soc.*, 1952, **74**, 650; (b) R. N. Haszeldine, *J. Chem. Soc.*, 1952, 3490; (c) E. K. Raunio and T. G. Frey, *J. Org. Chem.*, 1972, **36**, 345.
- ³² S. J. Blanksby and G. B. Ellison, *Acc. Chem. Res.*, 2003, **36**, 255.
- ³³ S. Z. Janicki, J. M. Fairgrieve and P. A. Petillo, *J. Org. Chem.*, 1998, **63**, 3694.
- ³⁴ D. V. Sevenard, A. V. Didenko, D. Lorenz, M. Vorobiev, J. Stelten, T. Dülcks and V. Ya. Sosnovskikh, *Tetrahedron*, 2017, **73**, 1495.
- ³⁵ D. Barnes-Seeman, M. Jain, L. Bell, S. Ferreira, S. Cohen, X.-H. Chen, J. Amin, B. Snodgrass and P. Hatsis, *ACS Med. Chem. Lett.*, 2013, **4**, 514.
- ³⁶ F. Wang, T. Luo, J. Hu, Y. Wang, H. S. Krishnan, P. V. Jog, S. K. Ganesh, G. K. S. Prakash and G. A. Olah, *Angew. Chem. Int. Ed.*, 2011, **50**, 7153.
- ³⁷ P. S. Nosik, S. V. Ryabukhin, O. O. Grygorenko and D. M. Volochnyuk, *Adv. Synth. Cat.*, 2018, **360**, 4104.

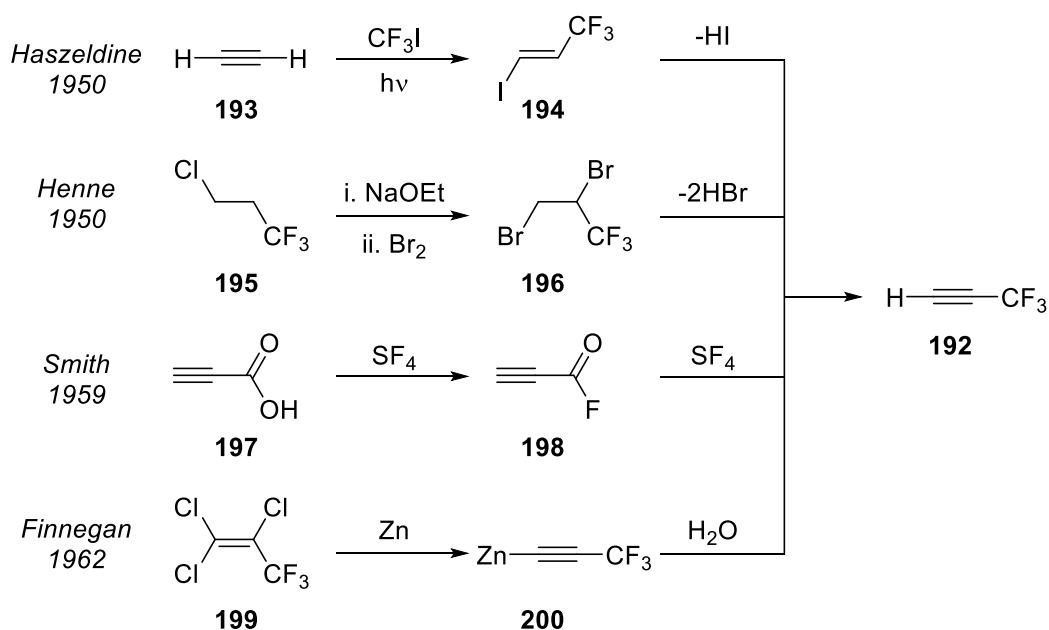
- ³⁸ P. Cyr, J. Flynn-Robitaille, P. Boissarie and A. Marinier, *Org. Lett.*, 2019, **21**, 2265.
- ³⁹ D. Gladow and H.-U. Reissig, *Helv. Chim. Acta*, 2012, **95**, 1818.
- ⁴⁰ G.-Q. Shi, X.-H. Huang and F. Hong, *J. Chem. Soc., Perkin Trans. 1*, 1996, 763.
- ⁴¹ P. Xiao, C. Schlinquer, X. Pannecoucke, J. P. Bouillon and S. Couve-Bonnaire, *J. Org. Chem.*, 2019, **84**, 2072.
- ⁴² M. Node, K. Kumar, K. Nishide, S.-I. Ohsugi and T. Miyamoto, *Tetrahedron Lett.*, 2001, **42**, 9207.
- ⁴³ W. S. Matthews, J. E. Bares, J. E. Bartmess, F. G. Bordwell, F. J. Cornforth, G. E. Drucker, Z. Margolin, R. J. McCallum, G. J. McCollum and N. R. Vanier, *J. Am. Chem. Soc.*, 1975, **97**, 7006.
- ⁴⁴ I. E. Kopka, Z. A. Fataftah and M. W. Rathke, *J. Org. Chem.*, 1987, **52**, 448.
- ⁴⁵ T. Yamazaki and N. Ishikawa, *Chem. Lett.*, 1985, **14**, 889.
- ⁴⁶ Y. Li and A. Studer, *Org. Lett.*, 2017, **19**, 666.
- ⁴⁷ A. Takaoka, H. Iwakiri and N. Ishikawa, *Bull. Chem. Soc. Japan.*, 1979, **52**, 3377.
- ⁴⁸ For alkoxide nucleophilicity: T. B. Phan and H. Mayr, *Can. J. Chem.*, 2005, **83**, 1554; for amine nucleophilicity: M. Breugst, F. C. Bautista and H. Mayr, *Chem. Eur. J.*, 2012, **18**, 127.
- ⁴⁹ J. Zhang, C. Xu, W. Wu and S. Cao, *Chem. Eur. J.*, 2016, **29**, 9902.
- ⁵⁰ L.-F. Jiang, B.-T. Ren, B. Li, G.-Y. Zhang, Y. Peng, Z.-Y. Guan and Q.H. Deng, *J. Org. Chem.*, 2019, **84**, 6557.

Chapter 4: Synthesis and Michael addition reactions of trifluoromethyl ynones

4.1 Introduction

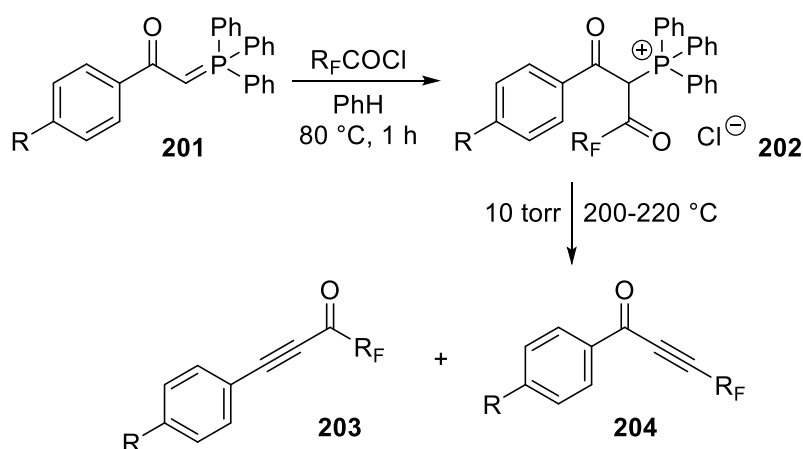
In the course of investigating reactions of **1** with various nucleophiles, as described in Chapter 3, we found that organolithium reagents did not react by an expected S_NV nucleophilic substitution process but, instead, eliminated lithium fluoride directly from **1** to form 3,3,3-trifluoropropyne (**192**). In this chapter, the synthetic utility of the trifluoroalkynyl systems that can be derived from **1** in this manner is explored.

The synthesis of **192** was first reported over 70 years ago by Haszeldine by the addition of CF_3^\bullet , derived photochemically from CF_3I , to acetylene (**193**) followed by dehydroiodination of the resulting iodoalkene **194** (Scheme 4.1).¹ Subsequent methods for the preparation of **192** have been described using successive bromination and elimination reactions of 1-chloro-3,3,3-trifluoropropane (**195**) via bromoalkene **196**,² deoxyfluorination of propiolic acid (**197**) with SF_4 via the corresponding acid fluoride **198**,³ and reaction of 1,1,2-trichloro-3,3,3-trifluoropropene (**199**) with zinc dust, which initially forms the zinc complex of **192** (**200**).⁴ By contrast to the reagents required by these older methods, **1** is relatively easy to handle and lacks the explosive potential of acetylene, the corrosiveness of SF_4 or the ozone-depleting nature of CFCs.



Scheme 4.1. Literature routes to 3,3,3-trifluoropropyne ¹⁻⁴

The main class of products formed from **192** in this Chapter are trifluoromethyl ynones, of which there are very few examples in the literature. Shen *et al.* reported the first synthesis of a CF₃-ynone in 1984 by reaction of phosphoranes (**201**) with perfluoroacyl chlorides to give perfluoroacylated phosphonium salts (**202**, Scheme 4.2).⁵ Pyrolysis gave the final products, in which the perfluoroalkyl group can be located either adjacent to the carbonyl (**203**) or at the alkynyl position (**204**). With trifluoromethyl phosphoranes, the carbonyl position is favoured whereas, with a bulkier perfluoro-*n*-propyl group, the ratio of carbonyl to alkyne becomes 1:1 (Table 4.1). With an electron-donating methoxy group on the phenyl ring, the yields for reactions involving both perfluoroalkyl groups were reduced but more so for the trifluoromethyl derivative.

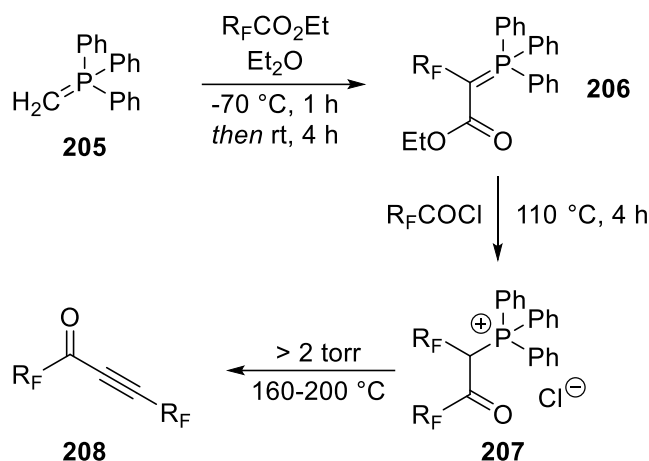


Scheme 4.2. Synthesis of perfluoroalkyl ynones by pyrolysis of perfluoroacyl phosphoranes⁵

Table 4.1. Substrate scope for pyrolysis of perfluoroacyl phosphoranes⁵

Product	R	R _F	% Yield 203	% Yield 204
203/204a	H	CF ₃	63	21
203/204b	H	<i>n</i> -C ₃ F ₇	43	43
203/204c	OMe	CF ₃	53	36
203/204d	OMe	<i>n</i> -C ₃ F ₇	42	42

This method was extended to prepare symmetrical perfluoroalkyl phosphoranes by reaction of methylenetriphenylphosphorane **205** with perfluoroalkyl esters (acid chlorides were ineffective for the first step) to give perfluoroalkyl-substituted phosphorane **206** followed by reaction with perfluoroacyl chlorides as above to give symmetrical phosphonium **207** (Scheme 4.3 and Table 4.2).⁶ Pyrolysis of the phosphorane derivatives afforded good yields of various perfluoroalkyl ynones **208** as a single regioisomer.

Scheme 4.3. Preparation of symmetrical perfluoroalkyl ynones⁶Table 4.2. Substrate scope for pyrolysis of symmetrical perfluorophosphoranes⁶

Product	R _F	% Yield
208a	CF ₃	70
208b	C ₂ F ₅	88
208c	<i>n</i> -C ₃ F ₇	96
208d	<i>n</i> -C ₇ F ₁₅	90

Subsequently, Chechulin *et al.* reported a lower temperature synthesis of the same structures by reaction of 1,3-dicarbonyl systems (**209**) with dihalophosphoranes (Scheme 4.4).⁷ As described above, this gave a mixture of isomers **203** and **204** with the carbonyl isomer **203** favoured for both CF₃ and *n*-C₃F₇ in this case (Table 4.3). Use of triphenylphosphonium dichloride over the corresponding dibromide was possible but required longer reaction times.

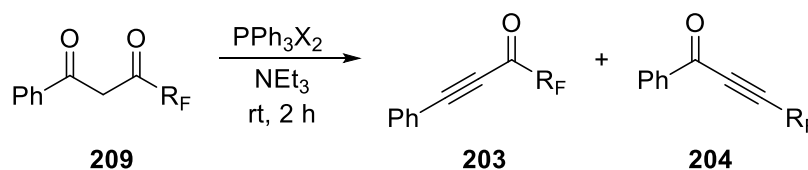
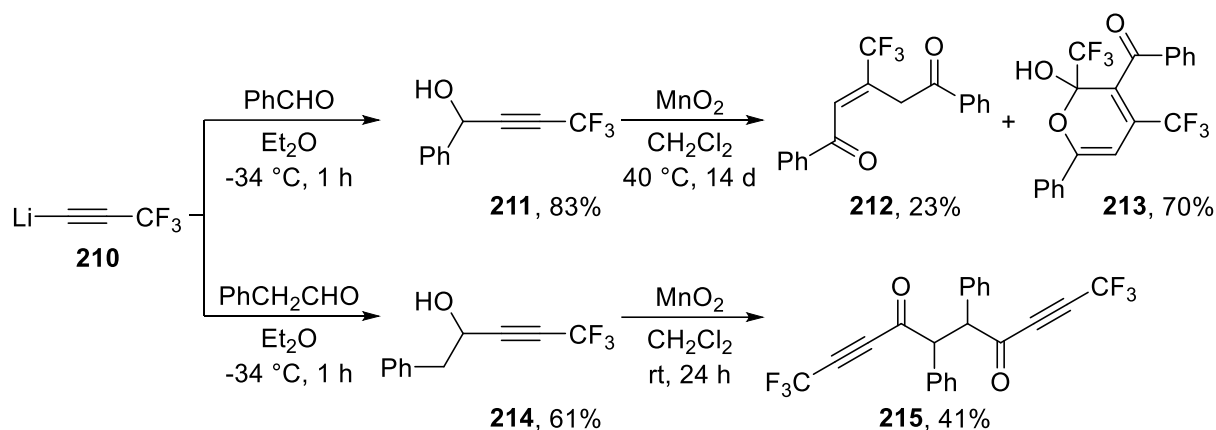
Scheme 4.4. Room temperature phosphorane-mediated synthesis of perfluoroalkyl ynones⁷

Table 4.3. Substrate scope for dihalophosphorane method

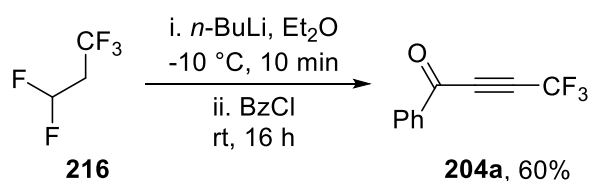
Product	X	R _F	% Yield 203	% Yield 204
203/204a	Br	CF ₃	28	10
203/204b	Br	<i>n</i> -C ₃ F ₇	70	24
203/204a	Cl	CF ₃	64	21
203/204b	Cl	<i>n</i> -C ₃ F ₇	84 (ratio not given)	

Tajammal and Tipping reported a different route to ynone **204a** (Scheme 4.5).⁸ Reaction of 3,3,3-trifluoropropynyl lithium (**210**), obtained by deprotonation of 3,3,3-trifluoropropyne (**192**) with *n*-BuLi, with benzaldehyde gave alcohol **211** in good yield but attempted oxidation reactions using pyridinium chlorochromate, Jones oxidation and mercury(I) oxide were all ineffective. Manganese (IV) oxide initially gave 17% conversion to **204a** but attempting to improve this with longer reaction times instead led to formation of some enedione **212** and pyran **213** as the major product, believed to form via a free radical cyclisation process. Tipping later reported another trifluoromethyl ynone synthesis from **210**, using phenacetaldehyde as the electrophile to give alcohol **214**.⁹ Oxidation of **214** with MnO₂ again did not give the expected ynone, instead forming diynone **215**, which is also believed to result from free radical coupling processes.



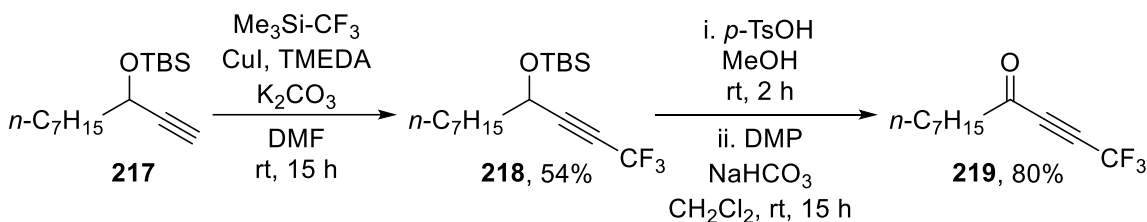
Scheme 4.5. Attempted syntheses of trifluoromethyl ynones from 3,3,3-trifluoropropynyl lithium⁸⁻⁹

A similar method was later reported by Brisdon and Crossley (Scheme 4.6).¹⁰ Treatment of the refrigerant 1,1,1,3,3-pentafluoropropane (HFC-245fa, **216**) with *n*-BuLi generated **210**, which reacted with benzaldehyde to give **211** as described above, albeit with a lower yield of 60%. However, by using benzoyl chloride as the electrophile, **204a** was synthesised in a single step without the need for subsequent oxidation. Bumgardner *et al.* had earlier reported a similar synthesis of **204a** from trifluoropropynyl zinc (**200**) and benzoyl chloride but gave no details of the procedure.¹¹



Scheme 4.6. Synthesis of **204a** from HFC-245fa via 3,3,3-trifluoropropynyl lithium¹⁰

Hoye *et al.* described a new multi-step method for the synthesis of trifluoromethyl ynones, beginning from a protected propargyl alcohol with an unsubstituted terminal alkyne (**217**, Scheme 4.7).¹² Trifluoromethylation of the terminal alkyne was carried out using the Ruppert-Prakash reagent (TMS-CF₃) with copper(I) iodide and tetramethylethylenediamine to give **218**. Deprotection of the silyl alcohol with *p*-toluenesulfonic acid was followed by oxidation using Dess-Martin periodinane to give heptyl ynone **219** in an overall yield of 43%, avoiding the radical cyclisation issues encountered by Tajammal and Tipping.



Scheme 4.7. Multi-step synthesis of a trifluoromethyl ynone from a free terminal alkyne ¹²

The initial phosphorane-based methods suffer from a lack of selectivity for the alkynyl-CF₃ isomer whilst other processes require either high global warming potential HFC starting materials or the use of the relatively expensive and atom uneconomical Ruppert-Prakash reagent. As such, there have been virtually no reports on the reactivity of this type of trifluoromethyl ynone structure. Consequently, the ability to synthesise these systems from an inexpensive and readily available building block such as **1** would be beneficial in allowing for the exploration of the reactivity of these ynone systems to access pharmaceutically relevant CF₃-substituted compounds.

4.2 Results and discussion

4.2.1 Synthesis of trifluoromethyl ynones

Formation of **192** from **1** was first observed in attempting to use lithium *N*-methylbenzylamide as a nucleophile for an S_NV reaction with **1** as described in Chapter 3. Similar reactivity was subsequently observed with *n*-butyl lithium, the Gilman reagent *n*-Bu₂CuLi, phenyl lithium, lithium phenylacetylide and sodium amide. **192** was identified on the basis of its ¹⁹F NMR spectrum, as shown in Figure 4.1, which was recorded from the reaction of **1** with *n*-BuLi in THF at -78 °C.

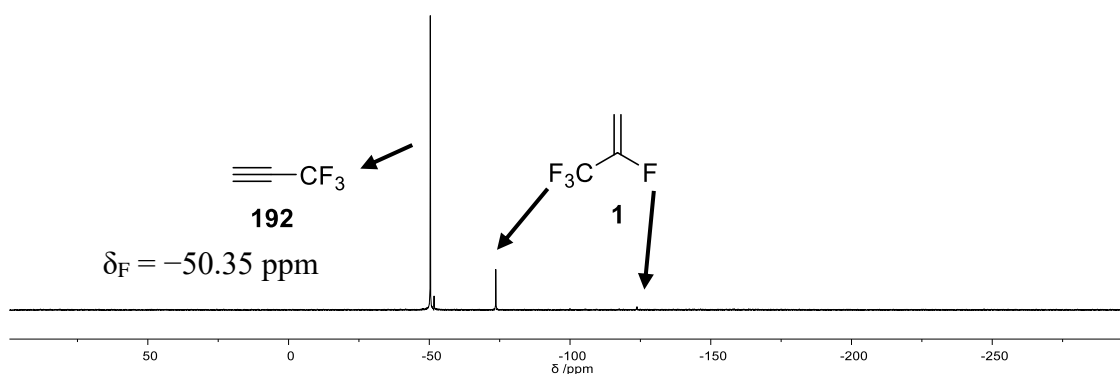


Figure 4.1. ^{19}F NMR spectrum of 3,3,3-trifluoropropyne formed from 2,3,3,3-tetrafluoropropene

On quenching the reaction with H_2O , a chemical shift for **192** was observed in the ^1H NMR spectrum consistent with the only known literature report for the NMR spectrum of **192**, which gave a δ_{H} of 2.80 ppm in CCl_4 compared to 2.45 ppm seen here in CDCl_3 (Figure 4.2).¹³ When the reaction was instead quenched with D_2O , no such signal was observed in the ^1H NMR spectrum whereas the ^{19}F NMR spectrum was unchanged. This suggests that, not only does elimination from **1** to form **192** occur, but also that the **192** formed is then deprotonated to form trifluoropropynyl lithium **210**.

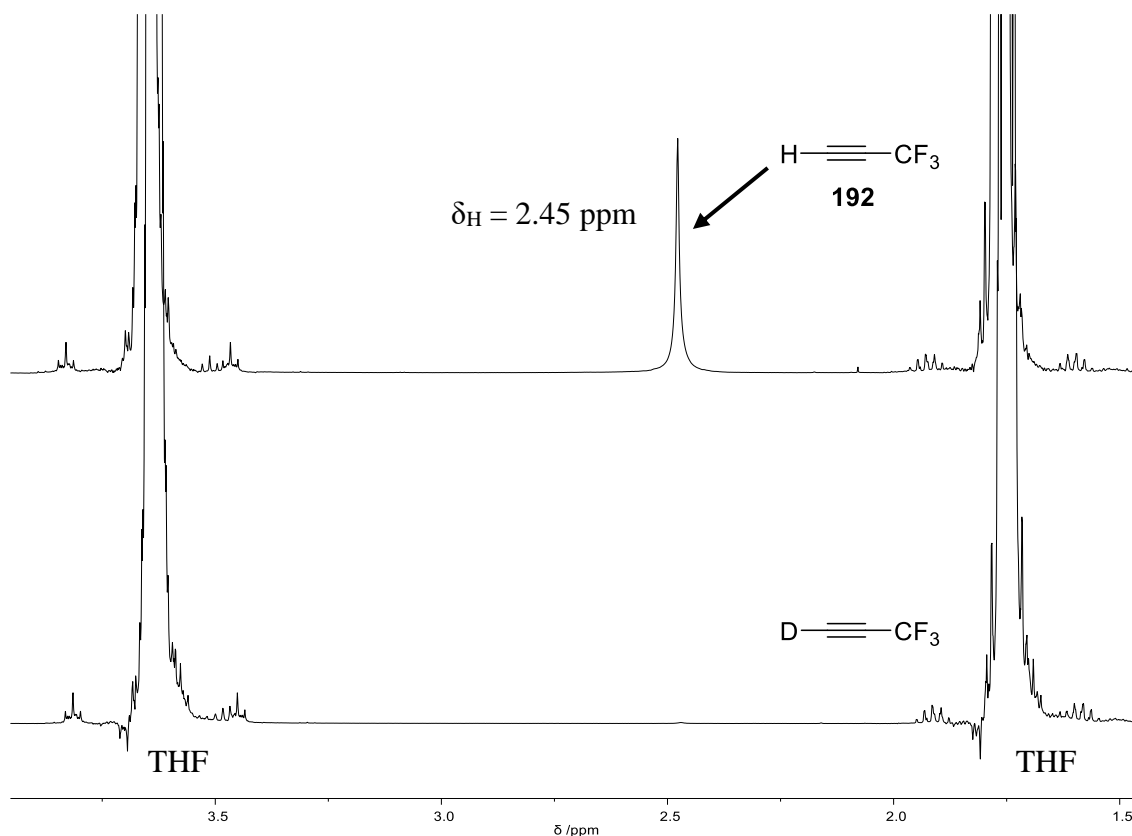


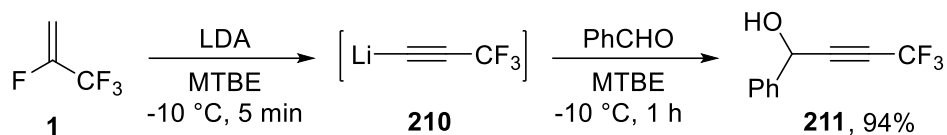
Figure 4.2. ^1H NMR spectrum of 3,3,3-trifluoropropyne formed from 2,3,3,3-tetrafluoropropene on quenching with H_2O (top) and D_2O (bottom)

The utility of using **210** formed by this process was then explored, firstly by attempting the reaction of **210** generated from **1** with benzaldehyde to form alcohol **211** (Scheme 4.8). Various conditions were screened (Table 4.4); initially, *n*-BuLi was used as the base but the Bu⁻ anion proved a better nucleophile than **210** and so low conversion to the desired alcohol was obtained. By using lithium diisopropylamine (LDA) instead, this competing reaction was prevented and so good conversion to **210** was observed. At -78 °C, the reaction proceeded cleanly but slowly in both diethyl ether and THF. At -10 °C, **210** formed much more rapidly but formed various side products in THF whilst the reaction in diethyl ether still gave clean conversion. This is consistent with Brisdon's report that **210** was more stable in diethyl ether than THF.¹⁰ However, diethyl ether is an undesirable solvent for process scale due to its volatility and tendency to form peroxides so alternative solvents were investigated. Methyl *tert*-butyl ether (MTBE), a safer and more environmentally benign alternative to diethyl ether,¹⁴ was found to give excellent conversion. Cyclopentyl methyl ether (CPME) also gave very good conversion and could be a viable alternative solvent if MTBE were still too volatile for a specific application. By contrast, di-*n*-butyl ether gave significantly lower conversion. Alternative hindered lithium amides to LDA, namely lithium tetramethylpiperidide (LTMP) and lithium hexamethyldisilazide (LHMDS), gave either low or no conversion to **210**. This suggests the p*K*_a of the protons of **1** lies approximately between 30 and 36.¹⁵

Table 4.4. Screening conditions for synthesis of alcohol **211**

Solvent	Base	Temperature /°C	Conversion /% ^[a]
Et ₂ O	<i>n</i> -BuLi	-78	1
Et ₂ O	LDA	-78	82
Et ₂ O	LDA	-10	97
Et ₂ O	LTMP	-10	14
Et ₂ O	LHMDS	-10	0
THF	LDA	-78	82
THF	LDA	-10	13
CPME	LDA	-10	91
MTBE	LDA	-10	98
<i>n</i> -Bu ₂ O	LDA	-10	70

^[a] determined by ¹⁹F NMR analysis of crude reaction mixture (Scheme 4.8) after quenching with water



Scheme 4.8. Optimised synthesis of CF_3 -alcohol **211** from HFO-1234yf

To gain further insight into the synthesis of trifluoromethyl ynone systems, the formation of **210** followed by its addition to benzaldehyde to form alcohol **211** was monitored by *in situ* IR spectroscopy using a MettlerToledo ReactIR probe (Figure 4.3). The results from this study show that both the formation and consumption of **210** is virtually instantaneous, i.e. complete within 15 seconds (Figure 4.4). The peaks associated with **210** are present from the beginning of the reaction (addition of **1**) and disappear as soon as benzaldehyde is added, with the new absorbances for **211** taking their place. The reaction of **210** with benzaldehyde to form **211** is so rapid that the characteristic C=O stretch of benzaldehyde group was not detected.

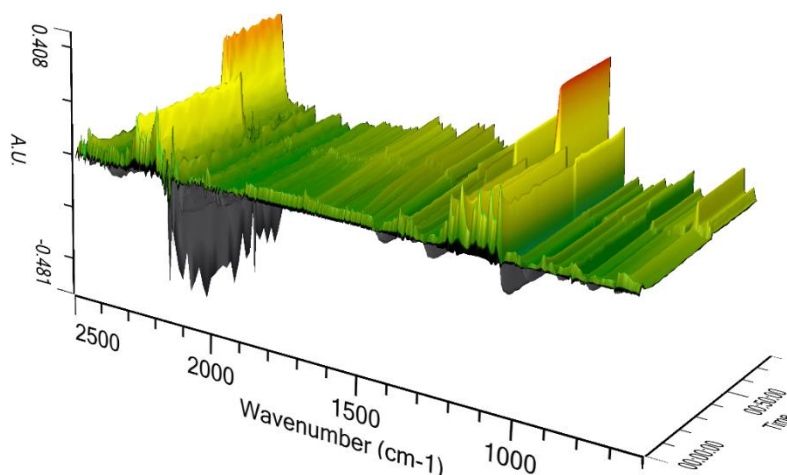


Figure 4.3. ReactIR spectra for reaction shown in Scheme 4.8

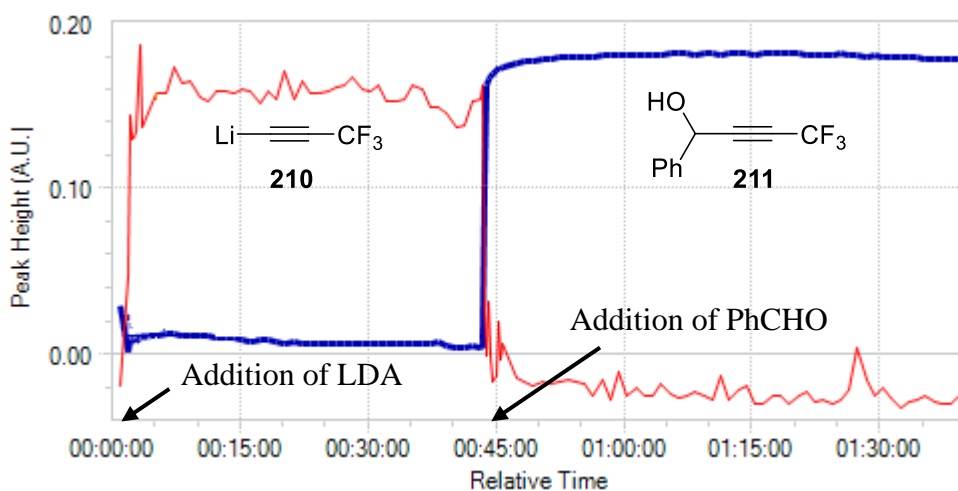
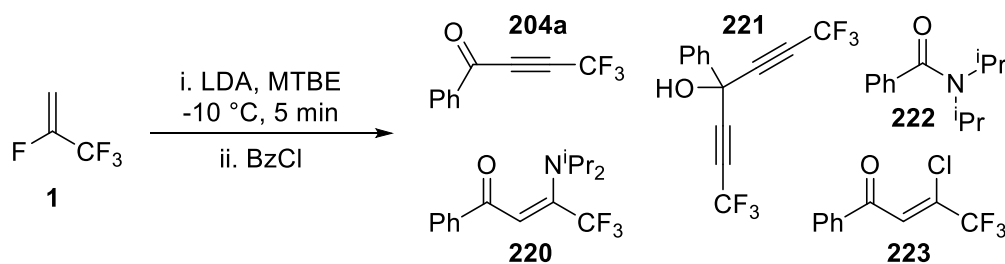


Figure 4.4. Absorbance for alkyne bonds of **210** (red, 2291 cm^{-1}) and **211** (blue, 2284 cm^{-1})

The most direct method for the preparation of targeted CF₃-ynone **204a** from **1** would be via reaction with an acid chloride. However, attempted reaction of **1** derived from **1** with benzoyl chloride under various conditions was unsuccessful in all cases owing to formation of inseparable side products (Table 4.5). Michael addition of diisopropylamine to any **204a** that did form was observed, forming both *E* and *Z* stereoisomers of enaminone **220** (Scheme 4.9). With excess **1**, overaddition was observed to form diyne species **221** whereas, with excess benzoyl chloride, diisopropylamine added to the acid chloride to form amide **222**. There was also some evidence by mass spectrometry of addition of chloride as a nucleophile to **204a** to give two isomers of enone **223**. All products were tentatively identified by GC-MS analysis of the crude reaction mixture after aqueous workup and the ratios were estimated based on the ¹⁹F NMR spectrum of the product mixture. Whilst clean conversion was observed to **204a** with 0.6 equivalents of LDA in MTBE after 20 minutes in the ¹⁹F NMR spectrum, ¹H NMR spectroscopy showed there was still 15% **222** present that could not be readily removed.



Scheme 4.9. Possible products formed from attempted synthesis of **204a** from **1** and benzoyl chloride

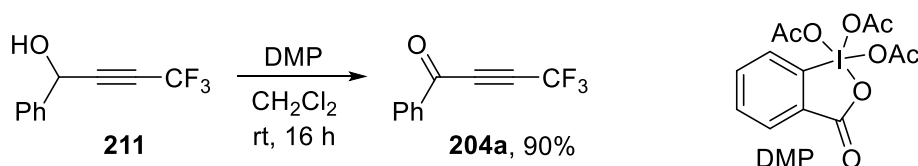
Table 4.5. Screening of conditions for synthesis of **204a** from **1** and benzoyl chloride

Conditions	204a ^[a]	220 ^[a]	221 ^[a]	Other ^[a]
1.5 eq. LDA, -78 °C, Et ₂ O, 1 h	33	7	0	60
2.3 eq. LDA, -78 °C, Et ₂ O, 1 h	11	3	0	86
2.3 eq. LDA, -78 °C, Et ₂ O, 2 h	37	3	0	60
2.3 eq. LDA, -78 °C, Et ₂ O, 16 h	51	10	2	37
1.9 eq. LDA, -78 °C, THF, 1 h	1	0	0	99
0.6 eq. LDA, -10 °C, MTBE, 1 h	81	0	0	19
0.7 eq. LDA, -10 °C, MTBE, 10 min	62	4	3	31
0.4 eq. LDA, -10 °C, MTBE, 20 min	85	1	4	10
0.6 eq. LDA, -10 °C, MTBE, 20 min	98	<1	<1	~1

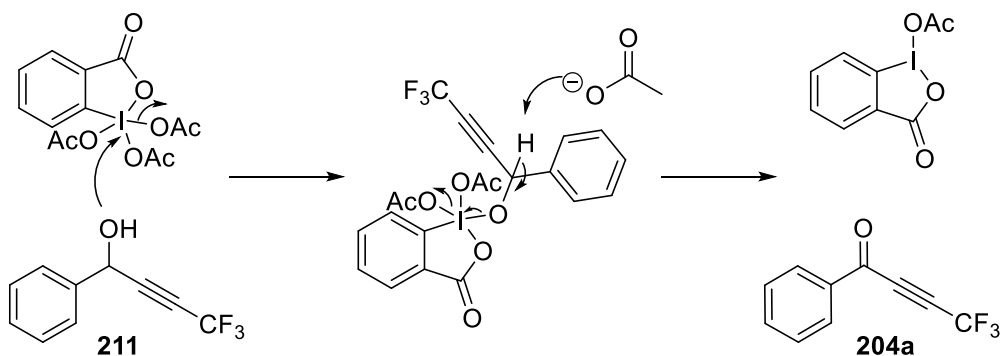
^[a] % conversion determined by ¹⁹F NMR analysis of crude reaction mixture after quenching with water

Attempted addition of morpholine as a reagent to mediate reactivity¹⁶ was unsuccessful, giving only 5% conversion to **204a**. Jeong *et al.* previously reported that reaction of **210** with Weinreb amides leads to formation of an ynone that is immediately attacked by the amine leaving group to give similar enamines to **220**.¹⁷ An ester starting material would likely react in a similar way to form enone ethers and so neither of these possible alternative starting materials were considered.

Oxidation of alcohol **211** was, therefore, considered as an alternative synthetic route to ynone **204a**. Hoye *et al.* showed that a CF₃-propargyl alcohol could be readily oxidised to the corresponding ynone using Dess-Martin periodinane (DMP) without any competing radical cyclisation.¹² DMP was also successfully used in previous syntheses of CF₂-substituted ynones as part of the synthesis of difluorinated analogs of musk lactones.¹⁸ Applying DMP oxidation conditions to **211** afforded the desired ynone **204a** in excellent yield and without the need for purification by column chromatography (Scheme 4.10). Fluorinated alcohols have previously been shown to react slowly with DMP due to their lower nucleophilicity¹⁹ but no such issues were encountered with **211** (Scheme 4.11). This meant that CF₃-ynones could now be prepared from **1** in just two steps without any resource-intensive purification procedures being required.



Scheme 4.10. Oxidation of alcohol **211** with Dess-Martin periodinane



Scheme 4.11. Mechanism of DMP-mediated oxidation of **211**

As hypervalent iodine species such as DMP are potentially energetic and reactions using this reagent have poor atom economy, alternative oxidation conditions were sought that

would be more suitable for larger scale reactions in future. Parikh–Doering oxidation²⁰ using pyridinium sulfur trioxide and DMSO was attempted. However, after two hours at room temperature, ¹⁹F NMR spectroscopy showed 45% starting material **211** and only 2% intended product **204a**. The remainder consisted of a range of small, unknown side products along with two larger signals with shifts indicative of a CF₃ alkene product. It is likely that some species in the reaction mixture is acting as a nucleophile and reacting with any **204a** that is formed. It is not clear from NMR spectroscopy or mass spectrometry what this nucleophile could be, and so the identity of this alkene remains uncertain. However, it is clear that any future synthesis of **204a** would need to avoid the presence of any potentially nucleophilic species. Whilst alternative conditions might still need to be developed for large-scale synthesis, the simplicity of the DMP procedure was preferred for an initial substrate scope. The oxidation of **211** to **204a** with DMP was also studied by *in situ* IR spectroscopy (Figure 4.5). The absorption of the C=O peak for **204a** increases rapidly at first before slowing with the reaction complete within around four hours (Figure 4.6). However, there appeared to be no significant side product formation and so, as with the synthesis of **211**, reactions could be left for longer if required for a given substrate.

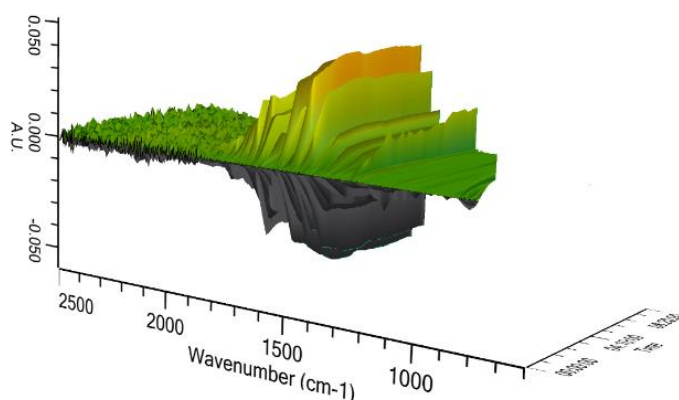


Figure 4.5. ReactIR spectra for reaction shown in Scheme 4.10

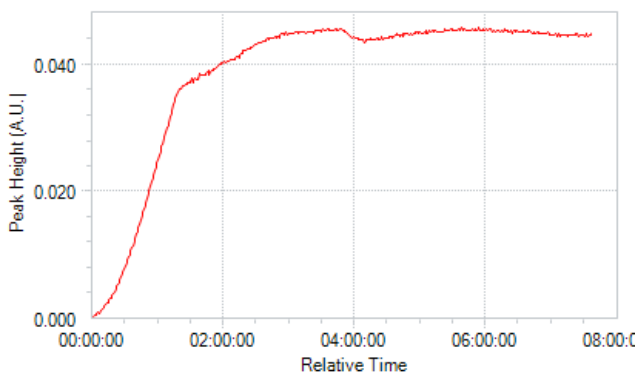
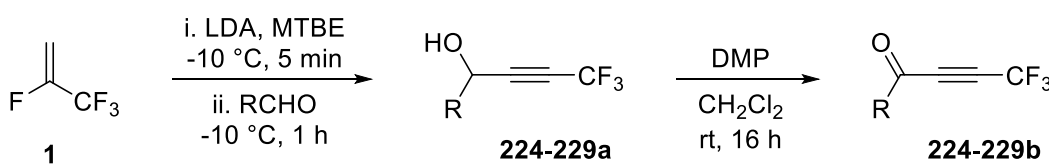
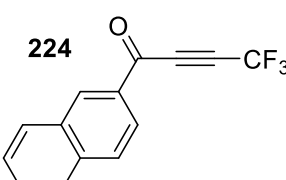
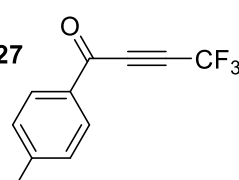
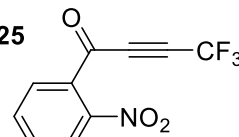
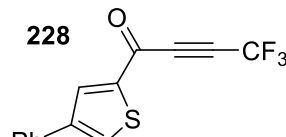
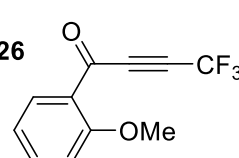
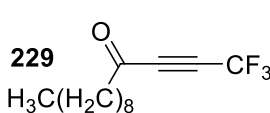


Figure 4.6. Absorbance for carbonyl bond of **211** (1648 cm⁻¹) over time

The substrate scope of aldehydes that could be used in the reaction was investigated (Table 4.6). 2-Naphthaldehyde afforded a crystalline product **224b**, the structure of which was confirmed by X-ray crystallography (Figure 4.7). Nitro (**225**), methoxy (**226**) and methyl (**227**) groups on the phenyl ring of benzaldehyde were all well tolerated in this synthetic process as was a thiophene substrate (**228**). The reaction could also be extended to aliphatic aldehydes, reacting with *n*-decyl aldehyde (**229**). In addition, MChem student Thomas Marsh was able to synthesise further examples from 3-fluorobenzaldehyde and 4-bromobenzaldehyde with 91% and 84% isolated yield respectively over the two steps and also found heating **224b** with triethylamine in THF led to a Meyer–Schuster-type rearrangement to form the equivalent CF₃-enone in 56% isolated yield.

Table 4.6. Substrate scope for synthesis of CF₃-ynones from HFO-1234yf

		224-229a		224-229b	
Compound	Yield a / %	Yield b / %	Compound	Yield a / %	Yield b / %
224 	94	95	227 	95	79
225 	82	79	228 	79	87
226 	86	93	229 	94	76

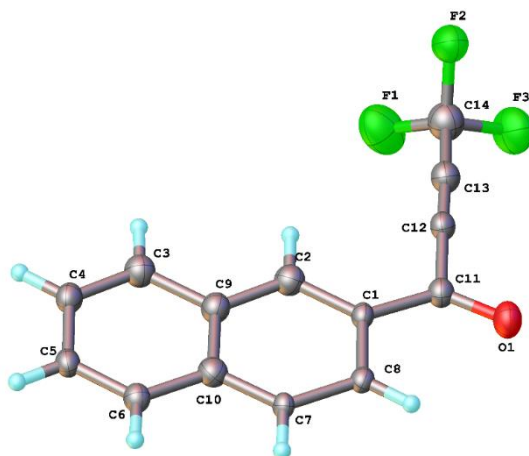
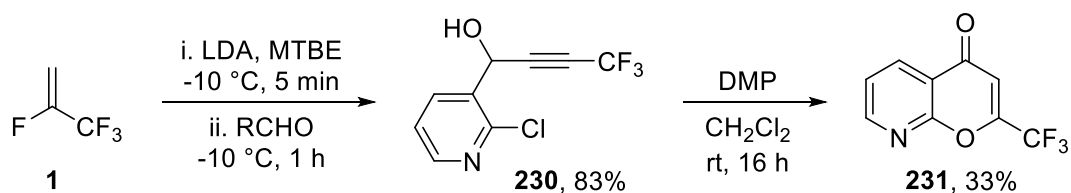
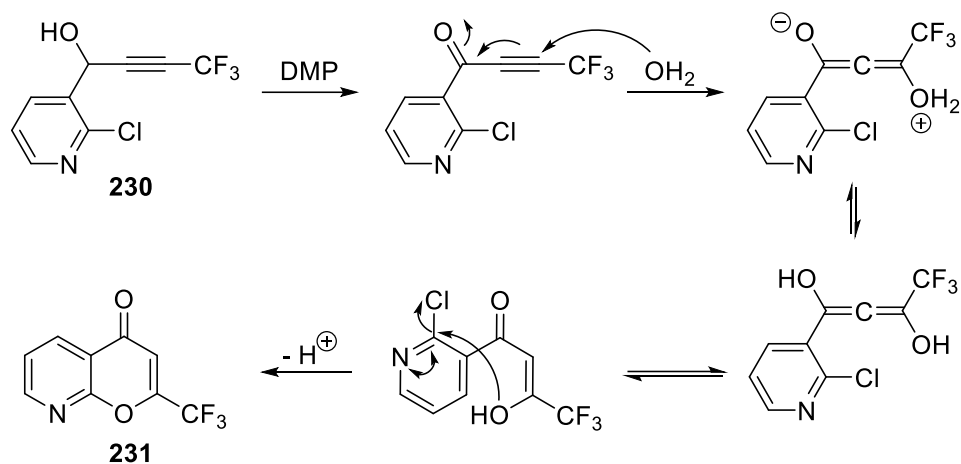


Figure 4.7. Structure of ynone **224b** as determined by X-ray crystallography

One exception to this generally good functional group tolerance was observed for pyridinyl aldehydes. 4-Pyridinecarboxaldehyde gave low mass recovery, up to a maximum of 15%, on reacting with trifluoropropyne **210**. Non-fluorinated pyridinyl propargylic alcohols are known to be unstable towards hydrolysis to enones via an allenol intermediate²¹ and so the CF₃-substituted analog would likely be even more reactive. In contrast, 2-chloro-3-pyridinecarboxaldehyde did react with **210** cleanly, forming alcohol **230** (Scheme 4.12). However, on oxidation a mixture of different products was obtained. Following column chromatography, the only product isolated was CF₃-azachromone **231**, which was likely formed by attack of water on the initially targeted ynone upon work-up. The resulting alcohol could then cyclise via an S_NAr reaction with the pyridinyl chloride moiety (Scheme 4.13). 5,7-Dimethyl-2-trifluoromethyl-8-azachromone was previously synthesised by Sosnovskikh *et al.* from ethyl trifluoroacetate²² but no other corresponding CF₃-azachromone derivatives are known. Indeed, azachromones appear to be an uncommon heterocyclic motif in the literature in general, although one notable example can be found in the antiallergenic drug amlexanox.²³

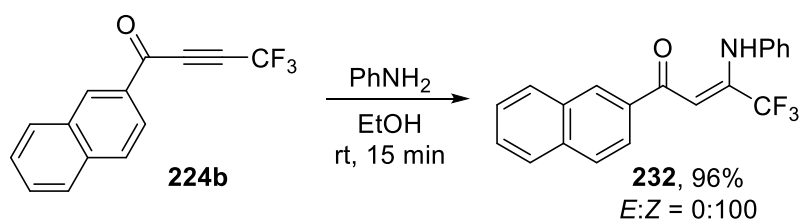


Scheme 4.12. Synthesis of CF₃-azachromone **231** from HFO-1234yf

Scheme 4.13. Proposed mechanism for formation of azachromone **231**

4.2.2 Reactions of trifluoromethyl ynones with amines

Trifluoromethyl ynones should be ideal Michael acceptors due to the presence of an electron withdrawing CF_3 group on the triple bond. Using **224b** as a model substrate, the addition of aniline as a nucleophile was investigated (Scheme 4.14). The reaction was found to be nearly instantaneous, giving complete conversion to a single product within a few minutes at room temperature as evidenced by ^{19}F NMR spectroscopy. The product is a highly crystalline, bright yellow solid and was identified by X-ray crystallography as being enaminone **232** (Figure 4.8). The stereoselectivity observed crystallographically in the solid state was further confirmed in solution through ^1H - ^1H NOE studies (Figure 4.9). The diagnostic through-space interaction to prove regioselectivity was that between the protons on C2 and C20 highlighted whilst the lack of interaction between the protons on C2 and C6/10 proves the *Z* stereochemistry. Jeong *et al.* previously reported the synthesis of a range of β -trifluoromethyl enaminones using ynones generated *in situ* from lithium 3,3,3-trifluoropropynide (**210**) and Weinreb amides.¹⁷ However, they obtained only 31% isolated yield for **232** following column chromatography whereas our method gives much higher yields and requires no resource intensive purification techniques.

Scheme 4.14. Michael addition reaction of CF_3 -ynone **224b** with aniline

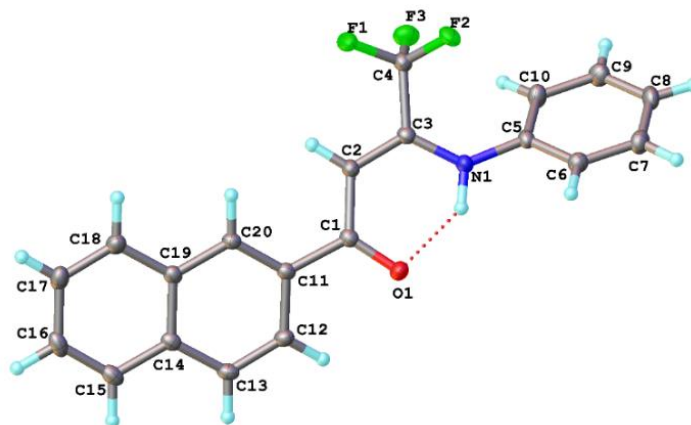


Figure 4.8. Structure of enaminone **232** as determined by X-ray crystallography

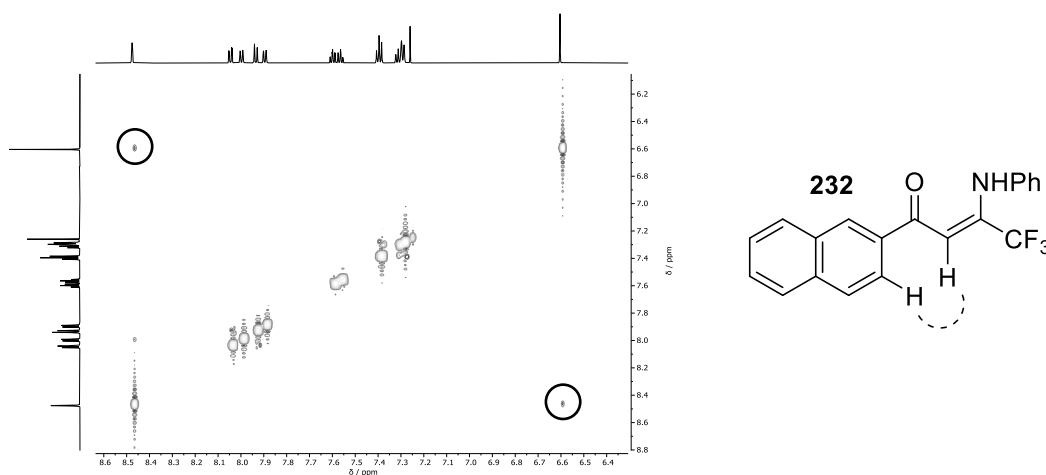
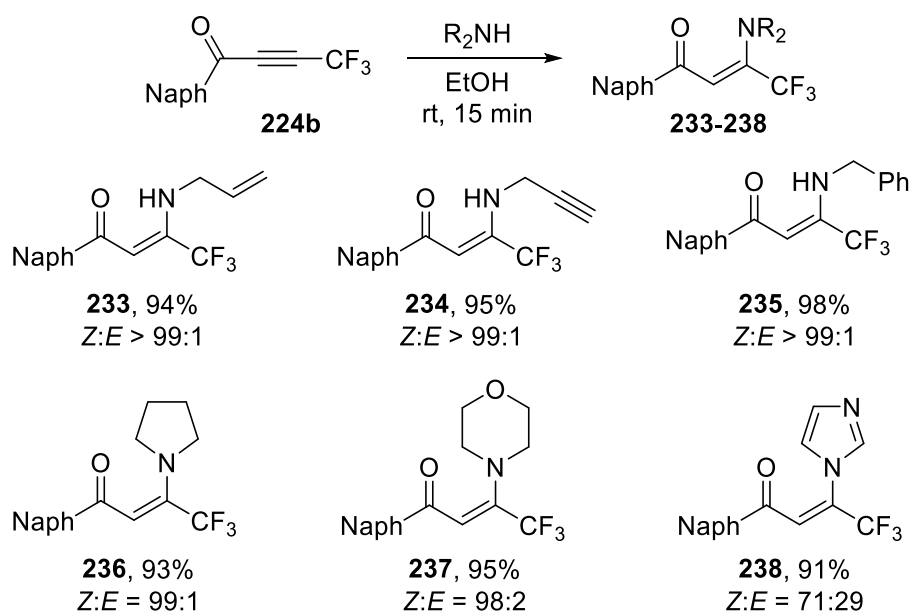


Figure 4.9. ^1H - ^1H NOE spectrum of enaminone **232**

Given the simplicity of this procedure, a brief substrate scope of different amines was investigated (Scheme 4.15). Reaction of **224b** with *tert*-butylamine led to formation of a mixture of products, likely due to the steric bulk reducing the rate of nucleophilic addition to such an extent that reaction of the solvent (ethanol) as a nucleophile occurred at a competitive rate. Reaction of **224b** with unprotected L-phenylalanine also gave a complex mixture, in this case likely due to competing side reactions involving the free carboxylic acid group. In all other cases, by using one equivalent of amine, the products were successfully isolated simply by removal of the solvent after just 15 minutes. The same regio- and stereoselectivity was observed by ^1H and ^{19}F NMR spectroscopy as seen for **232** in each case with primary amines (**233**, **234** and **235**) giving complete *Z* selectivity whilst, with secondary amines (**236** and **237**), trace amounts of *E* stereoisomer were observed. The use of imidazole (**238**) as a nucleophile reduced stereoselectivity further.



Scheme 4.15. Substrate scope for Michael addition reactions of CF_3 -ynone **224b** with amines

To better understand the selectivity in these reactions, DFT calculations were carried out to determine the ground state energies of the *E* and *Z* stereoisomers for phenylamino enaminone **232** (Figure 4.10). The lowest energy conformation of the *Z* isomer was found to be $6.8 \text{ kcal mol}^{-1}$ more stable than the lowest energy conformation of the *E* isomer, suggesting that selectivity is thermodynamically controlled. Michael addition reactions have long been known to be reversible,²⁴ lending further credibility to his argument. The calculated bond lengths and those determined experimentally through X-ray crystallography are all very similar, demonstrating that the theoretical structures are very similar to the values measured experimentally (Table 4.7).

Table 4.7. Comparison of calculated and crystallographic bond lengths for **232**; DFT calculations were carried out by Dr. Mark Fox (Durham University)

Bond	Calculated bond length / Å	Crystallography bond length / Å
C1-O1	1.251	1.247
C1-C2	1.449	1.446
C3-C4	1.523	1.520
C3-N1	1.356	1.352

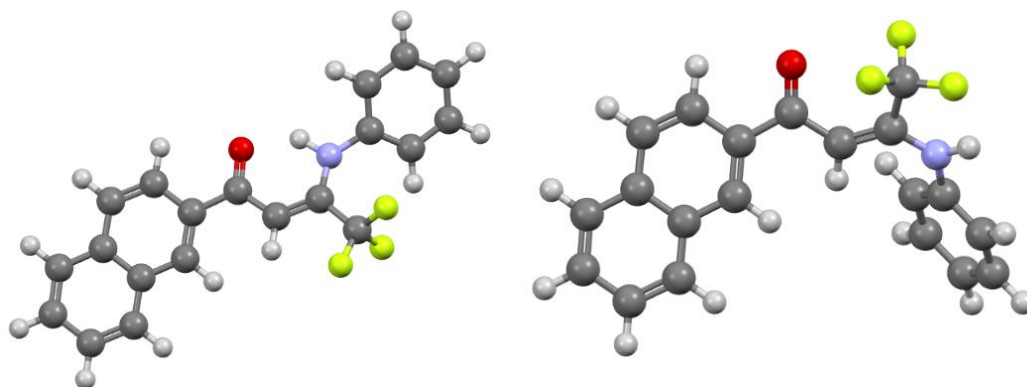
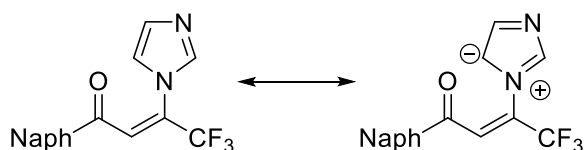


Figure 4.10. Calculated lowest energy conformations of *Z*-**232** (left) and *E*-**232** (right); DFT calculations were carried out by Dr. Mark Fox (Durham University)

One possible explanation for the difference in thermodynamic stability is that the *E* stereoisomer would have unfavourable electrostatic repulsion between the lone pairs of the fluorine atoms of the CF₃ group and those of the carbonyl oxygen. This can be seen in the calculated structure of *E*-**232**, where the fluorine atoms of the CF₃ group are orientated to maximise their distance from the carbonyl oxygen. The decrease in selectivity for secondary amine nucleophiles **236** and **237** can be attributed to the loss of the stabilising hydrogen bond interaction. However, the fact that stereoselectivity remains high for these compounds suggests this is a relatively minor factor compared to the electronic repulsion effect. DFT calculations on pyrrolidinyl enaminone **236** showed that the *Z*-stereoisomer is only 3.2 kcal mol⁻¹ more stable with undesirable steric interactions involving the CF₃ group affecting the preferred orientation of the pyrrolidinyl plane with respect to the carbon-carbon double bond for donation of electron density from nitrogen to the π_{CC} orbitals (Figure 4.11). Imidazolyl enaminone **238** does not suffer these unfavourable steric interactions and so the *Z*-isomer is only more stable by 0.8 kcal mol⁻¹. For **238**, a resonance structure where negative charge is located on the carbon closest to the carbonyl group and so electrostatic repulsion could occur there also (Scheme 4.16). Whilst less significant than the repulsion caused by the CF₃ group, this may also explain the decrease in selectivity for **238**.



Scheme 4.16. Contributing resonance forms of enaminone **238**

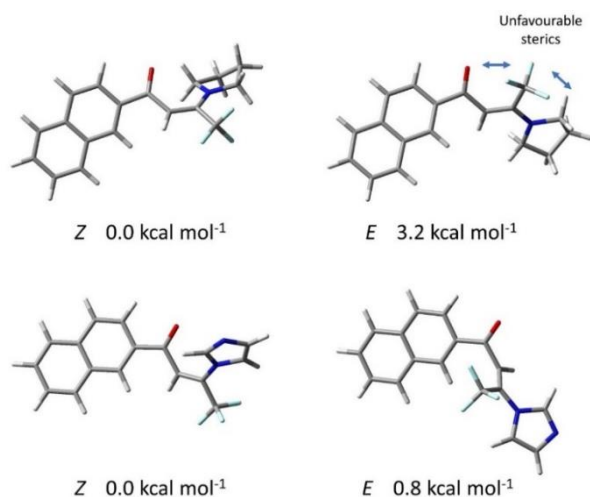
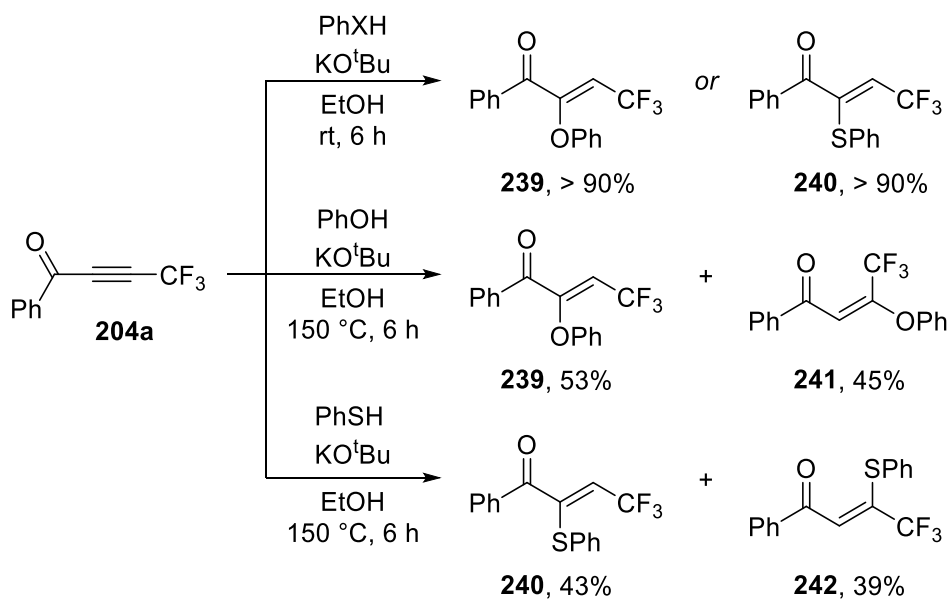


Figure 4.11. Optimised geometries of *E*- and *Z*-**236** (top) and *E*- and *Z*-**238** (bottom); DFT calculations were carried out by Dr. Mark Fox (Durham University)

4.2.2 Reactions of trifluoromethyl ynones with alcohols

One of the very few reactions of CF_3 -ynones reported in the literature was the addition of phenol and thiophenol as nucleophiles to **204a** by Bumgardner *et al.*,¹¹ who reported that the anti-Michael addition product (**239** or **240**) was favoured at room temperature (Scheme 4.17). At elevated temperatures, regular Michael addition selectivity became a competing reaction. For phenol, this gave predominantly the *E*-stereoisomer **241** whereas thiophenol gave mostly the *Z*-stereoisomer **242**.



Scheme 4.17. Literature report of reaction of CF_3 -ynones with phenol and thiophenol¹¹

However, attempting to replicate Bumgardner's conditions using naphthyl ynone **224b** led to formation of an intractable complex mixture. Optimised conditions were sought and selectivity, as determined by ^{19}F NMR spectroscopy, was found to be dependent on the amount of KO^tBu used, with a clear linear correlation between conversion to the major product and the equivalents of base used (Figure 4.12).

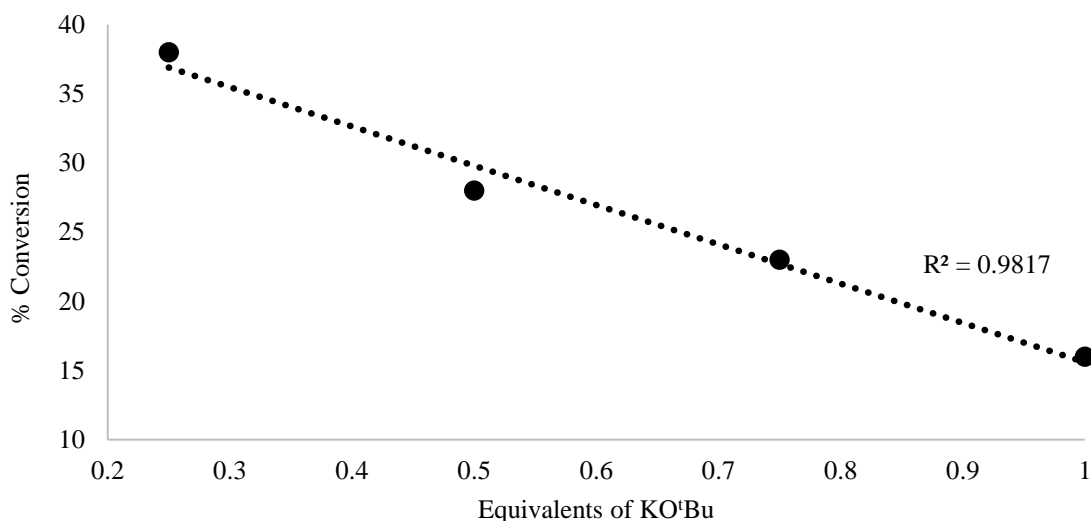
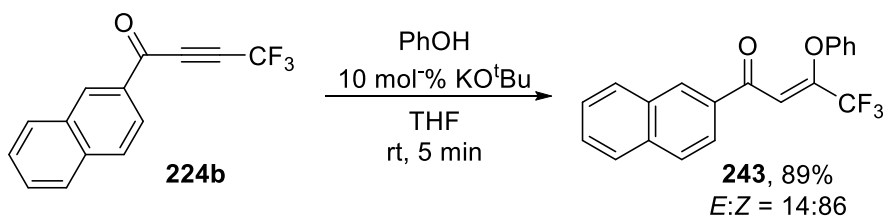


Figure 4.12. Effect of ratio of **224b**: KO^tBu on conversion in reaction of **224b** with phenol in ethanol

Using 10 mol-% KO^tBu and changing solvent from ethanol to THF, the reaction of **224b** with phenol was complete within five minutes, as opposed to the six hour reaction reported in the literature (Scheme 4.18). Evaporation of THF followed by addition of hexane allowed KO^tBu to be removed by filtration with no further purification required. The product enone **243** showed the same ^{19}F and ^1H NMR coupling patterns as enaminone **232**, strongly suggesting it has the same regio- and stereochemistry. This was further confirmed by ^1H - ^1H NOE spectroscopy, which also showed the same interactions as seen for **232** (Figure 4.13).



Scheme 4.18. Michael addition reaction of CF_3 -ynone **224b** with phenol

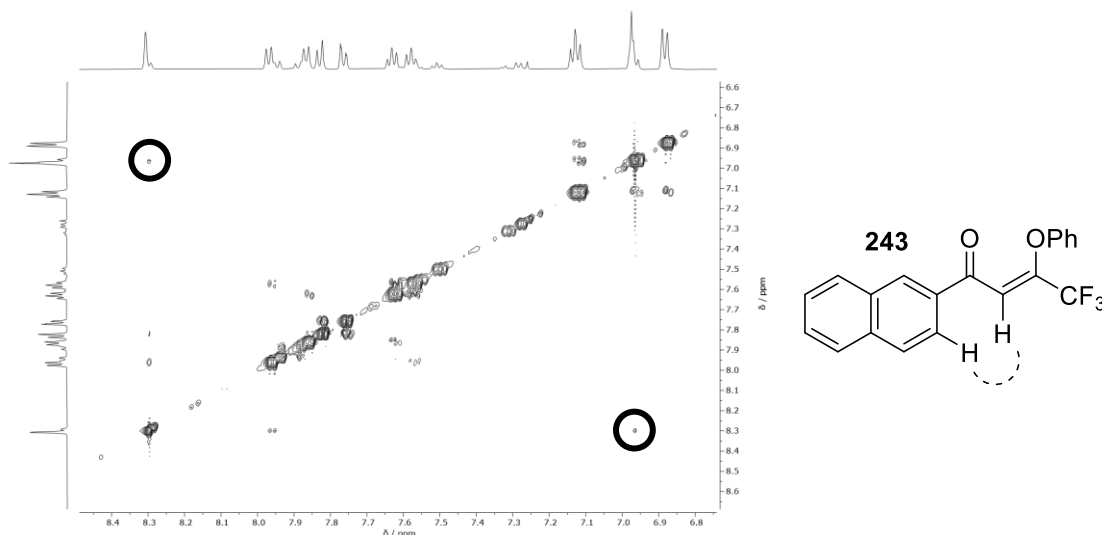


Figure 4.13. ^1H - ^1H NOE spectrum of enone ether **243**

Despite using exactly the same conditions, the anti-Michael addition reported by Bumgardner *et al.* could not be replicated nor was any anti-Michael product observed using our optimised conditions. The only difference between our reaction and that in the literature is, therefore, the use of naphthyl ynone **224b** instead of phenyl ynone **204a**. Such a significant shift in selectivity would not be expected from such a change in substrate structure. Chechulin *et al.*⁷ briefly mention in their reported synthesis of CF_3 -ynones that addition of ammonia leads to Michael-type selectivity as we have seen, although no details were given. Furthermore, reactions of commercially available CF_3 -ynoates with nucleophiles are also known in the literature to give Michael-type selectivity with various alcohols and thiols,²⁵ a range of different amines and phosphites^{26,27} and organolithium reagents.²⁸ Bumgardner's original reported anti-Michael products have distinct chemical shifts and coupling constants so the discrepancy cannot simply be attributed to a misinterpretation of the data. Therefore, it is possible that there was some experimental detail omitted from Bumgardner's paper that would lead to this change in reactivity, e.g. residual zinc from the CF_3 -ynone synthesis acting as a catalyst.

Stereoselectivity in the addition of phenol to form **243**, whilst still high, was significantly lower than for addition of aniline to form **232**. DFT calculations reveal that the *E*-stereoisomer is still the less stable for **243** but, in this case, the difference is only $0.6 \text{ kcal mol}^{-1}$ compared to $6.8 \text{ kcal mol}^{-1}$ for **232** (Figure 4.14).

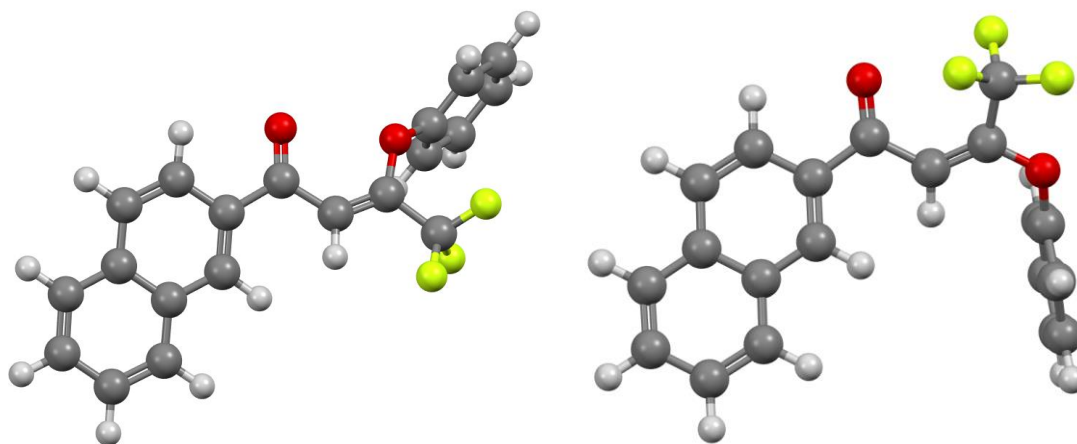


Figure 4.14. Calculated lowest energy conformations of *Z*-**243** (left) and *E*-**243** (right); DFT calculations were carried out by Dr. Mark Fox (Durham University)

To gain further insight into this reaction, the synthesis of **243** was carried out at various different temperatures and the *E*:*Z* ratio was measured by ^{19}F NMR spectroscopy (Figure 4.15). Above room temperature, no improvement in stereoselectivity was observed whereas, on reducing the temperature, selectivity dropped significantly to around 50:50 at 0 °C. Further reduction favoured formation of the less thermodynamically stable *E* stereoisomer, reaching a maximum of *E*:*Z* = 66:34 at -55°C and below. This suggests that the *E*-stereoisomer is the kinetically more favourable product, possibly due to favourable secondary orbital interactions between the π_{CO} and π_{CF^*} orbitals.

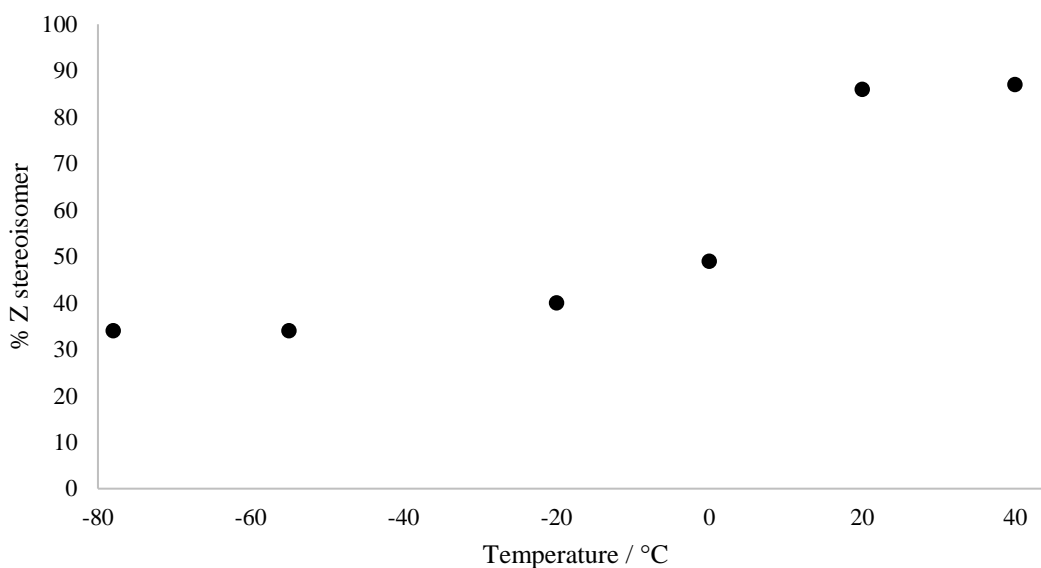
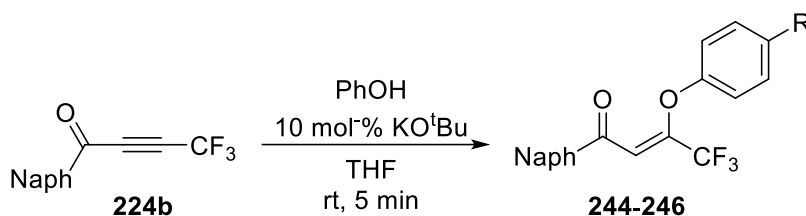


Figure 4.15. Change in stereoselectivity for synthesis of **243** with changing temperature

The addition of phenoxide nucleophiles to CF₃-ynones was expanded to phenols bearing other substituents (Table 4.8). Nitro (**244**), bromo (**245**) and alkyl (**246**) substituents were all well-tolerated. Reaction of **224b** with 4-nitrophenol was sufficiently slow that, initially, a 1:1 mixture of the *E* and *Z* stereoisomers of **244** was observed by ¹⁹F NMR spectroscopy (Figure 4.16). After five minutes, a 15:85 mixture of *E* and *Z* was seen, as for all other phenol nucleophiles, and this ratio was obtained as the final isolated product regardless of how long the reaction was allowed to continue for. This observation provides further proof that Michael addition to CF₃-ynones such as **224b** is indeed reversible and it is this reversibility that allows for the product mixture to become enriched in the more thermodynamically stable *Z*-stereoisomer.

Table 4.8. Substrate scope for addition of phenoxide nucleophiles to ynone **224b**



Product	R	% Isolated yield	<i>E</i> : <i>Z</i>
244	NO ₂	85	15:85
245	Br	84	11:89
246	<i>n</i> -(CH ₂) ₄ CH ₃	76	17:83

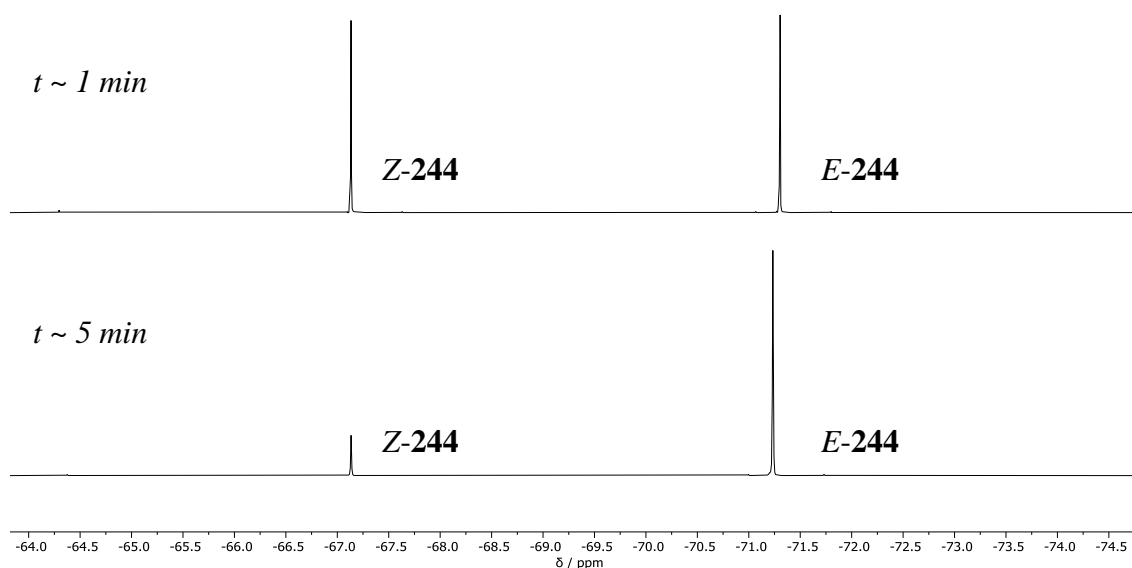
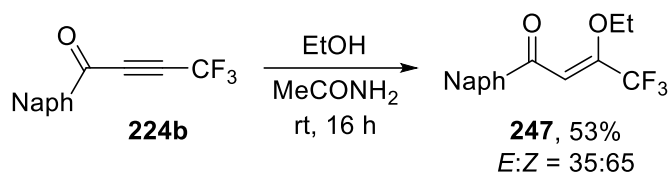


Figure 4.16. ¹⁹F NMR spectra from reaction of **224b** with 4-nitrophenol at different times

Attempting to extend these reaction to aliphatic alcohols, thiophenol or even 4-methoxyphenol under the same conditions were all unsuccessful, forming mixtures of products from which the enones could not be isolated. Reaction of **224b** with sodium ethoxide at room temperature and of **224b** with ethanol without base at reflux were both attempted and both gave intractable complex mixtures. In the course of investigating reactions of **224b** with amines, the use of acetamide as a nucleophile was trialled. However, this led to addition of the ethanol solvent as a nucleophile instead to form enone **247** (Scheme 4.19). Whilst the yield and stereoselectivity were lower than the reactions described above, **247** was the only product, which represents a remarkable improvement in selectivity over the other attempted reactions between **224b** and ethanol. The role of acetamide in the reaction is unclear but it could perhaps be acting as a very weak base.



Scheme 4.19. Michael addition reaction of ethanol to ynone **224b** mediated by acetamide

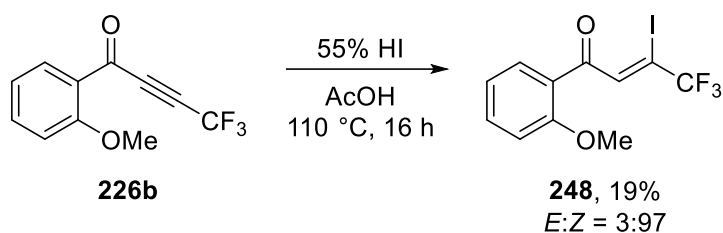
Screening of various conditions was attempted to increase selectivity for **247** and isolated yield (Table 4.9) but no improvement could be obtained. Furthermore, applying the same conditions to the reaction of **224b** with allyl alcohol or isopropanol led to complex mixtures from which no enone ether product was isolated.

Table 4.9. Screening conditions for acetamide mediated addition of ethanol; % conversion determined by ^{19}F NMR analysis of reaction mixture

Equivalents acetamide	$T / ^\circ\text{C}$	t / h	% Conversion
1	~20	16	95
4	100	1	95
1	100	0.5	84
0.5	100	0.5	92
1	80	0.5	93
0	80	0.5	71

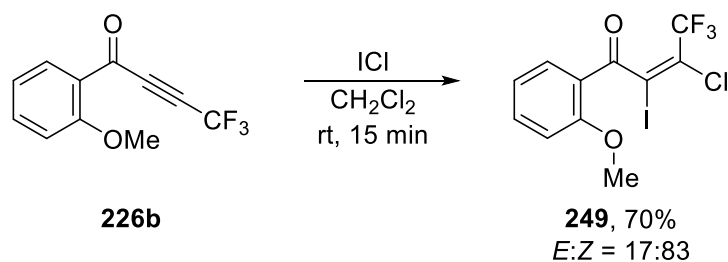
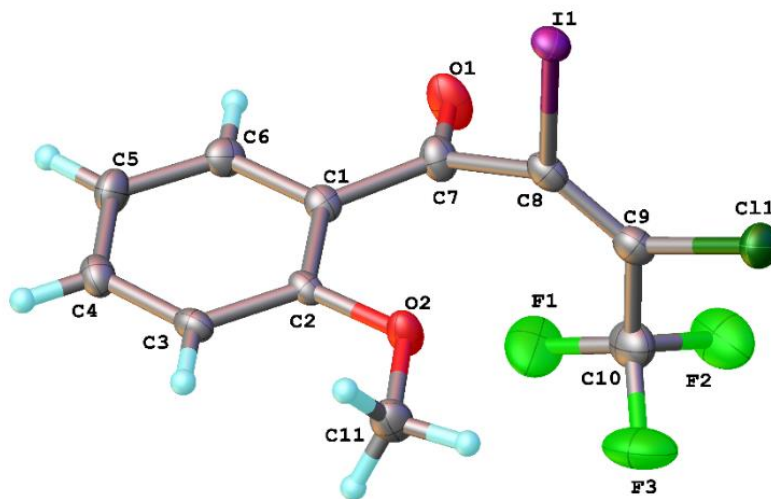
4.2.4 Intramolecular cyclisation reactions of trifluoromethyl ynones

The unintended formation of azachromone **231** described above prompted consideration of other possible intramolecular cyclisation processes. Demethylation of *ortho*-methoxy ynone **226b** using hydroiodic acid was attempted with the intention of forming the corresponding chromone. However, refluxing **226b** with HI in acetic acid led only to hydroiodination of the alkyne to give a low yield of iodoenone **248** (Scheme 4.20). The regio- and stereochemistry of the product was assumed to be that as would be expected for Michael addition of iodide to **226b** as described above.

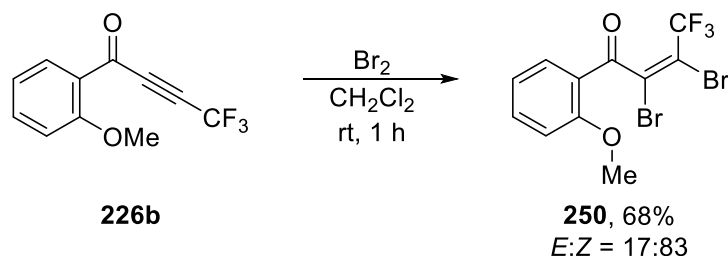


Scheme 4.20. Hydroiodination of a CF₃-ynones

Cyclisation of **226b** was attempted using the method of Larock *et al.*, i.e. formation of an iodonium cation from the alkyne that can then be attacked by the internal OMe nucleophile, with the methyl group then removed by iodide.²⁹ The reaction was initially sluggish using iodine in CH₂Cl₂, reaching 34% conversion in 16 hours. Addition of ceric ammonium nitrate to activate iodine³⁰ in either CH₂Cl₂ or MeCN was unsuccessful. Instead, iodine monochloride (as a 1.0 M solution in CH₂Cl₂) gave complete conversion in just 20 minutes. However, the desired CF₃-iodochromone was not formed but rather the electrophilic addition product **249** (Scheme 4.21). The major isomer of **249** was then separated via column chromatography and the structure confirmed by X-ray crystallography (Figure 4.17). The stereochemistry of the major product **249** is enforced by the geometry of the intermediate iodonium ion whilst the regioselectivity of **249** suggests that attack of the chlorine nucleophile occurs more favourably at the site adjacent to the CF₃ group because the other site is sterically hindered by the *ortho*-methoxyphenyl group and also due to the electron withdrawing inductive effect of the CF₃ group.

Scheme 4.21. Iodochlorination of a CF_3 -ynoneFigure 4.17. Structure of enone **249** as determined by X-ray crystallography

Similarly, reaction of **226b** with bromine simply gave dibromoalkene **250** with no evidence of any of the desired cyclisation. The stereochemistry of the bromination reaction was assumed to be the same as that observed for the iodochlorination reaction above given similarities in their NMR coupling constants and chemical shifts. The selectivity observed experimentally for both reactions is supported by DFT calculations assuming the most thermodynamically favourable pathways take place in these reactions (Figure 4.18).

Scheme 4.22. Bromination of a CF_3 -ynone

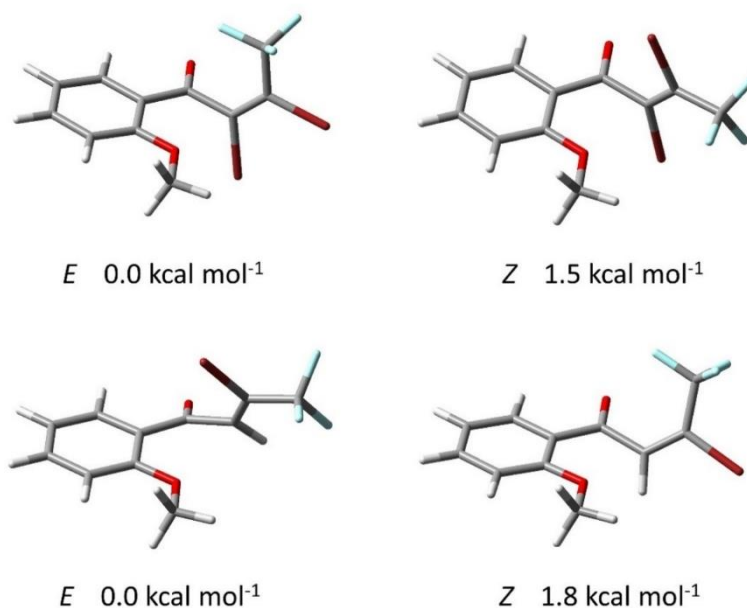


Figure 4.18. Optimised geometries of *E*- and *Z*-**250** (top) and a model for *E*- and *Z*-**249** (bottom)

N.B. iodine was not part of the basis set used for the calculations so bromine was used instead; DFT calculations were carried out by Dr. Mark Fox (Durham University)

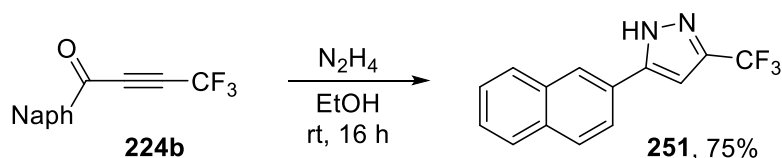
Attempted reaction of **226b** with *p*-nitrobenzene sulfonyl chloride as an electrophile was unsuccessful. These results are consistent with the findings of Larock *et al.*, who reported addition of ICl across the triple bond instead of cyclisation when using ynones with electron-poor aryl substituents since electron-withdrawing groups destabilize the expected carbocation-like iodonium intermediate, disfavoring cyclization.

Reduction of *ortho*-nitro ynone **225b** was attempted with the aim of reaching the *ortho*-amino derivative, which could then undergo cyclisation to form a trifluoromethyl quinoline. However, reduction of **225b** using iron and HCl in ethanol led to formation of a complex mixture with the major products observed by ¹⁹F NMR spectroscopy having chemical shifts more characteristic of a CF₃ alkene. Whilst some of the desired quinoline was detected by GC-MS, formation of an alkene suggests the alkyne is too susceptible to reduction to allow the nitro group to be selectively converted to the amine.

4.2.4 Reactions of trifluoromethyl ynones with dinucleophiles

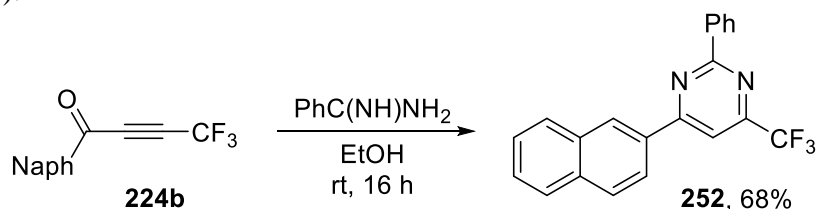
Given that addition of amine nucleophiles occurs selectively β to the carbonyl group, the reaction of CF₃-ynones with dinucleophiles was explored. The aim was for the second

nucleophilic site to cyclise through the carbonyl group following the initial Michael addition and so synthesise a range of different heterocyclic structures. Reaction of **224b** with hydrazine hydrochloride proceeded in the absence of any extra base and, after stirring overnight at room temperature, a precipitate formed that was determined to be pyrazole **251** (Scheme 4.23). Following a simple filtration, the product was isolated in an overall yield of 52% from HFO-1234yf (**1**) over three steps without the need for any further purification.



Scheme 4.23. Reaction of ynone **224b** with hydrazine to give CF_3 -pyrazole **251**

Reaction of **224b** with benzamidine gave pyrimidine **252** (Scheme 4.24) and, as before, the product precipitated from the reaction mixture, making isolation facile. A lower yield than for the reaction with hydrazine was obtained, corresponding to an overall yield of 32% from **1** over three steps, due to the relatively higher nucleophilicity of hydrazines compared to amidines. The structure of **252** was confirmed by X-ray crystallography (Figure 4.19).



Scheme 4.24. Reaction of ynone **224b** with benzamidine to give CF_3 -pyrimidine **252**

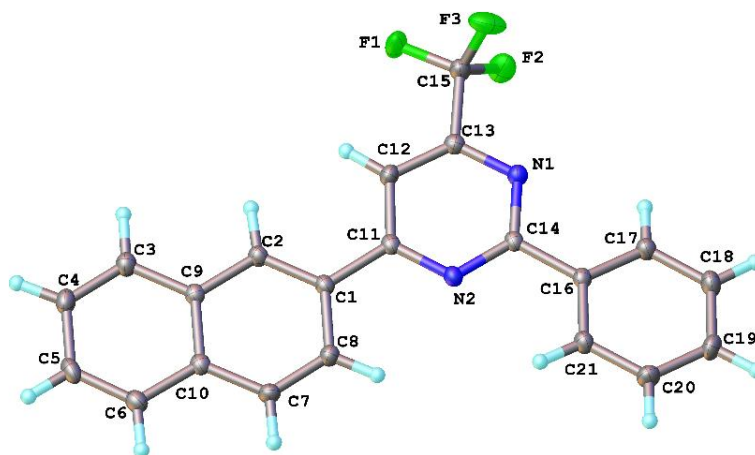
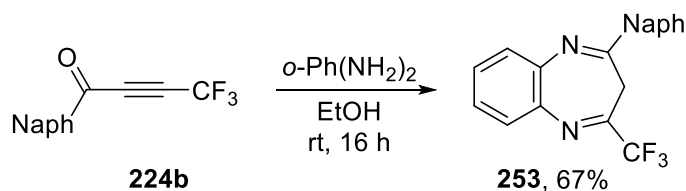


Figure 4.19. Structure of pyrimidine **252** as confirmed by X-ray crystallography

Reaction with *o*-phenylenediamine gave benzodiazepine **253** in an overall yield of 46% from **1** over three steps (Scheme 4.25). This reaction was much faster than the previous two, as the amine was used as the free base rather than the hydrochloride salt, but the product did not precipitate and so had to be isolated via an aqueous workup. However, excess diamine was simply removed by an acidic wash and no formation of any other side products was observed spectroscopically.

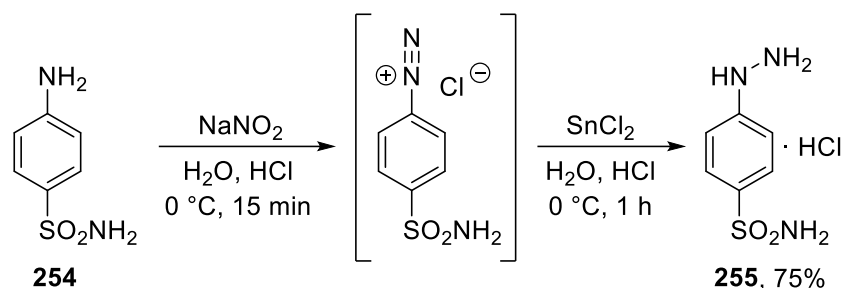


Scheme 4.25. Reaction of ynone **224b** with *o*-phenylenediamine to give CF₃-benzodiazepine **253**

Attempted reaction of **224b** with methyl thioglycolate and potassium carbonate via a Fiesselmann condensation reaction³¹ was unsuccessful, showing no conversion to the desired thiophene product. Likewise, attempted reaction of **224b** with 2-mercaptoacetaldehyde, generated *in situ* from its dimer with triethylamine,³² was also unsuccessful in forming a CF₃-thiophene derivative.

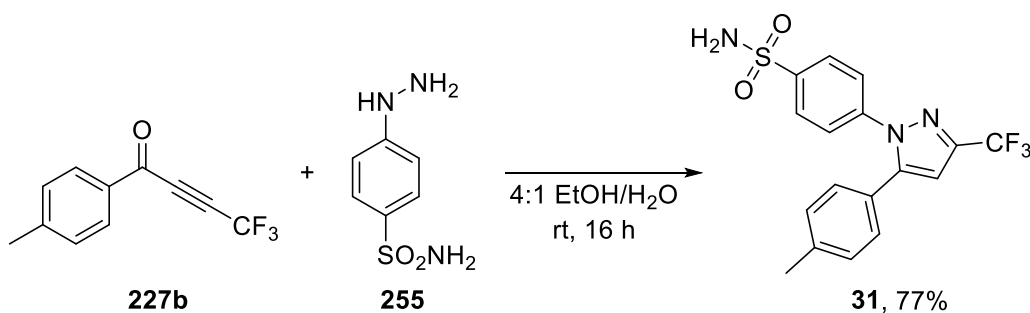
The use of trifluoromethyl ynones as building blocks for the synthesis of drug-like molecules was then explored. Celecoxib (**31**), also known by trade name Celebrex[®] (Pfizer), is a non-steroidal anti-inflammatory (NSAID) used for the relief of pain, primarily for patients with arthritis.³³ The commercial synthesis of **31** involves the reaction of the appropriately substituted hydrazine with a trifluoromethyl 1,3-diketone, which is ultimately derived from trifluoroacetic acid.³⁴ However, there can be issues with regioselectivity using this approach. In the commercial synthesis of celecoxib, the undesired regioisomer accounts for around 4% by weight of the product following the reaction of the dione with the hydrazine.³⁵ The crude product then requires up to three recrystallisations to remove the undesired regioisomer and yield pure celecoxib. By contrast, the addition of hydrazines to ynones is known to be highly regioselective³⁶ and so we envisioned that our methodology could be used to develop a new route to celecoxib using **1** as the key building block instead of TFA. The appropriate 4-methylphenyl ynones **227** was synthesised in 75% overall yield from **1** over two steps as described previously (Table 4.6). Reaction of *p*-sulfanilamide (**254**) with sodium nitrite gave the corresponding diazonium ion, which was then reduced *in situ* by tin(II) chloride to form hydrazine **255**

as its hydrochloride salt (Scheme 4.26). The unit cell parameters of a single crystal of **255** were determined and found to correspond to those of a previously characterised crystal.³⁷



Scheme 4.26. Synthesis of sulfonamide-hydrazine from p-sulfanilamide

The reaction of ynone **227b** with hydrazine **255** was then carried out to give celecoxib (**31**) in an overall isolated yield of 58% from **1** over just three steps (Scheme 4.27). Unfortunately, this process gave the same regioselectivity as the industrial process with 4% of the undesired regioisomer formed. However, this reaction does exemplify the potential of using a readily accessible refrigerant gas in drug manufacturing processes.



Scheme 4.27. Synthesis of celecoxib from 227b and 255

Some further examples of heterocycle formation from naphthyl ynone **224b** were carried out by MChem students Thomas Marsh and Alessia Santambrogio, included below for completeness in Figure 4.20. Bromophenyl and pyridinyl amidines gave pyrimidines **256** and **257**, albeit with lower yield than with unsubstituted benzamidine due to their relatively poor electron density. With 2-aminopyridine, an unusual pyrido[1,2-*a*]pyrimidine structure was formed with the pyridine nitrogen attacking as nucleophile first before cyclisation through the amine then reaction with the ethanol solvent to form **258**. Analogous to the reaction with hydrazine, reaction with hydroxylamine hydrochloride and potassium carbonate gave isoxazole **259** as a single regioisomer. Finally, a novel synthesis of CF₃-quinolines (**260a-e**) and chromenes (**261a-e**) was

developed by the reaction of **224b** with 2-amino or 2-hydroxy benzophenones and aldehydes. Following initial addition of the nucleophile, the intermediate allenolate cyclises through the *ortho*-carbonyl to form a range of polysubstituted CF₃-heterocyclic systems, some of which displayed interesting fluxional behaviour that was further studied by two-dimensional NMR, X-ray crystallography and DFT calculations.

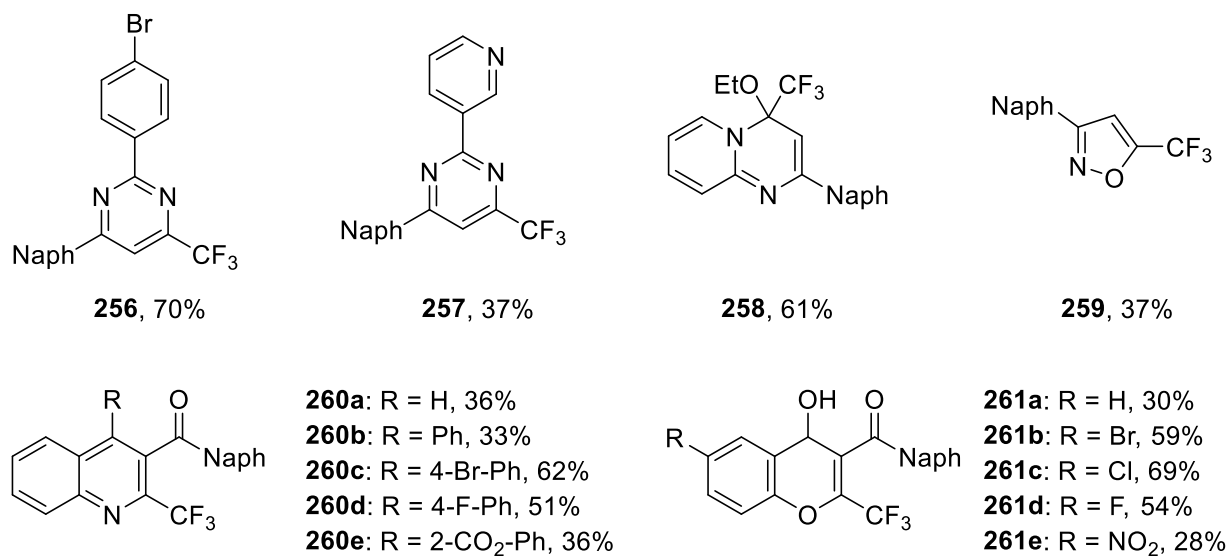
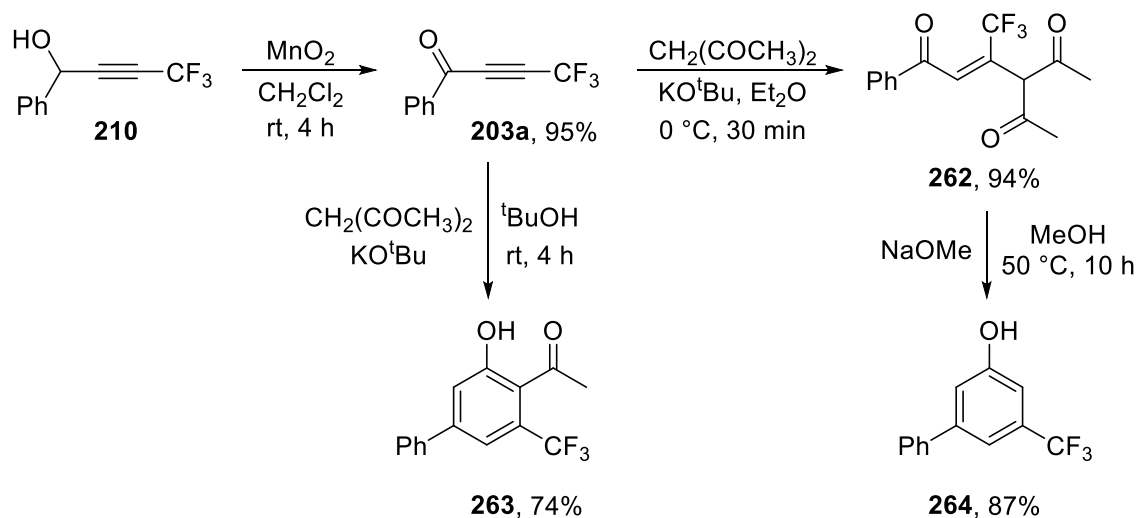


Figure 4.20. Heterocycles from **224b** by MChem students Thomas Marsh and Alessia Santambrogio

A few months after our work was published,³⁸ Yamazaki *et al.* reported a similar method for the synthesis of trifluoromethyl ynones.³⁹ The route also relies on addition of lithium 3,3,3-trifluoropropynide to aldehydes followed by oxidation of the resulting alcohol but, in their case, the alkynide was generated from 2-chloro or 2-bromo-3,3,3-trifluoropropene and MnO₂ was used as the oxidant. 10 equivalents of MnO₂ in CH₂Cl₂ gave good conversion for benzaldehyde derivatives in 2-4 hours but, for aliphatic aldehydes, suffered from side reactions and lower isolated yields. Yamazaki *et al.* were able to repeat our reactions of trifluoromethyl ynones with amidines to give pyrimidines, expanding the substrate scope in terms of amidine substituents as well as extending the reaction to ureas to form CF₃-aminopyrimidines. Base-mediated Michael addition of 1,3-dicarbonyl enolates to these ynones was also carried out and found to give the same regio- and stereoselectivity as our Michael addition reactions of amines and alcohols to give products such as **262**. By raising the temperature and extending the reaction time, an intramolecular cyclisation process was found to occur via formation of a second enolate, giving access to highly substituted CF₃-phenols such as **263** (Scheme 4.28). By changing

the base from potassium *tert*-butoxide to sodium methoxide, this cyclisation was accompanied by deacetylation to give phenol **264**.



Scheme 4.28. Yamazaki *et al.*'s synthesis of CF_3 -ynones and subsequent reactions³⁹

4.3 Conclusions

2,3,3,3-Tetrafluoropropene (HFO-1234yf, **1**) reacts with LDA to eliminate lithium fluoride and form 3,3,3-trifluoropropyne. With two equivalents of base, the alkyne formed is deprotonated and can be trapped with aldehydes to form corresponding CF_3 -substituted propargyl alcohols. After screening conditions and monitoring the reaction by *in situ* IR spectroscopy, lithium diisopropylamide and methyl *tert*-butyl ether were identified as the base and solvent to give the highest yields.

Reaction with a series of differently substituted aldehydes was carried out and subsequent oxidation of the resulting alcohols with Dess-Martin periodinane gave a range of trifluoromethyl ynones with excellent functional group tolerance and minimal purification required. Most of these were previously unknown compounds as the alkynyl- CF_3 ynone structure is remarkably rare in the literature. Michael-type reactions of trifluoromethyl ynones with various alcohols and amines led to formation of a range of CF_3 -enaminones and enones. These reactions show near complete selectivity for the *Z* stereoisomer, which was explored through DFT, crystallographic and NMR studies and found to result from the *Z* stereoisomer being the more thermodynamically stable product and the Michael addition reaction being reversible. Intramolecular nucleophilic addition gave access to CF_3 -azachromones whilst reaction with various electrophiles gave

halogenated CF₃-enones. With dinucleophiles, a range of CF₃-substituted heterocycles were synthesised including pyrazole, pyrimidine and benzodiazepine derivatives. Finally, this method was successfully applied to the synthesis of the blockbuster drug celecoxib, which was obtained in high yield in just three steps from HFO-1234yf, demonstrating the possibility of using refrigerants in the synthesis of complex CF₃-containing systems.

4.4 References for Chapter 4

- ¹ R. N. Haszeldine, *Nature*, 1950, **165**, 152.
- ² A. L. Henne and M. Nager, *J. Am. Chem. Soc.*, 1951, **73**, 1042.
- ³ W. C. Smith, C. W. Tullock, E. L. Muettterties, W. R. Hasek, F. S. Fawcett, V. A. Engelhardt and D. D. Coffman, *J. Am. Chem. Soc.*, 1959, **81**, 3165.
- ⁴ W. G. Finnegan and W. P. Norris, *J. Org. Chem.*, 1963, **28**, 1139
- ⁵ Y. Shen, Y. Xin, W. Cen and Y. Huang, *Synthesis*, 1984, **1**, 35
- ⁶ Y. Shen, W. Qiu, Y. Xin and Y. Huang, *Synthesis*, 1984, **11**, 924.
- ⁷ P. I. Chechulin, V. I. Filyakova and K. I. Pashkevich, *Bull. Acad. Sci. USSR Div. Chem. Sci.*, 1989, **38**, 189
- ⁸ S. Tajammal and A. E. Tipping, *J. Fluorine Chem.*, 1990, **47**, 45
- ⁹ L. Sibous and A. E. Tipping, *J. Fluorine Chem.*, 1993, **62**, 39.
- ¹⁰ A. K. Brisdon and I. R. Crossley, *Chem. Commun.*, 2002, 2420
- ¹¹ C. L. Bumgardner, J. E. Bunch and M.-H. Whangbo, *J. Org. Chem.*, 1986, **51**, 4082
- ¹² T. Wang, D. Niu and T. R. Hoye, *J. Am. Chem. Soc.*, 2016, **138**, 7832.
- ¹³ D. Rosenberg and W. Drenth, *Tetrahedron*, 1971, **27**, 3893
- ¹⁴ R. K. Henderson, C. Jiménez-González, D. J. C. Constable, S. R. Alston, G. G. A. Inglis, G. Fisher, J. Sherwood, S. P. Binks and A. D. Curzon, *Green Chem.*, 2011, **13**, 854.
- ¹⁵ I. E. Kopka, Z. A. Fataftah and M. W. Rathke, *J. Org. Chem.*, 1987, **52**, 448.
- ¹⁶ W. K. Shin, Y. R. Kim, S. H. Im, A. K. Jaladi, S. Gundeti and D. K. An, *Bull. Korean Chem. Soc.*, 2018, **39**, 683.
- ¹⁷ (a) I. H. Jeong, S. L. Jeon, Y. K. Min and B. T. Kim, *Tetrahedron Lett.*, 2002, **43**, 7171; (b) I. H. Jeong, S. L. Jeon, Y. K. Min and B. T. Kim, *J. Fluorine Chem.*, 2004, **125**, 1629; (c) S. L. Jeon, J. K. Kim, J. B. Son, B. T. Kim and I. H. Jeong, *J. Fluorine Chem.*, 2007, **128**, 153.
- ¹⁸ M. J. Corr, R. A. Cormanich, C. N. von Hahmann, M. Bühl, D. B. Cordes, A. M. Z. Slawin and D. O'Hagan, *Org. Biomol. Chem.*, 2016, **14**, 211.
- ¹⁹ R. J. Linderman and D. M. Graves, *J. Org. Chem.*, 1989, **54**, 661.
- ²⁰ J. R. Parikh and W. von E. Doering, *J. Am. Chem. Soc.*, 1967, **89**, 5505.
- ²¹ R. Erenler and J.-F. Biellmann, *Tetrahedron Lett.*, 2005, **46**, 5683.
- ²² V. Ya. Sosnovskikh and M. A. Barabanov, *J. Fluorine Chem.* 2003, **120**, 25
- ²³ A. Nohara, T. Ishiguro, K. Ukawa, H. Sugihara, Y. Maki and Y. Sanno, *J. Med. Chem.* 1985, **28**, 559.
- ²⁴ C. K. Ingold and W. J. Powell, *J. Chem. Soc., Trans.*, 1921, **119**, 1976.
- ²⁵ H. Yamanaka, K. Tamura, K. Funabiki, K. Fukunishi and T. Ishihara, *J. Fluorine Chem.*, 1992, **57**, 177.
- ²⁶ W. Cen, Y. Ni and Y. Shen, *J. Fluorine Chem.*, 1995, **73**, 161.

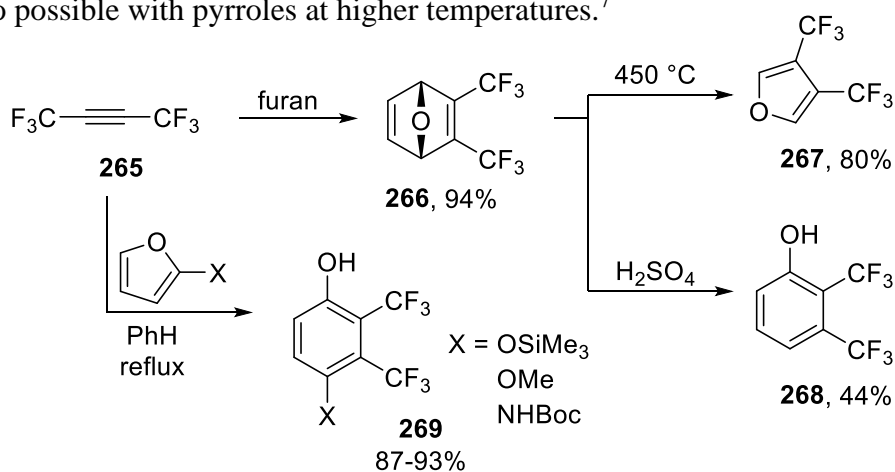
- ²⁷ G. Prié, S. Richard, J.-L. Parrian, A. Duchêne and M. Abarbri, *J. Fluorine Chem.*, 2002, **117**, 35.
- ²⁸ C. D. Poulter, P. L. Wiggins and T. L. Plummer, *J. Org. Chem.*, 1981, **46**, 1532.
- ²⁹ C. Zhou, A. V. Dubrovsky and R. C. Larock, *J. Org. Chem.*, 2006, **71**, 1626.
- ³⁰ P. R. Likhar, M. S. Subhas, M. Roy, S. Roy and M. L. Kantam, *Helv. Chim. Acta*, 2008, **91**, 259.
- ³¹ P. Fricero, L. Bialy, W. Czechtizky, M. Mendex and J. P. A. Harrity, *Org. Lett.*, 2018, **20**, 198.
- ³² E. C. Vatansever, K. Kılıç, M. S. Özer, G. Koza, N. Menges & M. Balci, *Tetrahedron Lett.*, 2015, **56**, 5386.
- ³³ T. D. Penning, J. J. Talley, S. R. Bertenshaw, J. S. Carter, P. W. Collins, S. Docter, M. J. Graneto, L. F. Lee, J. W. Malecha, J. M. Miyashiro, R. S. Rogers, D. J. Rogier, S. S. Yu, G. D. Anderson, E. G. Burton, J. N. Cogburn, S. A. Gregory, C. M. Koboldt, W. E. Perkins, K. Seibert, A. W. Veenhuizen, Y. Y. Zhang and P. C. Isakso, *J. Med. Chem.*, 1997, **40**, 1347.
- ³⁴ S. Dadiboyena and A. T. Hamme, *Curr. Org. Chem.*, 2012, **16**, 1390.
- ³⁵ J. J. Talley, T. D. Penning, P. W. Collins, D. J. Rogier Jr., J. W. Malecha, J. M. Miyashiro, S. R. Bertenshaw, I. K. Khanna, M. J. Graneto, R. S. Rogers and J. S. Carter, US5466823A, 1995.
- ³⁶ J. D. Kirkham, S. J. Edeson, S. Stokes and J. P. A. Harrity, *Org. Lett.*, 2012, **14**, 5354.
- ³⁷ A. M. Asiri, H. M. Faidallah, K. A. Alamry, S. W. Ng and E. R. T. Tiekink, *Acta Cryst.* 2012, **E68**, o1140.
- ³⁸ B. J. Murray, T. G. F. Marsh, D. S. Yufit, M. A. Fox, A. Harsanyi, L. T. Boulton and G. Sandford, *Eur. J. Org. Chem.*, 2020, 6236.
- ³⁹ T. Yamazaki, Y. Nakajima, M. Iida and T. Kawasaki-Takasuka, *Beilstein J. Org. Chem.*, 2021, **17**, 132.

Chapter 5: Cycloaddition reactions of trifluoromethyl ynones

5.1 Introduction

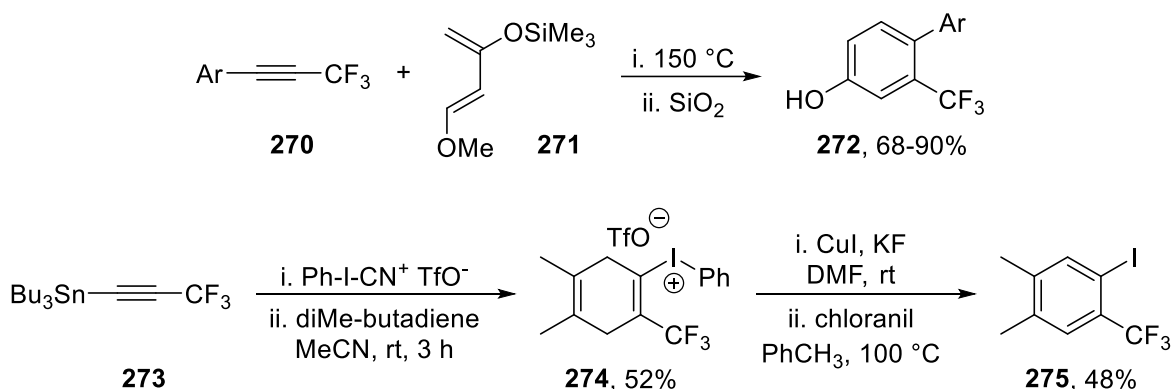
The exceptional electronegativity of the fluorine atom means that the presence of fluorine has a significant impact on the distribution of electrons in a π system and so can affect the rate, stereoselectivity and other attributes of pericyclic reactions.¹ The archetypal pericyclic reaction is the Diels-Alder, a [4+2] cycloaddition between diene and dienophile to generate a six-membered ring.² Traditionally, the Diels-Alder reaction involves an electron-rich diene with a high-energy HOMO and an electron-poor dienophile with a low-lying LUMO. As such, the electron-withdrawing effect of fluorine and fluoroalkyl groups means that alkenes and alkynes with these substituents, such as the CF_3 -ynones derived from **1** as described in Chapter 4, should be highly reactive dienophiles.

In this context, hexafluorobutyne (**265**) was first used in Diels-Alder reactions with benzene at 250 °C³ and subsequently with simple dienes.⁴ More pharmaceutically relevant highly substituted CF_3 -phenols were synthesised through the reaction of **265** with furan gave adduct **266**. Thermolysis of this adduct affected a retro-Diels-Alder reaction to give furan **267** whereas treatment with acid afforded phenol **268** (Scheme 5.1).⁵ It was later shown that reaction of **265** with furans bearing electron-donating groups in the 2-position formed an adduct that ring-opened *in situ* simply with heat in some cases or following filtration through silica, forming CF_3 -phenols such as **269**.⁶ Similar reactions were also possible with pyrroles at higher temperatures.⁷



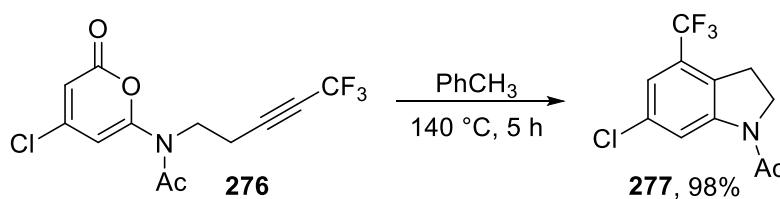
Scheme 5.1. Diels-Alder reactions of hexafluorobutyne with furans^{6,7}

Reaction of aryl CF_3 -alkynes (**270**) with the electron-rich Danishefsky's diene (**271**)⁸ at high temperature followed by reaction with silica provided a route to trifluoromethylated phenols such as **272** (Scheme 5.2).⁹ Alkynyl stannane **273** was converted to a hypervalent iodine species that could subsequently react with a simple diene to form adduct **274**, which was finally converted into trifluorotoluene derivative **275** featuring an iodine substituent as a useful handle for further functionalisation.¹⁰



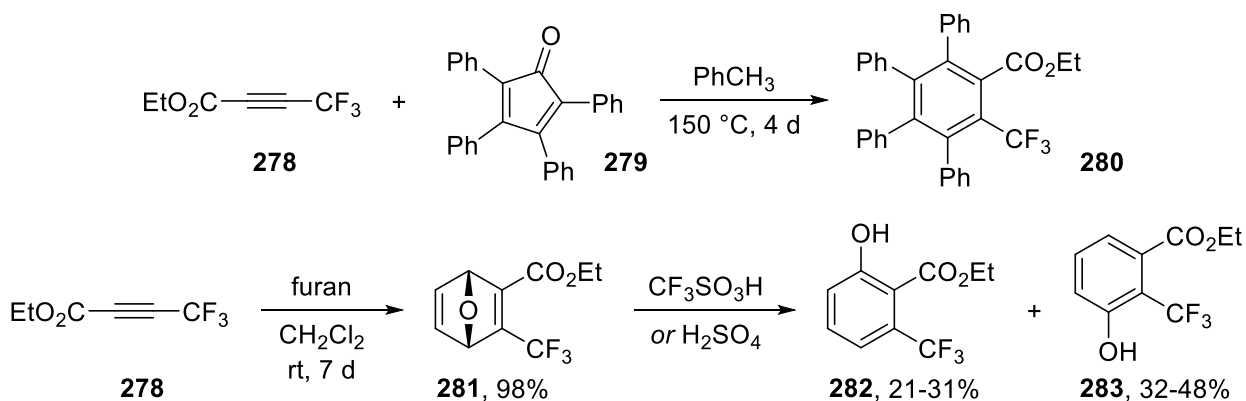
Scheme 5.2. Miscellaneous Diels-Alder routes from CF_3 -alkynes to CF_3 -aromatic systems^{9,10}

α -Pyrone are known to react in Diels-Alder reactions with alkynes and the resulting adduct can then extrude CO_2 to form highly substituted aromatic systems with predictable regiochemistry.¹¹ In terms of fluoroalkylated systems, reaction with α -pyrones has been demonstrated with $\text{ArC}\equiv\text{CCF}_2\text{Br}$ systems¹² and with $\text{SF}_5\text{C}\equiv\text{CCF}_3$.¹³ This methodology was more recently exemplified in an intramolecular synthesis from alkynyl pyrone **276** to form CF_3 -substituted indoline **277** (Scheme 5.3).¹⁴

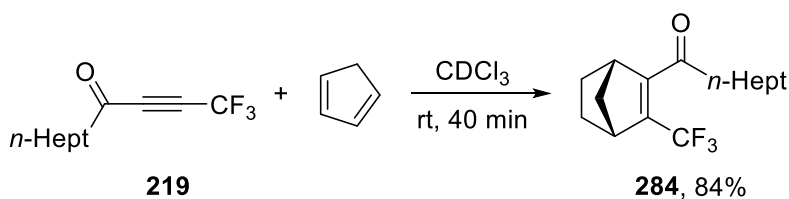


Scheme 5.3. Intramolecular Diels-Alder to form CF_3 -indolines¹⁴

CF_3 -ynoates have also been used in Diels-Alder cycloaddition reactions. Ethyl ester **278** and cyclopentadienone **279** at high temperature formed the highly substituted trifluorotoluene derivative **280** (Scheme 5.4).¹⁵ Reaction of **278** with furan was possible at room temperature but took one week to complete, forming adduct **281**, which then in turn reacted with acid to form a mixture of CF_3 -phenol regioisomers **282** and **283**.¹⁶

Scheme 5.4. Diels-Alder reactions of CF_3 -ynoates^{15,16}

Apart from the work of Bumgardner *et al.* discussed in Chapter 4, the only other reported reaction of CF_3 -ynones with the structure $CF_3C\equiv CCO_2R$ was the simple cycloaddition of *n*-heptyl CF_3 -ynone **219** with cyclopentadiene to give adduct **284** (Scheme 5.5).¹⁷ The rate of reaction was 1680 times greater for **219** than that of unsubstituted ynones and 20 times faster than the derivative with a methyl ester in place of the trifluoromethyl group.

Scheme 5.5. Diels-Alder reaction of a CF_3 -ynone¹⁷

The lack of precedent for the cycloaddition reactions of CF_3 -ynones, i.e. those synthesised from **1** in Chapter 4, is unsurprising given their scarcity in the literature. However, their high reactivity as Michael acceptors suggests the existence of a low-lying LUMO and so should be excellent dienophiles for cycloaddition reactions analogous to the literature examples discussed above. Given the low cost and ready availability of **1**, the synthesis of valuable, highly substituted CF_3 -aromatic systems from ynones derived from **1** would be advantageous and the use of cycloaddition reactions to achieve this might allow for greater regioselectivity than would be possible using established synthetic methods.

5.2 Results and discussion

5.2.1 Initial reactivity studies of cycloaddition reactions

We began our studies on the cycloaddition reaction of CF₃-ynones by conducting DFT calculations for a model compound, phenyl ynone **204a**. These revealed that the LUMO has a slightly greater contribution from the alkynyl carbon adjacent to the carbonyl than for that neighbouring the CF₃ group (Figure 5.1), which is useful information for predicting regio- and stereoselectivity in pericyclic reactions.

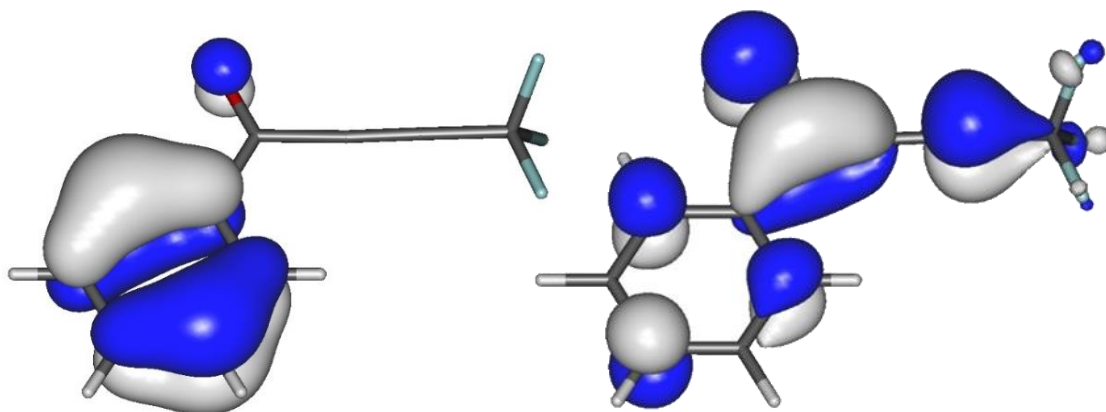
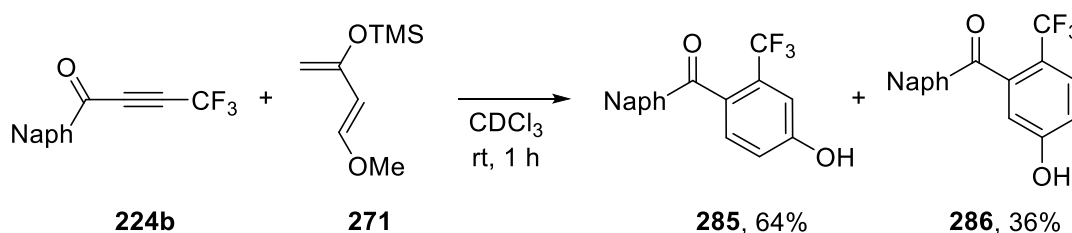
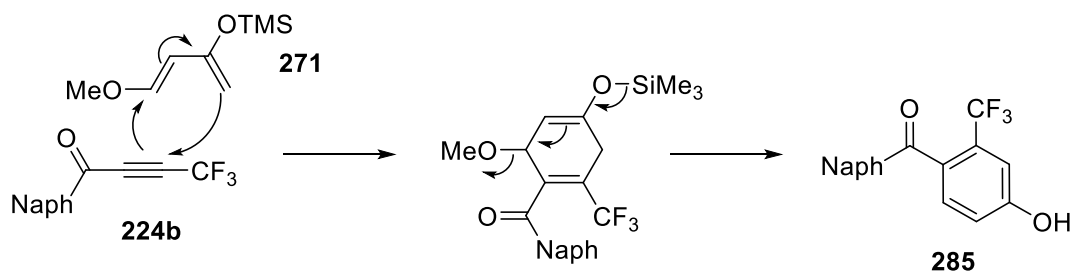


Figure 5.1. Calculated HOMO (left) and LUMO (right) of ynone **204a**; DFT calculations carried out by Dr. Mark Fox (Durham University)

As a proof of concept, naphthyl ynone **224b** was reacted with Danishefsky's diene (**271**) on an NMR tube scale (Scheme 5.6). Hydrolysis of the TMS group *in situ* with subsequent loss of methoxide is followed by rapid tautomerism to gain aromaticity and so form the phenolic products **285** and **286** (Scheme 5.7), the structures of which were proposed based on NMR spectroscopy and GC-MS data but were not proven. Regioselectivity was assumed to follow that predicted by the distribution of partial charges in diene **271** but this was not determined unequivocally. Regardless, the relatively poor selectivity may be also explained by the DFT calculations above, as there is not a great difference between the contributions of the two alkynyl carbon atoms to the LUMO.



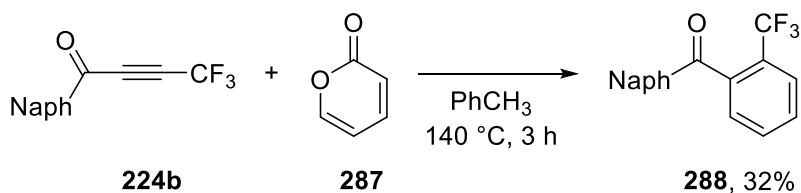
Scheme 5.6. Diels-Alder reaction of ynone **224b** and Danishefsky's diene (products not isolated)



Scheme 5.7. Proposed mechanism of formation of phenol 285

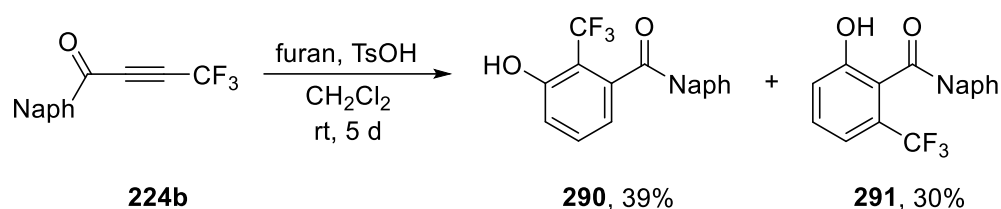
Complexation of the ynone carbonyl group with a Lewis acid would alter the distribution of electron density of the triple bond and so could improve the selectivity of the cycloaddition. However, repeating the reaction of **224b** and **271** in the presence of $\text{BF}_3 \cdot \text{OEt}_2$ led to violent formation of a polymeric mixture, even at -78°C . Lanthanum(III) triflate, a much milder Lewis acid, also led to formation of a polymeric mixture, albeit at a slower rate. Addition of aluminium trichloride to **224b** led to an immediate colour change, even in the absence of **271**, and ^{19}F NMR spectroscopy revealed the emergence of two peaks indicative of trifluoromethyl alkenes. This suggests that addition of a strong Lewis acid activates the ynone to such an extent that it immediately reacts with residual water as a nucleophile, limiting the utility of such an approach.

Moving to other dienes, **224b** and α -pyrone (**287**) showed poor conversion to the cycloadduct at room temperature. After three days, the reaction mixture was still composed of mostly unreacted **224b** along with several other unidentified products. The predicted cycloadduct product would still contain an electron-poor alkene and so might engage in further cycloaddition reactions as the diene was used in excess, leading to polymerisation. Using microwave irradiation, all **224b** was consumed in a few hours but low conversion to the targeted α - CF_3 benzophenone **288** was observed by ^{19}F NMR spectroscopy along with a wide array of side products, suggesting that prolonged heating or higher temperature further reduces selectivity (Scheme 5.8).

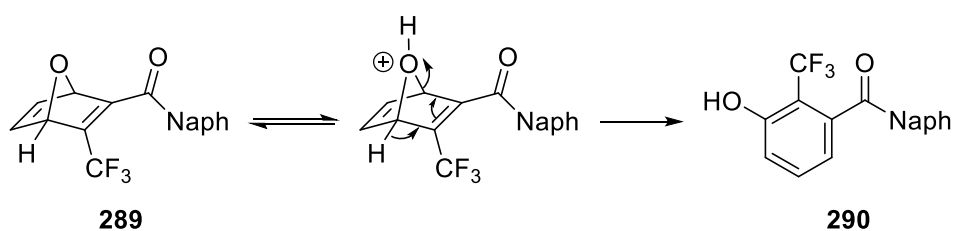


Scheme 5.8. Diels-Alder reaction of ynone 224b and α -pyrone 287 (product not isolated)

Reaction of **224b** with furan was then attempted and quantitative conversion to the expected adduct (**289**) was observed by ^{19}F NMR spectroscopy after 8 hours (Scheme 5.9). Furan was used in excess but no issues with polymerisation were encountered, perhaps because it is a less efficient diene in Diels-Alder reactions. Repeating the reaction on a preparative scale in the presence of *p*-toluenesulfonic acid led to a one-pot ring opening process, although very slowly, of **289** to what are believed to be CF_3 -substituted phenol isomers **290** and **291**, although neither was isolated so this could not be proven. The proton closest to the more electron-withdrawing CF_3 group was assumed to be the most labile and, therefore, **290** would be the major product but this was not confirmed as the two isomers proved difficult to separate (Scheme 5.10).

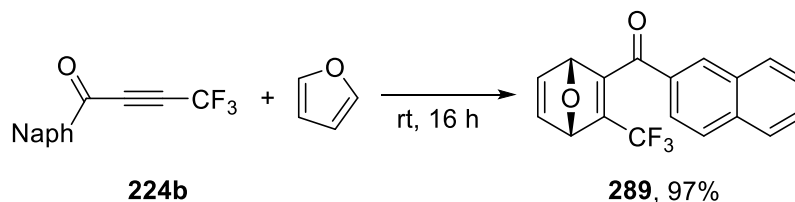


Scheme 5.9. Reaction of 224b with furan and acid-catalysed ring opening (products not isolated)



Scheme 5.10. Mechanism for formation of major isomer 290

Subsequently, the cycloaddition reaction was repeated under solvent free conditions and no side reactions were observed, allowing isolation of **289** in near quantitative yield (Scheme 5.11). However, **289** was found to be unstable at ambient temperature under air on storage after one week and so should be used as quickly as possible after synthesis.



Scheme 5.11. Diels-Alder reaction of ynone 224b with furan

A wide range of different Brønsted and Lewis acids were then screened to determine if appropriate conditions existed to selectively ring open **289** on a shorter timescale than with *p*-TsOH as described above (Scheme 5.9). These reactions were conducted in NMR tubes in deuterated acetonitrile overnight at room temperature (Table 5.1).

Table 5.1. Screening ring opening conditions for **289**

Acid	% Conversion from 289 ^[a]	Result
BF ₃ ·OEt ₂	38	complex mixture
FeCl ₃	6	complex mixture
ZnBr ₂	25	complex mixture
HCl	100	4 products – 3:17:31:49
AlCl ₃	94	4 products – 6:8:22:58
TiCl ₄	100	4 products – 3:15:43:38
<i>p</i> -TsOH	0	no reaction
CuOTf	0	no reaction
La(OTf) ₃	0	no reaction
CF ₃ CO ₂ H	5	single product

^[a] determined by ¹⁹F NMR spectroscopy

Under these conditions, *p*-toluenesulfonic acid, copper(I) triflate and lanthanum(III) triflate gave no reaction. Zinc(II) bromide, boron trifluoride diethyl etherate and iron(III) chloride all caused formation of complex mixtures of many unknown products with varying degrees of conversion. Hydrochloric acid, aluminium trichloride and titanium(IV) chloride gave a mixture of the same four unidentified products, albeit in different proportions. It seems likely, therefore, that the reactivity being observed is a result of HCl formed *in situ*. GC-MS analysis of the reaction mixture showed none of these products contained chlorine, based on the characteristic isotopic ratio pattern, so the origin of these four products is currently unknown although the ¹⁹F NMR chemical shifts would be consistent with CF₃-substituted alkenes or aromatic systems. The same mixture was obtained by treating **289** with 1.0 M HCl in Et₂O in CDCl₃, demonstrating that the solvent MeCN plays no active role in this reaction. Reaction of **289** and BF₃·OEt₂ was also attempted in dry CH₂Cl₂ at 0 °C and gave a cleaner but still complex mixture.

Trifluoroacetic acid catalysis gave only a single product, albeit in low conversion. Potential one-pot cycloaddition-ring opening was explored, again on an NMR tube scale overnight. The reaction of **224b** with furan was carried out using a range of acids as solvent, which meant the scope of acids that could be used was limited by the solubility of **224b** (Table 5.2). In all cases, conversion from **224b** to the Diels-Alder adduct **289** was quantitative. Formic acid and a 1.0 M solution of hydrochloric acid in acetic acid gave similar mixtures of four products as observed with HCl in acetonitrile above. Acetic and trifluoroacetic acid both gave the same, single product in 3% and 24% conversion from **289** respectively, compared to just 5% for TFA in acetonitrile.

*Table 5.2. Screening of one-pot cycloaddition-ring opening of **224b** with furan*

Acid	% Ring Opening	Ratio of products ^[a]
CF ₃ CO ₂ H	24	1:0
CH ₃ CO ₂ H	3	1:0
HCO ₂ H	100	11:29:53:7
HCl (1.0 M in AcOH)	100	11:34:50:5

^[a] determined by ¹⁹F NMR spectroscopy

The reaction was still slow and so raising the temperature was attempted. However, heating the Diels-Alder reaction of **224b** and furan in TFA in an attempt to increase the conversion of ring-opening led only to acid-catalysed polymerisation of the furan. Heating isolated **289** in TFA also led to polymerisation.

Therefore, a range of bases were screened, again on NMR tube scale using deuterated acetonitrile as the solvent (Table 5.3). Strong bases, DBU and 2-*tert*-butyl-1,1,3,3-tetramethylguanidine (Barton's base, BTMG), led to formation of complex mixtures whilst there was no observable reaction at all with KF, DABCO and quinuclidine. With all other bases, there appeared to be a clean reaction to form a single product but with low conversion in all cases. Reactions at elevated temperatures were again explored but, as with the acidic ring opening conditions, heating the reaction mixture led to a loss of selectivity and eventually to polymerisation.

Table 5.3. Screening of basic ring opening conditions for **289**

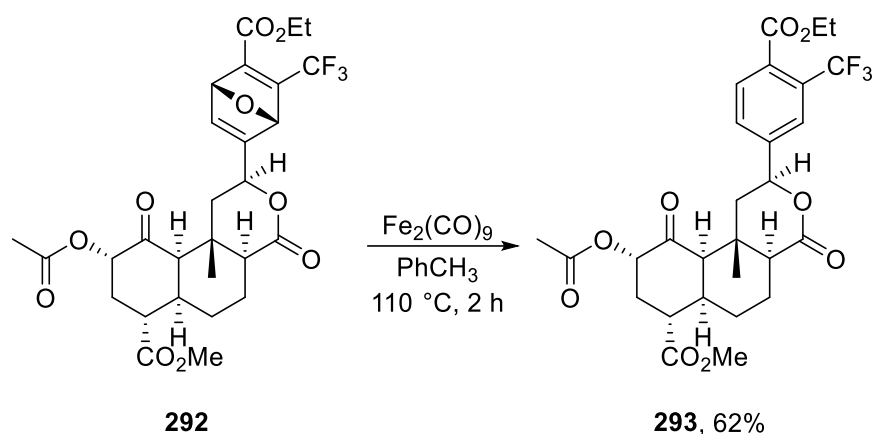
Base	% Conversion from 289 ^[a]	Result
NaOH	8	single product
Cs ₂ CO ₃	3	single product
KO ^t Bu	2	single product
K ₃ PO ₄	0.3	single product
KF	0	no reaction
DBU	50	complex mixture
DABCO	0	no reaction
Quinuclidine	0	no reaction
BTMG	50	complex mixture

^[a] determined by ¹⁹F NMR spectroscopy

Furans with nucleophilic groups in the 2-position were investigated as substrates because these could spontaneously ring open following cyclisation, as has been previously demonstrated with hexafluorobutyne⁶ and various non-fluorinated ynoates.¹⁸ 2-(*N*-Boc)aminofuran, 2-trimethylsilyloxyfuran and 2-methoxyfuran all reacted rapidly with **224b** to give the expected adducts with complete regioselectivity for a single product. However, spontaneous ring opening did not occur as anticipated, even when left for several days. Attempted use of heat or silica as a mildly acidic catalyst to encourage ring opening instead led to formation of intractable complex mixtures as described above.

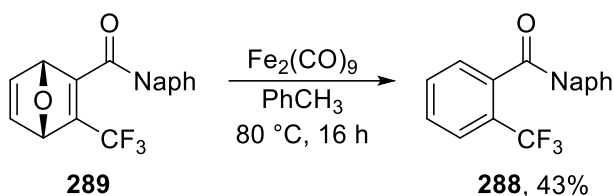
5.2.2 Deoxygenative aromatisation reactions

With acid or base-catalysed ring opening proving either too slow or unselective, deoxygenative ring-opening was instead explored using diironnonacarbonyl,¹⁹ an approach that was recently applied to the synthesis of CF₃-containing analogs of the hallucinogenic natural product salvinorin A by converting the Diels-Alder adduct of a furan with a CF₃-ynoate **292** to aromatic system **293**.²⁰ The mechanism of this reaction is believed to proceed by coordination of the iron complex to the bridging oxygen to form an O-Fe(CO)₄ intermediate species with loss of Fe(CO)₅. On heating, this O-Fe complex decomposes to form the aromatic product and some unknown iron-oxo complex.



Scheme 5.12. Fe₂(CO)₉ induced ring-opening in the synthesis of a CF₃-analog of a natural product²⁰

Applying the conditions shown in Scheme 5.12 to adduct **289** gave CF₃-benzophenone **288** in moderate yield, enabling isolation of the product that we previously attempted to synthesise from α -pyrone (Scheme 5.13).



Scheme 5.13. Deoxygenative ring opening reaction of Diels-Alder adduct **289**

Benzophenones are common motifs in natural products²¹ as well as being useful building blocks for organic synthesis, acting as precursors to functional groups such as oximes, cyanohydrins, carbazones, acetals and pinacols. The benzophenone moiety itself can also be found in various medications, such as ketoprofen,²² fenofibrate²³ and raloxifene,²⁴ and is also widely used in sunscreens. Previous methods for the synthesis of *ortho*-CF₃ benzophenones have relied on cross-coupling reactions of *ortho*-substituted trifluorotoluene derivatives,²⁵ trifluoromethylation of *ortho*-aminobenzophenones,²⁶ or superacidic Friedel-Crafts-type reactivity.²⁷ These methods suffer from either a lack of selectivity for the *ortho* isomer or needing to use directed lithiation procedures to control the selectivity and, in some cases, also need expensive trifluoromethylating reagents.

Whilst the deoxygenative ring opening reaction with Fe₂(CO)₉ was successful, the need for stoichiometric amounts of a toxic transition metal complex is disadvantageous for potential scale-up. Previous literature reports for deoxygenative ring opening have used

other low valent metal complexes derived from iron, titanium, tungsten or molybdenum, which can be generated *in situ* by reduction of the corresponding metal chloride with reagents such as *n*-BuLi and LiAlH₄, but these methods also require stoichiometric amounts of metal.²⁸

Murai *et al.* recently reported a similar reaction using 2.5 mol-% of a rhenium catalyst with a stoichiometric amount of triphenylphosphite as a sacrificial oxygen acceptor.²⁹ Applying these conditions to naphthyl ynone **224b** and furan in an attempted one-pot Diels-Alder/aromatisation process led to complete consumption of **224b** but only partial ring-opening (Table 5.4). GC-MS analysis showed the presence of significant amounts of phenol in the reaction mixture, presumably formed from triphenylphosphite. **224b** is known to be highly reactive towards nucleophiles even at ambient temperature so, with prolonged heating, the formation of a range of products is not unexpected. Further investigation was unable to establish other conditions using catalytic amounts of either other transition metals or stoichiometric additives.

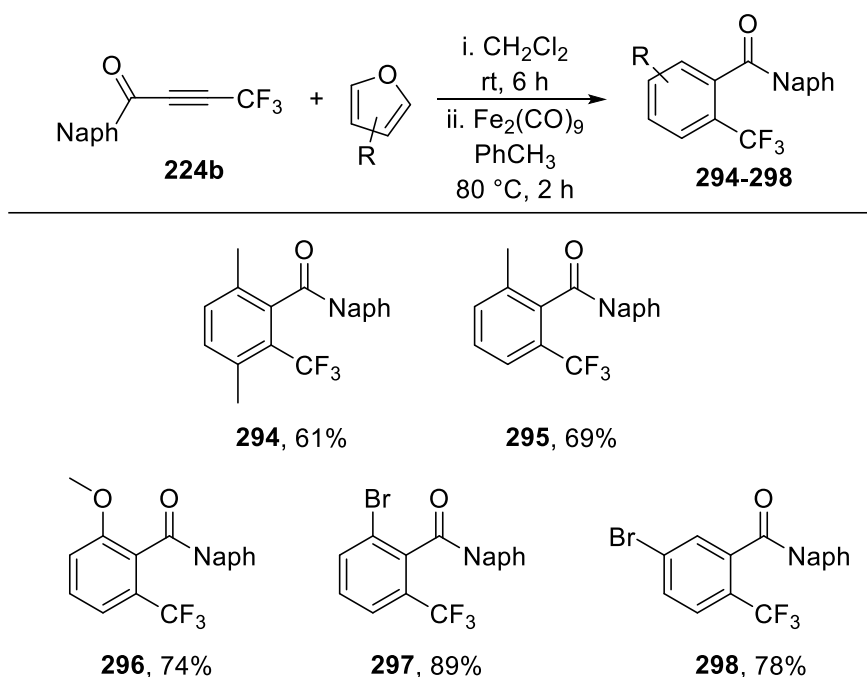
Table 5.4. Screening of conditions for catalytic deoxygenative aromatisation

Catalyst	Additive	Degassed	% Conversion ^[a]
NH ₄ ReO ₄	P(OPh) ₃	no	0
NH ₄ ReO ₄	P(OPh) ₃	yes	38
NH ₄ ReO ₄	PPh ₃	yes	15
NH ₄ ReO ₄	Fe	yes	0
Fe ₂ (CO) ₉	P(OPh) ₃	yes	0

^[a] determined by ¹⁹F NMR spectroscopy

Therefore, further examples of the deoxygenative aromatisation reaction with stoichiometric diironnonacarbonyl were investigated. The intermediate adduct was formed by reaction of naphthyl ynone **224b** either neat or with dichloromethane as a co-solvent if the furan was solid or too costly to use in excess. By reducing the reaction time from overnight to just two hours and changing purification from two filtrations through Celite followed by silica to a single filtration through alumina, improved yields were obtained (Scheme 5.14). 2-Ethyl furoate, 3-ethyl furoate and oxazole were unreactive in the initial cycloaddition reaction with **224b**, even at elevated temperatures. 2,5-Dimethyl

furan gave the symmetrical benzophenone **294** whilst unsymmetrical dienes gave only a single product in each case, namely **295** from 2-methylfuran, **296** from 2-methoxyfuran, **297** from 2-bromofuran and **298** from 3-bromofuran. No debromination was observed in the latter two cases, generating *ortho*-CF₃ benzophenones bearing a synthetically useful aryl bromide handle for further transformations.



Scheme 5.14. Substrate scope for deoxygenative aromatisation reactions

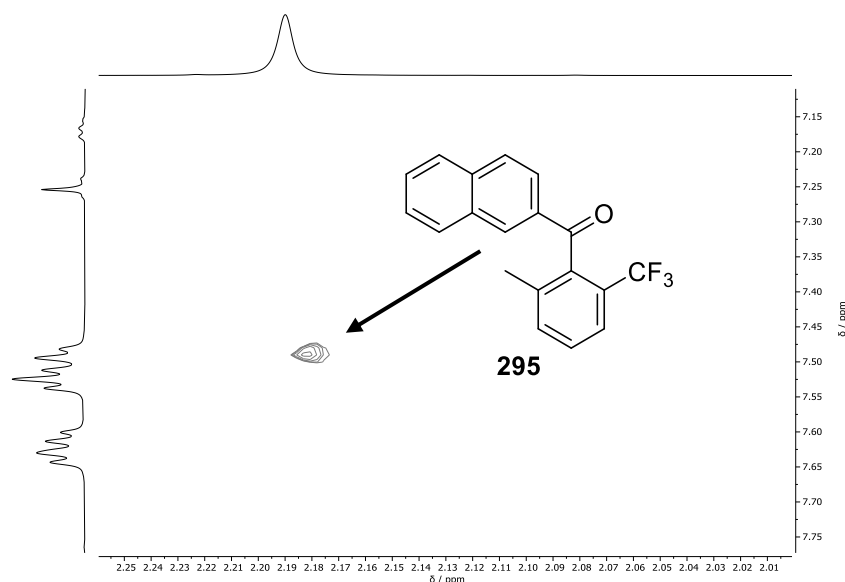


Figure 5.2. ¹H-¹H NOE spectrum of **295**

Complete regioselectivity was observed in each case for the isomers shown, with the structure determined by ¹H-¹H NOE spectroscopy. For example, methyl derivative **295**

showed a correlation between the protons of the methyl group and those on the naphthyl ring. This indicates spatial proximity between these protons and, therefore, that the sole regioisomer formed is that shown in Figure 5.2 as the other possible isomer would not give rise to this correlation. This selectivity matches the predicted outcome from the calculated LUMO of phenyl ynone **204a** shown in Figure 5.1

5.3 Conclusions

As demonstrated in Chapter 4, CF₃-ynones can be derived from the refrigerant gas 2,3,3,3-tetrafluoropropene (HFO-1234yf, **1**) in two steps without column chromatography in high yield and with high purity. These electron-poor systems proved to be reactive dienophiles for Diels-Alder cycloaddition reactions, reacting with a range of different dienes. However, in many cases attempted ring-opening of the resulting adducts to form more valuable CF₃-substituted systems was unsuccessful either due to poor conversion or polymerisation and a lack of selectivity leading to formation of intractable complex mixtures.

Reaction of CF₃-ynones with a range of variously substituted furans was rapid and clean, affording quantitative conversion at room temperature in a few hours at most. This contrasts with other CF₃-alkynes, even the structurally related CF₃-ynoates, which typically require much longer reaction times and/or higher temperatures. Subsequent reaction of the bicyclic *oxo*-adducts formed from CF₃-ynones and furans with diironnonacarbonyl led to deoxygenative aromatisation to form *ortho*-CF₃ benzophenones with generally high isolated yields and functional group tolerance. Whilst the need for stoichiometric amounts of a transition metal complex limits the scalability of this process, these reactions provide a new route to previously difficult to synthesise highly substituted CF₃-aromatic systems with complete and predictable regioselectivity and so could prove useful for smaller scale applications such as within medicinal chemistry discovery programmes.

5.4 References for Chapter 5

¹ I. S. Kondratov, N. A. Tolmachova and G. Haufe, *Eur. J. Org. Chem.*, 2018, **27**, 3618.

- ² O. Diels and K. Alder, *Justus Liebigs Ann. Chem.*, 1928, **460**, 98.
- ³ C. G. Krespan, B. C. McKusick and T. L. Cairns, *J. Am. Chem. Soc.*, 1961, **83**, 3428.
- ⁴ (a) J. A. Finkelstein and C. D. Perchonock, *Tetrahedron Lett.*, 1980, **21**, 3323; (b) I. Okamoto, T. Ohwada and K. Shudo, *J. Org. Chem.*, 1996, **61**, 3155; (c) H. Hopf and F. Th. Lenich, *Chem. Ber.*, 1974, **107**, 1891.
- ⁵ (a) A. B. Abubakar, B. L. Booth, N. N. E. Suliman and A. E. Tipping, *J. Fluorine Chem.*, 1992, **56**, 359; (b) M. G. Barlow, N. N. E. Suliman and A. E. Tipping, *J. Fluorine Chem.*, 1995, **70**, 95.
- ⁶ G.-D. Zhu, M. A. Staeger and S. A. Boyd, *Org. Lett.*, 2000, **2**, 3345.
- ⁷ (a) R. W. Kaesler and E. LeGoff, *J. Org. Chem.*, 1982, **47**, 4779; M. Visnick and M. A. Battiste, *J. Chem. Soc., Chem. Commun.*, 1985, 1621.
- ⁸ S. Danishefsky and T. Kitahara, *J. Am. Chem. Soc.*, 1974, **96**, 7807.
- ⁹ T. Hiyama and K. Sato, *Synlett*, 1990, 53.
- ¹⁰ M. Shimizu, Y. Takeda and T. Hiyama, *Chem. Lett.*, 2008, **37**, 1304.
- ¹¹ J. A. Reed, C. L. Schilling Jr., R. F. Tarvin, T. A. Rettig and J. K. Stille, *J. Org. Chem.*, 1969, **34**, 2188.
- ¹² V. M. Muzalevskiy, V. G. Nenajdenko, A. V. Shastin, E. S. Balenkova and G. Haufe, *Synthesis*, 2008, **18**, 2899.
- ¹³ B. Duda and D. Lentz, *Org. Biomol. Chem.*, 2015, **13**, 5625.
- ¹⁴ P. Gan, M. W. Smith, N. R. Braffman and S. A. Snyder, *Angew. Chem. Int. Ed.*, 2016, **55**, 3625.
- ¹⁵ A. Nezis, J. Fayn and A. Cambon, *J. Fluorine Chem.*, 1992, **56**, 29.
- ¹⁶ K. M. Guckian, E. Yin-Shiang Lin, L. Silvian, J. E. Friedman, D. Chin and D. M. Scott, *Bioorg. Med. Chem. Lett.*, 2008, **18**, 5249.
- ¹⁷ T. Wang, D. Niu and T. R. Hoye, *J. Am. Chem. Soc.*, 2016, **138**, 7832.
- ¹⁸ (a) A. Padwa, M. Dimitroff, A. G. Waterson and T. Wu, *J. Org. Chem.*, 1997, **62**, 4088; (b) M. Bobošíková, W. Clegg, S. J. Coles, M. Dandárová, M. B. Hursthouse, T. Kiss, A. Krutošíková, T. Liptaj, N. Prónayová and C. A. Ramsden, *J. Chem. Soc., Perkin Trans. I*, 2001, **7**, 680.
- ¹⁹ W. M. Best, P. A. Collins, R. K. McCulloch and D. Wege, *Aust. J. Chem.*, 1982, **35**, 843.
- ²⁰ A. Lozama, C. W. Cunningham, M. J. Caspers, J. T. Douglas, C. M. Dersch, R. B. Rothman and T. E. Prisinzano, *J. Nat. Prod.*, 2011, **74**, 718.
- ²¹ S.-B. Wu, C. Long and E. J. Kennelly, *Nat. Prod. Rep.*, 2014, **31**, 1158.
- ²² T. G. Kantor, *Pharmacotherapy*, **6**, 93.
- ²³ G. M. Keating, *Am. J. Cardiovasc. Drug.*, 2011, **11**, 227.
- ²⁴ C. D. Jones, M. G. Jevnikar, A. J. Pike, M. K. Peters, L. J. Black, A. R. Thompson, J. F. Falcone and J. A. Clemens, *J. Med. Chem.*, 1984, **27**, 1057.
- ²⁵ (a) J. Lichtenberger and F. Weiss, *Bull. Soc. Chim. France*, 1962, 587; (b) E. Brown, C. Chevalier, F. Huet, C. Le Grumelec, A. Lézé and J. Touet, *Tetrahedron Asymmetry*, 1994, **5**, 1191; (c) A. Fürstner, R. Singer and P. Knochel, *Tetrahedron Lett.*, 1994, **35**, 1047; (d) H. Gao and P. Knochel, *Synlett*, 2009, **8**, 1321; (e) F. Jafarpour, P. Rashidi-Ranjbar and A. O. Kashani, *Eur. J. Org. Chem.*, 2011, **11**, 2182; (f) H. Rao, L. Yang, Q. Shuai and C.-J. Li, *Adv. Synth. Catal.*, 2011, **353**, 1701; (g) P. Lei, G. Meng, Y. Ling, J. An, S. P. Nolan and M. Szostak *Org. Lett.*, 2017, **19**, 6510; (h) S. Panja, P. Maity and B. C. Ranu, *J. Org. Chem.*, 2018, **83**, 12609; (i) P. Ghosh, B. Ganguly and S. Das, *Appl. Organomet. Chem.*, 2018, **32**, 4173

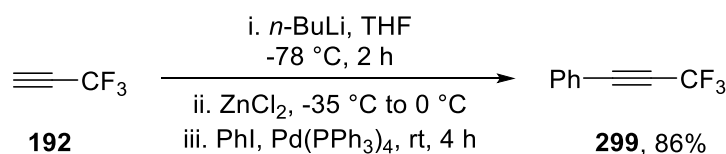
- ²⁶ (a) J. H. Clark, J. E. Denness, M. A. McClinton and A. J. Wynd, *J. Fluorine Chem.*, 1990, **50**, 411; (b) G. Danoun, B. Bayarmagnai, M. F. Grünberg and L. J. Gooßen, *Angew. Chem. Int. Ed.*, 2013, **52**, 7972; (c) J.-J. Dai, C. Fang, B. Xiao, J. Yi, J. Xu, Z.-J. Liu, X. Lu, L. Liu and Y. Fu, *J. Am. Chem. Soc.*, 2013, **135**, 8436; (d) B. Bayarmagnai, C. Matheis, E. Risto and L. J. Gooßen, *Adv. Synth. Catal.*, 2014, **356**, 2343.
- ²⁷ A. Kethe, A. F. Tracy and D. A. Klumpp, *Org. Biomol. Chem.*, 2011, **9**, 4545
- ²⁸ (a) H. Hart and G. Nwokogu, *J. Org. Chem.*, 1981, **46**, 1251; (b) Y. D. Xing and N. Z. Huang, *J. Org. Chem.*, 1982, **47**, 140; (c) H. Hart, C.-Y. Lai, G. C. Nwokogu and S. Shamouilian, *Tetrahedron*, 1987, **43**, 5203; (d) C.-H. Sun and T. J. Chow, *Heterocycles*, 1988, **27**, 217; (e) D. H. Blank and G. W. Gribble, *Tetrahedron Lett.*, 1997, **38**, 4761; (f) C. Bozzo and M. D. Pujol, *Synlett*, 2000, 550; (g) J. Lu, D. M. Ho, N. J. Vogelaar, C. M. Kraml and R. A. Pascal Jr., *J. Am. Chem. Soc.*, 2004, **126**, 11168; (h) F. Bailly, F. Cottet and M. Schlosser, *Synthesis*, 2005, 791.
- ²⁹ M. Murai, T. Ogita and K. Takai, *Chem. Commun.*, 2019, **55**, 2332.

Chapter 6: Towards a trifluoropropynylating reagent

6.1 Introduction

Alkynes are versatile building blocks for the synthesis of organic molecules with an enormous range of different structures.¹ Therefore, trifluoromethylalkynes have great potential utility for the introduction of CF₃ groups into complex multifunctional systems for diverse applications, notably in the synthesis of antiestrogenic drug panomifene² as well as various more recent uses in other syntheses such as in ring-opening metathesis,³ germylation⁴ or borylation⁵ followed by cross-coupling, hydration to form ketones,⁶ and via hydrogenation to introduce a trifluoropropyl group as a nitropropyl bioisostere.⁷ 3,3,3-Trifluoroprop-1-yne (**192**) would be the simplest source of a trifluoropropynyl group but is not commercially available on a useful scale and has a boiling point of -48 °C and so little chemistry has been reported since its first synthesis in the 1950s.⁸

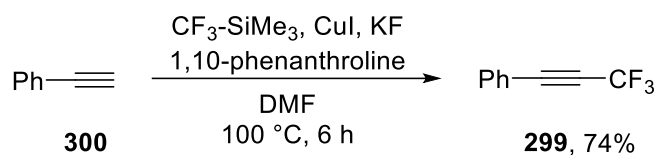
The first aryl trifluoropropynes were synthesised by Yagupolskii by bromination of CF₃-styrenes followed by two successive dehydrobromination reactions.⁹ A similar process involving dehydrochlorination was subsequently reported¹⁰ whilst Kobayashi *et al.* reported synthesis of aryl trifluoropropynes via an intramolecular Wittig process.¹¹ An alternative route from **192** was reported by Bunch & Bumgardner (Scheme 6.1).¹² The intermediate lithium acetylide (**210**) was trapped with zinc chloride to give the alkynyl zinc species, which then underwent a palladium-catalysed Negishi-type coupling with various aryl iodide derivatives to give trifluoromethylated alkynes such as **299**.



*Scheme 6.1. Example synthesis of aryl trifluoropropynes via Negishi coupling*¹²

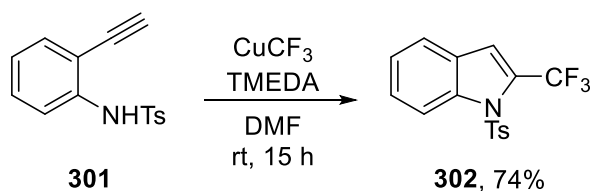
In modern times, aryl trifluoropropynes are more typically synthesised via trifluoromethylation of terminal alkynes. This was first demonstrated by Umemoto using his eponymous benzothiophenium CF₃⁺ salts with lithium alkynides.¹³ The first trifluoromethylation of free, unlithiated alkenes was not reported until 20 years later using the Ruppert-Prakash reagent, CF₃-SiMe₃, and copper catalysis, e.g. from **300** to **299** as in

Scheme 6.2.¹⁴ In this case, TMS-CF₃ acts as a source of the CF₃⁻ anion that then forms a CuCF₃ complex *in situ*, which then adds to the alkyne via an oxidative coupling process.



Scheme 6.2. Example synthesis of aryl trifluoropropyne using the Ruppert-Prakash reagent¹⁴

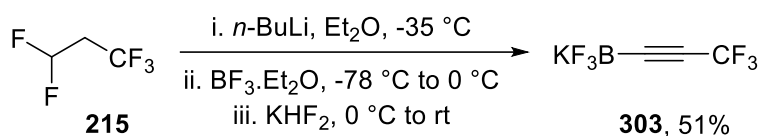
Copper-catalysed trifluoromethylation has since been used with the Umemoto reagent¹⁵ as well as with hypervalent iodine sources of CF₃⁺, the so-called Togni reagents, using either copper¹⁶ or gold¹⁷ catalysis. As an alternative to free alkyne substrates, alkynyltrifluoroborates can also be used as a reactant in copper-catalysed reactions with the Togni reagent¹⁸ or with the Langlois reagent (CF₃SO₂Na) via a radical mechanism.¹⁹ Copper/silver-catalysed decarboxylative trifluoromethylation of arylpropionic acids with TMS-CF₃ has been demonstrated²⁰ as has trifluoromethylation of terminal alkynes with CF₃I enabled by photoredox catalysis with *fac*-[Ir(ppy)₃].²¹ Another gaseous reagent, fluoroform (CF₃H), has been used to generate CuCF₃ as a less expensive source of CF₃ than the reagents listed above.²² Fluoroform, available on a very large scale as it is a by-product of the manufacture of PTFE, rapidly reacts with copper(I) chloride and potassium *tert*-butoxide to generate the CuCF₃ complex,²³ which can be stabilised using various amines, in this case tetramethylethylenediamine (TMEDA). This method was also employed in a one-pot cascade trifluoromethylation/cyclisation of 2-alkynyl anilines (**301**) to synthesise CF₃-substituted indoles (**302**, Scheme 6.3) via the appropriate trifluoropropynyl intermediate.²⁴



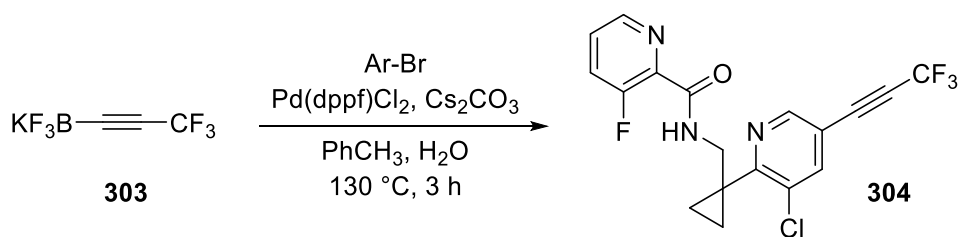
Scheme 6.3. Example synthesis of CF₃-indoles using CuCF₃ generated from fluoroform²⁴

These various methods for the trifluoromethylation of alkynes typically rely on reagents that are prohibitively expensive on process scales or CuCF₃, which can be derived from various sources but usually requires a super-stoichiometric excess of copper. Use of an alkyne as the key starting material can also be problematic as some alkynes are not

sufficiently stable to be stored in their unprotected forms and are less readily available than more common building blocks such as aryl halides. As such, trifluoropropynylation reactions of aryl halides or pseudo-halides would potentially be a more attractive route. Ramachandran & Mitsuhashi demonstrated that trifluoropropynyl lithium (**210**), generated *in situ* from HFC-245fa (**215**), could be trapped with $\text{BF}_3 \cdot \text{Et}_2\text{O}$ then treated with aqueous KHF_2 to give the trifluoropropynyl potassium trifluoroborate salt **303** (Scheme 6.4).²⁵ There is only one reported cross-coupling reaction of **303**, a Suzuki coupling to a bromopyridine as part of a Syngenta patent for carboxamide pesticide **304** (Scheme 6.5).²⁶



Scheme 6.4. Synthesis of a trifluoropropynyl trifluoroborate salt²⁵



Scheme 6.5. Use of a trifluoropropynyl trifluoroborate salt in Suzuki cross-coupling²⁶

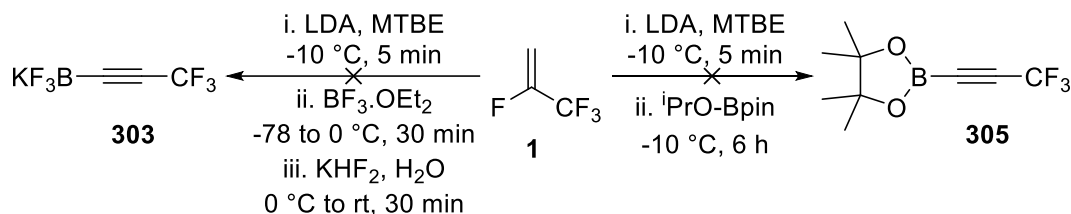
Together with the Negishi coupling using propyne **192**, as shown above in Scheme 6.1, cross-coupling of trifluoroborate salt **303** represents the only trifluoropropynylation reactions yet described in the literature. As shown in Chapter 4, lithium fluoride can be eliminated from HFO-1234yf (**1**) to generate **210** *in situ*. Therefore, we envisaged that trapping of **210** derived from **1** with different electrophiles might afford a bench-stable reagent that could act as a surrogate for gaseous **192** and so make trifluoropropynylation reactions a viable alternative to the trifluoromethylation of terminal alkynes.

6.2 Results and discussion

6.2.1 Initial lithium 3,3,3-trifluoropropynide trapping attempts

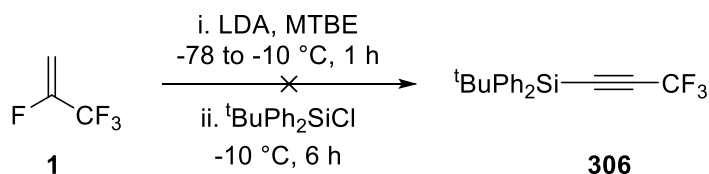
We attempted to repeat the method of Ramachandran *et al.* shown in Scheme 6.4 using alkynide **210** derived from **1** using the method outlined in Chapter 4 (LDA in MTBE).

No reaction was observable by ^{19}F NMR spectroscopy apart from the initial elimination (Scheme 6.6). Repeating this reaction with Ramachandran's later method for trapping **210** with K_3PO_4 instead of KHF_2 , which they found gave lower yields but caused less glass etching,²⁷ likewise gave no borylated product. Following the method of Harrity *et al.* for the borylation of unfluorinated propargyl alcohols,²⁸ reaction of **210** with $^i\text{PrO-Bpin}$ was also attempted but this did not give the intended fluorinated product **305**.



Scheme 6.6. Attempted application of literature borylation procedures to HFO-1234yf

Drakesmith *et al.* reported the trapping of alkyne **210** derived from 3,3,3-trifluoropropene with triethylsilyl chloride.²⁹ We attempted to use the bulkier *tert*-butyldiphenylsilyl chloride to synthesis of trifluoropropynyl silane **306** from **1** via **210** but no conversion was observed by ^{19}F NMR spectroscopy (Scheme 6.7). Trimethylsilyl chloride also gave no reaction under our conditions so steric hindrance alone cannot explain the lack of reactivity with **210** derived from **1**. Hanamoto & Yamada reported that **210**, generated from 2-bromo-3,3,3-trifluoropropene, was also unreactive with silanes.³⁰ They found that addition of 20 mol-% HMPA gave the corresponding trifluoromethyl silyl alkyne in good yield. HMPA is renowned for its carcinogenicity so we used DMPU as a less toxic alternative³¹ but this did not improve conversion from **1**.

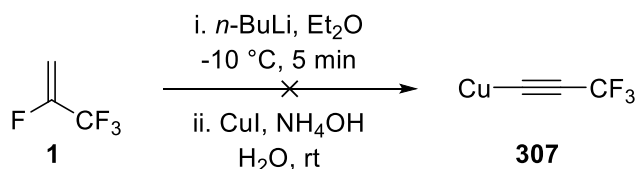


Scheme 6.7. Attempted synthesis of a trifluoropropynyl silane from HFO-1234yf

Lithium fluoride is produced from the elimination of **1** to form alkyne **210** and, whilst not soluble in MTBE, could be present in sufficient amounts to immediately cleave any C-Si bond formed and regenerate the free alkyne. It may, therefore, not be possible to synthesise any trifluoropropynyl silanes under these conditions without isolating the intermediate alkyne. However, subsequently to our work, Hoge *et al.* reported that **210**

derived from **1** did react with trimethylsilylchloride when using *n*-butyl lithium rather than LDA with dimethyl ether instead of MTBE as a solvent.³² Given the similarity in solvent choice, it seems likely that the presence of diisopropylamine is responsible for the lack of reaction in our case. This could be due to the amine decomposing the product directly or bringing sufficient lithium fluoride into solution to cause break-down of the alkynyl silane. The same mechanism may also be responsible for the decomposition of any trifluoropropynyl boranes, as alkynyl boranes are known to be somewhat unstable.³³

Copper alkynides are generally bench-stable solids but fairly poor nucleophiles, although simple copper acetylide is a known explosive.³⁴ Copper 3,3,3-trifluoropropynide (**307**) has only been prepared once before by the reaction of gaseous 3,3,3-trifluoropropyne with copper chloride and ammonium hydroxide.³⁵ Haszeldine described **307** as slowly breaking down with gentle heating whereas rapid heating “brought about the vigorous decomposition of larger quantities with occasionally a slight explosion”. In an attempt to isolate **307**, we carried out the reaction of **1** with *n*-BuLi in diethyl ether and the resulting solution of **210** was transferred via cannula into a solution of copper(I) iodide in a mixture of 5:3 ammonium hydroxide and ethanol (Scheme 6.8). A yellow precipitate appeared to form from the blue ammoniacal copper solution but in insufficient quantity to be readily isolated. An alternative approach was trialled by generating a solution of **210** in diethyl ether then quenching the reaction mixture with water. A continual flow of argon through the reaction mixture was used to carry the gaseous 3,3,3-trifluoropropyne formed and bubble it through an ammoniacal copper solution. However, using this approach, no visible precipitate was formed. Given the potential thermal instability of **307**, no further attempts were made to isolate it or the equivalent silver and mercury acetylides also reported in the literature by Haszeldine.³⁵



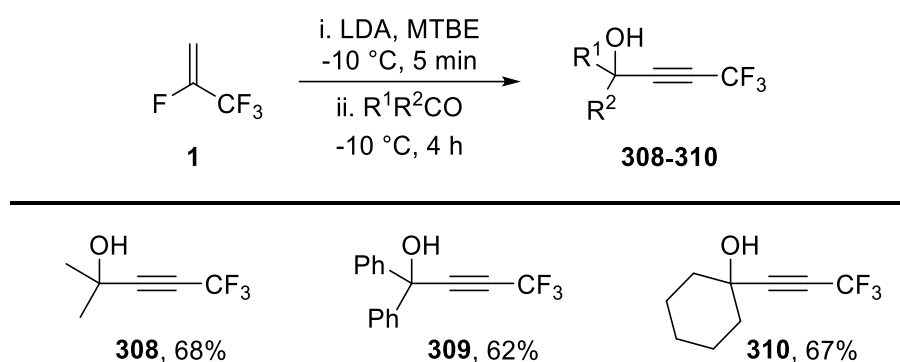
Scheme 6.8. Attempted synthesis of copper 3,3,3-trifluoropropynide from HFO-1234yf

6.2.2 Deacetonative Sonogashira coupling

Whilst direct palladium-catalysed cross-coupling of lithium alkynides has been recently described,³⁶ the use of free terminal alkynes or protected alkynes that are deprotected *in*

situ is much more commonplace. 2-Hydroxyprop-2-yl-alkynes can be used as a protected form of the equivalent free terminal alkyne³⁷ but this methodology has never been applied to the synthesis of corresponding trifluoromethyl alkynes. The hypothetical key building block for this process, 5,5,5-trifluoro-2-methyl-pent-3-yn-2-ol (**308**), has previously been prepared by addition of lithium 3,3,3-trifluoropropynide (**210**)²⁹ or the equivalent magnesium bromide³⁸ to acetone. Some simple transformations of **308**, namely reaction with elemental bromine³⁹ and hydrogenation with palladium on carbon,³⁸ have been reported along with various methods to form CF₃-allenes⁴⁰ and its use as a building block in the synthesis of CF₃-substituted pyrans.⁴¹ However, the use of **308**, or any structurally similar compound, to generate **192** via loss of a ketone has so far been unexplored and could be of great utility in the synthesis of trifluoromethyl alkynes.

In our case, alkynol **308** was synthesised from **1** using the same procedure as used for the trapping of **210** with aldehydes described in Chapter 4 but **308** required distillation to be isolated from MTBE due to its relatively low boiling point of 110 °C (Scheme 6.9). This step could be avoided by using diethyl ether as the solvent, which gave a lower isolated yield of 61% but was less labour-intensive. These reactions were also slower than for the equivalent addition to aldehydes, taking several hours to reach full conversion as observed by ¹⁹F NMR spectroscopy as opposed to the instantaneous reaction of alkynide **210** with benzaldehyde observed by *in situ* IR spectroscopy in Chapter 4.

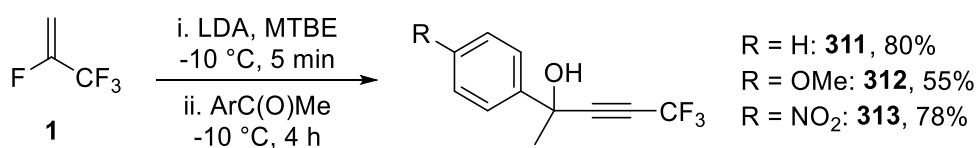


Scheme 6.9. Reactions of lithium 3,3,3-trifluoropropynide generated from **1** with ketones

Equivalent reactions with cyclohexanone and benzophenone gave alkynols **309** and **310**, respectively. **310** has previously been prepared from 2-bromo-3,3,3-trifluoropropene using an analogous approach⁴² whilst the synthesis of **309** is more well attested to in the literature with reports using 2-bromo-3,3,3-trifluoropropene,^{42a} 1,1-dichloro-3,3,3-

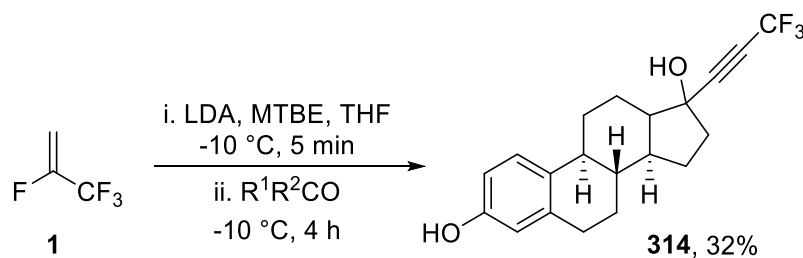
trifluoroacetone,^{40a} 1-chloro-3,3,3-trifluoropropene,⁴³ a trifluoropropynyl hexacarbonyl cobalt complex³⁹ and trifluoropropynyl magnesium bromide⁴⁴ as starting materials.

Expanding our scope further, addition of alkyne **192** derived from **1** to acetophenone gave alkynol **311** in good isolated yield (Scheme 6.10). This reaction could also be extended to acetophenone substrates with both electron-donating (*p*-OMe, **312**) and electron-withdrawing (*p*-NO₂, **313**) substituents on the aromatic ring. As would be expected, the more electron-poor carbonyl system proved more reaction and so the yield of **313** was greater than that of **312**.



Scheme 6.10. Reactions of lithium 3,3,3-trifluoropropynide generated from **1** with acetophenones

Reaction of the steroid estrone under these conditions afforded alkynol **314**, which has some pharmaceutical relevance as a trifluoromethylated analog of the birth control drug ethinyl estradiol (Scheme 6.11).⁴⁵ Two equivalents of the alkyne **192** were required as one was lost in deprotonating the phenol of the starting material. The poor solubility of estrone in MTBE led to the use of THF as a co-solvent but estrone was still barely soluble in THF and the final yield of **314** reflects these solubility issues. **314** has previously been synthesised by the reaction of a trifluoropropynyl magnesium bromide with estrone.⁴⁶

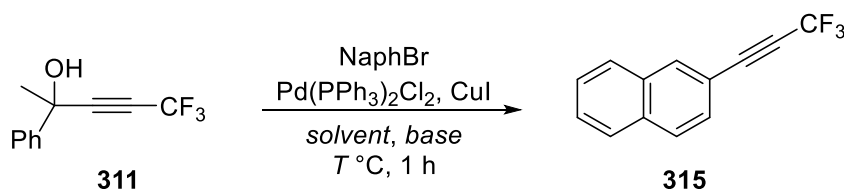


Scheme 6.11. Synthesis of a trifluoromethylated analog of ethinyl estradiol

With the CF₃-alkynols in hand, a one-pot deprotection/Sonogashira coupling reaction of acetophenone-derived **311** with naphthyl bromide to give alkyne **315** was attempted as a proof of concept. There have been numerous examples of equivalent deacetonative Sonogashira coupling reactions reported in the literature for the process with non-fluorinated alkenes.⁴⁷ Examples using phenylmethyl systems such as **311** are less

common, although not unprecedented.⁴⁸ A range of different solvents and bases were screened (Table 6.1) using a microwave reactor with sealed vials to contain any gaseous 3,3,3-trifluoropropyne (**192**) formed. No significant increase in pressure was detected in any case, suggesting at this scale that any **192** formed stays in solution. Whilst diisopropylamine and DMF both gave similar conversions at 80 °C, reaction in DMF had many more side products and so diisopropylamine was selected as the preferred solvent. The use of bases other than KOH also improved selectivity, suggesting that the hydroxide ion was interfering with the reaction by hydrolysing the alkyne. K₃PO₄ in particular gave very clean conversion to **315**. Whilst the reaction did occur without the presence of copper, conversion was decreased suggesting that *in situ* formation of copper 3,3,3-trifluoropropynide may occur but is not essential for the coupling reaction to proceed.

Table 6.1. Screening of conditions for Sonogashira coupling



Base	Solvent	<i>T</i> / °C	% Conversion ^[a]
KOH	DMF	100	59
KOH	DMF	80	51
KOH	DMF	60	41
KOH	MeCN	80	0
KOH	ⁱ PrNH ₂	80	54
K ₂ CO ₃	ⁱ PrNH ₂	80	82
Ag ₂ CO ₃	ⁱ PrNH ₂	80	0
KO ^t Bu	ⁱ PrNH ₂	80	0
K ₃ PO ₄	ⁱ PrNH ₂	80	95
K ₃ PO ₄ (no CuI)	ⁱ PrNH ₂	80	77

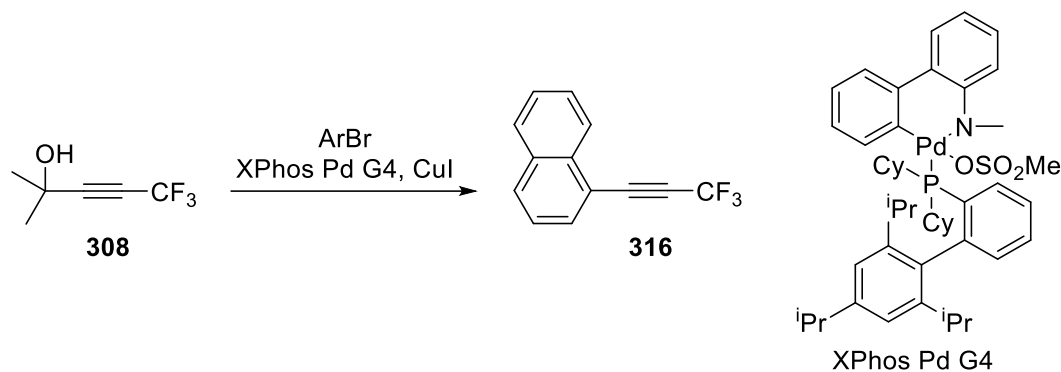
^[a] determined by ¹⁹F NMR spectroscopy analysis of crude reaction mixture

Whilst near quantitative conversion to **315** was obtained as determined by ¹⁹F NMR spectroscopy, the product was not isolated as this would require column chromatography or distillation to remove the acetophenone by-product. The acetone-derived adduct **308** should similarly be capable of Sonogashira cross-coupling. In that case, the only by-

product would be acetone, which is volatile and so should be easily removed by evaporation and the product aryl trifluoropropynes could be isolated without the need for resource-intensive purification procedures. However, reaction of **308** with 2-bromonaphthalene under the optimised conditions detailed above gave varied results with significant homocoupling of the aryl bromide to a range of unidentified fluorinated side products. It is possible the presence of acetophenone instead of acetone in the reaction mixture leads to more unwanted reactions via the more reactive enolate form of the ketone that interfere with the intended cross-coupling.

Therefore, further screening was carried out using **308** in an effort to improve reactivity for this sterically hindered system to form alkyne **316**, now using 1-bromonaphthalene as the substrate. Previous studies have shown that palladacycle complexes with the ligand XPhos can efficiently catalyse deacetonative Sonogashira reactions⁴⁹ whilst XPhos has also been used for deacetonative Sonogashira reactions of aryl chlorides in both acetonitrile⁵⁰ and in water.⁵¹ Therefore, the commercially available pre-catalyst XPhos Pd G4,⁵² consisting of palladium bonded to one XPhos ligand and a mesylate as part of a palladacycle, was used as the catalyst alongside copper(I) iodide (Table 6.2).

In contrast to the reactions with Pd(PPh₃)₂Cl₂, there was no reaction with tripotassium phosphate or potassium carbonate in the presence of the XPhos complex when DMF was used as the solvent. Potassium hydroxide showed improved conversion from 51% in previous work to 70% here but with the same hydrolytic side reactions. Amine bases gave low but measurable conversion, with DBU proving the best with 32%. Changing to various other solvents did not offer much improvement in conversion with triethylamine as the base. Tetrabutylammonium hydroxide (TBAOH), commercially available as a solution in methanol, has been shown in the literature to be an excellent base for cleavage of acetone from alkynes⁵³ and has previously been used as a base for Sonogashira-type cross-coupling reactions of free alkynes.⁵⁴ However, with **308** in DMF, TBAOH gave only 39% conversion and, as with KOH, the hydroxide ion led to the same hydrolysis side reactions to a mixture of unknown CF₃-alkene products.

Table 6.2. Screening of reaction conditions for Sonogashira coupling of **308**

Solvent	Base	% Conversion ^[a]
DMF	K ₃ PO ₄	0
DMF	K ₂ CO ₃	0
DMF	KOH	70
DMF	Et ₃ N	1
DMF	Et ₃ N	0
MeCN	Et ₃ N	0
MeOH	Et ₃ N	0
THF	Et ₃ N	0
EtOAc	Et ₃ N	0
PhCH ₃	Et ₃ N	0
Et ₃ N	-	0
DMF	ⁱ Pr ₂ NH	2
DMF	DBU	32
PhCH ₃	(<i>n</i> -Bu) ₄ NOH	39

^[a] determined by ¹⁹F NMR spectroscopy analysis of crude reaction mixture

In the course of this screening, a crystal structure was obtained of compound **317**, a complex of the ligand XPhos with copper (Figure 6.1). No crystal structure of an XPhos-copper complex has ever been reported before in the CCDC. The origin of the chloride in this example is not certain but the fact that **317** was isolated following column chromatography suggests that this complex has relatively high stability and so may not be catalytically active, hence the low reactivity observed in most cases. Further attempts

to optimise this reaction by MChem student Matthew Grannan, including the use of other amines, anhydrous conditions and iodoarenes instead of bromoarenes, confirmed that the desired deacetonative Sonogashira cross-coupling is not straightforward, with the low nucleophilicity of 3,3,3-trifluoropropyne likely a further complicating factor.

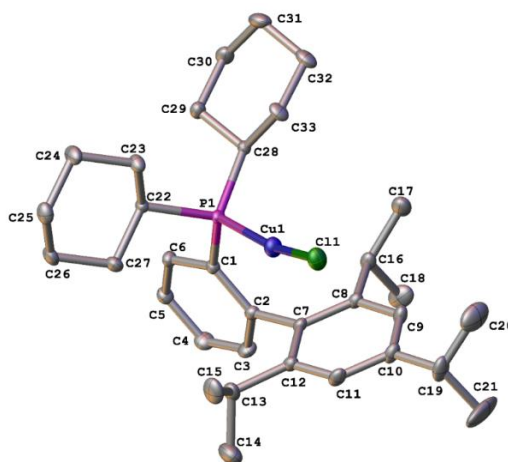
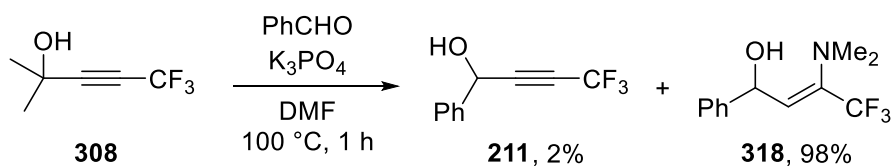


Figure 6.1. Structure of XPhos copper complex **317** as proven by X-ray crystallography

6.2.3 Deacetonative nucleophilic substitution reactions

In addition to the attempted deacetonative Sonogashira cross-coupling reactions described above, the use of **308** as a nucleophilic source of 3,3,3-trifluoropropyne without the need for palladium catalysis was also explored. Reaction of **308** with benzaldehyde was trialled as a model reaction, using K_3PO_4 as a base and DMF as a solvent (Scheme 6.12). The expected product, alkynol **211**, can be formed directly from **1** in 94% isolated yield on several gram scale, as described in Chapter 4, but a synthesis from **308** would offer a route in which there is no need for the user to handle gaseous reagents. However, ^{19}F NMR and GC-MS analysis of the reaction mixture showed the major product was not the desired alcohol **211** but rather enamine **318**. The dimethylamine nucleophile was likely formed by decomposition of the DMF solvent under these basic conditions. On aqueous workup, there was substantial decomposition (~50% by ^{19}F NMR spectroscopy) of **318** and so it was not purified further.



Scheme 6.12. Reaction of **308** with benzaldehyde in DMF (neither product isolated)

Different solvents and bases for the synthesis of alkynol **211** were explored (Table 6.3). Acetonitrile afforded a mixture of various products including **211**, THF gave only **211** but with low conversion whilst the only ^{19}F NMR signals observed in DMSO were for HF. Given that THF gave the cleanest conversion, albeit low, it was used as the solvent for further base screening. There was no reaction with sodium acetate, triethylamine or in a control reaction with no base whilst caesium carbonate gave clean but low conversion. With DBU, there was 39% conversion to **211**, 6% to an unknown product with the remaining 55% being unreacted **308**. Potassium *tert*-butoxide gave quantitative conversion to the same unknown product with seemingly no alkynol **211** formed after one hour at 80 °C. However, attempting to lower the temperature to 60 °C led to a significant reduction in conversion.

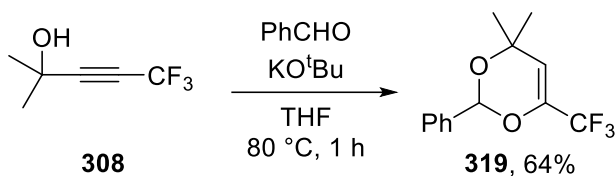
Table 6.3. Screening of conditions for reaction of **308** with benzaldehyde

Solvent	Base	$T / ^\circ\text{C}$	% Conversion ^[a]	
			211	other ^[b]
DMF	K ₃ PO ₄	100	2	98
DMSO	K ₃ PO ₄	80	0	0
MeCN/H ₂ O	K ₃ PO ₄	80	22	52
THF/H ₂ O	K ₃ PO ₄	80	6	0
THF	Et ₃ N	80	0	0
THF	DBU	80	39	6
THF	KO ^t Bu	80	0	100
THF/H ₂ O	Cs ₂ CO ₃	80	13	0
THF/H ₂ O	NaOAc	80	0	0
THF/H ₂ O	-	80	0	0
THF	KO ^t Bu	60	0	56

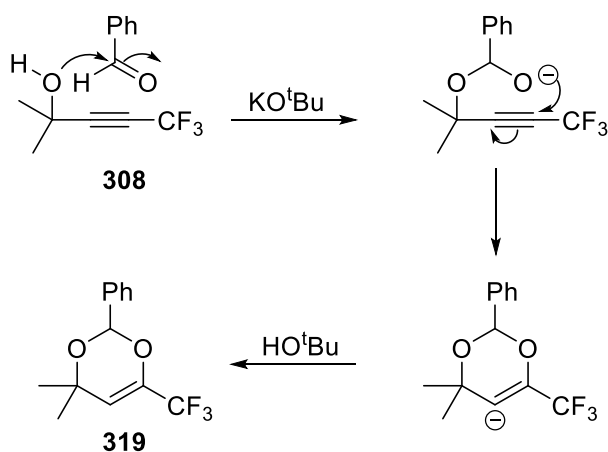
^[a] determined by ^{19}F NMR spectroscopy; ^[b] combined integral of all other peaks

Despite not giving any of the intended alkynol **211**, the reaction of **308** and benzaldehyde with potassium *tert*-butoxide in THF was repeated on a preparative scale to isolate and identify the product (Scheme 6.13). Analysis of the resulting NMR spectra suggested that cyclic acetal **319** was the sole product, which was confirmed by high resolution mass spectrometry. **319** was presumably formed by the hydroxyl moiety of **308** acting as a nucleophile towards benzaldehyde, generating an intermediate *gem*-diol that could then

cyclise via a Michael-type addition, as seen in the synthesis of enamine **318** above (Scheme 6.14).

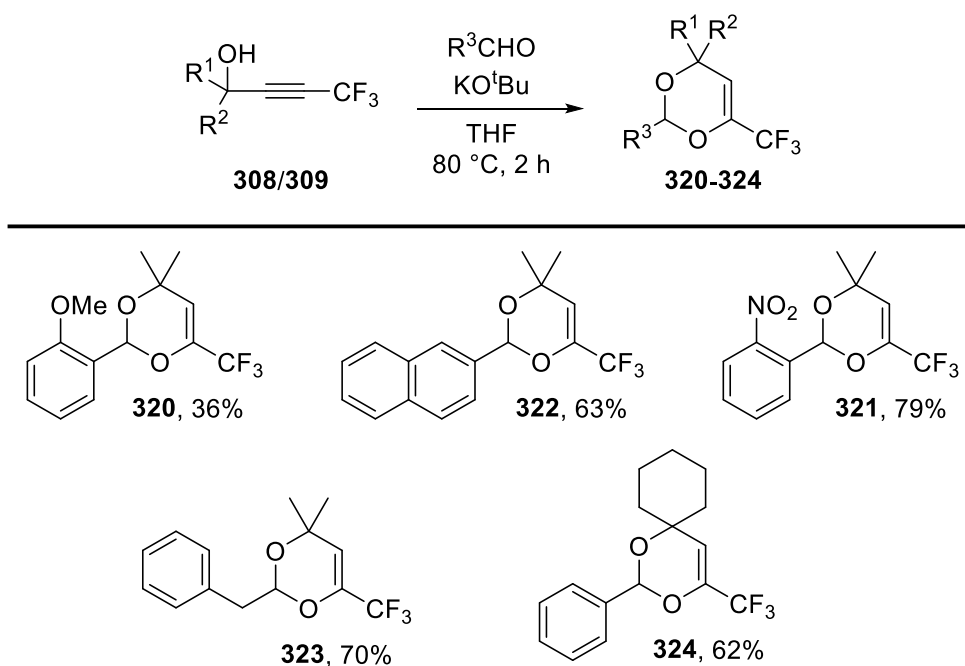


*Scheme 6.13. Unintended synthesis of acetal **319** from tertiary alcohol **308***



*Scheme 6.14. Proposed mechanism for formation of **319***

Trifluoromethylated dioxenes of this exact type were previously unknown in the literature but there have been several examples of other CF₃-substituted 1,3-dioxin-4-ones, which are typically prepared from trifluoromethyl ketones.⁵⁵ Similar non-fluorinated compounds with this type of structure have been used in the total synthesis of various complex, highly oxygenated natural products.⁵⁶ The scope of the cyclisation reaction was then expanded to a range of differently substituted aldehydes (Scheme 6.15), including methoxy- and nitro-substituted benzaldehydes, **320** and **321** respectively, 2-naphthaldehyde (**322**) and alkyl system phenylacetaldehyde (**323**). The CF₃-alkynol substrate could also be varied, with the use of cyclohexanone-derived **309** giving spirocyclic dioxene **324**.



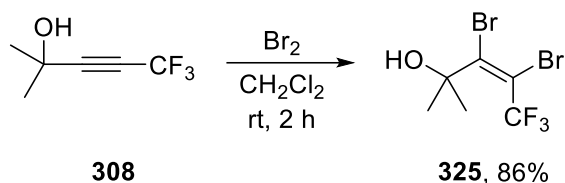
Scheme 6.15. Substrate scope for cyclisation reactions of CF₃-alkynols

In attempts to expand this reaction from aldehydes to ketones, **308** was mixed with KO^tBu and benzophenone and heated to 80 °C in THF for two hours and gave 22% conversion as determined by ¹⁹F NMR spectroscopy to the desired dioxene. However, on extending the reaction time to nine hours, an intractable complex mixture of various fluorinated products was formed. The equivalent reaction of **308** with benzophenone imine gave a similarly problematic mixture alongside some ¹⁹F NMR signals indicating formation of fluoride ions, suggesting decomposition of **308** was occurring.

6.2.4 Other reactions of trifluoropropynyl tertiary alcohols

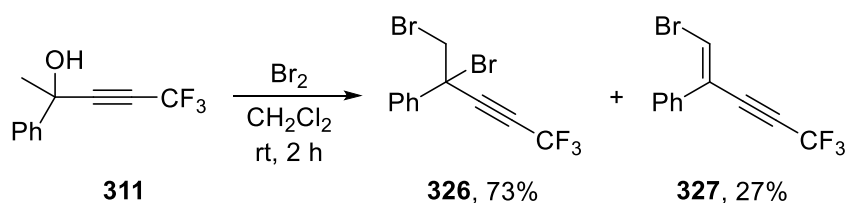
With mixed results from attempted deacetonative transformations of **308**, other classes of reaction for this compound were explored. Bromination of **308** afforded the dibromoalkane **325** as a single stereoisomer (Scheme 6.16). The stereoselectivity was assumed to be the same as that seen in the bromination of CF₃-ynones, as explained in Chapter 4, with the higher selectivity observed in this case ascribed to the greater steric bulk of a dimethyl tertiary alcohol compared to a planar aryl ketone in the same position. Preliminary DFT calculations did not offer any further insight due to the complicating factor of stabilising H-F or H-Br interactions in both possible stereoisomers. Suzuki coupling of **325** could, in principle, afford a diaryl allyl alcohol of the kind that has been

used in the preparation of indenenes,⁵⁷ furanones,⁵⁸ pyrans,⁵⁹ benzolactones⁶⁰ and dihydrofurans⁶¹ with non-fluorinated systems and so **325** could act as a precursor to trifluoromethylated analogs.

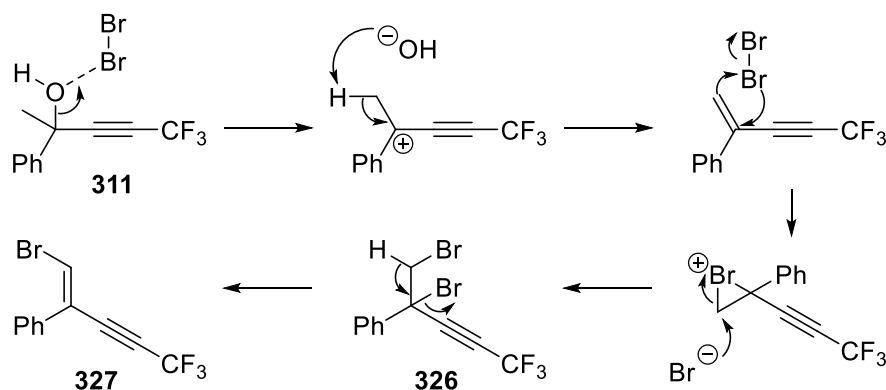


Scheme 6.16. Bromination of trifluoropropynyl alcohol 308

The bromination of acetophenone-derived alkynol **311** was then carried out under the same conditions (Scheme 6.17). However, this led to formation of a mixture of dibromo alkyne **326** and brominated enyne **327**, neither of which could be isolated due to their instability but the identities of both were confirmed by NMR spectroscopy and high-resolution mass spectrometry. In this case, bromine appears to promote dehydration of **311** to form an enyne and the more electron-rich alkene of this intermediate is preferentially brominated over the electron-poor CF₃-substituted alkene (Scheme 6.18). The reason why acetophenone-derived **311** undergoes the initial elimination where acetone-derived **308** did not is unknown but could be attributed to stabilisation afforded by delocalisation into the phenyl ring.

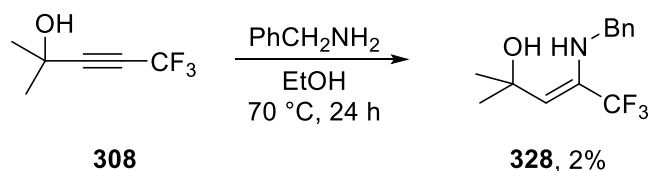


Scheme 6.17. Bromination of trifluoropropynyl alcohol 311 (neither product isolated, ratio determined by ¹⁹F NMR spectroscopy)



Scheme 6.18. Proposed mechanism for formation of trifluoromethylated enynes 326 and 327

Whilst the Michael addition of amines to CF_3 -ynones proceeded to full completion at room temperature in under 15 minutes, reaction of benzylamine with **308** was significantly slower. After refluxing in ethanol for 24 hours, only 2% of the expected Michael addition product **328** was observed in solution by ^{19}F NMR spectroscopy with the remainder being unreacted **308** (Scheme 6.19). However, a white precipitate formed from the reaction mixture that was sparingly soluble in water. Recrystallisation revealed via X-ray crystallography that this product was benzylammonium hexafluorosilicate (**329**, Figure 6.2). The synthesis of this particular salt has previously been reported utilising the reaction of benzylamine either directly with fluorosilicic acid⁶² or with pyridinium hexafluorosilicate⁶³ but this is the first reported crystal structure of **329**. A control reaction of refluxing benzylamine in ethanol in the same flask under identical conditions showed no solid precipitate. This demonstrated that the decomposition of **308** and subsequent reaction of reaction of the fluoride ions formed with the surface of the borosilicate glass vessel is necessary to cause formation of **329**. This confirms the earlier suggestion above of decomposition found when cyclisation of **308** was attempted with benzophenone imine and this lack of stability in the presence of amines may further explain why the deacetonative Sonogashira reactions of **308** attempted above were unsuccessful in amine solvents or solvents from which amines can be generated *in situ*, such as DMF.



Scheme 6.19. Attempted Michael addition to trifluoropropynyl alcohol **308** (product not isolated)

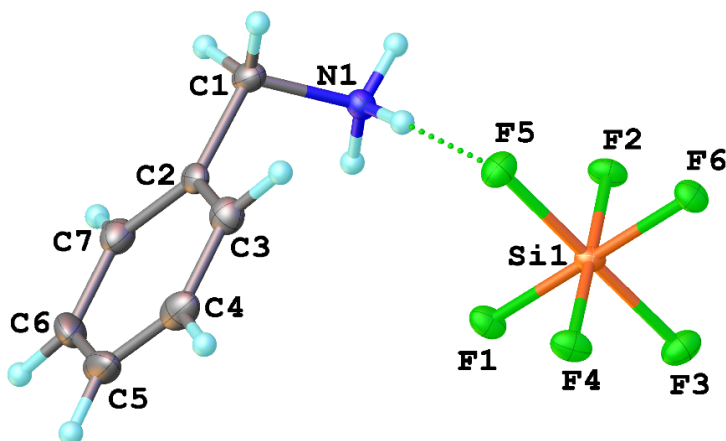


Figure 6.2. Structure of hexafluorosilicate salt **329** as proven by X-ray crystallography

6.3 Conclusions

Trifluoromethylated alkynes are a versatile building block for the preparation of a wide range of CF₃-substituted systems, including those of potential pharmaceutical relevance. Previous methods for the synthesis of this class of compound typically rely on trifluoromethylation of terminal alkynes. A trifluoropropynylation approach using HFO-1234yf as the trifluoropropyne source offers an alternative approach if a suitable bench-stable trifluoropropynylating reagent could be developed for general laboratory use with aryl halides or pseudo-halides as substrates, which typically have lower cost, greater stability and a wider range of differently substituted systems and are more readily commercially available than terminal alkynes. However, initial attempts to transform HFO-1243yf into potential trifluoropropynylating reagents including boron, silicon and copper derivatives proved unsuccessful.

A deketonative approach was then investigated, with a range of CF₃-substituted tertiary alkynols synthesised in generally high isolated yields by dehydrofluorination of **1** with LDA and subsequent trapping of lithium 3,3,3-trifluoropropynide with a range of different ketones. Of particular note, addition to estrone afforded a trifluoromethylated analog of the birth control drug ethinyl estradiol. Initially promising results were obtained for a palladium-catalysed deketonative Sonogashira reaction with aryl bromides to form aryl trifluoropropynes, losing a ketone as the by-product. However, isolation proved difficult with the acetophenone-derived adduct whilst the acetone-derived adduct gave rise to various side reactions so, whilst a promising route, further work would be needed to make this a viable synthetic pathway. Attempted deacetone trifluoropropynylation without palladium catalysis with benzaldehyde as the electrophile gave rise to an unexpected cyclisation reaction to form a novel cyclic acetal. The scope of the reaction using various aldehydes was then explored, forming several different CF₃-substituted dioxenes, potentially useful building blocks for the synthesis of other trifluoromethylated oxygen-rich systems.

6.4 References for Chapter 6

- ¹ (a) B. Godoi, R. F. Schumacher and G. Zeni, *Chem. Rev.*, 2011, **111**, 2937; (b) M. E. Muratore, A. Homs, C. Obradors and A. M. Echavarren, *Chem. Asian J.*, 2014, **9**, 3066; (c) I.-T. Trotsuş, T. Zimmermann and F. Schüth, *Chem. Rev.*, 2014, **114**, 1761; (d) L. Zhang, *Acc. Chem. Res.*, 2014, **47**, 877; (e) R. Chinchilla and C. Nájera, *Chem. Rev.*, 2014, **114**, 1783; (f) G. Fang and X. Bi, *Chem. Soc. Rev.*, 2015, **44**, 8124; (g) V. P. Boyarskiy, D. S. Ryabukhin, N. A. Bokach and A. V. Vasilyev, *Chem. Rev.*, 2016, **116**, 5894; (h) L. T. Boulton, in *Synthetic Methods in Drug Discovery*, ed. D. C Blakemore, P. M Doyle and Y. M Fobian, Royal Society of Chemistry, Cambridge, 2016, vol. 1, ch. 4, pp. 122-142.
- ² T. Konno, T. Daitoh, A. Noiri, J. Chae, T. Ishihara and H. Yamanaka, *Org. Lett.*, 2004, **6**, 933.
- ³ S. von Kugelgen, R. Sifri, D. Bellone and F. R. Fischer, *J. Am. Chem. Soc.*, 2017, **139**, 7577.
- ⁴ S. Schweizer, C. Tresse, P. Bissere, J. Lalevée, G. Evano and N. Blanchard, *Org. Lett.*, 2015, **17**, 1794.
- ⁵ Y. Yamamoto, E. Ohkubo and M. Shibuya, *Green Chem.*, 2016, **18**, 4628.
- ⁶ M. Cloutier, M. Roudias and J.-F. Paquin, *Org. Lett.*, 2019, **21**, 3866.
- ⁷ C.-C. Tseng, G. Baillie, G. Donvito, M. A. Mustafa, S. E. Juola, C. Zanato, C. Massarenti, S. Dall'Angelo, W. T. A. Harrison, A. H. Lichtman, R. A. Ross, M. Zanda and I. R. Greig, *J. Med. Chem.*, 2018, **62**, 5049.
- ⁸ R. N. Haszeldine, *J. Chem. Soc.*, 1951, 584.
- ⁹ L. M. Yagupolskii and Yu. A. Fialkov, *J. Gen. Chem. USSR*, 1960, **30**, 1291.
- ¹⁰ (a) G. Meazza, L. Capuzzi and P. Piccardi, *Synthesis*, 1989, **4**, 331; (b) H. Tamejiro, S. Kenichi and F. Makoto, *Bull. Chem. Soc. Japan*, 1989, **62**, 1352.
- ¹¹ Y. Kobayashi, T. Yamashita, K. Takahashi, H. Kuroda and I. Kumadaki, *Tetrahedron Lett.*, 1982, **23**, 343.
- ¹² J. E. Bunch and C.L. Bumgardner, *J. Fluorine Chem.*, 1987, **36**, 313.
- ¹³ T. Umemoto and S. Ishihara, *Tetrahedron Lett.*, 1990, **31**, 3579.
- ¹⁴ L. Chu and F.-L. Qing, *J. Am. Chem. Soc.*, 2010, **132**, 7262.
- ¹⁵ D.-F. Luo, J. Xu, Y. Fu and Q.-X. Guo, *Tetrahedron Lett.*, 2012, **53**, 2769.
- ¹⁶ Z. Weng, H. Li, W. He, L.-F. Yao, J. Tan, J. Chen, Y. Yuan and K.-W. Huang, *Tetrahedron*, 2012, **68**, 2527.
- ¹⁷ H.-S. M. Siah and A. Fiksdahl, *J. Fluorine Chem.*, 2017, **197**, 24.
- ¹⁸ H. Zheng, Y. Huang, Z. Wang, H. Li, K.-W. Huang, Y. Yuan and Z. Weng, *Tetrahedron Lett.*, 2012, **53**, 6646.
- ¹⁹ M. Pisset, D. Oehlrich, F. Rombouts and G. A. Molander, *J. Org. Chem.*, 2013, **78**, 12837.
- ²⁰ L. Yang, L. Jiang, Y. Li, X. Fu, R. Zhang, K. Jin and C. Duan, *Tetrahedron*, 2016, **72**.
- ²¹ N. Iqbal, J. Jung, S. Park and E. J. Cho, *Angew. Chem. Int. Ed.*, 2014, **53**, 539.
- ²² L. He and G. C. Tsui, *Org. Lett.*, 2016, **18**, 2800.
- ²³ A. Zanardi, M. A. Novikov, E. Martin, J. Benet-Buchholz and V. V. Grushin, *J. Am. Chem. Soc.*, 2011, **133**, 20901.
- ²⁴ Y. Ye, K. P. S. Cheung, L. He and G. C. Tsui, *Org. Lett.*, 2018, **20**, 1676.
- ²⁵ P. V. Ramachandran and W. Mitsuhashi, *Org. Lett.*, 2015, **17**, 1252.
- ²⁶ T. Pitterna, O. Loiseleur, T. Luksch and R. J. G. Mondiere, WO2014173921, 2014.
- ²⁷ P. V. Ramachandran and W. Mitsuhashi, *J. Fluorine Chem.*, 2016 **190**, 7.
- ²⁸ J. D. Kirkham, S. J. Edeson, S. Stokes and J. P. A. Harrity, *Org. Lett.*, 2012, **14**, 5354.

- ²⁹ F. G. Drakesmith, O. J. Stewart and P. Tarrant, *J. Org. Chem.*, 1968, **33**, 280.
- ³⁰ T. Hanamoto and K. Yamada, *J. Org. Chem.*, 2009, **74**, 7559.
- ³¹ M. Bengtsson and T. Liljefors, *Synthesis*, 1988, **3**, 250.
- ³² M. Keßler, S. Porath, H.-G. Stammer and B. Hoge, *Eur. J. Inorg. Chem.*, 2021, 907.
- ³³ A. J. J. Lennox and G. C. Lloyd-Jones, *J. Am. Chem. Soc.*, 2012, **134**, 7431.
- ³⁴ G. Evano, K. Jouvin, C. Theunissen, C. Guissart, A. Laouiti, C. Tresse, J. Heimburger, Y. Bouhoute, R. Veillard, M. Lecomte, A. Nitelet, S. Schweizer, N. Blanchard, C. Alayrac and A.-C. Gaumont, *Chem. Commun.*, 2014, **50**, 10008.
- ³⁵ R. N. Haszeldine, *J. Chem. Soc.*, 1951, 588.
- ³⁶ H. Helbert, P. Visser, J. G. H. Hermens, J. Buter and B. L. Feringa, *Nature Cat.*, 2020, **3**, 664.
- ³⁷ (a) P. G. M. Wuts and T. W. Greene, *Greene's Protective Groups in Organic Synthesis*, 4th Edition, John Wiley and Sons, Hoboken, NJ, 2007, pp. 927-933; (b) H. Qian, D. Huang, Y. Bi and G. Yan, *Adv. Synth. Catal.*, 2019, **361**, 3240; (c) A. Smeyanov and A. Schmidt, *Synth. Commun.*, 2013, **43**, 2809.
- ³⁸ A. L. Henne and M. Nager, *J. Am. Chem. Soc.*, 1952, **74**, 650.
- ³⁹ M. N. Bobrovnikov, *Russ. J. Org. Chem.*, 1994, **30**, 1850.
- ⁴⁰ (a) T. Yamazaki, T. Yamamoto and R. Ichihara, *J. Org. Chem.*, 2006, **71**, 6251; (b) M. Shimizu, M. Higashi, Y. Takeda, G. Jiang, M. Murai, T. Hiyama, *Synlett*, 2007, **7**, 1163; (c) Y. Watanabe and T. Yamazaki, *Synlett*, 2009, **20**, 3352; (d) P. Li, Z.-J. Liu and J.-T. Liu, *Tetrahedron*, 2010, **66**, 9729; (e) J.-L. Li, X.-J. Yang, M. Jiang and J.-T. Liu, *Tetrahedron Lett.*, 2017, **58**, 3377.
- ⁴¹ F.-L. Qing and W.-Z. Gao, *Tetrahedron Lett.*, 2000, **41**, 7727.
- ⁴² (a) T. Yamazaki, K. Mizutani and T. Kitzau, *J. Org. Chem.*, 1995, **60**, 6046; (b) A. R. Katritzky, M. Qi and A. P. Wells, *J. Fluorine Chem.*, 1996, **80**, 145.
- ⁴³ A. Miyagawa, M. Naka, T. Yamazaki and T. Kawasaki-Takasuka, *Eur. J. Org. Chem.*, 2009, **26**, 4395.
- ⁴⁴ M. N. Bobrovnikov, E. S. Turbanova, S. A. Shishenin, M. G. Peterleitner and A. A. Petrvo, *J. Org. Chem. USSR*, 1992, **28**, 1615.
- ⁴⁵ V. Petrow, *Chem. Rev.*, 1970, **70**, 713.
- ⁴⁶ C. Burgess, D. Burn, P. Feather, M. Howarth and V. Petrow, *Tetrahedron*, 1966, **22**, 2829.
- ⁴⁷ (a) H.-F. Chow, C.-W. Wan, K.-H. Low and Y.-Y. Yeung, *J. Org. Chem.*, 2001, **66**, 1910; (b) Z. Novák, P. Nemes and A. Kotschy, *Org. Lett.*, 2004, **6**, 4917; (c) E. Shirakawa, T. Kitabata, H. Otsuka and T. Tsuchimoto, *Tetrahedron*, 2005, **61**, 9878; (d) C. Y. Yi, R. M. Hua, H. X. Zeng and Q. F. Huang, *Adv. Synth. Catal.*, 2007, **349**, 1738; (e) T.-T. Hung, C.-M. Huang and F.-Y. Tsai, *ChemCatChem*, 2012, **4**, 540; (f) X. Li, S. Sun, F. Yang, J. Kang, Y. Wu and Y. Wu, *Org. Biomol. Chem.*, 2015, **13**, 2432; (g) F. Sun, M. Lia and Z. Gu, *Org. Chem. Front.*, 2016, **3**, 309; (h) Z. Mi, J. Tang, Z. Guan, W. Shi and H. Chen, *Eur. J. Org. Chem.*, 2018, **32**, 4479; (i) K. Yasui, N. Chatani and M. Tobisu, *Org. Lett.*, 2018, **20**, 2108.
- ⁴⁸ M. S. Shvartsberg, S. F. Vasilevskii, T. V. Anisimova and V. A. Gerasimov, *Bull. Acad. Sci. USSR Div. Chem. Sci.*, 1981, **30**, 1071.
- ⁴⁹ H. Hu, F. Yang and Y. Wu, *J. Org. Chem.*, 2013, **78**, 10506.
- ⁵⁰ K. Xu, S. Sun, G. Zhang, F. Yang and Y. Wu, *RSC Adv.*, 2014, **4**, 32643.
- ⁵¹ F. Chang and Y. Liu, *Synth. Commun.*, 2017, **47**, 961.
- ⁵² N. C. Bruno, N. Niljianskul and S. L. Buchwald, *J. Org. Chem.*, 2014, **79**, 4161.
- ⁵³ J. Li and P. Huang, *Beilstein J. Org. Chem.*, 2011, **7**, 426.

- ⁵⁴ (a); A. Mori, T. Shimada, T. Kondo and A. Sekiguchi, *Synlett*, 2011, 649; (b) C. E. D. Nazario, A. S. Santana, C. Y. Kawasoko, C. A. Carollo, G. R. Hurtado, L. H. Viana, S. L. Barbosa, P. G. Guerrero, F. A. Marques, V. B. Dabdoub, M. J. Dabdoub and A. C. M. Baroni, *Tetrahedron Lett.*, 2011, **54**, 4177.
- ⁵⁵ e.g. (a) M. Gautschi, W. B. Schweizer and D. Seebach, *Chem. Ber.*, 1994, **127**, 565; (b) J. Boivin, L. El Kaima and S. Z. Zard, *Tetrahedron*, 1995, **51**, 2585; (c) Y. Morita, R. Kamakura, M. Takeda and Y. Yamamoto.
- ⁵⁶ e.g. (a) Z. Kan-Yin, A. J. Borgerding and R. M. Carlson, *Tetrahedron Lett.*, 1988, **29**, 45, 5703; (b) S. Anné, W. Yong, M. Vandewalle, *Synlett*, 1999, **9**, 1435; (c) R. A. Aungst and R. L. Funk, *J. Am. Chem. Soc.*, 2001, **123**, 9455.
- ⁵⁷ X. Zhou, H. Zhang, X. Xie and Y. Li, *J. Org. Chem.*, 2008, **73**, 3958.
- ⁵⁸ Y. Liu, F. Song and S. Guo, *J. Am. Chem. Soc.*, 2006, **128**, 11332.
- ⁵⁹ R. C. Larock, Y. He, W. W. Leong, X. Han, M. D. Refvik and J. M. Zenner, *J. Org. Chem.*, 1998, **63**, 2154.
- ⁶⁰ A. Arcardi, G. Fabrizi, A. Goggiamani and F. Marinelli, *J. Org. Chem.*, 2015, **80**, 6986.
- ⁶¹ Y. Liu, F. Song and L. Cong, *J. Org. Chem.*, 2005, **70**, 6999.
- ⁶² A. A. Ennan, L. A. Gavrilova, A. N. Chobotarev and T. S. Borisenko, *Russ. J. Inorg. Chem.*, 1977, **22**, 688.
- ⁶³ K. S. Mohamed and D. K. Padma, *Indian J. Chem. A*, 1988, **27**, 712.

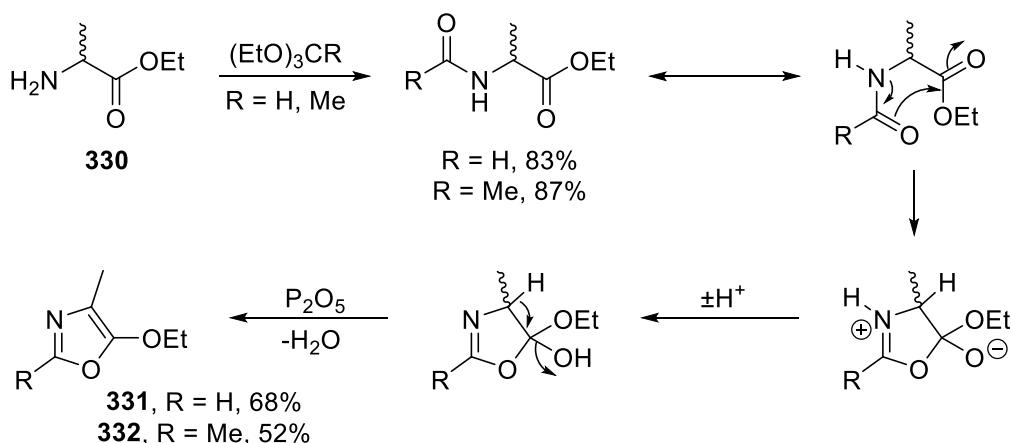
Chapter 7: Miscellaneous reactions of HFO-1234yf

7.1 Cycloaddition reactions of HFO-1234yf

7.1.1 Diels-Alder cycloaddition of HFO-1234yf

As previously discussed, there is limited literature precedent for reactions of **1** and so no cycloaddition reactions of **1** are known in the literature. However, the Diels-Alder reaction of structurally related 3,3,3-trifluoropropene was reported by McBee *et al.* as early as 1955.¹ They found that reactions proceeded only at high temperature with cyclopentadiene (135 °C for 60 hours), butadiene (180 °C for 24 hours) and anthracene (200 °C for 20 hours). Ojima *et al.* subsequently also found 3,3,3-trifluoropropene to be fairly unreactive, even with very electron-rich dienes such as Danishefsky's diene.²

Consistent with these reports, our attempted Diels-Alder cycloaddition of **1** and furan in a Carius tube gave no reaction of any kind observed by ¹H or ¹⁹F NMR spectroscopy after heating at 120 °C for 72 hours. Therefore, more electron-rich oxazole dienes were synthesised via the Robinson-Gabriel reaction (Scheme 7.1).³ *N*-Formyl and *N*-acetyl alanine ethyl esters were prepared from commercially available DL-alanine ethyl ester hydrochloride (**330**) using the appropriate triethyl orthoester. Cyclisation was then achieved by using phosphorus pentoxide as a dehydrating agent to give 4-methyl-5-ethoxyoxazole (**331**) and 2,4-dimethyl-5-ethoxyoxazole respectively (**332**).



Scheme 7.1. Robinson-Gabriel oxazole synthesis from DL-alanine ethyl ester hydrochloride

Subsequently, when **331** was heated overnight in a Carius tube with one equivalent of **1**, a range of unidentified decomposition and polymerisation products of the oxazole were observed in the ^1H NMR spectrum. Small amounts of several fluorinated products could also be detected by ^{19}F NMR spectroscopy with chemical shifts characteristic of a trifluoromethylated pyridinol⁴ (Figure 7.1) but none of these compounds could be isolated and no further reactions of this type were carried out due to the decomposition observed.

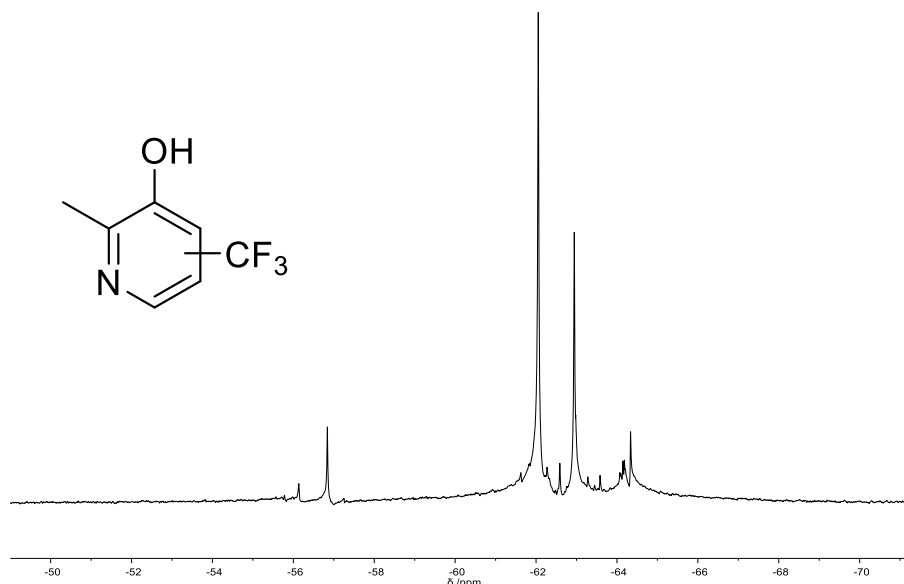
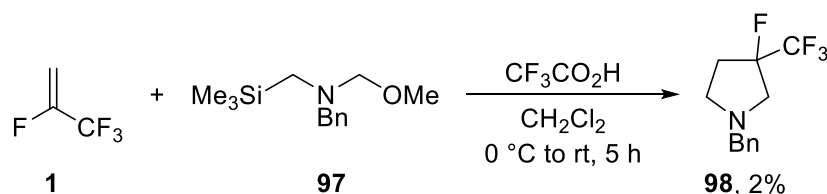


Figure 7.1. ^{19}F NMR spectrum after 20 hours at 120 °C from reaction of HFO-1234yf and oxazole **331** and structure of one of the possible products formed

7.1.2 1,3-Dipolar cycloaddition of HFO-1234yf

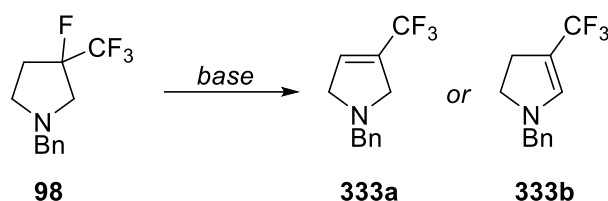
Work from Mykhailiuk *et al.* previously showed that various CF_3 -substituted alkenes underwent highly efficient 1,3-dipolar cycloaddition reactions with Achiwa's reagent (**97**), which forms an azomethine ylide on treatment with acid, to give CF_3 -pyrrolidines.⁵ Applying their conditions to the reaction between **1** and **97** gave tetrafluoropyrrolidine **98** following column chromatography, albeit in very low yield (Scheme 7.2).



Scheme 7.2. 1,3-Dipolar cycloaddition reaction of HFO-1234yf and Achiwa's reagent

respectively. Elimination of hydrogen chloride,⁹ bromide¹⁰ and iodide¹¹ all gave exclusively the 2,5-dihydropyrrole from the corresponding 3-halopyrrolidines. Various bases were screened for the dehydrofluorination of **98** (Table 7.1) but most gave poor conversion. Dehydrofluorination of inactivated systems is known to require somewhat more forcing conditions as the transition state has a high degree of E1cB character.¹²

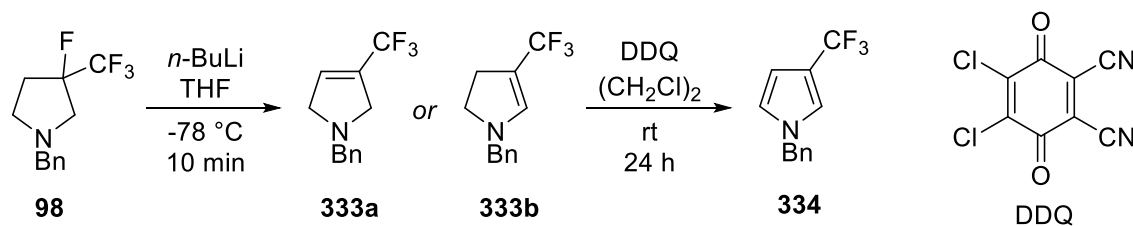
Table 7.1. Screening of bases for the dehydrofluorination of pyrrolidine **98**



Base	Conditions	% Conversion ^[a]
KO ^t Bu	THF, rt, 16 h	0
KO ^t Bu	THF, 70 °C, 16 h	29
KOMe	THF, 70 °C, 16 h	16
DBU	THF, rt, 24 h	0
<i>n</i> -BuLi	Et ₂ O, -78 °C, 10 min	39
LDA	Et ₂ O, -10 °C, 1 h	12

^[a] determined by ¹⁹F NMR analysis of crude reaction mixture after quenching with water

The mixture obtained following the reaction of **98** with *n*-BuLi was oxidised directly with DDQ, forming a complex mixture of products (Scheme 7.4). Following column chromatography, a mixture remained but with the major component still the tetrafluorinated pyrrolidine **98** (Figure 7.3). A signal consistent with the target pyrrole **334** was also observed with an estimated conversion of only 39% based on the relative integrals of each peak in the ¹⁹F NMR spectrum. However, this does suggest that all of the dihydropyrrole **333** that did form was oxidised by DDQ. The third product had a chemical shift of +21.16 ppm. Positive chemical shifts are unusual in the ¹⁹F NMR spectra of organofluorine compounds and typically only arise in organic systems from acyl fluorides or N-F species, although how either would form under these reaction conditions is not clear but both must involve some degradation of the CF₃ group. Therefore, the feasibility of this approach to trifluoromethylated pyrroles remains unproven.



Scheme 7.4. Dehydrofluorination of tetrafluoropyrrolidine **98** followed by oxidation with DDQ

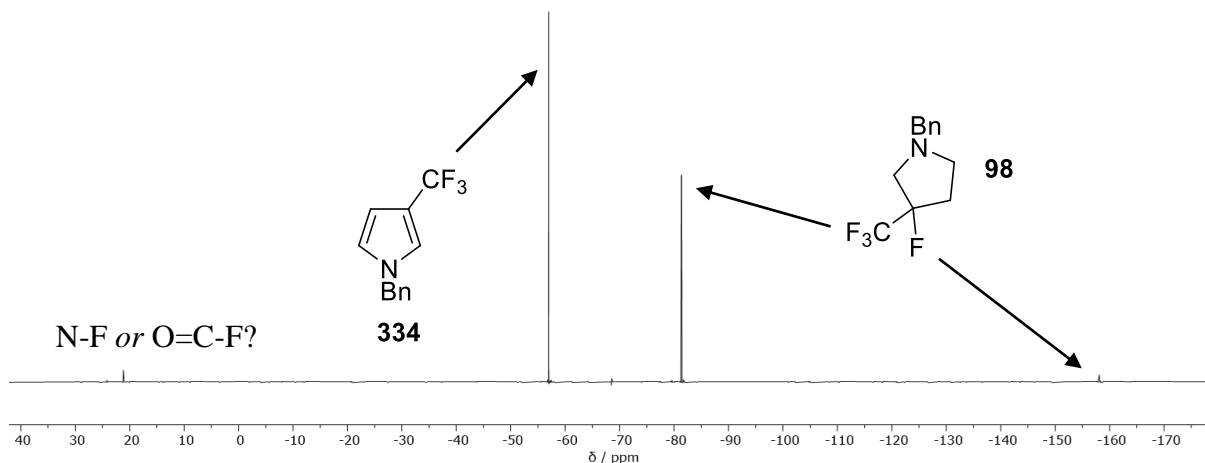


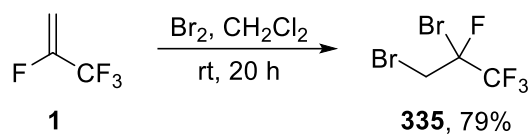
Figure 7.3. ^{19}F NMR spectrum (CDCl_3 , 376 MHz) of mixture from oxidation reaction with DDQ

7.2 Electrophilic addition to HFO-1234yf

7.2.1 Bromination of HFO-1234yf

The only reported electrophilic addition reactions to **1** come from a number of patents, using either harsh conditions (elemental chlorine¹³ or anhydrous hydrogen fluoride¹⁴) or milder conditions but with low yield and long reaction times, i.e. *N*-bromosuccinimide in acetic acid gave 21% yield of the cohalogenated product after 5 days.¹⁵ Perfluoroalkenes are generally known to be resistant to electrophilic addition, with such reactions typically requiring the presence of a Lewis acid and high temperatures.¹⁶ However, bromination of 3,3,3-trifluoropropene has long been known¹⁷ and so we attempted analogous conditions with **1**. Stirring a solution of elemental bromine in dichloromethane under an atmosphere of **1** provided by gas bladder afforded complete conversion overnight at room temperature as evidenced by the disappearance of the colour of Br_2 (Scheme 7.5). The reaction still proceeded whilst shielded from light, suggesting that the bromination likely proceeds via an ionic rather than radical mechanism. 1,2-Dibromo-2,3,3,3-tetrafluoropropane (**335**) was isolated via distillation of the reaction mixture in good yield and could be scaled up to produce around twenty grams of product without incident. Attempting this reaction

without solvent or using acetic acid or acetonitrile as the solvent led to no reaction at all detectable by ^{19}F NMR spectroscopy.



Scheme 7.5. Bromination of HFO-1234yf

The ^1H (Figure 7.4) and ^{19}F (Figure 7.5) NMR spectra of **335** show complex splitting patterns owing to the presence of four fluorine atoms and two diastereotopic hydrogen atoms. The two signals in the ^{19}F NMR spectrum show the expected 1:3 ratio of areas and the two bond F-F J-coupling (8.3 Hz) can be easily calculated by examining the proton-decoupled spectrum. The singular CBrF fluorine atom's quartet is further split into a doublet of doublets by the diastereotopic hydrogen atoms. These splittings have values of 20.9 Hz and 12.5 Hz, which can be attributed to the Karplus effect by which the value of J-coupling is at a maximum when the angle between nuclei is 0° or 180° and at a minimum at 90° .¹⁸ Assuming **335** adopts a staggered structure to minimise steric clash between the bromine atoms, these correspond to the protons as shown in Figure 7.4. Both protons also show small $^4J_{\text{HF}}$ couplings to the CF_3 fluorine atoms with values of 0.6 and 0.9 Hz for H_A and H_B respectively, the difference again attributable to the Karplus effect.

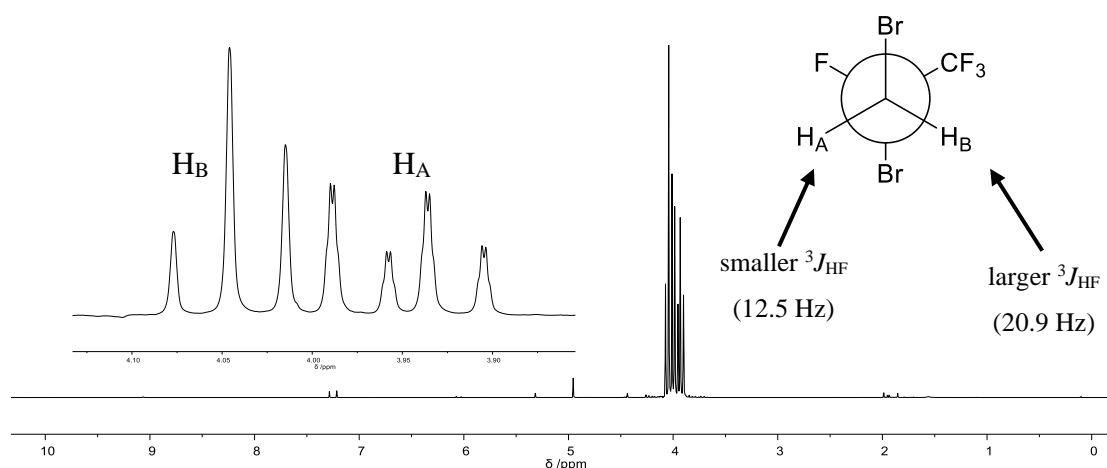


*Figure 7.4. ^1H NMR spectrum (400 MHz, CDCl_3) of **335***

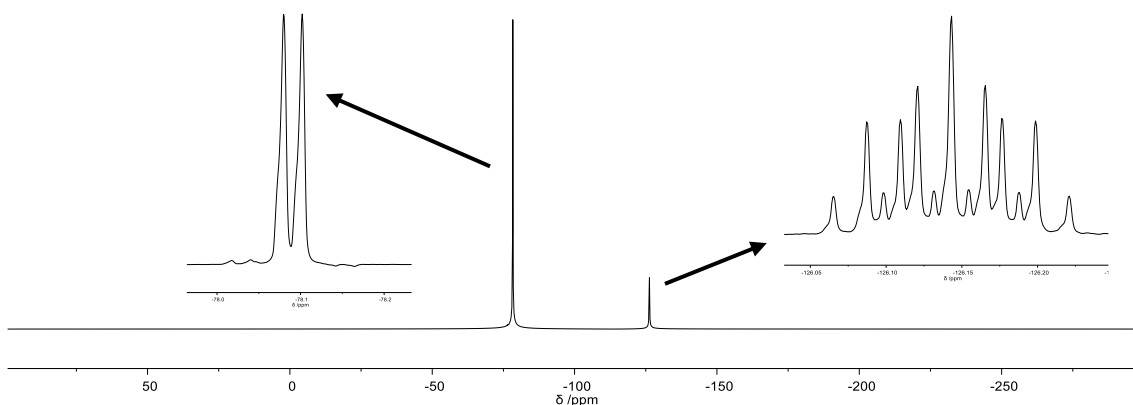


Figure 7.5. ^{19}F NMR spectrum (376 MHz, CDCl_3) of **335**

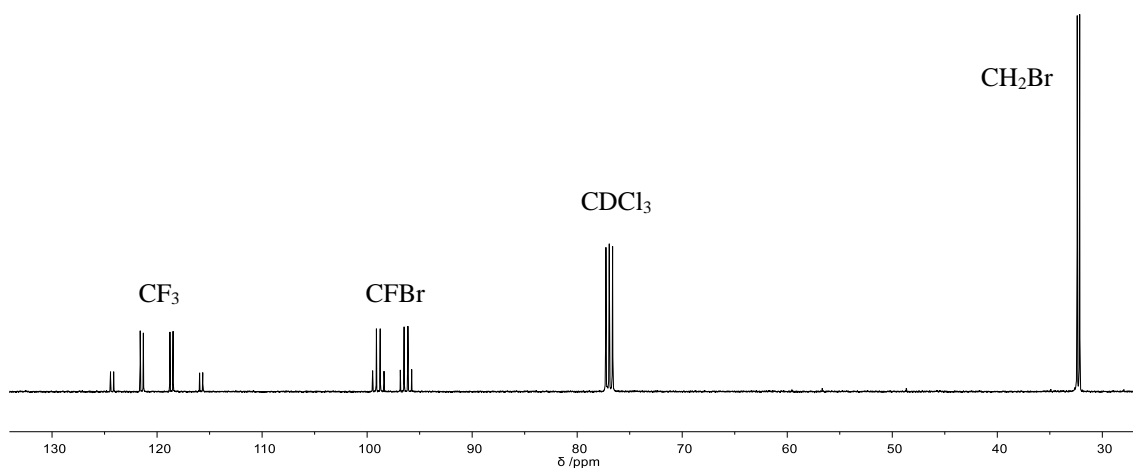


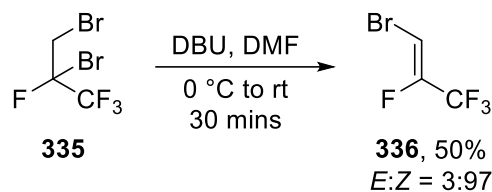
Figure 7.6. ^{13}C NMR spectrum (101 MHz, CDCl_3) of **335**

In the ^1H NMR spectrum, the integrals of the two diastereotopic hydrogen atoms is 1:1, as would be expected, but the similar chemical shifts mean the peaks are close together and so some overlap is seen, distorting the expected splitting patterns. The ^{13}C NMR spectrum (Figure 7.6) likewise shows a complex, but easily rationalised, splitting pattern. Finally, as further evidence, the mass spectrum of **335** also shows a characteristic 1:2:1 ratio for a dibrominated compound caused by the presence of both ^{79}Br and ^{81}Br isotopes.

7.2.2 Reactivity of 1,2-dibromo-2,3,3,3-tetrafluoropropane

Having synthesised dibromoalkane **335** in good yield at up to twenty-gram scale, the utility of this previously unknown compound was then explored. Bromination of $\alpha\text{-CF}_3$ enol ethers has previously been reported by Bonnet-Delpon *et al.* who then went on to demonstrate elimination of HBr using DBU in Et_2O to give the corresponding brominated enol ether.¹⁹ We applied these conditions to the dehydrobromination of **335** in the absence

of any solvent to give full conversion by ^{19}F NMR spectroscopy to **336** (Scheme 7.6). Based on the splitting patterns, *Z* was believed to be the major stereoisomer, comprising 96% of the product. However, isolation of **336** proved difficult due to it having a similar boiling point to the Et_2O solvent. The dehydrobromination reaction was carried out in 1,4-dioxane and the product was obtained in 32% yield following distillation at atmospheric pressure. By changing solvent to DMF the yield was further improved as, on addition of 1 M HCl, the product **336** formed a separate layer without any noticeable decomposition and could be easily separated and dried.



Scheme 7.6. Elimination of HBr from 335 to give 336

Whilst no other synthesis of **335** has yet been reported in the literature, during the course of this work a patent from 3M was published detailing the synthesis of **336** by the dehydrofluorination of 1,1,1,2,2-pentafluoro-3-bromopropane with potassium hydroxide under phase transfer conditions.²⁰ The pentafluorobromopropane starting material was prepared by reaction of the corresponding nonaflate with lithium bromide, with the nonaflate synthesised from the alcohol $\text{CF}_3\text{CF}_2\text{CH}_2\text{OH}$.

DFT calculations were carried out to explain the stereoselectivity observed in our dehydrobromination of **335**. Firstly, the chemical shifts for both *E* and *Z* stereoisomers of bromoalkene **336** were predicted and compared to experimental values. Whilst the absolute values differ by an average of 3.4 ppm, the same trend is predicted computationally as observed experimentally in that the *Z* stereoisomer has a lower chemical shift than the *E* stereoisomer, corroborating our assignments (Table 7.2).

Table 7.2. Comparison of calculated and experimentally observed chemical shifts for 336; calculations carried out by Dr. Mark Fox (Durham University)

Stereoisomer	Calculated δ_{F} /ppm		Experimental δ_{F} /ppm	
	CF_3	CF	CF_3	CF
<i>E</i>	-64.0	-110.1	-67.52	-116.68
<i>Z</i>	-68.0	-122.1	-71.96	-121.52

The relative energy of each stereoisomer of **336** was calculated and it was found that the *E* stereoisomer is 3.75 kcal mol⁻¹ less stable than the *Z* stereoisomer (Figure 7.7). Given that the *Z* conformation is the majority product (up to 98:2), this suggests that the dehydrobromination of **335** under these conditions is thermodynamically controlled and favours formation of the more stable *Z* stereoisomer.

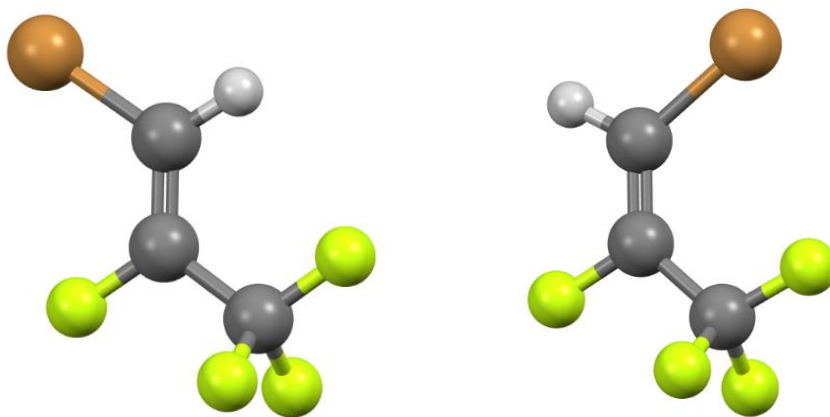
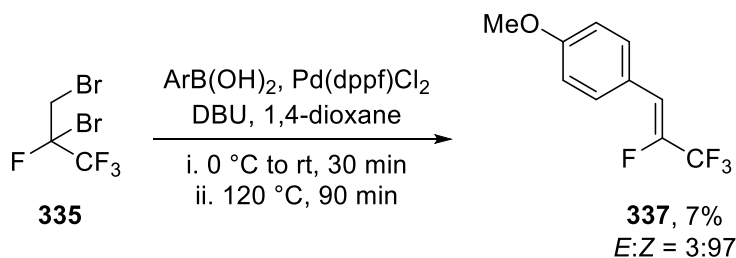


Figure 7.7. Optimised geometries of *Z*-**336** (left) and *E*-**336** (right) ; calculations carried out by Dr. Mark Fox (Durham University)

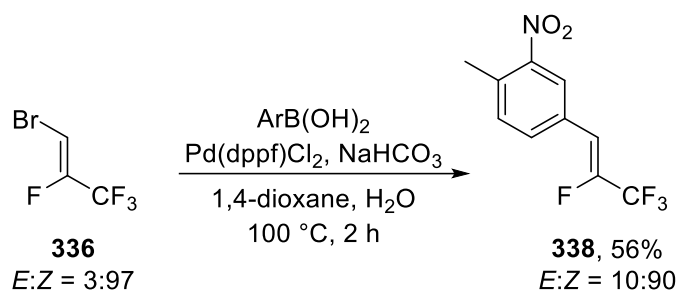
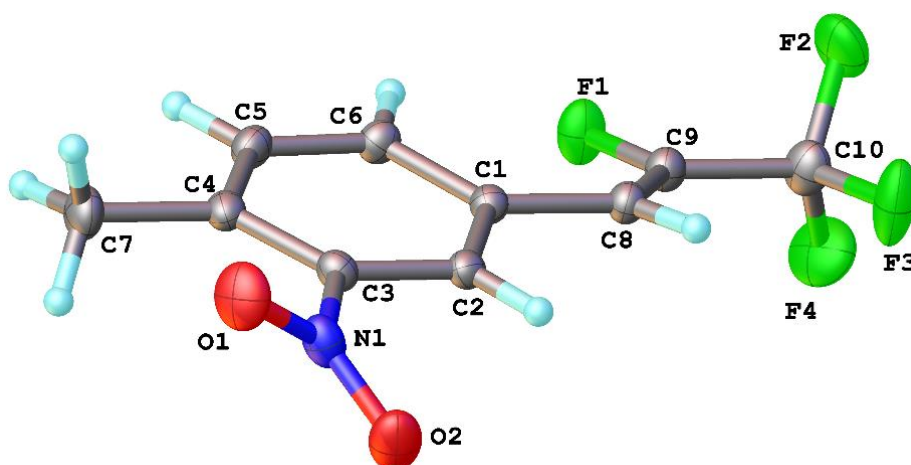
One-pot dehydrobromination-Suzuki coupling was previously reported by Deng *et al.* starting from 1,2-dibromo-3,3,3-trifluoropropane to form α -trifluoromethyl styrenes.²¹ Potassium hydroxide was used as a base in a 1:1:1 mixture of THF, 1,2-dimethoxyethane and water with catalytic Pd(PPh₃)₂Cl₂ and AsPh₃. A similar reaction of **335** was attempted as a proof of concept using Pd(dppf)Cl₂ as the catalyst in 1,4-dioxane. Using microwave irradiation for more efficient heating, complete consumption of **335** and 95% conversion from **336** to aryl alkene **337** was observed via ¹⁹F NMR spectroscopy. However, *E*:*Z* selectivity was reduced to 37:63 due to the use of potassium carbonate as a base instead of the bulky DBU. Following on from these results, the use of DBU as a base for both elimination and the Suzuki coupling was attempted. All reagents were added to the same vial at 0 °C then allowed to stir at room temperature for the elimination of HBr with DBU to occur. The same vial was then heated using microwave irradiation, an excess of DBU being used to also act as the base in the Suzuki coupling reaction to give quantitative conversion to **337** without a reduction in stereoselectivity as determined by ¹⁹F NMR spectroscopy (Scheme 7.7).

337 was isolated following filtration through a silica plug eluting with hexane, removing the palladium catalyst and DBU, followed by evaporation of the solvent. No significant protodeboronation or homocoupling of the boronic acid was observed and the intermediate bromoalkene **336** is volatile so no further purification was required, i.e. no aqueous workup or column chromatography. However, **337** itself was also quite volatile and, hence, a low isolated yield was obtained once the 1,4-dioxane and hexane were removed. An alternative solvent system was therefore sought and tetraglyme was selected as a high boiling solvent, which would allow **337** to be isolated by distillation in higher yields. However, when tetraglyme was used as a solvent, *E:Z* selectivity decreased to 6:94 and there was substantial protodeboronation of the boronic acid. As anisole and **337** have similar boiling points, this would have made isolation by distillation difficult.

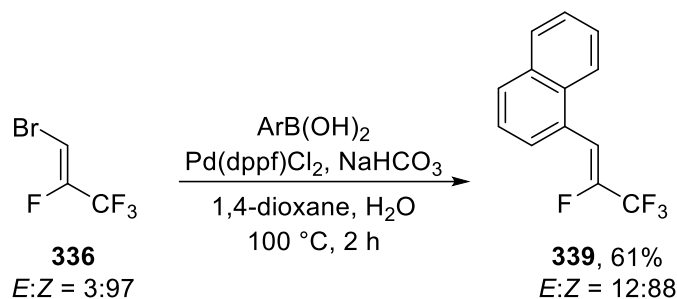


Scheme 7.7. Elimination of HBr from 335 followed by Suzuki coupling to give 337

Boronic acid coupling partners of greater molecular weight were, therefore, used in subsequent reactions to simplify purification. Initially, poor conversion was obtained using the one-pot methodology with less electron-rich boronic acids than the *para*-methoxy substituted analogue used above. Therefore, Suzuki cross-coupling of isolated **336** with 4-methyl-3-nitrophenylboronic acid was then carried out using an adaptation of the one-pot procedure conditions, swapping DBU for aqueous sodium bicarbonate as a much milder base (Scheme 7.8). This gave quantitative conversion to tetrafluoroalkene **338** and a good isolated yield following filtration of the crude reaction mixture through a simple silica plug eluting with ethyl acetate. However, the ratio of stereoisomers decreased from 3:97 in **336** to only 10:90 in **338**, suggesting some *cis-trans* isomerisation takes place during the reaction. **338** proved to be a crystalline solid and so the structure of the major product could be proved unequivocally by X-ray crystallography (Figure 7.8), demonstrating that it was indeed the *Z*-stereoisomer.

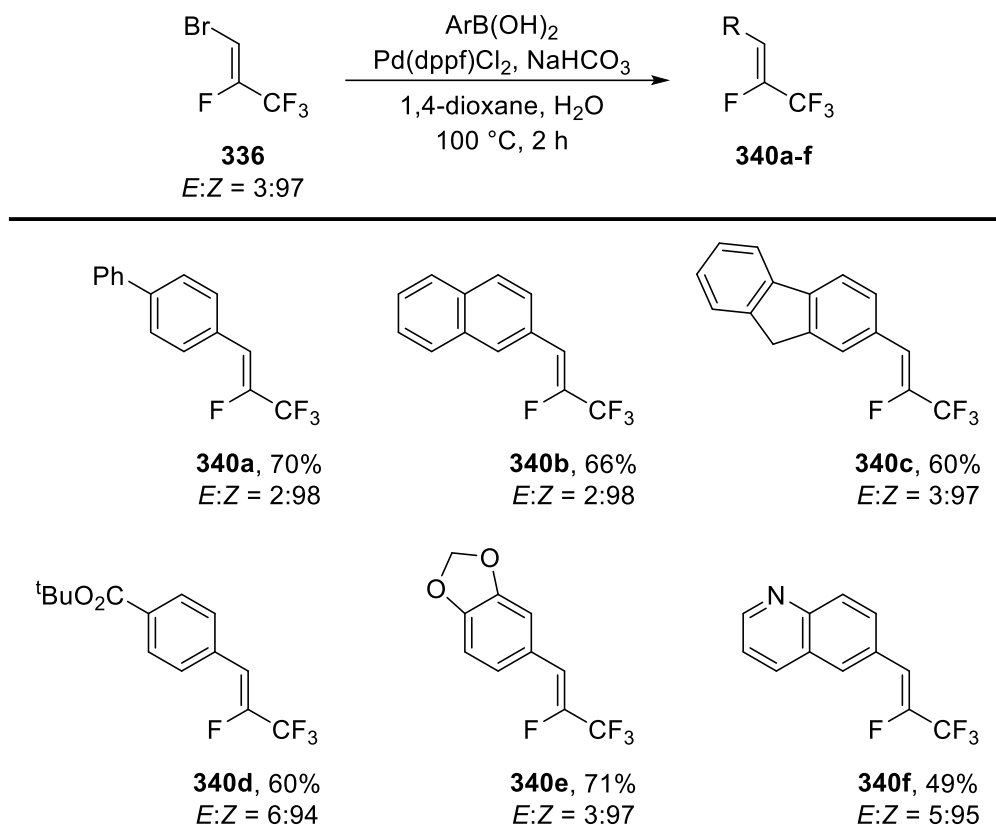
Scheme 7.8. Suzuki cross-coupling of bromoalkene **336**Figure 7.8. Structure of **338** as proven by X-ray crystallography

Changing coupling partner to 1-naphthylboronic acid, literature conditions for the cross-coupling of 1-bromo-3,3,3-trifluoropropene were used instead,²² which required a lower temperature and a shorter reaction time and so would hopefully reduce the amount of *cis-trans* isomerisation (Scheme 7.9). Tetrafluoroalkene **339** was obtained in good yield but again showed a decrease in stereoselectivity compared to the starting material.

Scheme 7.9. Suzuki cross-coupling of bromoalkene **336**

Some further examples of the Suzuki cross-coupling reaction of **336** were then conducted by MChem student Jonathan Holland, as shown in Scheme 7.10 for completeness. Several

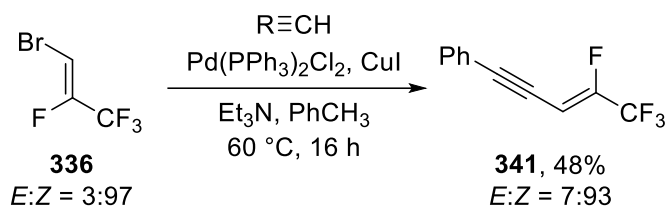
hydrocarbon substrates were successfully employed, with the structure of fluorenyl derivative **340c** also confirmed by X-ray crystallography to be the *Z*-stereoisomer and so reaffirming the previously determined stereoselectivity of these reactions. The reaction conditions were also tolerant of more electron-poor aryl boronic acids (ester derivative **340d**) as well as heterocyclic systems (dioxole **340e** and quinoline **340f**).



Scheme 7.10. Examples of the Suzuki coupling of **336** carried out by MChem student Jonathan Holland

Lu *et al.* showed that the tetrafluorostyrenes such as **338** can be obtained through direct oxidative Heck coupling of **1** with boronic acids.²³ Therefore, our three-step procedure from **1** to such systems is significantly less efficient and so would only be of use with boronic acids with substituents particularly sensitive towards oxidative reaction conditions. However, bromoalkene **336** offers further utility as it could be used in other classes of cross-coupling reactions. To that end, the Sonogashira reaction of **336** with phenylacetylene was attempted to form tetrafluoroenyne **341** (Scheme 7.11). After 1.5 hours at $80\text{ }^\circ\text{C}$, only 6% conversion was observed by ^{19}F NMR spectroscopy. Extending the reaction time to 24 hours afforded clean conversion of **336** to enyne **341** as determined by ^{19}F NMR spectroscopy. However, ^1H NMR spectroscopy showed that there was also

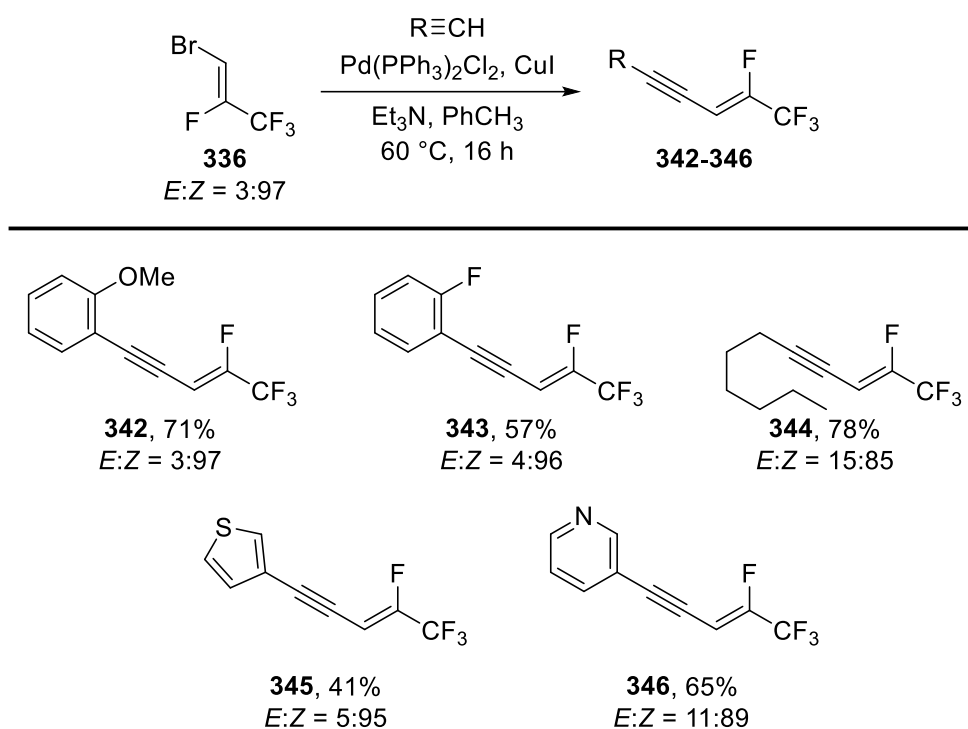
significant amount of 1,4-diphenyl-1,3-butadiyne formed from homocoupling of phenylacetylene and the identity of this by-product was confirmed by X-ray crystallography. Purification by column chromatography was attempted but this gave **341** in only 10% isolated yield, suggesting that prolonged exposure to silica may degrade tetrafluorinated enynes of this type. The synthesis of **341** was repeated using a larger excess of the bromoalkene **336** with respect to the alkyne, which reduced the amount of homocoupling but there was still a significant amount of diyne in the crude product mixture. More thorough degassing of the reaction mixture eliminated homocoupling but led to formation of a complex mixture of unidentified fluorinated products. However, by reducing the reaction temperature from 80 °C to 60 °C, replacing triethylamine with toluene as the solvent and instead adding one equivalent of triethylamine, the reaction became selective for only enyne **341** with minimal homocoupling observed.



Scheme 7.11. Sonogashira coupling reaction of bromoalkene 336

The only previously reported preparation of tetrafluoroenyne was by the analogous reaction of 1-iodo-2,3,3,3-tetrafluoropropene, which is not commercially available and is prepared by a three-step synthesis from $\text{CF}_3\text{CF}_2\text{CH}_2\text{OH}$.²⁴ Addition of alkynyl lithium reagents to these enynes gave 3-trifluoromethylated hex-3-ene-1,5-diyne. Separately, dehydrofluorination of tetrafluoroenyne gives CF_3 -substituted diynes,²⁵ which can then react via carbocupration or hydrostannylation²⁶ reactions to provide an alternative route to CF_3 -hexenediyne. Other CF_3 -substituted enynes have been synthesised previously by Sonogashira coupling of 1-chloro-2,3,3,3-tetrafluoropropene,²⁷ the reaction of 1,1-difluoro-1-alken-3-ols with diethylaminosulfur trifluoride²⁸ or, more frequently, an oxidative Sonogashira coupling of trimethylsilyl-substituted CF_3 -alkenes.²⁹ **1** is a more readily available and more environmentally benign starting material than any other substrate used previously in the literature. Enynes with a single trifluoromethyl substituent prepared via these means have been used in the synthesis of CF_3 -furans³⁰ and CF_3 -indoles,³¹ demonstrating the utility of such systems as building blocks for the preparation of compounds of potential pharmaceutical relevance.

We then undertook some further examples of the Sonogashira reaction of **336** (Scheme 7.12). Both electron-donating and withdrawing substituents on the phenyl ring of the acetylene substrates were tolerated with 2-fluorophenylacetylene giving **342** and 2-methoxyphenylacetylene **343**, respectively. Reaction with 1-octyne gave clean conversion to the desired enyne product **344** and, finally, heterocyclic alkynes were also found to be suitable substrates with the successful preparation of thiophene and pyridine derivatives **345** and **346** respectively.

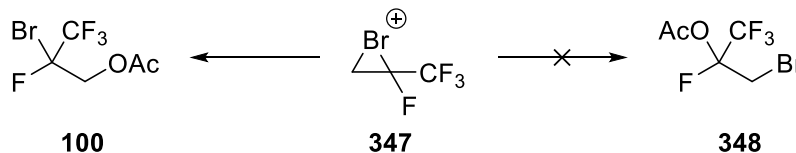


Scheme 7.12. Substrate scope for Sonogashira coupling reactions of bromoalkene 336

7.2.2 Other electrophilic addition reactions of HFO-1234yf

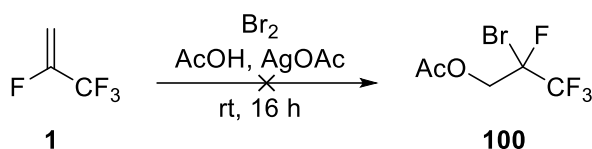
Various other attempted electrophilic addition reactions of **1** at room temperature and atmospheric pressure were unsuccessful, namely: cohalogenation with bromine and acetic acid, benzyl alcohol or *t*-butanol; iodine; iodine monochloride; and electrophilic fluorinating reagents (SelectfluorTM or the more reactive³² pentachloro-*N*-fluoropyridinium triflate). The Mexichem patent¹⁵ describing cohalogenation of **1** with *N*-bromosuccinimide and acetic acid suggests that electrophilic addition to **1** is not trivial, requiring heating to 80 °C over five days to give an ultimately low yield of 21% (Scheme

7.13). The process was reported to be regioselective for the product derived from attack at the least hindered carbon of the bromonium intermediate (**347**). This would suggest that steric hindrance plays a significant role in the reactivity of such species, thus favouring formation of **100** over **348**.



Scheme 7.13. Regioselectivity in Mexichem patented cohalogenation of HFO-1234yf¹⁵

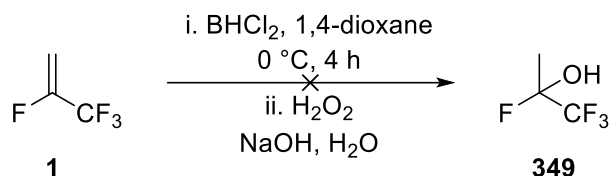
Knunyants *et al.* demonstrated that cohalogenation of 3,3,3-trifluoropropene was possible using bromine in acetic acid with stoichiometric mercury acetate.³³ Subsequently, Ramachandran tested a series of metal acetates (Ag, Cu, Fe, Mn, Ni and Zn) as non-toxic alternatives and found stoichiometric silver acetate was a viable substitute, albeit giving a lower yield.³⁴ However, our attempted reaction of **1** with bromine and acetic acid with silver acetate led to the formation of none of the intended product **100** (Scheme 7.14), only the previously observed bromination product **335**. Likewise, no cohalogenation with bromine, trifluoroacetic acid and silver trifluoroacetate was observed.



Scheme 7.14. Attempted silver-mediated cohalogenation of 1 with acetic acid and bromine

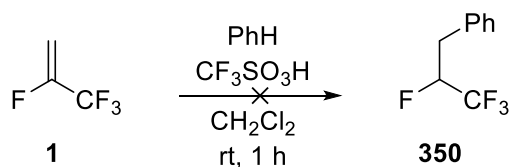
Along with halogenation reactions, the hydroboration of alkenes is another textbook example of electrophilic addition. Whilst no hydroboration reaction of **1** has been reported in the literature, Brown *et al.* did develop the hydroboration of 3,3,3-trifluoropropene.³⁵ They found that optimal yields and stereoselectivity (81%, 98:2 secondary:primary) were obtained using BHCl_2 . We attempted the reaction of **1** with the commercially available complex of BHCl_2 with 1,4-dioxane (3.0 M in CH_2Cl_2) followed by oxidation with NaOH and H_2O_2 (Scheme 7.15). This would be expected to give alcohol **349** as the main product. However, no fluorinated product was observed by NMR spectroscopy following aqueous work-up. This could either be due to a lack of reactivity with **1** or the possible instability of **349**, which may eliminate fluoride to form the highly volatile 1,1,1-trifluoroacetone.

α -Fluoroalcohols are known in the literature to be unstable with respect to forming the corresponding ketone.³⁶ Subsequent work by Ramachandran demonstrated that inversion of selectivity, i.e. the anti-Markovnikov product, could be obtained with other trifluoromethyl alkenes by using dicyclohexylborane.³⁷ However, dicyclohexylborane is not commercially available and would have to be prepared whilst other dialkylboranes, such as 9-BBN, were described as being “inert to such alkenes”.



Scheme 7.15. Attempted hydroboration of **1**

Nenadjenko *et al.* reported that 1-aryl-2,3,3,3-tetrafluoropropenes, which they derived from aldehydes through copper-catalysed olefination reactions with CF_3CBr_3 , could be protonated by triflic acid and the resulting carbocation underwent Friedel-Crafts type reactions with various arenes.³⁸ Attempting to apply their procedure to **1**, a solution of triflic acid in dry dichloromethane was stirred under an atmosphere of **1** provided via gas bladder (Scheme 7.16). Benzene was then added dropwise with the aim of forming tetrafluorinated propylbenzene **350**. However, after one hour at room temperature followed by aqueous workup, ^{19}F NMR spectroscopy showed no fluorinated compounds.



Scheme 7.16. Attempted Friedel-Crafts reaction of carbocation derived from **1** with benzene

7.3 Conclusions

The reticence of 2,3,3,3-tetrafluoropropene (HFO-1234yf, **1**) to undergo cycloaddition or electrophilic addition reactions is reflective of its broader reactivity as discussed in earlier chapters. Whilst it is beneficial for a refrigerant to be relatively chemically inert, this can be disadvantageous when attempting to use **1** as a building block in organic chemistry. Nevertheless, under suitable conditions, transformations of **1** towards more pharmaceutically relevant trifluoromethylated organic systems are possible. The

attempted Diels-Alder reaction of **1** with furan gave no reaction despite the elevated temperatures and pressures used. Cycloaddition with oxazoles did give some reaction but provided only an intractable complex mixture of fluorinated products. Greater success was obtained with the 1,3-dipolar cycloaddition reaction of **1** with an azomethine ylide to give a tetrafluorinated pyrrolidine, a reaction which was carried out previously in the literature but for which we were able to obtain the first crystallographic proof of structure. Further reactions of this pyrrolidine were explored and, whilst there is potential for a new route to CF₃-substituted pyrroles, this work requires further optimisation.

Similarly, attempted electrophilic addition reactions of **1** were generally unsuccessful. This lack of reactivity is instructive as it reveals that **1** is more akin to perfluoroalkenes than to 3,3,3-trifluoropropene in its reactivity with electrophiles. This contrasts with the results in Chapter 3 where the reactivity of **1** towards nucleophiles was found to be significantly less than that of perfluoroalkenes. The one electrophilic addition reaction of **1** that was found to work, bromination using Br₂ in dichloromethane, proceeded at ambient temperature and pressure to give clean conversion to 1,2-dibromo-2,3,3,3-tetrafluoropropane, a compound which has not previously been described in the literature but has great potential utility as a multi-functional CF₃-containing building block.

Dehydrobromination gave 1-bromo-3,3,3-trifluoropropene, an alkene that has only recently been described elsewhere in the literature and for which no other reactions have yet been reported despite the simplicity of its structure. The elimination reaction was found to be highly selective for the *Z* stereoisomer, which DFT calculations revealed to be a thermodynamic effect as the *E* stereoisomer was less stable. The bromoalkene was a competent partner in both Suzuki and Sonogashira cross-coupling reactions, forming a range of tetrafluorinated aryl alkenes and enynes respectively. Similar structures have been employed in the literature for the preparation of various trifluoromethylated heterocycles of pharmaceutical relevance as well as highly conjugated systems useful for organic materials applications, all of which may now, in principle, be accessed from **1**.

7.4 References for Chapter 7

¹ E. T. McBee, C. G. Hsu, O. R. Pierce and C. W. Roberts, *J. Am. Chem. Soc.*, 1955, **77**, 915.

- ² I. Ojima, M. Yatabe and T. Fuchikami, *J. Org. Chem.*, 1982, **47**, 2051.
- ³ (a) A. Dean, A. Venzo, M. G. Ferlin, G. G. Bombi, P. Brun, I. Castagliuolo and V. B. Di Marco, *Dalton Trans.*, 2007, 1689; (b) A. Dean, M. G. Ferlin, M. Cvijovic, P. Djurdjevic, F. Dotto, D. Badocco, P. Pastore, A. Venzo and V. B. Di Marco, *Polyhedron*, 2014, **67**, 520.
- ⁴ e.g. M. Surowiec and M. Małosza, *Tetrahedron*, 2004, **60**, 5019.
- ⁵ V. S. Yarmolchuk, O. V. Shishkin, V. S. Starova, O. A. Zaporozhets, O. Kravchuk, S. Zozulya, I. V. Komarov and P. K. Mykhailiuk, *Eur. J. Org. Chem.*, 2013, **15**, 3086.
- ⁶ D. Meyer and M. El Qacemi, *Org. Lett.*, 2020, **22**, 3479.
- ⁷ Y. Guo, K. Fujiwara, H. Amii and K. Uneyama, *J. Org. Chem.*, 2007, **72**, 8523.
- ⁸ I. McAlpine, M. Tran-Dubé, F. Wang, S. Scales, J. Matthews, M. R. Collins, S. K. Nair, M. Nguyen, J. Bian, L. Martinez Alsina, J. Sun, J. Zhong, J. S. Warmus and B. T. O'Neill, *J. Org. Chem.*, 2015, **80**, 7266.
- ⁹ K. Tomita, Y. Tsuzuki, K.-I. Shibamori, M. Tashima, F. Kajikawa, Y. Sato, S. Kashimoto, K. Chiba and K. Hino, *J. Med. Chem.*, 2002, **45**, 5564.
- ¹⁰ (a) A. M. Pohlit and C. R. D. Correia, *Heterocycles*, 1997, **45**, 2321; (b) M. D'hooghe, W. Aelterman and N. De Kimpe, *Org. Biomol. Chem.*, 2009, **7**, 135; (c) J. Chen, L. Zhou and Y.-Y. Yeung, *Org. Biomol. Chem.*, 2012, **10**, 3808.
- ¹¹ (a) A. Boto, R. Hernández, Y. de León and E. Suárez, *J. Org. Chem.*, 2001, **66**, 7796; (b) N. Shangguan and M. Joullié, *Tetrahedron Lett.*, 2009, **50**, 6748; (c) S. Phae-Nok, C. Kuhakarn, M. Pohmakotr, V. Reutrakula and D. Soorukram, *Org. Biomol. Chem.*, 2015, **13**, 11807.
- ¹² J. M. Percy, *Synthesis: Carbon with No Attached Heteroatoms in Comprehensive Organic Functional Group Transformations*, eds. A. R. Katritzky, O. Meth-Cohn and C. W. Rees, 1995, Elsevier.
- ¹³ T. Taniguchi, S. Furuta and H. Shiota, US 297918, 2018.
- ¹⁴ J. Lyu, J. Zeng, X. Tang, S. Han, W. Zhang, J. Kang, B. Wang, Z. Hao, Z. Yang and F. Li, CN 105439805, 2016.
- ¹⁵ J. H. Murray and A. P. Sharratt, WO2018/197897, 2018.
- ¹⁶ R. D. Chambers, *Fluorine in Organic Chemistry*, 2004, Blackwell Publishing Ltd., Oxford, pg. 191-7.
- ¹⁷ (a) A. L. Henne and M. Nager, *J. Am. Chem. Soc.*, 1951, **73**, 1042; (b) R. N. Haszeldine, *J. Chem. Soc.*, 1951, 2495; (c) R. N. Haszeldine and K. Leedham, *J. Chem. Soc.*, 1952, 3483.
- ¹⁸ M. Karplus, *J. Chem. Phys.*, 1959, **30**, 11.
- ¹⁹ D. Bonnet-Delpon, D. Bouvet, M. Ourévitch and M. H. Rock, *Synthesis*, 1998, **3**, 288.
- ²⁰ S. M. Smith, M. G. Costello, M. J. Bulinski, H. Ren and F. A. Coughlin, WO2020/128964, 2020, A2.
- ²¹ R.-Q. Pan, X.-X. Liu and M.-Z. Deng, *J. Fluorine Chem.*, 1999, **95**, 167.
- ²² D. A. Wacker, K. A. Rossi and Y. Wang, US2009/23702, 2009, A1.
- ²³ Y. Li, D.-H. Tu, Y.-J. Gu, B. Wang, Y.-Y. Wang, Z.-T. Liu, Z.-W. Liu and J. Lu, *Eur. J. Org. Chem.*, 2015, **20**, 4340
- ²⁴ T. Konno, M. Kishi, T. Ishihara and S. Yamada, *J. Fluorine Chem.*, 2013, **156**, 144.
- ²⁵ T. Konno, M. Kishi and T. Ishihara, *Beilstein J. Org. Chem.*, 2012, **8**, 2207.
- ²⁶ T. Konno, M. Kishi, T. Ishihara and S. Yamada, *Tetrahedron Lett.*, 2015, **70**, 2455.
- ²⁷ M. Naka, T. Kawasaki-Takasuka and T. Yamazaki, *Beilstein J. Org. Chem.*, 2013, **9**, 2182.
- ²⁸ F. Tellier and R. Sauvêtre, *J. Fluorine Chem.*, 1993, **62**, 183.

- ²⁹ A. Ikeda, M. Omote, K. Kusumoto, A. Tarui, K. Sato and A. Ando, *Org. Biomol. Chem.*, 2015, **8**, 8886.
- ³⁰ J. Zhang, X. Zhao, Y. Li and L. Lu, *Tetrahedron Lett.*, 2006, **47**, 4737.
- ³¹ A. Ikeda, M. Omote, K. Kusumoto, M. Komori, A. Tarui, K. Sato and A. Ando, *Org. Biomol. Chem.*, 2016, **14**, 2127.
- ³² N. Rozatian, I. W. Ashworth, G. Sandford and D. R. W. Hodgson, *Chem. Sci.*, 2018, **9**, 8692.
- ³³ I. L. Knunyants, E. Ya. Pervova and V. V. Tyuleneva, *Bull Acad. Sci. USSR, Div. Chem. Sci.*, 1961, **10**, 77.
- ³⁴ P. V. Ramachandran and K. J. Padiya, *J. Fluorine Chem.*, 2007, **128**, 1255.
- ³⁵ H. C. Brown, G.-M. Chen, M. P. Jennings and P. V. Ramachandran, *Angew. Chem. Int. Ed.*, 1999, **38**, 2052.
- ³⁶ T. Hayasaka, Y. Katsubara, T. Kume and T. Yamazaki, *Tetrahedron*, 2011, **67**, 2215.
- ³⁷ (a) P. V. Ramachandran, M. P. Jennings and H. C. Brown, *Org. Lett.*, 1999, **1**, 1399;
(b) P. V. Ramachandran and M. P. Jennings, *Chem. Commun.*, 2002, 386.
- ³⁸ M. A. Sandzhieva, A. N. Kazakova, I. A. Boyarskaya, A. Yu. Ivanov, V. G. Nenajdenko and A. V. Vasilyev, *J. Org. Chem.*, 2016, **81**, 5032.

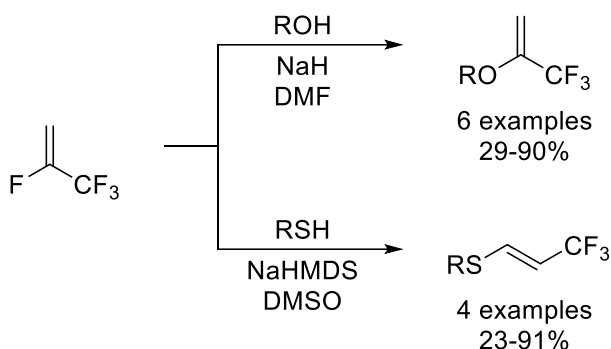
Chapter 8: Conclusions and future work

The incorporation of fluorine into organic compounds has wide-ranging effects on the properties and reactivity of such systems, which can be beneficial for pharmaceuticals, agrochemicals and organic materials. Fluorinated organic compounds and, in particular, those bearing a trifluoromethyl group are commonplace in these applications. Whilst great strides have been made in recent years to develop methods for the trifluoromethylation of various substrates, such processes often have poor atom economy and can be prohibitively expensive for large scale applications. The preparation of trifluoromethyl-substituted compounds on process scale and above is, therefore, typically limited to the use of trifluoroacetic acid or trifluorotoluene derivatives as building blocks, which limits the number of trifluoromethylated structures that can be easily synthesised.

Refrigerant gases containing a trifluoromethyl group have been produced on an enormous scale for several decades, at first in chlorofluorocarbons (CFCs) then in hydrofluorocarbons (HFCs) and now in low global warming potential hydrofluoroolefins (HFOs), such as 2,3,3,3-tetrafluoropropene (HFO-1234yf). As HFOs replace HFCs, their cost is decreasing and availability increasing. The presence of a trifluoromethyl group attached to a carbon-carbon double bond provides the opportunity to use these refrigerant gases as feedstocks for various transformations to access more complex trifluoromethylated organic compounds of greater relevance to the pharmaceutical sector. At the beginning of this project, there had only been five scientific papers and a handful of patents published on the use of HFO-1234yf in organic synthesis but the work in this thesis, and several reports from other groups that were published in the same period, have demonstrated the benefits of this approach.

Our studies began by investigating a discrepancy in the literature wherein the reaction of HFO-1234yf with alkoxide nucleophiles gave either an α -CF₃ or β -CF₃ enol ether product, as reported in Chapter 3. Both literature reports were found to be accurate and the different regioselectivity arises as hard nucleophiles under aprotic conditions favour the α -regioisomer whereas reactions of softer nucleophiles in protic solvents favour the β -regioisomer, a mechanistic proposal supported by trapping of intermediates with deuterium and DFT calculations. After optimising conditions, a range of α -CF₃ enol ethers were synthesised from alkoxides with more pharmaceutically relevant heterocyclic

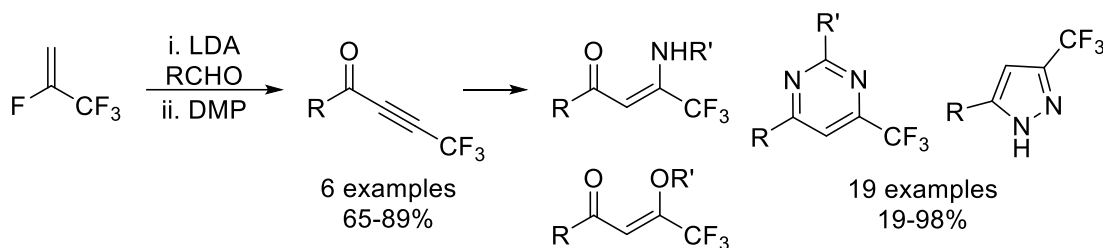
and sp^3 -rich structures. By contrast, reaction with thiolates gave β - CF_3 vinyl sulfides whilst attempts at addition of nitrogen- or carbon-centred nucleophiles to HFO-1234yf led to dehydrofluorination rather than nucleophilic substitution. Attempted Heck coupling and cyclopropanation reactions of the α - CF_3 enol ethers derived from HFO-1234yf were generally unsuccessful. We intended to further explore these reactions using high-throughput techniques at GlaxoSmithKline but this placement was not possible due to restrictions imposed by the COVID-19 pandemic.



Scheme 8.1. Nucleophilic substitution reactions of HFO-1234yf carried out in Chapter 3

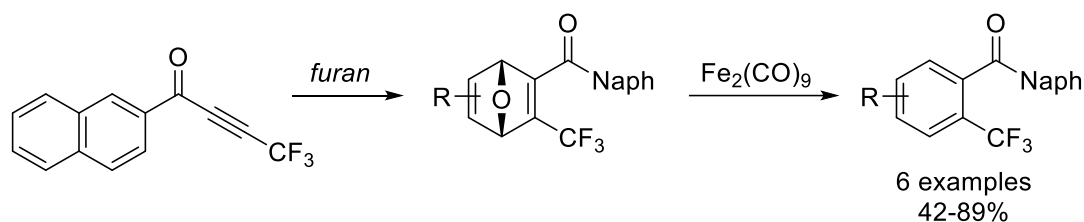
Whilst no nucleophilic substitution was observed with carbon-centred nucleophiles, Chapter 4 described how organolithium reagents did react with HFO-1234yf to affect dehydrofluorination to form 3,3,3-trifluoropropyne. Deuterium trapping demonstrated that, with two equivalents of organolithium reagent, the alkyne was deprotonated to form lithium 3,3,3-trifluoropropynide. Solvents and bases were screened to optimise the addition reaction of this propynide nucleophile to benzaldehyde, aided by *in situ* IR spectroscopy studies. A range of CF_3 -propargyl alcohols were synthesised and subsequently oxidised with Dess-Martin periodinane, forming CF_3 -ynones. Surprisingly, there have been very few previous studies of the synthesis of ynones with an alkynyl CF_3 group and even fewer exploring their reactivity. We found that addition of amine nucleophiles was rapid and clean, occurring exclusively next to the CF_3 group in a Michael-type process to form various CF_3 -enaminones. Reaction with phenoxides gave the equivalent CF_3 -enone ethers and, supported by DFT calculations and NMR studies, stereoselectivity was found to be governed by thermodynamic control to give a single stereoisomer. These reactions were extended to dinucleophiles, forming CF_3 -substituted pyrazoles, pyrimidines and benzodiazepines with the product heterocycle simply precipitating from solution, making this method highly scalable. Finally, the

pharmaceutical relevance of these reactions was demonstrated with a novel synthesis of the anti-arthritis blockbuster drug celecoxib in just three steps from HFO-1234yf.



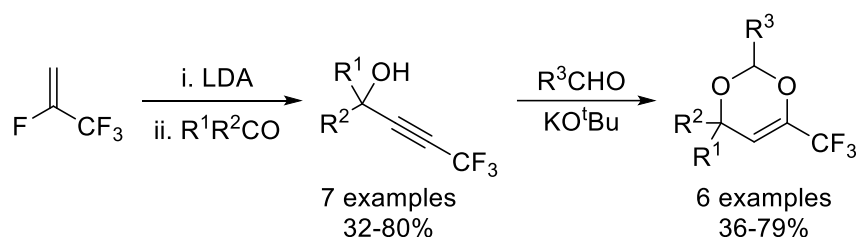
Scheme 8.2. Synthesis and reactivity of trifluoromethyl ynones explored in Chapter 4

In Chapter 5, the reaction of the CF_3 -ynones derived from HFO-1234yf was extended beyond Michael addition reactions to cycloaddition processes. Reactions with various dienes via a Diels-Alder [4+2] process were explored and were generally successful but the adducts formed were of little value. Attempted ring-opening of some of these adducts to access more pharmaceutically relevant structures was generally unselective. However, a deoxygenative process using the adduct formed between CF_3 -ynones and furans using diironnonacarbonyl was developed and gave complete regioselectivity for *ortho*- CF_3 benzophenones with a 1,2,3-substitution pattern from 2-substituted furans or 1,3,4 from 3-substituted furans. The preparation of trifluoromethylated aromatic systems with such regioselectivity through classical transformations of benzene rings is not trivial. Future work could expand the scope of either these cycloaddition processes or the aforementioned nucleophilic addition reactions. The ability to synthesise CF_3 -ynones in a single step from HFO-1234yf would improve the practicality of this process. Whilst our attempts to react lithium 3,3,3-trifluoropropynide with acid chlorides led to intractable mixtures, further work could be done to optimise conditions to improve selectivity. In particular, the use of flow chemistry techniques could be useful to limit the amount of time the two reagents are in contact and to more accurately control the equivalents of gaseous starting material used with a mass flow controller.



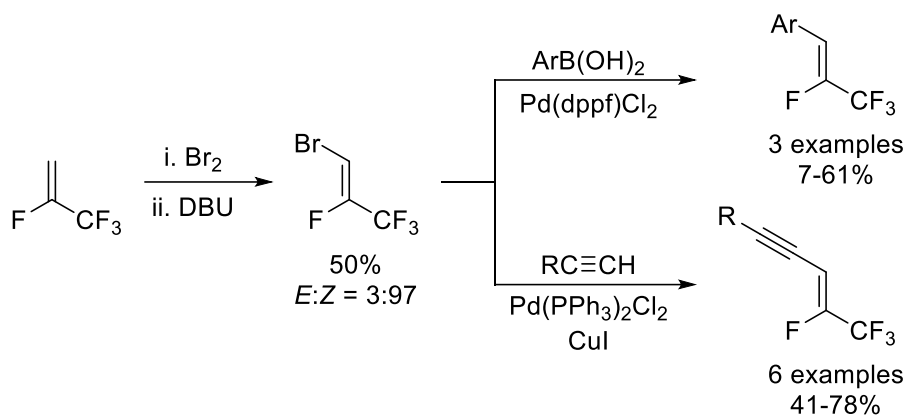
Scheme 8.3. Cycloaddition reactions of trifluoromethyl ynones discussed in Chapter 5

Lithium 3,3,3-trifluoropropynide formed from HFO-1234yf was also trapped with ketones to form tertiary alcohol systems, as shown in Chapter 6. The acetone adduct formed via this process was found to be a bench-stable liquid that, on heating with base, released 3,3,3-trifluoropropyne. Some initial attempts were made to leverage this process for deacetonative Sonogashira cross-coupling and nucleophilic substitution reactions but with limited success. Greater success was obtained in transforming these CF₃-substituted tertiary alcohols into a range of unusual heterocyclic and alkenyl building blocks, the utility of which to access novel trifluoromethylated systems could be explored in future work. Future work could also develop alternative conditions for the deacetonative Sonogashira trifluoropropyne reaction, possibly enabled by other phosphine ligands that might mitigate the low nucleophilicity of the trifluoropropynide anion. If successful, the simplicity of the deacetonative mechanism and the ease with which the starting CF₃-alkynol can be synthesised might make such a process widely applicable to preparation of CF₃-alkynes, especially when compared to the current leading methods for trifluoromethylation of terminal alkynes.



Scheme 8.4. Synthesis and reactivity of CF₃-tertiary alcohols as shown in Chapter 6

Finally, Chapter 7 examined the reaction of HFO-1234yf with electrophiles and through cycloaddition reactions. Whilst an unreactive dienophile in Diels-Alder reactions, HFO-1234yf was a good dipolarophile for 1,3-dipolar cycloaddition with azomethine ylides to form a tetrafluorinated pyrrolidine. Future work could look at other 1,3-dipolar cycloaddition reactions of HFO-1234yf and also investigate routes from the tetrafluorinated pyrrolidine product to trifluoromethylated pyrroles or analogs of proline for use in peptide chemistry. Bromination of HFO-1234yf occurred readily at ambient temperature and pressure and the resulting dibromoalkane, following dehydrobromination, was a useful building block for cross-coupling reactions to prepare tetrafluorinated styrenes and enynes. In future work, further examples of these cross-coupling reactions could be investigated as well as other related processes, such as Heck reactions to form tetrafluorinated dienes or carbonylative cross-coupling reactions.



Scheme 8.5. Synthesis and reactivity of 1-bromo-2,3,3,3-tetrafluoropropene investigated in Chapter 7

Taken together, the work in this thesis has significantly expanded our understanding of the reactivity of the 4th generation refrigerant gas HFO-1234yf. As befits a refrigerant, HFO-1234yf is inert towards many reagents but, under the right conditions, can react with nucleophiles, electrophiles, bases and through cycloaddition processes. Combined with other work on the reactivity of HFO-1234yf published by others in the same timeframe, most textbook reactions of alkenes have now been investigated with one notable exception being radical processes. This is likely a promising area for further development as trifluoromethyl alkenes have long been known to react via various free radical pathways and these transformations have seen a resurgence in popularity in recent years, particularly using photocatalytic conditions.

The work that has been done with HFO-1234yf so far in this thesis and beyond demonstrates that somewhat harsh reagents, such as organolithium reagents, are often required for any reaction to occur. However, the reactions that do proceed are usually highly selective with few side products. By using HFO-1234yf in excess, isolation of products is typically straightforward as the gaseous starting material is facile to remove and so chromatography or distillation can often be avoided, making reactions easier to increase to process scale and beyond. When one also considers the low global warming potential, low purchasing cost and low chemical hazards associated with HFO-1234yf, this synthetic utility makes it an ideal feedstock for further transformations towards pharmaceutically relevant systems and chemical intermediates.

Chapter 9: Experimental

9.1 General information

2,3,3,3-Tetrafluoropropene, (HFO-1234yf, 1), was purchased from Apollo Scientific in 100 gram cylinders. Unless otherwise stated, all other chemicals were purchased from Acros Organics, Fisher Scientific, Fluorochem or Sigma Aldrich and were used without any further purification. Glassware was oven-dried prior to use but no other precautions were taken to exclude air or moisture unless otherwise stated. Gas bladder reactions were performed using a 242 mL rubber gas expansion bag purchased from Sigma Aldrich, which was then fitted with a B19 Teflon® tap adapter.

Thin layer chromatography was carried out using Macherey-Nagel™ standard SIL G silica layers (5-17 µm with fluorescence indicator UV254, with compounds visualised under UV light) on Polygram™ polyester sheets purchased from Fisher Scientific. Manual column chromatography was carried out using LC401 silica gel (40-63 µm) purchased from Fluorochem and automated column chromatography was carried out on a Teledyne Isco CombiFlash NextGen 100 with RediSep® Normal-phase Silica Flash Columns (35-70 µm). In both cases, crude products were adsorbed onto LC401 silica gel prior to loading onto columns for purification.

Proton, carbon and fluorine nuclear magnetic resonance (NMR) spectra were recorded on a Bruker 400 Ultrashield (¹H NMR at 400 MHz; ¹³C NMR at 101 MHz; ¹⁹F NMR at 376 MHz) a Varian VNMRS-600 (¹H NMR at 600 MHz; ¹³C NMR at 151 MHz) or a Varian VNMRS-700 (¹H NMR at 700 MHz; ¹³C NMR at 176 MHz) spectrometer with residual solvent peaks as the internal standard (¹H NMR, CHCl₃ at 7.26 ppm; ¹³C NMR, CDCl₃ at 77.16 ppm) or relative to an external standard (¹⁹F NMR, CFCl₃ at 0.00 ppm). NMR spectroscopic data are reported as follows: chemical shift (ppm), integration, multiplicity (s=singlet, d=doublet, t=triplet, q=quartet, m=multiplet, br s = broad singlet), coupling constant(s, Ar) (Hz), assignment. NMR assignments were made using COSY, DEPT-135, HSQC and HMBC experiments where appropriate and spectra were analysed using MestReNova software.

Low resolution LC-MS data were recorded on a Waters TQD mass spectrometer equipped with Acquity UPLC BEH C18 1.7 μm column (2.1 mm x 50 mm). GC-MS data were recorded on a Shimadzu QP2010-Ultra equipped with a Rxi-17Sil MS column (0.15 μm x 10 m x 0.15 mm) at 70 eV using a helium carrier gas. Accurate mass analysis was achieved with a Waters QtoF Premier mass spectrometer equipped with an accurate solids analysis probe (ASAP) or a Waters LCT Premier XE mass spectrometer equipped with Acquity UPLC and ASAP.

Infra-red (IR) spectra for isolated compounds were recorded on a Perkin Elmer FTIR Spectrum Two fitted with an ATR probe and selected absorption maxima are reported in wavenumbers. In situ IR spectroscopy was performed using a Mettler Toledo React IR instrument equipped with a diamond probe.

Melting points were measured with a manually operated Gallenkamp apparatus in open capillary tubes at atmospheric pressure.

9.2 Experimental data for Chapter 2

Solubility screening.

5 mL of solvent was added to a 10 mL glass vial, which was then sealed with a septum cap. **1** was bubbled through the solvent to fill a balloon attached to the septum via a needle to approximately the same volume (~10 mL). The solvent was then stirred under this atmosphere of **1** for one hour at room temperature. 0.7 mL of the resulting solution was then removed and the concentration of **1** determined relative to an internal standard (0.01 mL) of 2,2,2-trifluoroethanol (for water) or fluorobenzene (for all other solvents) by ^{19}F NMR spectroscopy. For stability tests, NMR tubes from the initial screening were left either open to the air or sealed with a standard NMR tube cap at room temperature for the indicated time without any further alterations.

Carius tubes.

The use of glass Carius tubes for reactions of gases is a well-established approach and was used occasionally in this work. Figure 9.1 shows how to vacuum transfer gaseous reagents into vessels such as a Carius tube. Firstly, a cylinder of gas (**A**) connected to a

standard vacuum line equipped with a vacuum gauge (**B**) is used. A Young's tube (**C**) is attached to the vacuum line, evacuated and then cooled to below the boiling point of the gas with cooling generally achieved using liquid nitrogen. The tap to the pump is closed, creating a sealed system under static vacuum. The cylinder can then be opened, allowing gas to travel through the Schlenk line and condense into the cold Young's tube, monitored by the vacuum gauge. The mass of gas used can then also be determined by weighing the Carius tube before and after transfer, although there will be some error from condensation on the outside of the tube. Separately, the Carius tube (**D**) is charged with the other non-gaseous reactants, attached to the Schlenk line, evacuated and cooled to below the boiling point of the gas. On warming to room temperature, the gas inside the Young's tube evaporates through the vacuum line to condense inside the cooled Carius tube.



Figure 9.1. Example of a Carius tube being charged with gas

The Carius tube is then sealed by melting the glass at one end and then placed inside a steel container with loose-fitting lid to contain any issues due to over pressurisation (Figure 9.2). This ensemble is then heated inside a furnace, which at Durham has been custom-built to contain high pressure reactions and is located in a specially designed fire-proof room. The furnace can reach a maximum temperature of 500 °C, which is monitored

by a thermocouple and can be controlled from outside the furnace room. Once the reaction is complete, the Carius tube can be withdrawn, cracked open and the contents extracted.



Figure 9.2. Carius tube (top-left) with steel container (bottom-left) and furnace (right)

Hastelloy autoclave.

Carius tubes are a relatively simple way to run reactions of gaseous substrates at above ambient pressures and useful for initial screening and smaller scale reactions but have a safe maximum rating of around 15 to 20 bar, depending on the thickness of glass used in their manufacture, and mixing the reagents during the reaction is difficult. For reactions at higher pressures, allowing for even larger scale reactions and higher temperatures, a Hastelloy autoclave can be employed. This apparatus consists of a sealable, heavy-walled metal cylinder which can be charged with gas via vacuum transfer in much the same way as a Carius tube. Figure 9.3 shows an example of a Hastelloy autoclave. Sealing is simpler than for a Carius tube, simply being closed with a large screw thread with a disposable aluminium washer then secured using the bolts on top. The tap allows for connection via rubber tubing to a Schlenk line once the autoclave has been charged with non-volatile reagents. There is a bursting disc system on the right side for release of excessive build-up of pressure (up to 200 bar). The descending metal rod is hollow and so a thermocouple can be inserted to monitor the reaction temperature.

Durham has a specially constructed high-pressure laboratory (HPL) for autoclave reactions, designed so that any sudden release of pressure can be safely contained (Figure 9.4). The building is constructed from steel-reinforced concrete up to 18 inches thick with a curved, blow-off roof designed to absorb pressure. The HPL contains several individual cells, each sealed off from the others, and the interiors are designed to prevent debris from

escaping with no direct path to the outside. The HPL is also equipped with a variety of gas lines, including H₂ and CO, which can be piped directly into equipment.

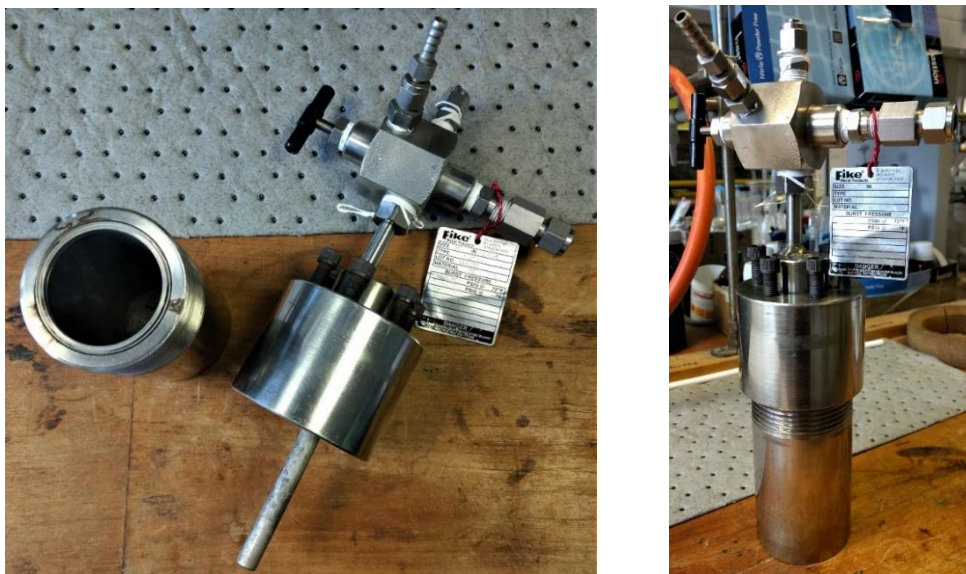


Figure 9.3. Interior of autoclave (left) and when fully assembled and sealed (right)



Figure 9.4. Durham HPL exterior

The autoclave can be placed inside a rocking furnace to facilitate mixing of reagents with temperature monitoring by a thermocouple. Once the reaction is complete, the autoclave is cooled and opened, and the contents extracted. Figure 9.5 shows the interior of an HPL cell with the rocking furnace (A) and various gas lines (B). The control room allows for remote monitoring of the cell via the wall-mounted monitor (C), which is connected to a camera controlled by the PC (D). The temperature of the furnace is controlled by the blue control box (E) and the piped gas lines by the handles to the right (F). Entry to the cell

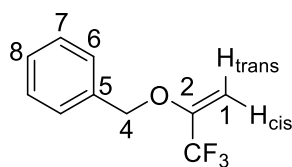
requires the key attached to the power lever (G) below the monitor, which prevents access without first shutting down all equipment in the cell.



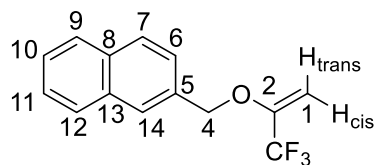
Figure 9.5. Inside an example cell (left) and the control room (right) of Durham HPL

9.3 Experimental data for Chapter 3

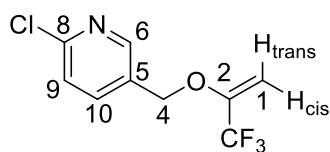
General procedure: α -trifluoromethyl enol ether synthesis. NaH (60% suspension in mineral oil, 1.5 eq.) under an argon atmosphere was washed with hexane then anhydrous DMF was added. The alcohol (as a solution in anhydrous DMF if alcohol solid at room temperature, 1 eq.) was added dropwise at 0 °C then stirred at room temperature for 30 minutes. The resulting alkoxide solution was then stirred under an atmosphere of **1** (excess), introduced via a gas bladder. The reaction mixture was stirred at room temperature for 3 hours, unless otherwise indicated, then carefully quenched with saturated aqueous ammonium chloride and filtered through a Celite plug, which was then washed with ethyl acetate. The aqueous phase was extracted with ethyl acetate then the combined organic extracts were washed twice with 0.5 M HCl then with brine, dried over MgSO₄ and concentrated *in vacuo* to give the product without further purification unless otherwise specified.

2-Benzyloxy-3,3,3-trifluoroprop-1-ene (80a).

Benzyl alcohol (12.5 g, 0.116 mol), **1** (25.5 g, 0.224 mol) and NaH (7.95 g, 0.331 mol) in DMF (250 mL) gave 2-benzyloxy-3,3,3-trifluoroprop-1-ene, **80a** (20.8 g, 89%), as a colourless oil. δ_{H} (400 MHz; CDCl_3) 4.53 (1H, dt, $^2J_{\text{HH}}$ 3.9, $^4J_{\text{HF}}$ 1.9, H_{trans}), 4.90 (1H, d, $^2J_{\text{HH}}$ 3.9, H_{cis}), 4.91 (2H, s, CH_2), 7.37-7.45 (5H, m, Ph). δ_{F} (376 MHz; CDCl_3) -72.42 ($^4J_{\text{HF}}$ 1.9). δ_{C} (101 MHz; CDCl_3) 70.6 (C4), 88.3 (q, $^3J_{\text{CF}}$ 3.6, C1), 119.9 (q, $^1J_{\text{CF}}$ 273.3, CF_3), 127.4 (s, Ar), 128.4 (s, Ar), 128.7 (s, Ar), 135.3 (s, Ar), 150.2 (d, $^2J_{\text{CF}}$ 34.6, C2). IR ν_{max} / cm^{-1} 2922, 2853, 1656, 1457, 1377, 1347, 1195, 1153, 1028. GC-MS (EI+) m/z 202 ($[\text{M}+\text{H}]^+$, 6%), 92 ($[\text{Bn}+\text{H}]^+$, 95), 91 ($[\text{Bn}]^+$, 100), 65 ($[\text{C}_5\text{H}_5]^+$, 51), 39 ($[\text{C}_3\text{H}_3]^+$, 15). HRMS (ASAP, AI+) m/z calc. for $[\text{M}]^+$ $\text{C}_{10}\text{H}_9\text{OF}_3$ 201.0527; found 201.0530. Spectroscopic data consistent with literature values.¹

2-(2'-Naphthylmethyloxy)-3,3,3-trifluoroprop-1-ene (149).

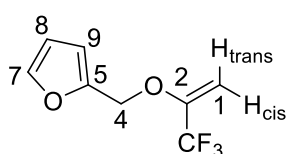
2-Naphthalenemethanol (3.08 g, 19.4 mmol), **1** (5.23 g, 45.9 mmol) and NaH (1.40 g, 58.5 mmol) in DMF (60 mL) gave 2-(2'-naphthylmethyloxy)-3,3,3-trifluoroprop-1-ene, **149** (4.01 g, 82%), as a white solid, m.p. 44-45 °C. δ_{H} (400 MHz; CDCl_3) 4.56 (1H, dq, $^2J_{\text{HH}}$ 3.9, $^4J_{\text{HF}}$ 1.9, H_{trans}), 4.90 (1H, d, $^2J_{\text{HH}}$ 3.9, H_{cis}), 5.06 (2H, s, CH_2), 7.46-7.51 (3H, m, Ar-H), 7.81-7.87 (4H, m, Ar-H). δ_{F} (376 MHz; CDCl_3) -72.37 (d, $^4J_{\text{HF}}$ 1.9). δ_{C} (101 MHz; CDCl_3) 70.8 (s, C4), 88.6 (q, $^3J_{\text{CF}}$ 3.6, C1), 119.9 (q, $^1J_{\text{CF}}$ 273.3, CF_3), 125.0 (s, C6), 126.4 (s, C7/14), 126.5 (s, C7/14), 126.5 (s, C9-12), 127.9 (s, C9-12), 128.1 (s, C9-12), 128.6 (s, C9-12), 132.7 (s, C5), 133.3 (s, C8/13), 133.3 (s, C8/13), 150.2 (q, $^2J_{\text{CF}}$ 34.6, C1). IR ν_{max} / cm^{-1} 1650, 1341, 1123, 1022, 1000. ASAP-MS (AI+) m/z 252 ($[\text{M}]^+$, 30%), 251 ($[\text{M}-\text{H}]^+$, 100), 141 ($[\text{NaphCH}_2]^+$, 81). HRMS (AI+) m/z calc. for $[\text{M}-\text{H}]^+$ $\text{C}_{14}\text{H}_{10}\text{OF}_3$ 251.0684; found 251.0696.

2-(6-Chloro-3-pyridinylmethyloxy)-3,3,3-trifluoroprop-1-ene (150).

6-Chloro-3-pyridinylmethanol (0.71 g, 4.9 mmol), **1** (2.38 g, 20.9 mmol) and NaH (0.54 g, 14 mmol) in DMF (20 mL) gave 2-(6-chloro-3-pyridinylmethyloxy)-3,3,3-trifluoroprop-1-ene, **150** (1.06 g, 90%), as a yellow oil. δ_{H} (400 MHz; CDCl_3) 4.54 (1H, dq, $^2J_{\text{HH}}$ 4.1, $^4J_{\text{HF}}$ 1.9, H_{trans}), 4.87 (2H, s, CH_2), 4.94 (1H, d, $^2J_{\text{HH}}$ 4.1, H_{cis}), 7.36 (1H, dd, $^3J_{\text{HH}}$ 8.2, $^4J_{\text{HH}}$ 0.7, Ar-H), 7.69 (1H, ddt, $^3J_{\text{HH}}$ 8.2, $^4J_{\text{HH}}$ 2.5, $^4J_{\text{HH}}$ 0.7,

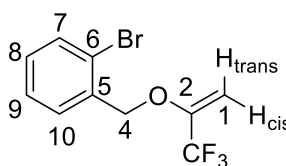
Ar-H), 8.38 (1H, dd, $^4J_{\text{HH}}$ 2.5, $^4J_{\text{HH}}$ 0.7, Ar-H). δ_{F} (376 MHz; CDCl_3) -72.46 (d, $^4J_{\text{HF}}$ 1.9). δ_{C} (101 MHz; CDCl_3). 67.1 (s, C4), 88.9 (q, $^3J_{\text{CF}}$ 3.6, C1), 119.6 (q, $^1J_{\text{CF}}$ 273.2, CF_3), 124.5 (s, Ar), 129.8 (s, Ar), 138.0 (s, Ar), 148.6 (s, C6), 149.8 (q, $^2J_{\text{CF}}$ 35.1, C2), 151.7 (s, C8). IR $\nu_{\text{max}}/\text{cm}^{-1}$ 1660, 1593, 1570, 1463, 1398, 1342, 1189, 1133, 1102, 1022. LC-MS (ESI+) m/z 239 ($[\text{M}^{(37}\text{Cl})+\text{H}]^+$, 22%), 238 ($[\text{M}^{(35}\text{Cl})+\text{H}]^+$, 100), 152 (29), 124 ($[\text{C}_4\text{H}_4\text{OF}_3+\text{H}]^+$, 48), 101 ($[\text{C}_5\text{H}_3\text{N}^{(35}\text{Cl})+\text{H}]^+$, 11). HRMS (ESI+) m/z calc. for $[\text{M}+\text{H}]^+$ $\text{C}_9\text{H}_8\text{NOF}_3^{(35}\text{Cl})$ 238.0247; found 238.0271.

2-(Furyl-2-methoxy)-3,3,3-trifluoroprop-1-ene (151).



Furfuryl alcohol (0.55 g, 5.6 mmol), **1** (3.02 g, 26.5 mmol) and NaH (0.52 g, 13 mmol) in DMF (20 mL) gave 2-(furyl-2-methoxy)-3,3,3-trifluoroprop-1-ene, **151** (0.32 g, 30%), as a yellow oil. δ_{H} (400 MHz; CDCl_3) 4.62 (1H, dq, $^2J_{\text{HH}}$ 4.0, $^4J_{\text{HF}}$ 1.9, H_{trans}), 4.85 (2H, s, CH_2), 4.92 (1H, d, $^2J_{\text{HH}}$ 4.0, H_{cis}), 6.41 (1H, dd, $^3J_{\text{HH}}$ 3.3, $^3J_{\text{HH}}$ 1.8, Ar-H), 6.47 (1H, dd, $^3J_{\text{HH}}$ 3.3, $^4J_{\text{HH}}$ 0.7, Ar-H), 7.47 (1H, dd, $^3J_{\text{HH}}$ 1.8, $^4J_{\text{HH}}$ 0.7, Ar-H). δ_{F} (376 MHz; CDCl_3) -72.38 (d, $^4J_{\text{HF}}$ 1.9). δ_{C} (101 MHz; CDCl_3) 62.9 (s, C4), 88.4 (q, $^3J_{\text{CF}}$ 3.7, C1), 110.7 (s, Ar), 110.9 (s, Ar), 119.8 (q, $^1J_{\text{CF}}$ 273.3, CF_3), 143.5 (s, Ar), 148.7 (s, Ar), 150.0 (q, $^2J_{\text{CF}}$ 34.8, C2). IR $\nu_{\text{max}}/\text{cm}^{-1}$ 1656, 1505, 1385, 1341, 1188, 1132, 1015. LC-MS (ESI-) m/z 365 ($[\text{2M-F}+\text{H}]^-$, 100%), 301 ($[\text{2M-F-C}_4\text{H}_5\text{O}]^-$, 51), 113 ($[\text{C}_3\text{H}_4\text{F}_3\text{O}]^-$, 12). HRMS (ESI-) m/z calc. for $[\text{M-H}]^-$ $\text{C}_8\text{H}_6\text{O}_2\text{F}_3$ 191.0320; found 191.0327.

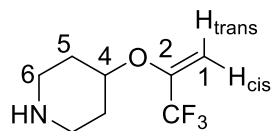
2-(2-Bromobenzyloxy)-3,3,3-trifluoroprop-1-ene (152).



2-Bromobenzyl alcohol (1.22 g, 6.52 mmol), **1** (1.50 g, 13.2 mmol) and NaH (0.40 g, 10 mmol) in DMF (20 mL) after 16 hours gave 2-(2-bromobenzyloxy)-3,3,3-trifluoroprop-1-ene, **152** (1.48 g, 43%), as a yellow oil. δ_{H} (400 MHz; CDCl_3) 4.55 (1H, dq, $^2J_{\text{HH}}$ 4.0, $^4J_{\text{HF}}$ 1.9, H_{trans}), 4.92 (1H, d, $^2J_{\text{HH}}$ 4.0, H_{cis}), 4.96 (2H, s, CH_2), 7.21 (1H, td, $^3J_{\text{HH}}$ 7.7, $^4J_{\text{HH}}$ 1.7, Ar-H), 7.36 (1H, td, $^3J_{\text{HH}}$ 7.7, $^4J_{\text{HH}}$ 1.2, Ar-H), 7.48 (1H, dd, $^3J_{\text{HH}}$ 7.7, $^4J_{\text{HH}}$ 1.7, Ar-H), 7.58 (1H, dd, $^3J_{\text{HH}}$ 7.7, $^4J_{\text{HH}}$ 1.2, Ar-H). δ_{F} (376 MHz; CDCl_3) -72.31 (d, $^4J_{\text{HF}}$ 1.9). δ_{C} (101 MHz; CDCl_3) 69.8 (s, C4), 88.7 (q, $^3J_{\text{CF}}$ 3.6, C1), 119.9 (q, $^1J_{\text{CF}}$ 273.3, CF_3), 122.3 (s, Ar), 127.8 (s, Ar), 128.7 (s, Ar), 129.7 (s, Ar), 132.8 (s, Ar), 134.7 (s, Ar), 149.9 (q, $^2J_{\text{CF}}$ 34.8, C2). IR $\nu_{\text{max}}/\text{cm}^{-1}$ 1659, 1396, 1344, 1188, 1135, 1027.

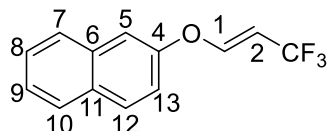
LC-MS (ESI⁻) m/z 281 ($[M(^{81}\text{Br})-H]^-$, 100%), 279 ($[M(^{79}\text{Br})-H]^-$, 50), 113 ($\text{C}_3\text{H}_2\text{FO}$, 53). HRMS (ESI⁻) m/z calc. for $[M-H]^- \text{C}_{10}\text{H}_7\text{OF}_3(^{79}\text{Br})$ 278.9632; found 278.9629.

2-(4-Piperidinyloxy)-3,3,3-trifluoroprop-1-ene (153).



4-Hydroxypiperidine (0.58 g, 5.7 mmol), **1** (2.64 g, 23.2 mmol) and NaH (0.59 g, 15 mmol) in DMF (20 mL) after 3 hours to give 2-(4-piperidinyloxy)-3,3,3-trifluoroprop-1-ene, **153** (0.33 g, 29%, 87:13 α : β), as a brown oil. NMR assignments are given for α -regioisomer only.² δ_{H} (400 MHz; CDCl_3) 1.68 (2H, dtd, $^3J_{\text{HH}}$ 12.2, $^3J_{\text{HH}}$ 7.8, $^3J_{\text{HH}}$ 3.7, C(5)H axial), 1.96 (2H, m, C(5)H equatorial), 1.96 (1H, br s, N-H), 2.73 (2H, ddd, $^3J_{\text{HH}}$ 12.2, $^3J_{\text{HH}}$ 8.4, $^2J_{\text{HH}}$ 3.6, C(6)H axial), 3.09 (2H, ddd, $^3J_{\text{HH}}$ 11.2, $^3J_{\text{HH}}$ 6.7, $^2J_{\text{HH}}$ 3.6, C(6)H equatorial), 4.20 (1H, tt, $^3J_{\text{HH}}$ 7.8, $^3J_{\text{HH}}$ 3.7, C(4)H), 4.41 (1H, dq, $^2J_{\text{HH}}$ 4.2, $^4J_{\text{HF}}$ 2.0, H_{cis}), 4.86 (1H, d, $^2J_{\text{HH}}$ 4.2, H_{trans}). δ_{F} (376 MHz; CDCl_3) -72.75 (d, $^4J_{\text{HF}}$ 1.9). δ_{C} (101 MHz; CDCl_3) 31.2 (s, C5), 43.6 (s, C6), 74.16 (s, C4), 88.0 (q, $^3J_{\text{CF}}$ 3.7, C1), 120.0 (q, $^1J_{\text{CF}}$ 273.6, CF_3), 148.5 (q, $^2J_{\text{CF}}$ 33.7, C2). IR $\nu_{\text{max}}/\text{cm}^{-1}$ 2951 (br), 1652, 1133, 1156, 1455, 1439, 1387, 1351, 1333, 1320, 1260, 1035. LC-MS (ESI⁺) m/z 197 ($[M+2H]^+$, 40%), 196 ($[M+H]^+$, 100), 195 ($[M]^+$, 60). HRMS (ESI⁺) m/z calc. for $[M+H]^+ \text{C}_9\text{H}_{15}\text{NOF}_3$ 196.0949; found 196.0965.

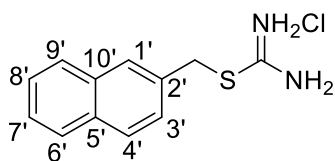
(E)-1-(2-Naphthyloxy)-3,3,3-trifluoroprop-1-ene (159).



Following the general procedure for alcohols, 2-naphthol (1.52 g, 13.3 mmol), **1** (2.28 g, 20.0 mmol) and NaH (0.51 g, 13 mmol) in DMF (25 mL) after 16 hours at 60 °C gave the crude product as a brown oil. Hexane (10 mL) was added, the resulting mixture filtered through a silica plug and then the filtrate was concentrated *in vacuo* to give (E)-1-(2-naphthyloxy)-3,3,3-trifluoroprop-1-ene, **159** (0.15 g, 5%), as a white solid, m.p. 35-36 °C. δ_{H} (400 MHz; CDCl_3) 5.09 (1H, qd, $^3J_{\text{HF}}$ 8.0, $^3J_{\text{HH}}$ 6.9, C(1)H), 6.89 (1H, d, $^3J_{\text{HH}}$ 6.9, C(2)H), 7.26-7.29 (1H, m, Ar-H), 7.37-7.42 (1H, m, Ar-H), 7.45-7.52 (2H, m, Ar-H), 7.77-7.81 (1H, m, Ar-H), 7.81-7.85 (2H, m, Ar-H). δ_{F} (376 MHz; CDCl_3) -57.60 (d, $^3J_{\text{HF}}$ 8.0). δ_{C} (101 MHz; CDCl_3) 99.8 (q, $^3J_{\text{CF}}$ 35.3, C2), 112.5 (s, Ar), 118.4 (s, Ar), 122.7 (d, $^1J_{\text{CF}}$ 213.0, CF_3), 125.5 (s, Ar), 127.1 (s, Ar), 127.4 (s, Ar), 127.9 (s, Ar), 130.3 (s, Ar), 149.2 (q, $^3J_{\text{CF}}$ 5.4, C1), 154.5 (s, C4). IR $\nu_{\text{max}}/\text{cm}^{-1}$ 1675, 1627, 1596, 1508, 1485, 1465, 1444, 1417, 1386, 1357, 1266, 1246, 1212, 1144, 1103 (vs), 1048, 965, 918, 849, 824, 788, 753, 685, 645, 579, 479. ASAP-MS (AI⁺) m/z 239 ($[M+H]^+$, 100%), 219 ($[M-F]^+$, 7), 199 ($[M-2F]^+$, 18). HRMS (AI⁺) m/z calc. for $[M]^+$

$C_{13}H_9OF_3$ 238.0605; found 238.0616. Spectroscopic data consistent with literature values.³

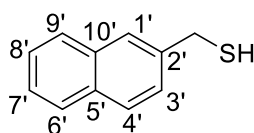
***S*-(2-Naphthyl)isothiuronium chloride.**



2-Bromomethylnaphthalene (1.09 g, 4.91 mmol) and thiourea (0.419 g, 5.50 mmol) were dissolved in 95% ethanol (199 mL) heated to 85 °C for 6 hours. The mixture was diluted with water (50 mL) then acidified with concentrated

hydrochloric acid (100 mL). Ethanol was allowed to evaporate and the resulting white precipitate filtered and washed with cold water then diethyl ether to give *S*-(2-naphthyl)isothiuronium chloride (0.79 g, 60%), as a white solid, m.p. 186-187 °C (lit. 186-188 °C).⁴ δ_H (400 MHz; DMSO-*d*₆) 4.71 (2H, s, CH₂), 7.51-7.58 (3H, m, Ar-H), 7.90-7.97 (4H, m, Ar-H), 9.29-9.37 (4 H, m, NH₂). δ_C (101 MHz; CDCl₃) 34.4 (s, CH₂), 126.4 (s, Ar), 126.6 (s, Ar), 126.8 (s, Ar), 127.6 (s, Ar), 127.7 (s, Ar), 128.5 (s, Ar), 132.3 (s, Ar), 132.7 (s, Ar), 169.0 (s, SC(NH₂)₂). IR ν_{max} /cm⁻¹ 3050 (br), 1649, 1599, 1509, 1434, 1361, 1236, 1149, 1124, 1081, 1019. LC-MS (ESI+) *m/z* 218 [M-Cl+H]⁺, 100%), 217 ([M-Cl]⁺, 54), 141 (5). HRMS (ESI+) *m/z* calc. for [M-Cl]⁺ C₁₂H₁₃N₂S 217.0799; found 217.0798. Spectroscopic data consistent with literature.⁴

2-Mercaptomethylnaphthalene.

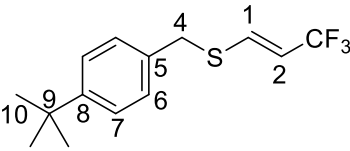


S-(2-Naphthyl)isothiuronium chloride (0.779 g, 3.20 mmol) and potassium hydroxide (0.686 g, 12.2 mmol) were added to water (100 mL) then heated to reflux to 100 °C for 2 hours. The reaction

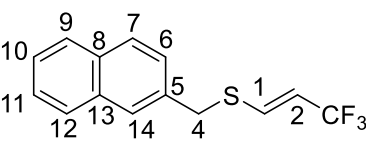
mixture was allowed to cool to room temperature and neutralised with 6M HCl. The resulting solid was filtered, washed with water and dried in a vacuum desiccator over P₂O₅ to give 2-mercaptomethylnaphthalene, (0.378 g, 73%), as a yellow solid, m.p. 45-48 °C (lit. 48-49 °C).⁵ δ_H (400 MHz; CDCl₃) 3.72 (2H, s, CH₂S), 7.31-7.35 (1H, m, SH), 7.45-7.53 (3H, m, Ar-H), 7.76-7.83 (4H, m, Ar-H). δ_C (101 MHz; CDCl₃) 43.7 (CH₂S), 126.1 (s, Ar), 126.4 (s, Ar), 127.4 (s, Ar), 127.9 (s, Ar), 127.9 (s, Ar), 128.4 (s, Ar), 128.4 (s, Ar), 132.7 (s, Ar), 133.3 (s, Ar), 134.6 (s, Ar). IR ν_{max} /cm⁻¹ 3297 (br), 1599, 1548, 1507, 1421, 1359, 1275, 1222, 1123. ASAP-MS (AI+) 173 ([M]⁺, 5%) 141 (27), 115 (2). HRMS (AI+) *m/z* calc. for [M-H]⁺ C₁₁H₉S 173.0425; found 173.0419. Spectroscopic data consistent with literature.⁵

General procedure: β -trifluoromethyl vinyl sulfide synthesis. The thiol (1 eq.) was dissolved in anhydrous DMSO under an argon atmosphere then NaHMDS (2M in THF, 2 eq.) was added dropwise and the resulting mixture stirred at room temperature for 30 minutes. The reaction mixture was stirred under an atmosphere of **1** (excess) provided via gas bladder for 3 hours then carefully quenched, filtered and subjected to aqueous workup as for the enol ethers described above to give the product without further purification unless otherwise specified.

(E)-1-(4-(*tert*-Butyl)benzyl)thio-3,3,3-trifluoroprop-1-ene (183**).**

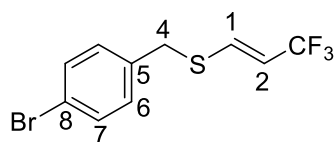
 4-(*tert*-Butyl)benzyl mercaptan (0.498 g, 2.75 mmol), **1** (1.65 g, 14.5 mmol) and NaHMDS (2.5 mL, 5.0 mmol) in anhydrous DMSO (15 mL) gave (E)-1-(4-(*tert*-butyl)benzyl)thio-3,3,3-trifluoroprop-1-ene, **183** (0.688 g, 91%) as a yellow oil. δ_{H} (400 MHz; CDCl₃) 1.36 (9H, s, ¹Bu), 3.97 (2H, s, CH₂), 5.57 (1H, dq, ²J_{HH} 11.0, ³J_{HF} 8.5, C(2)H), 6.69 (1H, dq, ²J_{HH} 11.0, ⁴J_{HF} 1.0, C(1)H), 7.27-7.32 (2H, m, Ar-H), 7.38-7.43 (2H, m, Ar-H). δ_{F} (376 MHz; CDCl₃) -59.88 (dd, ³J_{HF} 8.5, ⁴J_{HF} 1.0). δ_{C} (101 MHz; CDCl₃) 31.4 (s, ¹Bu), 34.7 (s, ¹Bu), 60.5 (s, ¹Bu), 112.8 (q, ²J_{CF} 35.0, C2), 123.6 (q, ¹J_{CF} 270.9, CF₃), 125.9 (s, Ar), 128.9 (s, Ar), 133.5 (s, Ar), 138.7 (q, ³J_{CF} 5.1, C1), 150.9 (s, Ar). IR ν_{max} /cm⁻¹ 2963, 1737, 1615, 1516, 1464, 1364, 1268, 1203, 1111, 1047, 1018. GC-MS (EI+) *m/z* 274 ([M]⁺, 17%), 147 ([¹BuPhCH₂]⁺, 100), 117 ([¹PrPh]⁺, 40), 105 ([PhMe₂]⁺, 25), 91 ([Bn]⁺, 19). HRMS (ESI+) *m/z* calc. for [M+MeCN]⁺ C₁₆H₂₀NF₃S 315.1269; found 315.1037.

(E)-1-(Naphthyl-2-methylthio)-3,3,3-trifluoroprop-1-ene (184**).**

 2-Mercaptomethylmethanol (0.229 g, 1.32 mmol), NaHMDS (1.5 mL, 3 mmol) and **1** (1.85g, 16.2 mmol) gave the crude product as a brown oil, which was then diluted with hexane and filtered through a silica plug then concentrated *in vacuo* to give (E)-1-(naphthyl-2-methylthio)-3,3,3-trifluoroprop-1-ene, **184** (0.299 g, 85%), as a yellow solid, m.p. °C. δ_{H} (400 MHz; CDCl₃) 4.11 (2H, s, C(4)H), 5.52 (1H, dq, ²J_{HH} 11.1, ³J_{HF} 8.6, C(1)H), 6.64 (1H, dq, ²J_{HH} 11.1, ⁴J_{HF} 1.0, C(2)H), 7.49 (3H, C(6/7/14)H), 7.77-7.82 (4H, m, C(9-12)H). δ_{F} (376 MHz; CDCl₃) -59.94 (dd, ³J_{HF} 8.6, ⁴J_{HF} 1.0). δ_{C} (101 MHz; CDCl₃) 38.8 (s, C4), 113.2 (q, ²J_{CF} 35.0, C2), 123.5 (q, ¹J_{CF} 270.7, CF₃), 126.4 (s, Ar), 126.6 (s, Ar), 126.8 (s, Ar), 127.8 (s, Ar), 127.9 (s, Ar), 127.9 (s, Ar), 129.1 (s, Ar), 132.9

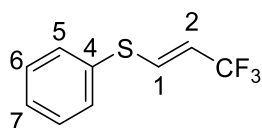
(s, C8/13), 133.3 (s, C8/13), 133.9 (s, C5), 138.1 (q, $^3J_{CF}$ 5.1, C1). GC-MS (EI+) m/z 269 ($[M+H]^+$, 3%), 268 ($[M]^+$, 14), 141 ($[NaphCH_2]^+$, 100). HRMS (ESI-) m/z calc. for $[M-H]^-$ $C_{14}H_{10}F_3S$ 267.0455; found 267.0448.

(E)-1-(4-Bromobenzyl)thio-3,3,3-trifluoroprop-1-ene (185).

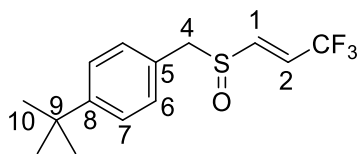


4-Bromobenzyl mercaptan (0.967 g, 4.76 mmol), **1** (2.06 g, 18.1 mmol) and NaHMDS (5.0 mL, 10 mmol) in anhydrous DMSO (15 mL) gave (*E*)-1-(4-(bromobenzyl)thio-3,3,3-trifluoroprop-1-ene, **185** (0.69 g, 48%) as a yellow oil. δ_H (400 MHz; $CDCl_3$) 3.91 (2H, s, C(4)H), 5.56 (1H, dq, $^2J_{HH}$ 11.1, $^3J_{HF}$ 8.5, C(2)H), 6.57 (1H, dq, $^2J_{HH}$ 11.0, $^4J_{HF}$ 1.0, C(1)H), 7.18-7.22 (2H, m, Ar-H), 7.46-7.51 (2H, m, Ar-H). δ_F (376 MHz; $CDCl_3$) -59.92 (dd, $^3J_{HF}$ 8.5, $^4J_{HF}$ 1.0). δ_C (101 MHz; $CDCl_3$) 38.0 (q, $^5J_{CF}$ 1.7, C4), 113.6 (q, $^2J_{CF}$ 35.1, C2), 121.8 (s, C5/8), 123.4 (q, $^1J_{CF}$ 270.8, CF_3), 130.7 (s, C6/7), 132.1 (s, C6/7), 135.6 (s, C5/8), 137.9 (q, $^3J_{CF}$ 5.0, C1). IR ν_{max}/cm^{-1} 1615, 1488, 1403, 1365, 1265, 1205, 1106, 1070. LC-MS (ESI+) m/z 296 (M^+ , 24%), 273 (52), 112 (100). HRMS (ESI+) m/z calc. for $[M+H]^+$ $C_{10}H_9F_3S(^{79}Br)$ 296.9560; found 296.9571.

(E)-1-Phenylthio-3,3,3-trifluoroprop-1-ene (189).



Following the general procedure for alcohols, sodium thiophenolate (0.23 g, 1.74 mmol), sodium hydride (0.19 g, 8.0 mmol), **1** (1.54 g, 13.5 mmol) in DMSO (20 mL) the crude product as a brown oil. Hexane (10 mL) was added, the resulting mixture filtered through a silica plug and then the filtrate was concentrated *in vacuo* to give (*E*)-1-phenylthio-3,3,3-trifluoroprop-1-ene, **189** (0.080 g, 23%), as a yellow oil. δ_H (400 MHz; $CDCl_3$) 5.65 (1H, dq, $^3J_{HH}$ 10.9, $^3J_{HF}$ 8.5, C(2)H), 6.88 (1H, dq, $^3J_{HH}$ 10.9, $^4J_{HF}$ 0.9, C(1)H), 7.35-7.39 (3H, m, Ar-H), 7.43-7.48 (2H, m, Ar-H). δ_F (376 MHz; $CDCl_3$) -59.82 (dd, $^3J_{HF}$ 8.5, $^4J_{HF}$ 0.9). δ_C (101 MHz; $CDCl_3$) 113.2 (q, $^2J_{CF}$ 35.3, C2), 123.4 (q, $^1J_{CF}$ 270.8, CF_3), 128.5 (s, C7), 129.6 (s, C6), 131.4 (s, C5), 134.3 (s, C4), 140.0 (q, $^3J_{CF}$ 5.0, C1). IR ν_{max}/cm^{-1} 2924, 2855, 1613, 1480, 1459, 1442, 1360, 1263, 1203, 1119 (vs), 1025, 860 805, 739, 709, 689, 577, 563, 517, 472, 415. GC-MS (EI+) m/z 204 ($[M]^+$, 90%), 183 ($[M-F]^+$, 12), 135 ($[M-CF_3]^+$, 100), 109 ($[SPh]^+$, 27), 77 ($[C_6H_5]^+$, 25). HRMS (ESI+) m/z calc. for $[M]^+$ $C_9H_7F_3S$ 204.0221; found 204.0576. Spectroscopic data consistent with literature reports.⁶

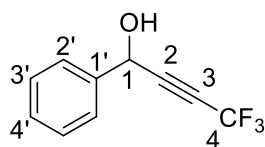
(E)-1-(4-(tert-Butyl)benzyl)sulfinyl-3,3,3-trifluoroprop-1-ene (190).

4a (0.30 g, 1.1 mmol) and mCPBA (1.4 g, 8.2 mmol) were dissolved to DCM (10 mL) and stirred at room temperature for 24 hours. Saturated aqueous sodium metabisulfite (10 mL) was then added and the resulting mixture stirred at room temperature for 30 minutes then neutralised with saturated aqueous sodium bicarbonate. The organic layer was separated and dried over MgSO_4 then concentrated *in vacuo* to give (E)-1-(4-(tert-butyl)benzyl)sulfinyl-3,3,3-trifluoroprop-1-ene, **190** (0.27 g, 84%), as an orange oil. δ_{H} (400 MHz; CDCl_3) 1.32 (9H, s, C(10)H), 4.36 (2H, s, C(4)H), 6.29 (1H, dq, $^2J_{\text{HH}}$ 12.4, $^3J_{\text{HF}}$ 8.5, C(2)H), 6.57 (1H, d, $^2J_{\text{HH}}$ 12.4, C(1)H), 7.28-7.33 (2H, m, C(7)H), 7.40-7.45 (2H, m, C(6)H). δ_{F} (376 MHz; CDCl_3) -57.31 (d, $^3J_{\text{HF}}$ 8.5). δ_{C} (101 MHz; CDCl_3) 31.3 (s, C10), 34.8 (s, C9), 61.7 (s, C4), 120.1 (q, $^1J_{\text{CF}}$ 273.3, CF_3), 123.3 (s, C8), 126.3 (s, C6/7), 130.4 (q, $^2J_{\text{CF}}$ 39.2, C2), 130.8 (s, C6/7), 138.6 (q, $^3J_{\text{CF}}$ 5.2, C1), 152.8 (s, C5). IR (neat) $\nu_{\text{max}}/\text{cm}^{-1}$ 2965, 1735, 1516, 1456, 1415, 1366, 1331, 1269, 1246, 1192, 1124, 1046, 1021, 887, 840, 820, 776, 743, 664, 647, 588, 556, 508, 472, 441. GC-MS (EI+) m/z 291 ($[\text{M}+\text{H}]^+$, 2%), 147 ($[\text{tBuPhCH}_2]^+$, 100), 132 (48), 117 ($[\text{tPrPh}^+]$, 36), 105 ($[\text{PhMe}_2]^+$, 20), 91 ($[\text{Bn}]^+$, 14). HRMS (ESI+) m/z calc. for $[\text{M}+\text{MeCN}+\text{H}]^+$ $\text{C}_{16}\text{H}_{21}\text{NOF}_3\text{S}$ 332.1296; found 332.1327.

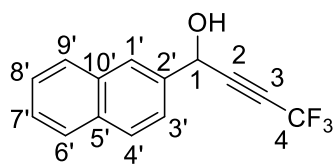
9.4 Experimental data for Chapter 4

General procedure: lithiation and reaction with aldehydes.

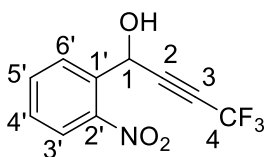
Diisopropylamine (2 eq.) was dissolved in a stock solution of **1** (1 eq.) in anhydrous MTBE under argon. *n*-Butyllithium (2.5 M in hexanes, 2 eq.) was added dropwise at -78°C . The resulting solution of lithium diisopropylamide was stirred for 30 minutes at -10°C . The aldehyde (as a solution in anhydrous MTBE if solid) was then added dropwise then the reaction was stirred at -10°C for the indicated time period. The reaction mixture was allowed to warm to room temperature then quenched by adding saturated aqueous sodium bisulfite and stirred vigorously for 30 minutes. The aqueous layer was separated and extracted with MTBE then the combined organic extracts washed twice with 1M HCl then with brine, dried over MgSO_4 and concentrated *in vacuo* to give the product without further purification unless otherwise specified.

1-Phenyl-4,4,4-trifluorobut-2-yn-1-ol (211).

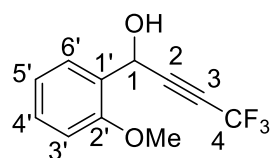
Following the general procedure, diisopropylamine (2.7 mL, 18 mmol), *n*-butyllithium (7.2 mL, 18 mmol), **1** (1.00 g, 8.77 mmol) and benzaldehyde (0.52 g, 4.9 mmol) in MTBE after 1 hour gave 1-phenyl-4,4,4-trifluorobut-2-yn-1-ol, **211** (0.919 g, 94%), as a colourless oil. δ_{H} (400 MHz; CDCl_3) 2.89 (br s, OH), 5.54 (1H, q, $^5J_{\text{HF}}$ 3.0, C(1)H), 7.41-7.48 (5H, m, Ar-H). δ_{F} (376 MHz; CDCl_3) -50.53 (d, $^5J_{\text{HF}}$ 3.0). δ_{C} (101 MHz; CDCl_3) 65.4 (s, C1), 73.3 (q, $^2J_{\text{CF}}$ 52.9, C3), 86.6 (q, $^3J_{\text{CF}}$ 6.5, C2), 114.1 (q, $^1J_{\text{CF}}$ 257.7, C4), 126.6 (s, C4'), 129.0 (s, C2'/3'), 129.2 (s, C2'/3'), 138.0 (C1'). IR (neat) $\nu_{\text{max}}/\text{cm}^{-1}$ 3371 (br, O-H), 2278 (C \equiv C), 1760, 1659, 1496, 1456, 1271, 1133, 1040, 1003. LC-MS (ESI $^-$) m/z 199 ($[\text{M}-\text{H}]^-$, 16%), 113 ($[\text{M}-\text{PhCH}]^-$, 6). HRMS (ESI $^-$) m/z calc. for $[\text{M}-\text{H}]^-$ $\text{C}_{10}\text{H}_6\text{OF}_3$ 199.0371; found 199.0363. Spectroscopic data are consistent with the literature.⁷

1-(2'-Naphthyl)-4,4,4-trifluorobut-2-yn-1-ol (224a).

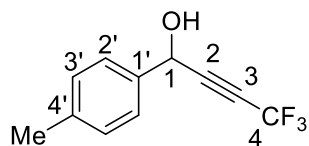
Following the general procedure, diisopropylamine (3.5 mL, 25.2 mmol), **1** (1.43 g, 12.6 mmol) in MTBE (100 mL), *n*BuLi (10.1 mL, 2.5 M, 25.2 mmol) and 2-naphthaldehyde (1.78 mL, 11.3 mmol) gave 1-(2'-naphthyl)-4,4,4-trifluoromethylbut-2-yn-1-ol, **224a** (2.78 g, 94%), as a yellow solid, m.p. 78-80 °C. δ_{H} (400 MHz; CDCl_3) 2.46 (br s, O-H), 5.73 (1H, q, $^5J_{\text{HF}}$ 3.0, C(1)H), 7.53-7.57 (2H, m, C(4'/3')H), 7.48-7.61 (1H, m, C(1')H), 7.86-7.93 (4H, m (C6'-9')H). δ_{F} (376 MHz; CDCl_3) -50.53 (d, $^5J_{\text{HF}}$ 3.0). δ_{C} (101 MHz; CDCl_3) 64.3 (d, $^4J_{\text{CF}}$ 1.3, C1), 73.8 (q, $^2J_{\text{CF}}$ 53.0, C3), 86.5 (q, $^3J_{\text{CF}}$ 6.4, C2), 114.2 (q, $^1J_{\text{CF}}$ 257.9, C4), 124.1 (s, Ar), 125.9 (s, Ar), 126.9 (s, Ar), 127.0 (s, Ar), 127.9 (s, Ar), 128.4 (s, Ar), 129.3 (s, Ar), 133.2 (s, C5'/10'), 133.7 (s, C5'/10'), 135.3 (s, C2'). IR (neat) $\nu_{\text{max}}/\text{cm}^{-1}$ 3324 (br, O-H), 2278 (C \equiv C), 2160, 2032, 1603, 1508, 1420, 1323, 1289, 1120, 1020. GC-MS (EI $^+$) m/z 250 (M^+ , 98%), 232 ($[\text{M}-\text{F}+\text{H}]^+$, 24), 201 (38), 183 (32), 152 (36), 129 ($[\text{M}-\text{C}_4\text{H}_2\text{OF}_3]^+$, 100). HRMS (ESI $^+$) m/z calc. for $[\text{M}+\text{H}]^+$ $\text{C}_{14}\text{H}_{10}\text{OF}_3$ 251.0684; found 251.0683. Spectroscopic data are consistent with the literature.⁸

1-(2'-Nitrophenyl)-4,4,4-trifluorobut-2-yn-1-ol (225a).

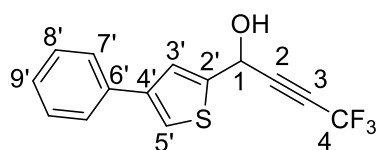
Following the general procedure, diisopropylamine (3.5 mL, 25 mmol), *n*-butyllithium (10 mL, 25 mmol), **1** (1.32 g, 11.6 mmol) and 2-nitrobenzaldehyde (1.49 g, 9.46 mmol) in MTBE (100 mL) after 1 hour gave 1-(2'-nitrophenyl)-4,4,4-trifluorobut-2-yn-1-ol, **225a** (1.92 g, 82%), as a dark red oil. δ_{H} (400 MHz; CDCl_3) 3.89 (br s, OH), 6.16 (1H, q, $^5J_{\text{HF}}$ 2.9), 7.56 (1H, ddd, $^3J_{\text{HH}}$ 8.1, $^3J_{\text{HH}}$ 7.6, $^4J_{\text{HH}}$ 1.4, C(4')H), 7.74 (1H, td, $^3J_{\text{HH}}$ 7.6, $^4J_{\text{HH}}$ 1.3, C(5')H), 7.91 (1H, dd, $^3J_{\text{HH}}$ 7.6, $^4J_{\text{HH}}$ 1.4, C(6')H), 8.09 (1H, dd, $^3J_{\text{HH}}$ 8.1, $^4J_{\text{HH}}$ 1.3, C(3')H). δ_{F} (376 MHz; CDCl_3) -50.78 (q, $^5J_{\text{HF}}$ 2.9). δ_{C} (101 MHz; CDCl_3) 60.7 (q, $^4J_{\text{CF}}$ 1.4, C1), 73.0 (q, $^2J_{\text{CF}}$ 53.2, C3), 84.9 (q, $^3J_{\text{CF}}$ 6.5, C2), 113.9 (q, $^1J_{\text{CF}}$ 258.1, C4), 125.6 (s, C3'-6'), 129.3 (s, C3'-6'), 130.2 (s, C3'-6'), 133.2 (s, C1'), 134.5 (s, C3'-6'), 147.4 (s, C2'). IR (neat) ν_{max} / cm^{-1} 3411 (br s), 2281 (C \equiv C), 1525 (N-O), 1346, 1270, 1130, 1055, 1040. GC-MS (EI+) m/z 227 ([M-OH] $^+$, 2%), 183 ([M-NO $_3$] $^+$, 64), 169 ([M-OH $_3$ F $_3$] $^+$, 84), 163 ([M-NO $_3$ F] $^+$, 100), 151 ([M-C $_3$ F $_3$] $^+$, 49), 133 ([M-C $_3$ F $_3$ OH] $^+$, 85), 121 ([M-PhNO $_2$] $^+$, 49). HRMS (ESI-) m/z calc. for [M-H] $^-$ C $_{10}$ H $_5$ NO $_3$ F $_3$ 244.0222; found 244.0246.

1-(2'-Methoxyphenyl)-4,4,4-trifluorobut-2-yn-1-ol (226a).

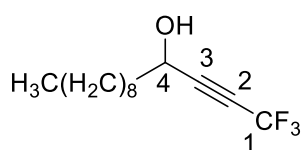
Following the general procedure, diisopropylamine (5.0 mL, 36 mmol), *n*-butyllithium (14 mL, 35 mmol), **1** (1.76 g, 15.4 mmol) and 2-methoxybenzaldehyde (2.00 g, 14.7 mmol) in MTBE (100 mL) after 1 hour gave 1-(2'-methoxyphenyl)-4,4,4-trifluorobut-2-yn-1-ol, **226a** (2.91 g, 86%), as a yellow oil. δ_{H} (400 MHz; CDCl_3) 3.29 (br s, OH), 3.92 (3H, s, OMe), 5.68 (1H, q, $^5J_{\text{HF}}$ 3.1, C(1)H), 6.96-6.73 (2H, m, Ar-H), 7.37-7.42 (2H, m, Ar-H). δ_{F} (376 MHz; CDCl_3) -50.37 (d, $^5J_{\text{HF}}$ 3.1). δ_{C} (101 MHz; CDCl_3) 55.7 (s, OMe), 61.2 (q, $^4J_{\text{CF}}$ 1.4, C1), 72.3 (q, $^2J_{\text{CF}}$ 52.7, C3), 86.9 (q, $^3J_{\text{CF}}$ 6.5, C2), 111.3 (s, C3'-6'), 114.3 (d, $^1J_{\text{CF}}$ 257.4, C4), 121.2 (s, C3'-6'), 126.5 (s, C2'), 128.0 (s, C3'-6'), 130.6 (s, C3'-6'), 156.9 (s, C1'). IR (neat) ν_{max} / cm^{-1} 3382 (O-H), 2277 (C \equiv C), 1603, 1493, 1466, 1441, 1397, 1271, 1246, 1129, 1026. LC-MS (ESI+) m/z 230 ([M] $^+$, 16%), 121 ([M-PhOMe] $^+$, 9). HRMS (ESI+) m/z calc. for C $_{11}$ H $_{10}$ O $_2$ F $_3$ [M+H] $^+$ 231.0633; found 231.0651. Spectroscopic data are consistent with the literature.⁹

1-(4'-Methylphenyl)-4,4,4-trifluorobut-2-yn-1-ol (227a).

Following the general procedure, diisopropylamine (4.1 mL, 29 mmol), *n*-butyllithium (11.8 mL, 29.4 mmol), **1** (1.67 g, 14.6 mmol) and 4-methylbenzaldehyde (1.63 g, 13.7 mmol) in MTBE (100 mL) after 1 hour gave 1-(4'-methylphenyl)-4,4,4-trifluorobut-2-yn-1-ol, **227a** (2.78 g, 95%), as a yellow oil. δ_{H} (400 MHz; CDCl_3) 2.38 (3H, s, Me), 2.59 (br s, O-H), 5.50 (1H, q, $^5J_{\text{CF}}$ 3.0, C(1)H), 7.20-7.26 (2H, m, Ar-H), 7.34-7.41 (2H, m, Ar-H). δ_{F} (376 MHz; CDCl_3) -50.53 (d, $^5J_{\text{CF}}$ 3.0). δ_{C} (101 MHz; CDCl_3) 21.3 (s, Me), 64.0 (q, $^4J_{\text{CF}}$ 1.4, C1), 73.4 (q, $^2J_{\text{CF}}$ 52.8, C3), 86.8 (q, $^3J_{\text{CF}}$ 6.4, C2), 115.5 (q, $^1J_{\text{CF}}$ 257.7, C1), 126.7 (s, C2'/3'), 129.8 (s, C2'/3'), 135.2, (s, C1'/C4'), 139.4 (s, C1'/C4'). IR (neat) ν_{max} / cm^{-1} . LC-MS (ESI+) m/z 215 ($[\text{M}+\text{H}]^+$, 52%), 137 ($[\text{C}_5\text{H}_4\text{F}_3\text{O}]^+$, 100). HRMS (ESI+) m/z calc. for $\text{C}_{13}\text{H}_{13}\text{OF}_3$ $[\text{M}+\text{MeCN}+\text{H}]^+$ 256.0949; found 256.0956. Spectroscopic data are consistent with the literature.¹⁰

1-(4'-Phenyl-2'-thiophenyl)-4,4,4-trifluorobut-2-yn-1-ol (228a).

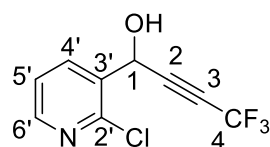
Following the general procedure, diisopropylamine (1.0 mL, 3.57 mmol), *n*-butyllithium (2.9 mL, 7.3 mmol), **1** (0.407 g, 3.57 mmol) and 4-phenylthiophene-2-carboxaldehyde (0.580 g, 3.08 mmol) in MTBE (25 mL) after 1 hour gave 1-(4'-phenyl-2'-thiophenyl)-4,4,4-trifluorobut-2-yn-1-ol, **228a** (0.678 g, 79%), as a yellow solid, m.p. 96-98 °C. δ_{H} (400 MHz; CDCl_3) 2.31 (1H, br s, O-H), 5.80 (1H, q, $^5J_{\text{CF}}$ 2.9), 7.30-7.34 (1H, m, C(9')H), 7.39-7.44 (2H, m, Ar-H), 7.44-7.49 (2H, m, Ar-H), 7.55-7.59 (2H, m, Ar-H). δ_{F} (376 MHz; CDCl_3) -50.76 (d, $^5J_{\text{CF}}$ 2.9). δ_{C} (101 MHz; CDCl_3) 60.0 (s, C1), 73.2 (q, $^2J_{\text{CF}}$ 53.3, C3), 85.5 (q, $^3J_{\text{CF}}$ 6.4, C2), 114.1 (q, $^1J_{\text{CF}}$ 258.2, C4), 121.8 (s, Ar), 125.8 (s, Ar), 126.5 (s, Ar), 127.7 (s, Ar), 129.1 (s, Ar), 135.3 (s, Ar), 141.9 (s, Ar), 142.5 (s, Ar). HRMS (ESI+) m/z calc. for $[\text{M}+\text{OH}_2]^+$ $\text{C}_{14}\text{H}_{11}\text{O}_2\text{F}_3\text{S}$ 300.0432; found 300.0432.

1,1,1-Trifluorotridec-2-yn-4-ol (229a).

Following the general procedure, diisopropylamine (0.50 mL, 3.62 mmol), *n*-butyllithium (1.5 mL, 3.75 mmol), **1** (0.204 g, 1.79 mmol) and decanal (0.30 mL, 1.61 mmol) in MTBE (25 mL) after 1 hours gave 1,1,1-trifluorotridec-2-yn-4-ol, **229a** (0.382 g, 94%), as a yellow oil. δ_{H} (400 MHz; CDCl_3) 0.85-0.90 (3H, m, C(13)H₃), 1.20-1.38 (11H, m, C(7-12)H₂), 1.43-1.47 (2H, m, C(6)H₂), 1.75-1.79 (2H, m, C(5)H₂), 2.09

(br s, O-H), 4.47 (1H, tt, $^3J_{\text{HH}}$ 6.3, $^5J_{\text{CF}}$ 3.0, C(4)H). δ_{F} (376 MHz; CDCl_3) -50.40 (d, $^5J_{\text{HF}}$ 3.0). δ_{C} (101 MHz; CDCl_3) 14.2 (s, C13), 22.8 (s, C5-12), 24.9 (s, C5-12), 29.2 (s, C5-12), 29.4 (s, C5-12), 29.5 (s, C5-12), 29.6 (s, C5-12), 32.0 (s, C5-12), 36.8 (s, C5-12), 61.9 (q, $^4J_{\text{CF}}$ 1.5, C4), 72.1 (q, $^2J_{\text{CF}}$ 52.7, C2), 88.1 (q, $^3J_{\text{CF}}$ 6.4, C3), 114.2 (q, $^1J_{\text{CF}}$ 257.3, C1). IR (neat) ν_{max} / cm^{-1} 3332 (O-H), 2926, 2857, 2263 (C \equiv C), 1273, 1139. HRMS (ESI+) m/z calc. for $\text{C}_{13}\text{H}_{22}\text{OF}_3$ $[\text{M}+\text{H}]^+$ 251.1623; found 251.0029. Spectroscopic data are consistent with the literature.¹⁰

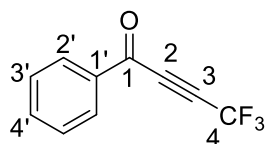
1-(2'-Chloro-3'-pyridinyl)-4,4,4-trifluorobut-2-yn-1-ol (**230**).



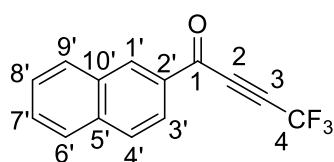
Following the general procedure, diisopropylamine (1.0 mL, 7.1 mmol), *n*-butyllithium (3.5 mL, 8.75 mmol), **1** (0.502 g, 4.40 mmol) and 2-chloro-3-pyridinecarboxaldehyde (0.490 g, 3.46 mmol) in MTBE (25 mL) after 1 hour gave 1-(2'-chloro-3'-pyridinyl)-4,4,4-trifluorobut-2-yn-1-ol, **230** (0.677 g, 83%), as a yellow oil. δ_{H} (400 MHz; CDCl_3) 3.37 (br s, OH), 5.89 (1H, q, $^5J_{\text{HF}}$ 2.9, C(1)H), 7.38 (1H, dd, $^3J_{\text{HH}}$ 7.7, $^3J_{\text{HH}}$ 4.8, C(5')H), 8.06 (1H, dd, $^3J_{\text{HH}}$ 7.7, $^4J_{\text{HH}}$ 1.9, C(4')H), 8.42 (1H, dd, $^3J_{\text{HH}}$ 4.8, $^4J_{\text{HH}}$ 1.9, C(6')H). δ_{F} (376 MHz; CDCl_3) -50.82 (d, $^5J_{\text{HF}}$ 2.9). δ_{C} (101 MHz; CDCl_3) 60.6 (s, C1), 73.4 (d, $^2J_{\text{CF}}$ 53.3, C3), 84.6 (q, $^3J_{\text{CF}}$ 6.3, C2), 113.8 (q, $^1J_{\text{CF}}$ 258.3, C1), 123.2 (s, C4'/5'), 132.5 (s, C3'), 137.0 (s, C4'/5'), 149.4 (s, C2'), 149.9 (s, C6'). IR (neat) ν_{max} / cm^{-1} 3208 (O-H), 2261 (C \equiv C), 1579, 1413, 1269, 1251, 1182, 1123, 1085, 1042. ASAP-MS (AI+) m/z 236 ($[\text{M}+\text{H}]^+$, 100%), 218 ($[\text{M}-\text{OH}_2]^+$, 26), 200 ($[\text{M}-\text{HCl}]^+$, 21). HRMS (AI+) m/z calc. for $[\text{M}+\text{H}]^+$ $\text{C}_9\text{H}_6\text{NO}^{(35}\text{Cl)}\text{F}_3$ 236.0090; found 236.0100.

General procedure: oxidation of alcohols.

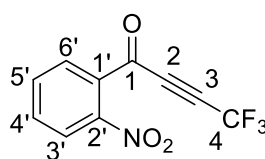
The CF_3 -substituted alcohol (1 eq.) was dissolved in CH_2Cl_2 and Dess-Martin periodinane (2 eq.) was added. The reaction mixture was stirred at room temperature overnight then a 1:1 mixture of saturated aqueous sodium thiosulfate and sodium bicarbonate was added and the resulting mixture stirred vigorously for 30 minutes. The organic layer was separated then washed with sodium thiosulfate, sodium bicarbonate then brine, dried over MgSO_4 and concentrated *in vacuo* to give the CF_3 -ynone product without further purification unless otherwise specified.

1-Phenyl-4,4,4-trifluorobut-2-yn-1-one (204a).

Following the general procedure, **211** (0.50 g, 2.5 mmol) and DMP (2.12 g, 5.0 mmol) in CH_2Cl_2 (100 mL) after 15 hours gave 1-phenyl-4,4,4-trifluorobut-2-yn-1-one, **204a** (0.46 g, 90%), as a yellow oil. δ_{H} (400 MHz; CDCl_3) 7.51-7.57 (2H, m, Ar-H), 7.68-7.71 (1H, m, C(4')H), 8.08-8.13 (2H, m, Ar-H). δ_{F} (376 MHz; CDCl_3) -51.57 (s). δ_{C} (101 MHz; CDCl_3) 75.50 (q, $^2J_{\text{CF}}$ 54.5, C3), 80.1 (q, $^3J_{\text{CF}}$ 6.5, C2), 113.9 (q, $^1J_{\text{CF}}$ 260.0, C4), 129.2 (s, C2'/3'), 129.9 (s, C2'/3'), 135.3 (s, C1'/C4'), 135.7 (s, C1'/C4'), 175.1 (s, C1). GC-MS (EI+) m/z 198 ($[\text{M}]^+$, 100%), 169 ($[\text{M}-\text{CHO}]^+$, 49), 151 ($[\text{M}-\text{CF}_3]^+$, 40), 129 ($[\text{M}-\text{CF}_3]^+$, 65), 105 ($[\text{M}-\text{C}_2\text{CF}_3]^+$, 31), 77 ($[\text{C}_6\text{H}_5]^+$, 57), 51 ($[\text{C}_4\text{H}_4]^+$, 52). HRMS (ESI+) m/z calc. for $[\text{M}]^+$ $\text{C}_{10}\text{H}_5\text{OF}_3$ 198.0293; found 198.1853. Spectroscopic data are consistent with the literature.¹¹

1-(2'-Naphthyl)-4,4,4-trifluorobut-2-yn-1-one (224b).

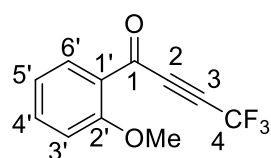
Following the general procedure, **224a** (2.00 g, 7.99 mmol) and DMP (6.78 g, 16.0 mmol) in DCM (80 mL) after 16 hours gave 1-(2'-naphthyl)-4,4,4-trifluorobut-2-yn-1-one, **224b** (1.89 g, 95%) as an orange solid, m.p. 47-48 °C. δ_{H} (400 MHz; CDCl_3) 7.64-7.69 (2H, m, Ar-H), 7.91-7.96 (2H, m, Ar-H), 8.07 (2H, m, Ar-H), 8.65-8.69 (1H, m, C(1')H). δ_{F} (376 MHz; CDCl_3) -51.37 (s). δ_{C} (101 MHz; CDCl_3) 80.4 (q, $^3J_{\text{CF}}$ 6.5, C2), 87.7 (q, $^2J_{\text{CF}}$ 51.9, C3), 114.1 (q, $^1J_{\text{CF}}$ 260.1, C4), 123.3 (s, Ar), 127.7 (s, Ar), 128.2 (s, Ar), 129.4 (s, Ar), 130.2 (s, Ar), 130.3 (s, Ar), 132.4 (s, C5'/10'), 132.9 (s, C5'/10'), 134.1 (s, Ar), 136.8 (s, C2'), 175.0 (s, C1). IR (neat) ν_{max} / cm^{-1} 2160 (C≡C), 1648 (C=O), 1624, 1354, 1250, 1218, 1158, 1133, 1018. GC-MS (EI+) m/z 248 (M^+ , 100%), 220 (38), 179 (25), 170 (17), 155 (17), 127 (55). HRMS (ESI+) m/z calc. for $[\text{M}+\text{OH}_3]^+$ $\text{C}_{14}\text{H}_{10}\text{O}_2\text{F}_3$ 267.0633; found 267.0634.

1-(2'-Nitrophenyl)-4,4,4-trifluorobut-2-yn-1-one (225b).

Following the general procedure, **225a** (1.56 g, 5.97 mmol) and DMP (4.25 g, 10.0 mmol) in CH_2Cl_2 (100 mL) after 16 hours gave 1-(2'-nitrophenyl)-4,4,4-trifluorobut-2-yn-1-one, **225b** (1.23 g, 79%), as a dark red oil. δ_{H} (400 MHz; CDCl_3) 7.75-7.81 (3H, m, Ar-H), 8.02-8.05 (1H, m, Ar-H). δ_{F} (376 MHz; CDCl_3) -51.93 (s). δ_{C} (101 MHz; CDCl_3) 75.7 (q, $^2J_{\text{CF}}$ 54.8, C3), 79.3 (q, $^3J_{\text{CF}}$ 6.5, C2), 113.7 (q, $^1J_{\text{CF}}$ 260.7, C4), 124.8 (s, C3'-6'),

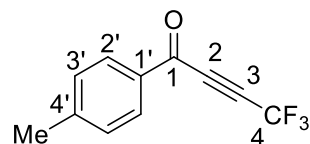
130.2 (s, C3'-6'), 132.3 (s, C1'), 133.9 (s, C3'-6'), 134.0 (s, C3'-6'), 147.5 (s, C2'), 173.5 (q, $^4J_{CF}$ 1.8, C1). IR (neat) ν_{max}/cm^{-1} 2248 (C≡C), 1698 (C=O), 1530 (N-O), 1347, 1253, 1188, 1143, 1061, 1015. LC-MS (ESI-) m/z 260 ([M+OH₂]⁻, 38), 113 ([M-NO₃CF₃]⁻, 12). HRMS (ESI-) m/z calc. for [M+OH₂]⁻ C₁₀H₆NO₄F₃ 260.0171; found 260.0154.

1-(2'-Methoxyphenyl)-4,4,4-trifluorobut-2-yn-1-one (226b).



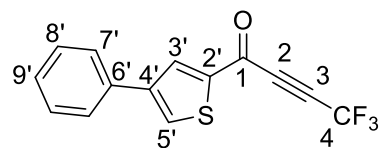
Following the general procedure, **226a** (2.53 g, 11.0 mmol) and DMP (5.13 g, 12.1 mmol) in CH₂Cl₂ (200 mL) after 24 hours gave 1-(2'-methoxyphenyl)-4,4,4-trifluorobut-2-yn-1-one, **226b** (2.34 g, 93%), as a yellow solid, m.p. 32-33 °C. δ_H (400 MHz; CDCl₃) 3.95 (3H, s, OMe), 7.01-7.06 (2H, m, Ar-H), 7.58-7.63 (1H, m, Ar-H), 7.90-7.94 (1H, m, Ar-H). δ_F (376 MHz; CDCl₃) -51.46 (s). δ_C (101 MHz; CDCl₃) 55.7 (s, OMe), 74.1 (q, $^2J_{CF}$ 53.9, C3), 82.6 (q, $^3J_{CF}$ 6.6, C2), 112.5 (s, Ar-H), 114.3 (q, $^1J_{CF}$ 259.2, C4), 120.9 (s, Ar-H), 124.8 (s, C2'), 132.1 (s, Ar-H), 136.9 (s, Ar-H), 160.7 (s, C1'), 173.3 (d, $^4J_{CF}$ 1.6, C1), 189.9 (s, C1). IR (neat) ν_{max}/cm^{-1} 2245 (C≡C), 1629 (C=O), 1597, 1486, 1467, 1437, 1303, 1254, 1228, 1163, 1134, 1055, 1014. LC-MS (ESI+) m/z 229 ([M+H]⁺, 100%), 115 (16). HRMS (ESI+) m/z calc. for [M+H]⁺ C₁₁H₈O₂F₃ 229.0476; found 229.0479.

1-(4'-Methylphenyl)-4,4,4-trifluorobut-2-yn-1-one (227b).



Following the general procedure, **227a** (2.75 g, 12.9 mmol) and DMP (10.77 g, 25.4 mmol) in CH₂Cl₂ (200 mL) after 16 hours gave 1-(4'-methylphenyl)-4,4,4-trifluorobut-2-yn-1-one, **227b** (2.17 g, 79%), as a yellow oil. δ_H (400 MHz; CDCl₃) 2.46 (3H, s, Me), 7.32-7.36 (2H, m, Ar-H), 7.97-7.81 (2H, m, Ar-H). δ_F (376 MHz; CDCl₃) -51.49 (s). δ_C (101 MHz; CDCl₃) 22.1 (s, Me), 75.0 (q, $^2J_{CF}$ 54.2, C3), 80.3 (q, $^3J_{CF}$ 6.4, C2), 114.0 (q, $^1J_{CF}$ 259.9, C4), 129.9 (s, C4'), 130.1 (s, C2'/3'), 133.0 (s, C2'/3'), 147.3 (s, C1'), 174.7 (q, $^5J_{CF}$ 1.5, C1). HRMS (ESI-) m/z calc. for [M]⁻ C₁₁H₇OF₃ 229.0464; found 229.0476.

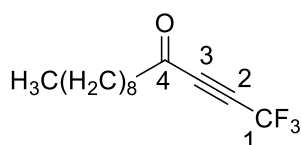
1-(4-Phenylthiophen-2-yl)-4,4,4-trifluorobut-2-yn-1-one (228b).



Following the general procedure, **228a** (0.715 g, 2.56 mmol) and DMP (1.12 g, 2.64 mmol) in CH₂Cl₂ (100 mL) after 16 hours gave 1-(4-phenylthiophen-2-yl)-4,4,4-trifluorobut-2-yn-1-one, **228b** (0.626 g, 87%), as a yellow solid, m.p. 85-87 °C. δ_H (400 MHz; CDCl₃) 7.37-7.41 (1H, m, C(9')H), 7.45-7.49 (2H, m, C(7'/8')H), 7.55-7.61 (2H,

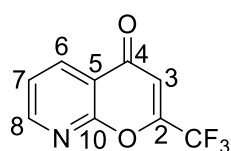
m, C(7'/8')H), 7.92-7.95 (1H, m, C(3'/5')H), 8.15-8.19 (1H, m, C(3'/5')H). δ_F (376 MHz; CDCl₃) -51.51 (s). δ_C (101 MHz; CDCl₃) 74.3 (q, $^2J_{CF}$ 54.7, C3), 79.7 (q, $^3J_{CF}$ 6.3, C2), 113.9 (q, $^1J_{CF}$ 260.3, C4), 126.5 (s, Ar), 128.5 (s, Ar), 129.3 (s, Ar), 132.3 (s, Ar), 135.4 (s, Ar), 143.3 (s, Ar), 144.5 (s, Ar), 176.5 (s, C1). HRMS (ESI+) m/z calc. for [M+H]⁺ C₁₄H₈OF₃S 281.0248; found 281.0241.

1,1,1-Trifluorotridec-2-yn-4-one (229b).



Following the general procedure, **229a** (0.341 g, 1.36 mmol) and DMP (1.30 g, 3.07 mmol) in CH₂Cl₂ (100 mL) after 16 hours gave 1,1,1-trifluorotridec-2-yn-4-one, **229b** (0.258 g, 76%), as a yellow oil. δ_H (400 MHz; CDCl₃) 0.85-0.91 (3H, m, C(13)H₃), 1.19-1.33 (12H, m, C(7-12)H₂), 1.65-1.69 (2H, m, C(6)H₂), 2.64-2.68 (2H, m, C(5)H₂). δ_F (376 MHz; CDCl₃) -51.75 (s). δ_C (101 MHz; CDCl₃) 14.2 (s, C13), 22.8 (s, C5-12), 23.4 (s, C5-12), 28.9 (s, C5-12), 29.3 (s, C5-12), 29.4 (s, C5-12), 31.9 (s, C5-12), 45.5 (s, C5-12), 73.0 (q, $^2J_{CF}$ 54.4, C2), 80.8 (q, $^3J_{CF}$ 6.4, C3), 113.9 (q, $^1J_{CF}$ 260.1, C1), 185.2 (s, C4). IR (neat) ν_{max} /cm⁻¹ 2927, 2857, 2263 (C≡C), 1699 (C=O), 1255, 1152. LC-MS (ESI-) m/z 247 ([M-H]⁻, 100%), 113 ([C₈H₁₇]⁻, 41). HRMS (ESI-) m/z calc. for [M-H]⁻ C₁₃H₁₈OF₃ 247.1310; found 247.1315.

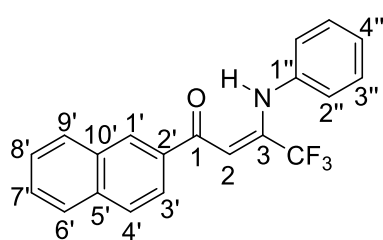
2-Trifluoromethyl-4H-pyrano[2,3-b]pyridin-4-one (331).



Following the general procedure, **330** (0.657 g, 2.80 mmol) and DMP (1.59 g, 3.75 mmol) in CH₂Cl₂ (100 mL) after 16 hours gave the crude product as a brown oil, which was purified by manual flash column chromatography (9:1 hexane/ethyl acetate over silica gel) to give 2-trifluoromethyl-4H-pyrano[2,3-b]pyridin-4-one, **331** (0.201 g, 33%), as a yellow oil. δ_H (400 MHz; CDCl₃) 7.42 (1H, q, $^4J_{CF}$ 0.8, C(3)H), 7.43 (1H, dd, $^3J_{HH}$ 7.7, $^3J_{HH}$ 4.8, C(7)H), 7.99 (1H, dd, $^3J_{HH}$ 7.7, $^4J_{HH}$ 2.0, C(6)H), 8.58 (1H, dd, $^3J_{HH}$ 4.8, $^4J_{HH}$ 2.0, C(8)H). δ_F (376 MHz; CDCl₃) -70.27 (d, $^4J_{CF}$ 0.8). δ_C (101 MHz; CDCl₃) 119.8 (q, $^1J_{CF}$ 274.2, CF₃), 123.1 (s, C6'-8'), 127.9 (q, $^3J_{CF}$ 3.8, C3), 130.7 (d, $^2J_{CF}$ 38.8, C2), 133.7 (s, C5), 139.77 (s, C6'-8'), 148.4 (s, C10), 152.9 (s, C6'-8'), 187.9 (s, C4). IR (neat) ν_{max} /cm⁻¹ 1678 (C=O), 1623, 1577, 1560, 1445, 1399, 1273, 1189, 1147, 1091, 1063, 1020. LC-MS (ESI+) 216 ([M+H]⁺, 87%), 151 (16), 130 (51), 105 (41). HRMS (ESI+) m/z calc. for [M+H]⁺ C₉H₅NO₂F₃ 216.0272; found 216.0271.

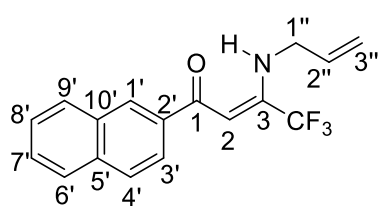
General procedure: Michael addition of amines.

Ynone **224b** (1 eq.) and the amine (1 eq.) were dissolved in ethanol (5 mL) and stirred at room temperature for 10 minutes. The reaction mixture was then concentrated *in vacuo* to afford the enaminone product without further purification unless specified. Where a mixture of *E* and *Z* stereoisomers was obtained, ^1H and ^{13}C NMR data are reported for the major product only.

(Z)-1-(2'-Naphthyl)-3-phenylamino-4,4,4-trifluorobut-2-en-1-one (232).

224b (0.048 g, 0.19 mmol) and aniline (0.017 mL, 0.19 mmol) gave 1-(2'-naphthyl)-3-phenylamino-4,4,4-trifluorobut-2-en-1-one, **232** (0.063 g, 96%) as a yellow solid, m.p. 106-108 °C. δ_{H} (400 MHz; CDCl_3) 6.61 (1H, s, C(3)H), 7.28-7.33 (3H, m, Ar), 7.37-7.41 (2H, m, Ar),

7.57-7.60 (2H, m, Ar), 7.88-7.93 (2H, m, Ar), 7.99-8.01 (1H, m, Ar), 8.04-8.06 (1H, m, Ar), 8.46-8.49 (1H, m, Ar), 12.43 (1H, br s, N-H). δ_{F} (376 MHz; CDCl_3) -62.97 (d, $^4J_{\text{HF}}$ 1.5, *E*), -61.81 (s, *Z*). δ_{C} (101 MHz; CDCl_3) 92.0 (q, $^3J_{\text{CF}}$ 4.8, C2), 120.2 (q, $^1J_{\text{CF}}$ 278.4, C4), 123.7 (s, Ar), 126.0 (s, Ar), 126.7 (s, Ar), 127.1 (s, Ar), 127.8 (s, Ar), 128.1 (s, Ar), 128.5 (s, Ar), 128.6 (s, Ar), 129.0 (s, Ar), 129.5 (s, Ar), 132.7 (s, Ar), 135.3 (s, Ar), 135.9 (s, Ar), 137.8 (s, Ar), 148.5 (q, $^2J_{\text{CF}}$ 31.5, C3), 191.2 (s, C1). HRMS (ESI+) m/z calc. for $[\text{M}+\text{H}]^+$ $\text{C}_{20}\text{H}_{15}\text{NOF}_3$ 342.1106; found 342.1102.

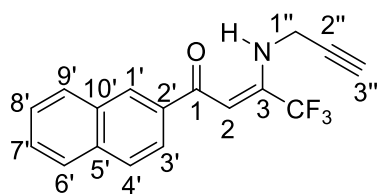
(Z)-1-(2'-Naphthyl)-3-allylamino-4,4,4-trifluorobut-2-en-1-one (233).

224b (0.033 g, 0.13 mmol) and allylamine (0.010 mL, 0.13 mmol) gave 1-(2'-naphthyl)-3-allylamino-4,4,4-trifluorobut-2-en-1-one, **233** (0.037 g, 94%) as a yellow oil. δ_{H} (400 MHz; CDCl_3) 4.07 (2H, t, $^3J_{\text{HH}}$ 5.7, C(1''')H), 5.27 (1H, d, $^3J_{\text{HH}}$ 10.3, C(3''')H), 5.36 (1H, d, $^3J_{\text{HH}}$ 17.1,

C(3''')H), 5.96 (1H, ddt, $^3J_{\text{HH}}$ 17.1, $^3J_{\text{HH}}$ 10.6, $^3J_{\text{HH}}$ 5.7, C(2''')H), 6.42 (1H, d, $^4J_{\text{HF}}$ 1.7, C(2)H), 7.54-7.58 (2H, m, C(3'/4')H), 7.78-8.09 (4H, m, C(6'-9')H), 8.40-8.43 (1H, m, C(1')H), 10.88 (1H, br s, N-H). δ_{F} (376 MHz; CDCl_3) -66.44 (d, $^4J_{\text{HF}}$ 1.8). δ_{C} (101 MHz; CDCl_3) 46.8 (q, $^4J_{\text{CF}}$ 2.8, C1'''), 89.9 (q, $^3J_{\text{CF}}$ 5.2, C2), 117.5 (s, Ar), 120.3 (q, $^1J_{\text{CF}}$ 277.9, CF_3), 123.8 (s, Ar), 126.7 (s, Ar), 127.8 (s, Ar), 128.0 (s, Ar), 128.3 (s, Ar), 128.5 (s, Ar), 129.5 (s, Ar), 132.8 (s, Ar), 133.4 (s, Ar), 135.2 (s, Ar), 136.3 (s, Ar), 149.9 (q, $^2J_{\text{CF}}$ 31.1,

C3), 190.9 (s, C1). HRMS (ESI+) m/z calc. for $[M+H]^+$ $C_{17}H_{15}NOF_3$ 306.1106; found 306.1106.

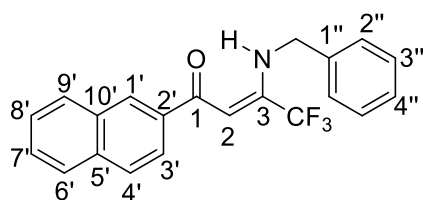
(Z)-1-(2'-Naphthyl)-3-propargylamino-4,4,4-trifluorobut-2-en-1-one (234).



224b (0.040 g, 0.16 mmol) and propargylamine (0.010 mL, 0.16 mmol) gave 1-(2'-naphthyl)-3-propargylamino-4,4,4-trifluorobut-2-en-1-one, **234** (0.046 g, 95%) as a yellow solid, m.p. 99-101 °C. δ_H (400 MHz; $CDCl_3$) 2.39

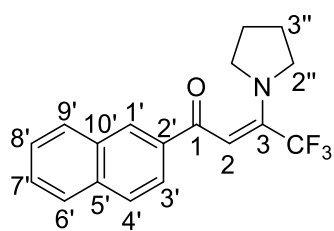
(1H, t, $^4J_{HH}$ 2.5, C(3'')H), 4.21 (2H, d, $^4J_{HH}$ 2.5, C(2'')H), 6.46 (1H, d, $^4J_{HF}$ 1.7, C(2)H), 7.51-7.63 (2H, m, C(3'/4')H), 7.82-8.04 (4H, m, C(6'-9')H), 8.42 (1H, s, C(1')H), 10.75 (1H, br s, N-H). δ_F (376 MHz; $CDCl_3$) -66.38 (d, $^4J_{HF}$ 1.7). δ_C (101 MHz; $CDCl_3$) 34.0 (d, $^4J_{CF}$ 3.4, C1''), 73.1 (s, C3''), 78.4 (s, C2''), 91.3 (q, $^4J_{CF}$ 5.2, C2), 120.2 (q, $^1J_{CF}$ 277.7, CF_3), 123.8 (s, Ar), 126.8 (s, Ar), 127.9 (s, Ar), 128.2 (s, Ar), 128.6 (s, Ar), 128.6 (s, Ar), 129.6 (s, Ar), 132.8 (s, Ar), 135.3 (s, Ar), 136.0 (s, Ar), 148.6 (q, $^2J_{CF}$ 31.2, C3), 191.1 (s, C1). HRMS (ESI+) m/z calc. for $[M+H]^+$ $C_{17}H_{13}NOF_3$ 304.0949; found 304.0947.

(Z)-1-(2'-Naphthyl)-3-benzylamino-4,4,4-trifluorobut-2-en-1-one (235).

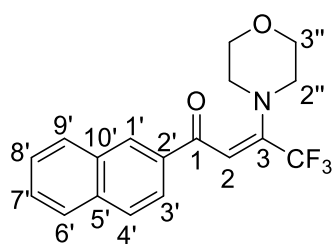


224b (0.039 g, 0.16 mmol) and benzylamine (0.017 mL, 0.16 mmol) gave 1-(2'-naphthyl)-3-benzylamino-4,4,4-trifluorobut-2-en-1-one, **235** (0.056 g, 98%) as a yellow oil. δ_H (400 MHz; $CDCl_3$)

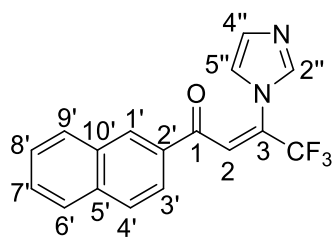
4.65 (2H, s, N-CH₂), 6.48 (1H, d, $^4J_{CF}$ 1.7, C(2)H), 7.33-7.41 (5H, m, C(1'''-4''')H), 7.54-7.56 (2H, m, C(3'/4')H), 7.92-7.96 (4H, m, C(6'-9')H), 8.42-8.44 (1H, m (C1')H), 11.12 (1H, br s, N-H). δ_F (376 MHz; $CDCl_3$) -66.16 (d, $^4J_{CF}$ 1.7). δ_C (101 MHz; $CDCl_3$) 48.5 (q, $^4J_{CF}$ 2.8, N-CH₂), 90.0 (q, $^3J_{CF}$ 5.2, C2), 120.3 (q, $^1J_{CF}$ 277.9, CF_3), 123.8 (s, Ar), 126.7 (s, Ar), 127.4 (s, Ar), 127.8 (s, Ar), 128.0 (s, Ar), 128.1 (s, Ar), 128.3 (s, Ar), 128.4 (s, Ar), 129.1 (s, Ar), 129.5 (s, Ar), 132.8 (s, Ar), 135.2 (s, Ar), 136.2 (s, Ar), 137.1 (s, Ar), 149.7 (q, $^2J_{CF}$ 31.0, C3), 190.9 (s, C1). HRMS (ESI+) m/z calc. for $[M+H]^+$ $C_{21}H_{19}NOF_3$ 358.1419; found 358.1415.

(Z)-1-(2'-Naphthyl)-3-pyrrolidinyl-4,4,4-trifluorobut-2-en-1-one (236).

224b (0.034 g, 0.14 mmol) and pyrrolidine (0.012 mL, 0.14 mmol) gave 1-(2'-naphthyl)-3-pyrrolidinyl-4,4,4-trifluorobut-2-en-1-one, **236** (0.042 g, 93%) as a white solid, m.p. 86-88 °C. δ_{H} (400 MHz; CDCl_3) 1.98-2.02 (4H, m, C(3'')H), 3.45-3.51 (4H, m, C(2'')H), 6.34 (1H, s, C(2)H), 7.54-7.57 (2H, m C(3'/4')H), 7.94-7.99 (4H, m, C(5'-8')H), 8.39-8.42 (1H, m, C(3')H). δ_{F} (376 MHz; CDCl_3) -65.23 (s). δ_{C} (101 MHz; CDCl_3) 25.6 (s, C3''), 52.8 (s, C2''), 94.3 (q, $^3J_{\text{CF}}$ 5.1, C2), 121.3 (q, $^1J_{\text{CF}}$ 279.3, CF_3), 124.7 (s, Ar), 126.6 (s, Ar), 127.8 (s, Ar), 127.9 (s, Ar), 128.3 (s, Ar), 129.4 (s, Ar), 129.5 (s, Ar), 132.8 (s, Ar), 135.1 (s, Ar), 137.3 (s, Ar), 144.1 (q, $^2J_{\text{CF}}$ 29.8, C3), 186.7 (s, C1). HRMS (ESI+) m/z calc. for $[\text{M}+\text{H}]^+$ $\text{C}_{18}\text{H}_{17}\text{NOF}_3$ 320.1262; found 320.1249.

(Z)-1-(2'-Naphthyl)-3-morpholinyl-4,4,4-trifluorobut-2-en-1-one (237).

224b (0.074 g, 0.30 mmol) and pyrrolidine (0.026 mL, 0.30 mmol) gave 1-(2'-naphthyl)-3-morpholinyl-4,4,4-trifluorobut-2-en-1-one, **237** (0.095 g, 95%) as a yellow oil. δ_{H} (400 MHz; CDCl_3) 3.32-3.36 (4H, m, C2''/3''), 3.78-3.82 (4H, m, C2''/3''), 6.46 (1H, s, C(2)H), 7.55-7.58 (2H, m, C(5'/10')H), 7.91-7.96 (4H, m, C(6'-9')H), 8.38-8.40 (1H, m, C(1')H). δ_{F} (376 MHz; CDCl_3) -63.70 (s). δ_{C} (101 MHz; CDCl_3) 51.6 (s, C2''/3''), 66.8 (s, C2''/3''), 97.6 (q, $^3J_{\text{CF}}$ 4.6, C2), 121.6 (q, $^1J_{\text{CF}}$ 279.6, CF_3), 124.3 (s, Ar), 126.8 (s, Ar), 127.9 (s, Ar), 128.3 (s, Ar), 128.5 (s, Ar), 129.6 (s, Ar), 129.5 (s, Ar), 132.3 (s, Ar), 135.4 (s, Ar), 136.8 (s, Ar), 147.2 (q, $^2J_{\text{CF}}$ 29.6, C3), 187.6 (s, C1). HRMS (ESI+) m/z calc. for $[\text{M}+\text{H}]^+$ $\text{C}_{18}\text{H}_{17}\text{NO}_2\text{F}_3$ 336.1211; found 336.1200.

(Z)-1-(2'-Naphthyl)-3-imidazolyl-4,4,4-trifluorobut-2-en-1-one (238).

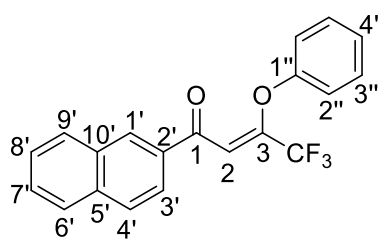
224b (0.044 g, 0.18 mmol) and imidazole (0.012 g, 0.18 mmol) gave 1-(2'-naphthyl)-3-imidazolyl-4,4,4-trifluorobut-2-en-1-one, **238** (0.051 g, 91%) as a red oil. δ_{H} (400 MHz; CDCl_3) 6.99 (1H, dd, $^3J_{\text{HH}}$ 1.5, $^4J_{\text{HH}}$ 0.9, C(4''/5'')H), 7.01-7.03 (1H, m, $^4J_{\text{HH}}$ 0.9, C(4''/5'')H), 7.46 (1H, q, $^4J_{\text{HF}}$ 0.9, C(2)H), 7.55 (1H, d, $^4J_{\text{HH}}$ 0.9, C(2'')H), 7.66 (2H, m, C(3'/4')H), 7.84-7.86 (1H, m, C(4''/5'')H), 7.95-7.80 (4H, m, C(6'-9')H), 8.29-8.31 (1H, m, C(1')H). δ_{F} (376 MHz;

CDCl₃) -69.09 (d, ⁴J_{HF} 0.9, *E*, 29%), -63.76 (s, *Z*, 71%). δ_C (101 MHz; CDCl₃) 120.1 (q, ¹J_{CF} 275.2, CF₃), 123.2 (s, Ar), 127.4 (s, Ar), 127.7 (q, ³J_{CF} 3.4, C2), 128.0 (s, Ar), 129.3 (s, Ar), 129.6 (s, Ar), 129.7 (s, Ar), 130.5 (s, Ar), 131.0 (s, Ar), 131.5 (s, Ar), 132.2 (s, Ar), 132.5 (s, Ar), 136.3 (s, Ar), 137.8 (s, Ar), 188.6 (s, C1). HRMS (ESI+) *m/z* calc. for [M+H]⁺ C₁₇H₁₂N₂O₂F₃ 317.0902; found 317.0891.

General procedure: Michael addition of phenols.

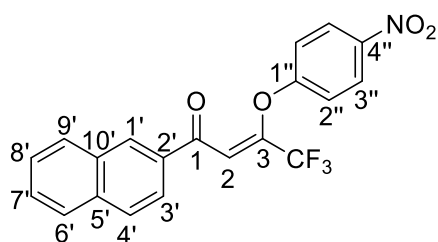
Ynone **224b** (1 eq.) and the phenol (1 eq.) were dissolved in anhydrous THF (5 mL) with KO^tBu (0.1 eq.) and stirred at room temperature for 10 minutes. The reaction mixture was then concentrated *in vacuo* then hexane was added, the resulting solid filtered and filtrate concentrated *in vacuo* to afford the enone ether product without further purification unless specified. Where a mixture of *E* and *Z* stereoisomers was obtained, ¹H and ¹³C NMR data are reported for the major product only.

(*Z*)-1-(2'-Naphthyl)-3-phenyloxy-4,4,4-trifluorobut-2-en-1-one (**243**).



224b (0.165 g, 0.665 mmol), phenol (0.061 g, 0.67 mmol) and KO^tBu (0.0056 g, 0.050 mmol) gave 1-(2'-naphthyl)-3-phenyloxy-4,4,4-trifluorobut-2-en-1-one, **243** (0.202 g, 89%) as a yellow oil. δ_H (400 MHz; CDCl₃) 6.86-6.89 (2H, m, C(2''/3''))H), 6.95-6.98 (2H, m, C(4'')H and C(2)H overlapping), 7.59-7.62 (2H, m, Naph-H), 7.78-7.81 (2H, m, Naph-H), 7.90-7.93 (2H, m, Naph-H), 8.30-8.32 (1H, m, C(3')H). δ_F (376 MHz; CDCl₃) -67.32 (d, ⁴J_{HF} 1.0, *E*, 14%), -71.11 (s, *Z*, 86%). δ_C (101 MHz; CDCl₃) 113.2 (q, ³J_{CF} 4.1, C2), 117.8 (q, ¹J_{CF} 275.8, CF₃), 120.5 (s, Ar), 120.9 (s, Ar), 123.7 (s, Ar), 124.1 (s, Ar), 127.1 (s, Ar), 127.9 (s, Ar), 128.8 (s, Ar), 129.1 (s, Ar), 129.6 (s, Ar), 129.8 (s, Ar), 131.0 (s, Ar), 132.4 (s, Ar), 134.07(s, Ar), 147.7 (q, ²J_{CF} 35.3, C3), 156.3 (s, C2'), 188.6 (C1). HRMS (ESI+) *m/z* calc. for [M+H]⁺ C₂₀H₁₄O₂F₃ 343.0946; found 343.0935.

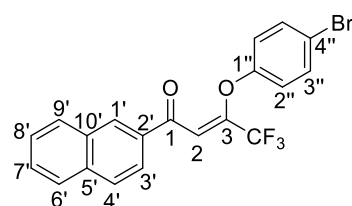
(*Z*)-1-(2'-Naphthyl)-3-(4''-nitrophenyl)oxy-4,4,4-trifluorobut-2-en-1-one (**244**).



224b (0.118 g, 0.475 mmol), 4-nitrophenol (0.066 g, 0.475 mmol) and KO^tBu (0.0053 g, 0.0475 mmol) gave 1-(2'-naphthyl)-3-(4''-nitrophenyl)oxy-4,4,4-trifluorobut-2-en-1-one, **244** (0.156 g, 85%) as a yellow oil. δ_H (400 MHz; CDCl₃) 7.04-7.07 (2H, m,

C(2'')H), 7.31 (1H, s, C(2)H), 7.62-7.64 (2H, m, Naph-H), 7.81-7.84 (1H, m, Naph-H), 7.86-7.89 (2H, m, Naph-H), 7.97-7.99 (1H, m, Naph-H), 8.13-8.15 (2H, m, C(3'')H), 8.34-8.36 (1H, m, Naph-H). δ_F (376 MHz; CDCl₃) -67.09 (d, $^4J_{HF}$ 0.7, *E*, 15%), -71.13 (d, $^4J_{HF}$ 0.5, *Z*, 85%). δ_C (101 MHz; CDCl₃) 115.8 (q, $^3J_{CF}$ 3.9, C2), 119.8 (q, $^1J_{CF}$ 275.9, CF₃), 116.6 (s, Ar), 119.9 (s, Ar), 123.4 (s, Ar), 123.7 (s, Ar), 125.9 (s, Ar), 126.5 (s, Ar), 128.4 (s, Ar), 127.5 (s, Ar), 128.1 (s, Ar), 129.6 (s, Ar), 131.2 (s, Ar), 132.4 (s, Ar), 133.6 (s, Ar), 136.2 (s, Ar), 143.8 (s, Ar), 148.8 (q, $^2J_{CF}$ 35.1, C3), 160.9 (s, Ar), 187.3 (s, C1). HRMS (ESI+) m/z calc. for [M+H]⁺ C₂₀H₁₃NO₄F₃ 388.0797; found 388.0767.

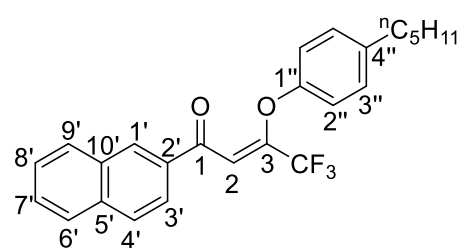
(Z)-1-(2'-Naphthyl)-3-(4''-bromophenyl)oxy-4,4,4-trifluorobut-2-en-1-one (245).



224b (0.041 g, 0.17 mmol), 4-bromophenol (0.029 g, 0.17 mmol) and KO^tBu (0.002 g, 0.02 mmol) gave 1-(2'-naphthyl)-3-(4''-bromophenyl)oxy-4,4,4-trifluorobut-2-en-1-one, **245** (0.060 g, 84%) as a yellow oil. δ_H (400 MHz; CDCl₃) 6.77-6.79 (2H, m, Ph-H), 7.04 (1H, d, $^4J_{HF}$ 0.6,

C(2)H), 7.22-7.24 (1H, m, Naph-H), 7.60-7.65 (3H, m, Naph-H), 7.77-7.79 (1H, m, Naph-H), 7.87-7.89 (2H, m, Ph-H), 7.98-7.99 (1H, m, Naph-H), 8.30-8.32 (1H, m, Naph-H). δ_F (376 MHz; CDCl₃) -67.33 (d, $^4J_{HF}$ 0.8, *Z*, 11%), -71.08 (d, $^4J_{HF}$ 0.6, *E*, 89%). δ_C (101 MHz; CDCl₃) 114.7 (q, $^3J_{CF}$ 3.5, C2), 118.8 (q, $^1J_{CF}$ 276.4, CF₃), 116.1 (s, Ar), 119.5 (s, Ar), 122.8 (s, Ar), 123.3 (s, Ar), 125.4 (s, Ar), 126.1 (s, Ar), 127.9 (s, Ar), 126.9, 127.6 (s, Ar), 129.1 (s, Ar), 130.7 (s, Ar), 132.0 (s, Ar), 133.1 (s, Ar), 135.7 (s, Ar), 142.3 (s, Ar), 148.3 (q, $^2J_{CF}$ 35.1, C3), 160.5 (s, Ar), 186.7 (s, C1). HRMS (ESI+) m/z calc. for [M+H]⁺ C₂₀H₁₃O₂F₃(⁷⁹Br) 421.0051; found 421.0042.

(Z)-1-(2'-Naphthyl)-3-[4''-(*n*-pentyl)phenyl]oxy-4,4,4-trifluorobut-2-en-1-one (246).

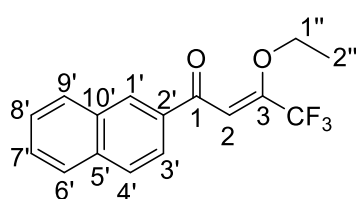


224b (0.044 mg, 0.18 mmol), 4-(*n*-pentyl)phenol (0.030 mL, 0.18 mmol) and KO^tBu (0.002 g, 0.018 mmol) gave 1-(2'-naphthyl)-3-[4''-(*n*-pentyl)phenyl]oxy-4,4,4-trifluorobut-2-en-1-one, **246** (0.056 g, 76%) as a yellow oil. δ_H (400 MHz;

CDCl₃) 0.89-0.92 (3H, m, *n*-pentyl CH₃), 1.30-1.38 (8H, m, *n*-pentyl), 6.76-6.78 (2H, m, C(2'')/3'')H), 6.88-6.90 (2H, m, C(2'')/3'')H), 7.62-7.64 (2H, m, C(6'-9')H), 7.77-7.80 (2H, m, C(6'-9')H), 7.89-7.90 (1H, m, C(3'/4')H), 7.97-7.99 (1H, m, C(3'/4')H), 8.29-8.30 (1H, m, C(1')H). δ_F (376 MHz; CDCl₃) -67.34 (s, *E*, 17%), -71.16 (s, *Z*, 83%). δ_C

(101 MHz; CDCl₃) 14.1 (s, *n*-pentyl CH₃), 22.6 (s, *n*-pentyl CH₂), 31.2 (s, *n*-pentyl CH₂), 31.4 (s, *n*-pentyl CH₂), 35.1 (s, *n*-pentyl CH₂), 112.4 (q, ³J_{CF} 3.3, C2), 117.1 (s, C2''/3''), 120.0 (q, ¹J_{CF} 276.2, CF₃), 123.7 (s, Ar), 127.0 (s, Ar), 127.9 (s, Ar), 128.7 (s, Ar), 129.0 (s, Ar), 129.4 (s, C2''/3''), 129.8 (s, Ar), 131.0 (s, Ar), 132.4 (s, Ar), 134.1 (s, Ar), 135.9 (s, Ar), 138.8 (s, Ar), 141.4 (s, Ar), 148.1 (q, ²J_{CF} 35.1, C3), 188.9 (s, C1). HRMS (ESI+) *m/z* calc. for [M+H]⁺ C₂₅H₂₄O₂F₃ 413.1720; found 413.1728.

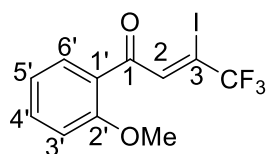
(Z)-1-(2'-Naphthyl)-3-ethoxy-4,4,4-trifluorobut-2-en-1-one (247).



224b (0.139 g, 0.560 mmol) and acetamide (0.033 g, 0.56 mmol) were dissolved in the ethanol (5 mL) and stirred at room temperature for 16 hours. The reaction mixture was then concentrated *in vacuo* then the residue partitioned

between ethyl acetate and water. The aqueous layer was extracted with ethyl acetate then the combined organic extracts washed with 6M HCl then brine, dried over MgSO₄ and concentrated *in vacuo* to give 1-(2'-naphthyl)-3-ethoxy-4,4,4-trifluorobut-2-en-1-one, **247** (0.087 g, 53%) as a yellow oil. Product obtained as a mixture of *E* and *Z* stereoisomers, ¹H and ¹³C NMR data reported for major product only. δ_H (400 MHz; CDCl₃) 1.50 (3H, t, ³J_{HH} 7.0, C(2'')H), 4.06 (2H, q, ³J_{HH} 7.0, C(1'')H), 6.11 (1H, s, C(2)H), 7.58-7.60 (2H, m, C(3'/4')H), 7.92-7.95 (4H, m, C(6'-9')H), 8.41-8.42 (1H, m, C(1')H). δ_F (376 MHz; CDCl₃) -67.28 (d, ⁴J_{HF} 0.9, *Z*, 65%), -71.93 (s, *E*, 35%). δ_C (101 MHz; CDCl₃) 14.1 (s, C2''), 65.7 (s, C1''), 103.5 (q, ³J_{CF} 1.8, C2), 119.4 (q, ¹J_{CF} 276.4, CF₃), 124.1 (s, Ar), 127.0 (s, Ar), 127.9 (s, Ar), 128.7 (s, Ar), 128.8 (s, Ar), 129.7 (s, Ar), 131.2 (s, Ar), 132.5 (s, Ar), 134.8 (s, Ar), 135.8 (s, Ar), 151.5 (q, ²J_{CF} 36.4, C3), 189.8 (s, C1). HRMS (ESI+) *m/z* calc. for [M+H]⁺ C₁₆H₁₄O₂F₃ 295.0946; found 295.0958.

(E)-1-(2'-Methoxyphenyl)-3-iodo-4,4,4-trifluorobut-2-en-1-one (248).



226b (1.574 g, 6.90 mmol) was dissolved in acetic acid (20 mL) then 55% HI (6 mL) was added and the resulting mixture heated to 110 °C for 16 hours. On cooling to room temperature, the reaction mixture was quenched with saturated aqueous sodium

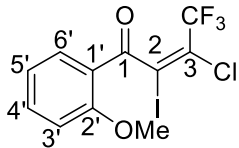
bicarbonate and sodium thiosulfate then extracted twice with ethyl acetate. The combined organic extracts were washed with sodium thiosulfate, twice with sodium bicarbonate, then with brine, dried over MgSO₄ and concentrated *in vacuo* to give (*E*)-1-(2'-methoxyphenyl)-3-iodo-4,4,4-trifluorobut-2-en-1-one, **248** (0.459 g, 19%) as an orange

oil. A 97:3 mixture of *E:Z* stereoisomers was obtained – ^1H and ^{13}C NMR data reported for major product only. δ_{H} (400 MHz; CDCl_3) 3.90 (3H, s, OMe), 6.99 (1H, dd, $^3J_{\text{HH}}$ 8.5, $^4J_{\text{HH}}$ 1.0, C(3')H), 7.07 (1H, ddd, $^3J_{\text{HH}}$ 7.9, $^3J_{\text{HH}}$ 7.3, $^4J_{\text{HH}}$ 1.0, C(5')H), 7.57 (1H, ddd, $^3J_{\text{HH}}$ 8.5, $^3J_{\text{HH}}$ 7.3, 1.8, C(4')H), 7.86 (1H, dd, $^3J_{\text{HH}}$ 7.9, $^4J_{\text{HH}}$ 1.8, C(6')H), 7.88 (1H, q, $^4J_{\text{CF}}$ 1.3, C(2)H). δ_{F} (376 MHz; CDCl_3) –60.68 (s, *Z*), –65.81 (d, $^4J_{\text{HF}}$ 1.3, *E*). δ_{C} (101 MHz; CDCl_3) 55.8 (s, OMe), 89.4 (q, $^2J_{\text{CF}}$ 36.9, C3), 112.0 (s, C3'-6'), 121.1 (q, $^1J_{\text{CF}}$ 272.5, CF_3), 121.3 (s, C3'-6'), 125.7 (s, C2'), 131.4 (s, C3'-6'), 135.7 (s, C3'-6'), 141.4 (q, $^3J_{\text{CF}}$ 5.2, C2), 159.7 (s, C1'), 189.9 (s, C1). IR (neat) ν_{max} / cm^{-1} 1660 (C=O), 1597, 1484, 1466, 1438, 1302, 1255, 1209, 1162, 1133, 1015. GC-MS (EI+) m/z 356 (M^+ , 15%), 209 ($[\text{C}_2\text{HF}_3\text{I}]^+$, 25), 135 ($[\text{M}-\text{C}_3\text{HF}_3\text{I}]^+$, 100), 77 ($[\text{C}_6\text{H}_5]^+$, 38). HRMS (ESI+) m/z calc. for $[\text{M}+\text{H}]^+$ $\text{C}_{11}\text{H}_9\text{O}_2\text{F}_3\text{I}$ 356.9599; found 356.9595.

General procedure: electrophilic addition.

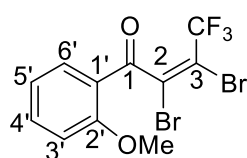
Ynone **226b** (1 eq.) was dissolved in dichloromethane (30 mL) and the electrophile (1.1 eq.) was then added. The reaction mixture was stirred at room temperature for the indicated time then quenched with sodium thiosulfate solution. The aqueous layer was separated and extracted with CH_2Cl_2 then the combined organic extracts were washed with sodium thiosulfate then brine, dried over MgSO_4 and concentrated *in vacuo* to give the product without further purification unless otherwise specified.

(*Z*)-1-(2'-Methoxyphenyl)-2-chloro-3-iodo-4,4,4-trifluorobut-2-en-1-one (**249**).

 **226b** (0.697 g, 3.05 mmol) and iodine monochloride (1.0 M in CH_2Cl_2 , 4.5 mL, 4.5 mmol) after 20 minutes gave 1-(2'-methoxyphenyl)-2-chloro-3-iodo-4,4,4-trifluorobut-2-en-1-one, **249** (0.832 g, 70%) as a yellow solid, m.p. 61-62 °C. A 13:87 mixture of *E:Z* stereoisomers was obtained – ^1H and ^{13}C NMR data reported for major product only. Subsequent purification by column chromatography (CombiFlash NextGen 100TM, hexane/ethyl acetate, 0-100% over 9 minutes) afforded a sample of pure *Z*-**249** for analysis by X-ray crystallography. δ_{H} (400 MHz; CDCl_3) 3.87 (3H, s, OMe), 6.97-6.99 (1H, m, Ar-H), 7.06-7.07 (1H, m, Ar-H), 7.57-7.59 (1H, m, Ar-H), 7.94-7.95 (1H, m, Ar-H). δ_{F} (376 MHz; CDCl_3) –62.23 (s, *E*), –63.01 (s, *Z*). δ_{C} (101 MHz; CDCl_3) 55.8 (s, OMe), 112.2 (s, C3'-6'), 113.0 (q, $^3J_{\text{CF}}$ 2.9, C2), 119.0 (q, $^1J_{\text{CF}}$ 275.4, C4), 121.2 (s, C3'-6'), 121.6 (s, C2'), 126.1 (q, $^2J_{\text{CF}}$ 39.2, C3), 132.2 (s, C3'-6'), 136.6 (s, C3'-6'), 159.8 (s, C1'), 186.9 (s, C1). IR (neat) ν_{max} / cm^{-1} 1653, 1590, 1483, 1454, 1435, 1288, 1265, 1249,

1219, 1187, 1161, 1138, 1115, 1035, 1016. LC-MS (ESI+) m/z 391 ($[M+H]^+$, 72%) 390 ($[M]^+$, 58). HRMS (ESI+) m/z calc. for $[M+H]^+$ $C_{11}H_8O_2F_3(^{35}Cl)I$ 390.9210; found 390.9223.

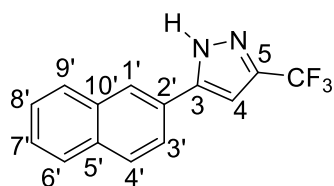
(Z)-1-(2'-Methoxyphenyl)-2,3-dibromo-4,4,4-trifluorobut-2-en-1-one (250).



226b (0.193 g, 0.0845 mmol) and bromine (0.1 mL, 1.95 mmol) after 1 hour gave 1-(2'-methoxyphenyl)-2,3-dibromo-4,4,4-trifluorobut-2-en-1-one, **250** (0.223 g, 68%) as a yellow solid, m.p. 44-45 °C. A 20:80 mixture of *E*:*Z* stereoisomers was obtained – 1H

and ^{13}C NMR data reported for major product only. δ_H (400 MHz; $CDCl_3$) 3.89 (3H, s, OMe), 7.00-7.02 (1H, m, Ar-H), 7.07-7.08 (1H, m, Ar-H), 7.60-7.61 (1H, m, Ar-H), 7.93-7.95 (1H, m, Ar-H). δ_F (376 MHz; $CDCl_3$) -60.14 (s, *E*), -61.01 (s, *Z*). δ_C (101 MHz; $CDCl_3$) 56.0 (s, OMe), 112.3 (s, C3'-6'), 112.8 (q, $^2J_{CF}$ 39.1, C3), 117.6 (q, $^1J_{CF}$ 245.0, C4), 121.2 (s, C3'-6'), 122.0 (s, C2'), 132.2 (s, C3'-6'), 135.1 (q, $^3J_{CF}$ 3.7, C2), 136.8 (s, C3'-6'), 160.0 (s, C1'), 185.0 (s, C1). IR (neat) ν_{max}/cm^{-1} 1655, 1619, 1597, 1578, 1484, 1465, 1296, 1261, 1249, 1222, 1138, 1115, 1066, 1038, 1012. LC-MS (ESI+) m/z 391 ($[M(^{81}Br)_2+H]^+$, 51%), 389 ($[M(^{79}Br^{81}Br)+H]^+$, 100), 387 ($[M(^{79}Br)_2+H]^+$, 48) 282 ($[COC_2Br_2CF_3]^+$, 16). HRMS (ESI+) m/z calc. for $[M+H]^+$ $C_{11}H_8O_2F_3(^{79}Br)_2$ 386.8843; found 386.8853.

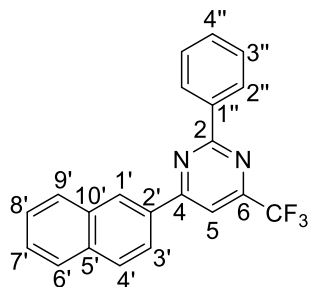
3-(2'-Naphthyl)-5-(trifluoromethyl)-1H-pyrazole (251).



224b (0.135 g, 0.544 mmol) and hydrazine hydrochloride (0.094 g, 1.37 mmol) were dissolved in ethanol (20 mL) and stirred at room temperature for 16 hours. The resulting precipitate was filtered, washed with ethanol then dried *in vacuo* to give 3-(2'-naphthyl)-5-(trifluoromethyl)-1H-pyrazole, **251** (0.107 g, 75%), as a yellow solid, m.p. 161-162 °C (lit. 178-179 °C from toluene).¹² δ_H (400 MHz; $CDCl_3$) 1.69 (br s, N-H), 7.55-7.58 (2H, m, Ar-H), 7.66 (1H, d, $^4J_{CF}$ 1.1, C(2)H), 7.90-7.93 (3H, m, Ar-H), 8.02-8.04 (1H, m, Ar-H), 8.09-8.10 (1H, m, Ar-H). δ_F (376 MHz; $CDCl_3$) -74.16 (d, $^4J_{CF}$ 1.1). δ_C (101 MHz; $CDCl_3$) 120.2 (q, $^1J_{CF}$ 273.2, CF_3), 123.75(C4), 126.5 (q, $^2J_{CF}$ 38.2, C5), 126.9 (s, Ar), 128.0 (s, Ar), 128.0 (s, Ar), 128.1 (s, Ar), 128.9 (s, Ar), 129.1 (s, Ar), 129.1 (s, Ar), 131.3 (s, Ar), 133.1 (s, Ar), 135.0 (s, Ar), 157.7 (s, C3). IR (neat) ν_{max}/cm^{-1} 3050 (N-H), 2160, 2039, 1561, 1288, 1260, 1183, 1154, 1128, 1056. GC-MS (EI+) m/z 262 ($[M]^+$, 100%), 214 (11), 165 (18), 131 (11). HRMS (AI+) m/z calc.

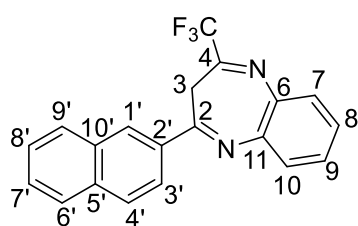
for $[M+H]^+$ $C_{14}H_8N_2F_3$ 263.0796; found 263.0803. Spectroscopic data consistent with literature results.⁹

2-Phenyl-4-(2'-naphthyl)-6-(trifluoromethyl)pyrimidine (**252**).



224b (0.191 g, 0.770 mmol) and benzamidine hydrochloride (0.194 g, 12.4 mmol) were dissolved in ethanol (20 mL) and stirred at room temperature for 16 hours. The resulting precipitate was filtered, washed with ethanol then dried *in vacuo* to give 2-phenyl-4-(2'-naphthyl)-6-(trifluoromethyl)pyrimidine, **252** (0.126 g, 47%), as a white solid, m.p. 140-141 °C. δ_H (400 MHz; $CDCl_3$) 7.55-7.61 (5H, m, Ph), 7.93-7.94 (1H, m, Naph), 8.02-8.05 (3H, m, Naph), 8.37-8.39 (1H, m, Naph), 8.67-8.70 (2H, m, Naph), 8.76 (1H, s, C(5)H). δ_F (376 MHz; $CDCl_3$) -69.94 (s). δ_C (101 MHz; $CDCl_3$) 110.2 (q, $^3J_{CF}$ 2.9, C5), 121.1 (q, $^1J_{CF}$ 275.4, CF_3), 123.9 (s, C4''), 127.0 (s, Ar), 127.9 (s, Ar), 128.1 (s, Ar), 128.2 (s, Ar), 128.8 (s, Ar), 128.9 (s, Ar), 129.1 (s, Ar), 129.3 (s, Ar), 131.7 (s, Ar), 133.2 (s, C5'/10'), 133.3 (s, C5'/10'), 135.2 (s, C2'/1''), 136.7 (s, C2'/1''), 156.8 (q, $^2J_{CF}$ 35.5, C6), 165.5 (C4), 166.5 (C2). IR (neat) ν_{max} / cm^{-1} 1569, 1592, 1547, 1474, 1457, 1440, 1389, 1376, 1304, 1262, 1238, 1206, 1160, 1136, 1100, 1055, 1021, 1003. LC-MS (ESI+) m/z 351 ($[M+H]^+$, 100%). HRMS (ESI+) m/z calc. for $[M+H]^+$ $C_{21}H_{14}N_2F_3$ 351.1109; found 351.1119.

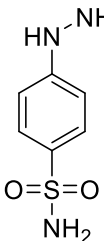
2-(2'-Naphthyl)-4-trifluoromethyl-3H-benzo[*b*][1,4]diazepine (**253**).



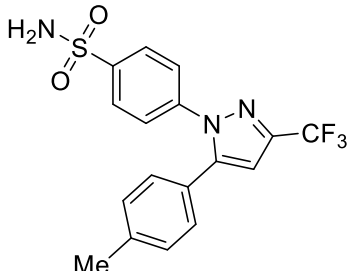
224b (0.126 g, 0.508 mmol) and 1,2-phenylenediamine (0.15 g, 1.4 mmol) were dissolved in ethanol (30 mL) and stirred at room temperature for 16 hours. Ethanol was removed *in vacuo* and the residue was partitioned between ethyl acetate and 1M HCl. The organic layer was washed with 1M HCl then brine, dried over $MgSO_4$ and concentrated *in vacuo* to give 2-(2'-naphthyl)-4-trifluoromethyl-3H-benzo[*b*][1,4]diazepine, **253** (0.117 g, 67%), as an orange solid, m.p. 158-160 °C. δ_H (400 MHz; $CDCl_3$) 2.75 (2H, s, C(3)H), 7.41-7.43 (2H, m, Ar-H), 7.58-7.61 (2H, m, Ar-H), 7.72-7.74 (2H, m, Ar-H), 7.89-7.91 (2H, m, Ar-H), 7.98-7.99 (1H, m, Ar-H), 8.03-8.04 (1H, m, Ar-H), 8.47-8.49 (1H, m, Ar-H). δ_F (376 MHz; $CDCl_3$) -64.11 (s). δ_C (101 MHz; $CDCl_3$) 26.8 (s, C3), 118.8 (d, $^1J_{CF}$ 271.0, CF_3), 124.0 (s, Ar), 124.9 (s, Ar), 126.9 (s, Ar), 127.9 (s, Ar), 128.6 (s, Ar), 128.6 (s, Ar), 129.7

(s, Ar), 130.4 (s, Ar), 132.6 (s, Ar), 134.6 (s, Ar), 135.8 (s, Ar), 140.7 (d, $^2J_{CF}$ 40.8, C4), 198.6 (s, C2). IR (neat) ν_{max}/cm^{-1} 1678, 1627, 1597, 1551, 1500, 1463, 1401, 1362, 1317, 1285, 1192, 1166, 1140, 1128, 1006. ASAP-MS (AI+) m/z 339 ($[M+H]^+$, 100%), 281 (13), 245 (10), 187 (68), 171 (19). HRMS (AI+) m/z calc. for $[M+H]^+$ $C_{20}H_{14}N_2F_3$ 339.1109; found 339.1107.

4-Hydrazinobenzene-1-sulfonamide hydrochloride (**255**).

 Using a modified literature procedure,¹³ 4-aminobenzenesulfonamide (**254**, 10.12 g, 58.8 mmol) was dissolved in 37% HCl (200 mL) and heated to 100 °C until solids dissolved then cooled to 0 °C. A solution of NaNO₂ (4.87 g, 70.6 mmol) in water (50 mL) was added slowly over 5 minutes then stirred at 0 °C for a further ten minutes. A solution of SnCl₂·2H₂O (40.75 g, 181 mmol) in 37% HCl (100 mL) was then added slowly over 5 minutes at 0 °C and then the reaction mixture allowed to warm to room temperature over an hour. The resulting precipitate was filtered and washed with cold water then ethanol to give 4-hydrazinobenzene-1-sulfonamide hydrochloride, **255** (8.62 g, 75%), as a yellow solid, m.p. 204-209 °C (lit. 205-211 °C).¹⁴ δ_H (400 MHz; DMSO-*d*₆) 7.03-7.05 (2H, m, Ar-H), 7.21 (1H, br s, SO₂-NH), 7.69-7.72 (2H, m, Ar-H), N-H, 8.92 (1H, br s, ArNH), 10.52 (3H, br s, NH₃Cl). δ_C (101 MHz; CDCl₃) 113.4 (s, C-H), 127.0 (s, C-H), 136.2 (s, C-N/S), 148.4 (s, C-N/S). IR (neat) ν_{max}/cm^{-1} 3191 (N-H), 2691 (N-H), 2160 (N-H), 2130 (N-H), 1595, 1506, 1415, 1313, 1260, 1154, 1099, 1060, 1013. HRMS (AI+) calc. for $[M]^+$ $C_6H_9N_3O_2S$ 187.0415; found 187.0406. Spectroscopic data consistent with literature results.¹⁵

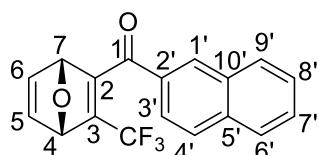
Celecoxib (**31**).

 Ynone **227b** (0.253 g, 1.19 mmol) and hydrazine **255** (0.267 g, 1.20 mmol) were dissolved in ethanol and stirred at room temperature for 16 hours. The solvent was removed *in vacuo* to afford celecoxib, **31** (0.351 g, 78%) as a yellow solid, m.p. 161-162 °C (lit. 160-161 °C).¹⁶ δ_H (400 MHz; CDCl₃) 2.38 (3H, Me), 4.94 (2H, br s, N-H), 6.74 (1H, s, pyrazole-H), 7.10-7.12 (2H, m, Ar-H), 7.17-7.19 (2H, m, Ar-H), 7.47-7.49 (2H, m, Ar-H), 7.89-7.91 (2H, m, Ar-H). δ_F (376 MHz; CDCl₃) -62.45 (s). δ_C (101 MHz; CDCl₃) 21.4 (s, C10), 106.5 (s, Ar), 121.1 (q, $^1J_{CF}$ 272.6, CF₃), 125.6 (s, Ar), 125.8 (s, Ar), 127.6

(s, Ar), 128.8 (s, Ar), 129.9 (s, Ar), 139.9 (s, Ar), 141.4 (s, Ar), 142.7 (s, Ar), 144.3 (q, $^2J_{CF}$ 38.4, C3) 145.4 (s, Ar). HRMS (AI+) m/z calc. for $[M+H]^+$ $C_{17}H_{15}N_3O_2F_3S$ 382.0837; found 382.0831. Spectroscopic data consistent with literature results.¹⁶

9.5 Experimental data for Chapter 5

(3-Trifluoromethyl-7-oxa-norborna-2,5-dien-2-yl)-(2'-naphthyl) ketone (**289**).

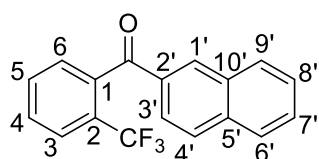


224b (0.557 g, 2.24 mmol) and furan (10 mL) were stirred at room temperature for 6 hours then concentrated *in vacuo* to give (3-trifluoromethyl-7-oxa-norborna-2,5-dien-2-yl)-(2'-naphthyl) ketone, **289** (0.688 g, 97%), as a yellow oil. δ_H (400 MHz; $CDCl_3$) 5.67 (1H, q, $^4J_{HF}$ 1.1, C(4)H), 5.82 (1H, t, $^3J_{HH}$ 1.8, C(7)H), 7.26-7.27 (1H, m, C(5)H), 7.45 (1H, dd, $^3J_{HH}$ 5.3, $^3J_{HH}$ 1.8, C(6)H), 7.61-7.63 (2H, m, C(3'/4')H), 7.93-7.96 (4H, m, (C6'-9')H), 8.36 (1H, s, C(1')H). δ_F (376 MHz; $CDCl_3$) -62.48 (d, $^4J_{HF}$ 1.1). δ_C (101 MHz; $CDCl_3$) 83.9 (q, $^3J_{CF}$ 2.2, C4), 86.9 (s, C7), 122.1 (q, $^1J_{CF}$ 268.9, CF_3), 127.3 (s, Ar), 128.0 (s, Ar), 129.0 (s, Ar), 129.4 (s, Ar), 130.0 (s, Ar), 132.4 (s, Ar), 132.6 (s, Ar), 133.3 (s, Ar), 136.4 (s, Ar), 142.1 (s, Ar), 143.8 (s, Ar), 145.6 (q, $^2J_{CF}$ 36.5, C3), 156.4 (q, $^3J_{CF}$ 4.8, C2), 191.4 (s, C1). HRMS (ESI+) m/z calc. for $[M+H]^+$ $C_{18}H_{12}O_2F_3$ 317.0789; found 317.0781.

General procedure: deoxygenative ring opening.

Ynone **224b** (1 eq.) and the diene (1 eq.) were dissolved in CH_2Cl_2 and stirred at room temperature for 6 hours. The resulting solution was then concentrated *in vacuo* then the residue dissolved in toluene. Diironnonacarbonyl (2 eq.) was added and heated to 80 °C for 2 hours before being allowed to cool to room temperature. The reaction mixture was filtered through a plug of alumina, which was washed with toluene and the combined washings concentrated *in vacuo* to give the benzophenone product without further purification unless otherwise specified.

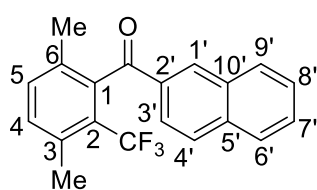
Naphthalen-2-yl-[2-(trifluoromethyl)-phenyl]-methanone (**288**).



Adduct **289** (0.459 g, 1.45 mmol) and diiron nonacarbonyl (1.509 g, 4.15 mmol) gave naphthalen-2-yl-[2-(trifluoromethyl)-phenyl]-methanone, **288** (0.187 g, 43%), as

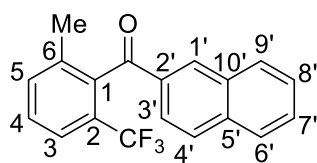
a yellow oil. δ_{H} (400 MHz; CDCl_3) 7.47-7.48 (1H, m), 7.53-7.54 (1H, m), 7.62-7.64 (1H, m), 7.66-7.68 (2H, m), 7.85-7.89 (4H, m), 8.03-8.04 (1H, m), 8.10-8.12 (1H, m). δ_{F} (376 MHz; CDCl_3) -57.94 (s). δ_{C} (101 MHz; CDCl_3) 123.8 (d, $^1J_{\text{CF}}$ 274.0), 124.7 (s, Ar), 126.9 (q, $^3J_{\text{CF}}$ 4.6), 127.0 (s, Ar), 128.0 (s, Ar), 128.4 (s, Ar), 128.4 (d, $^2J_{\text{CF}}$ 32.3), 128.7 (s, Ar), 129.1 (s, Ar), 129.8 (s, Ar), 129.9 (s, Ar), 131.6 (s, Ar), 132.3 (s, Ar), 133.4 (s, Ar), 133.96 (s, Ar), 136.0 (s, Ar), 138.6 (s, Ar), 195.6 (s, C=O). HRMS (ESI+) m/z calc. for $[\text{M}+\text{H}]^+$ $\text{C}_{18}\text{H}_{12}\text{OF}_3$ 301.0840; found 301.0831.

Naphthalen-2-yl-[2-(trifluoromethyl)-3,6-(dimethyl)-phenyl]-methanone (**294**).

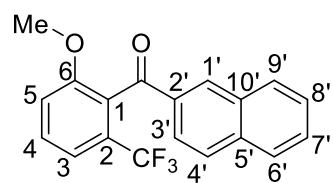


224b (0.033 g, 0.14 mmol), 2,5-dimethylfuran (0.015 mL, 0.14 mmol) and diiron nonacarbonyl (0.098 g, 2.7 mmol) gave naphthalen-2-yl-[2-(trifluoromethyl)-3,6-(dimethyl)-phenyl]-methanone, **294** (0.027 g, 61%), as a yellow solid, m.p. $^{\circ}\text{C}$. δ_{H} (400 MHz; CDCl_3) 2.12 (3H, s, Me), 2.56 (3H, s, Me), 7.33-7.35 (2H, m, Ar), 7.56-7.58 (2H, m, Ar), 7.91-7.96 (5H, m, Ar). δ_{F} (376 MHz; CDCl_3) -54.63 (s). δ_{C} (101 MHz; CDCl_3) 19.3 (s, Me), 20.1 (s, Me), 123.2 (q, $^2J_{\text{CF}}$ 31.9, C2), 124.1 (s, Ar), 126.2 (q, $^1J_{\text{CF}}$ 274.1, CF_3) 126.9 (s, Ar), 128.0 (s, Ar), 128.9 (s, Ar), 129.9 (s, Ar), 131.8 (s, Ar), 132.7 (s, Ar), 132.7 (s, Ar), 133.1 (s, Ar), 133.7 (s, Ar), 134.4 (s, Ar), 135.3 (s, Ar), 135.4 (s, Ar), 136.0 (s, Ar), 138.4 (s, Ar), 197.4 (s, C=O). HRMS (ESI+) m/z calc. for $[\text{M}+\text{H}]^+$ $\text{C}_{20}\text{H}_{16}\text{OF}_3$ 329.1153; found 329.1159.

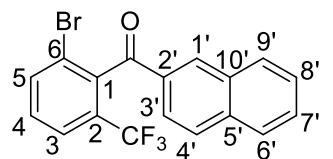
Naphthalen-2-yl-[2-(trifluoromethyl)-6-(methyl)-phenyl]-methanone (**295**).



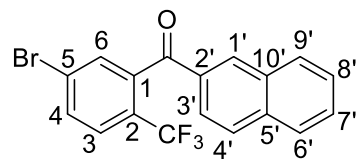
224b (0.086 g, 0.35 mmol), 2-methylfuran (0.0031 mL, 0.35 mmol) and diiron nonacarbonyl (0.247 g, 0.679 mmol) gave naphthalen-2-yl-[2-(trifluoromethyl)-6-(methyl)-phenyl]-methanone, **295** (0.075 g, 69%), as a yellow oil. δ_{H} (400 MHz; CDCl_3) 2.19 (3H, s, Me), 7.52-7.55 (3H, m, Ar-H), 7.62-7.65 (2H, m, Ar-H), 7.89-7.92 (3H, m, Ar-H), 7.99-8.00 (1H, m, Ar-H), 8.11 (1H, s, C(3')H). δ_{F} (376 MHz; CDCl_3) -57.64 (s). δ_{C} (101 MHz; CDCl_3) 19.6 (s, Me), 123.9 (q, $^1J_{\text{CF}}$ 274.3, CF_3), 124.1 (d, $^3J_{\text{CF}}$ 4.8, C1/3), 124.2 (s, Ar), 127.0 (s, Ar), 128.0 (q, $^2J_{\text{CF}}$ 31.6, C2), 128.0 (s, Ar), 128.9 (s, Ar), 129.1 (s, Ar), 129.1 (s, Ar), 129.2 (s, Ar), 129.9 (s, Ar), 132.3 (s, Ar), 132.6 (s, Ar), 134.1 (s, Ar), 134.2 (s, Ar), 136.2 (d, $^3J_{\text{CF}}$ 3.2, C1/3), 137.9 (q, $^4J_{\text{CF}}$ 2.1, C4-6), 196.8 (s, C=O). HRMS (ESI+) m/z calc. for $[\text{M}+\text{H}]^+$ $\text{C}_{19}\text{H}_{14}\text{OF}_3$ 315.0997; found 315.0994.

Naphthalen-2-yl-[2-(trifluoromethyl)-6-methoxyphenyl]-methanone (296).

224b (0.073 g, 0.294 mmol), 2-methoxyfuran (0.027 mL, 0.294 mmol) and diiron nonacarbonyl (0.239 g, 0.657 mmol) gave naphthalen-2-yl-[2-(trifluoromethyl)-6-methoxyphenyl]-methanone, **296** (0.072 g, 74%), as a yellow oil. δ_{H} (400 MHz; CDCl_3) 3.72 (3H, s, OMe), 7.20 (1H, m, C(2'-5')H), 7.39 (1H, m, C(2'-5')H), 7.52 (1H, m, C(2'-5')H), 7.59 (2H, m, C(3'/4')H), 7.89 (3H, m, C(6'-9')H), 7.99 (1H, m, C(6'-9')H), 8.16 (1H, m, C(1')H). δ_{F} (376 MHz; CDCl_3) -58.05 (s). δ_{C} (101 MHz; CDCl_3) 56.31 (s, OMe), 114.67 (s, Ar), 118.44 (q, $^3J_{\text{CF}}$ 4.7, C1), 123.56 (q, $^1J_{\text{CF}}$ 274.4, CF_3), 124.35 (s, Ar), 126.82 (s, Ar), 127.85 (s, Ar), 127.97 (s, Ar), 128.58 (s, Ar), 128.84 (s, Ar), 129.33 (q, $^2J_{\text{CF}}$ 32.2, C2), 129.89 (s, Ar), 130.81 (s, Ar), 132.05 (s, Ar), 132.62 (s, Ar), 134.61 (s, Ar), 136.07 (s, Ar), 157.26 (s, C6), 194.48 (s, C=O). HRMS (ESI+) m/z calc. for $[\text{M}+\text{H}]^+$ $\text{C}_{19}\text{H}_{14}\text{O}_2\text{F}_3$ 331.0946; found 331.0943.

Naphthalen-2-yl-[2-(trifluoromethyl)-6-bromophenyl]-methanone (297).

224b (0.076 g, 0.031 mmol), 2-bromofuran (0.045 mL, 0.031 mmol) and diiron nonacarbonyl (0.220 g, 0.062 mmol) gave naphthalen-2-yl-[2-(trifluoromethyl)-phenyl]-methanone, **297** (0.104 g, 89%), as a yellow oil. δ_{H} (400 MHz; CDCl_3) 7.23-7.24 (1H, m, Ar), 7.37-7.38 (1H, m, Ar), 7.62-7.65 (3H, m, Ar), 7.93-7.95 (2H, m, Ar), 8.00-8.02 (2H, m, Ar), 8.36-8.37 (1H, m, Ar). δ_{F} (376 MHz; CDCl_3) -63.41 (s). δ_{C} (101 MHz; CDCl_3) 119.3 (q, $^3J_{\text{CF}}$ 4.7, C1), 121.0 (s, Ar), 123.7 (q, $^1J_{\text{CF}}$ 274.4, CF_3), 124.4 (s, Ar), 125.7 (s, Ar), 127.1 (s, Ar), 128.1 (s, Ar), 128.3 (q, $^2J_{\text{CF}}$ 32.4, C2), 129.0 (s, Ar), 129.3 (s, Ar), 130.0 (s, Ar), 130.7 (s, Ar), 131.3 (s, Ar), 132.6 (s, Ar), 136.3 (s, Ar), 136.7 (s, Ar), 172.2 (s, C6), 193.3 (s, C=O). HRMS (ESI+) m/z calc. for $[\text{M}+\text{H}]^+$ $\text{C}_{18}\text{H}_{11}\text{OF}_3(^{79}\text{Br})$ 378.9945; found 378.9954.

Naphthalen-2-yl-[2-(trifluoromethyl)-5-bromophenyl]-methanone (298).

224b (0.171 g, 0.689 mmol), 3-bromofuran (0.061 mL, 0.69 mmol) and diiron nonacarbonyl (0.664 g, 1.83 mmol) gave naphthalen-2-yl-[2-(trifluoromethyl)-5-bromophenyl]-methanone, **298** (0.204 g, 78%), as a yellow oil. δ_{H} (400 MHz; CDCl_3) 7.52-7.55 (2H, m, Ar), 7.63-7.64 (1H, m, Ar), 7.78-7.79 (1H, m, Ar), 7.89-7.93 (5H, m, Ar), 8.12-8.13 (1H, m, Ar). δ_{F} (376 MHz; CDCl_3) -58.07 (s).

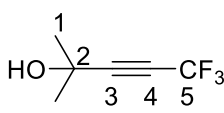
δ_C (101 MHz; $CDCl_3$) 119.2 (q, $^3J_{CF}$ 4.6, C1), 121.0 (s, Ar), 123.7 (q, $^1J_{CF}$ 274.2, CF_3), 124.3 (s, Ar), 125.7 (s, Ar), 127.1 (s, Ar), 128.1 (s, Ar), 128.3 (q, $^2J_{CF}$ 32.3, C2), 129.0 (s, Ar), 129.2 (s, Ar), 130.0 (s, Ar), 130.7 (s, Ar), 131.2 (s, Ar), 132.6 (s, Ar), 136.2 (s, Ar), 136.7 (s, Ar), 172.2 (s, C5), 193.3 (s, C=O). HRMS (ESI+) m/z calc. for $[M+H]^+$ $C_{18}H_{11}OF_3(^{79}Br)$ 378.9945; found 378.9960.

9.6 Experimental data for Chapter 6

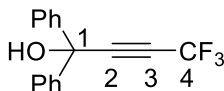
General procedure: addition of trifluoropropynide to ketones

Anhydrous diisopropylamine (2 eq.) was dissolved in a solution of **1** (1 eq.) in either anhydrous diethyl or methyl *tert*-butyl ether under argon at -78 °C. *n*-Butyl lithium (2.5 M in hexanes, 2 eq.) was added dropwise and the resulting solution stirred at 0 °C for 5 minutes. The ketone (as a solution in the appropriate ether if solid, 0.9 eq.) was added dropwise at -78 °C then the reaction mixture was stirred at 0 °C for 4 hours. The reaction mixture was allowed to warm to room temperature then quenched by pouring into saturated aqueous ammonium chloride. The aqueous layer was separated and extracted twice with the appropriate ether then the combined organic extracts washed with 1M HCl then with brine, dried over $MgSO_4$ then concentrated *in vacuo* to give the tertiary alcohol product without further purification unless otherwise specified.

2-Methyl-5,5,5-trifluoropent-3-yn-2-ol (**308**).

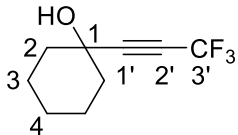

 Following the general procedure, **1** (1.64 g, 14.4 mmol), diisopropylamine (4.0 mL, 29 mmol), *n*-butyl lithium (11.5 mL, 28.9 mmol) and acetone (0.9 mL, 0.12 mmol) in Et_2O (80 mL) gave 2-methyl-5,5,5-trifluoropent-3-yn-2-ol, **308** (1.11 g, 61%), as a colourless oil. δ_H (400 MHz; $CDCl_3$) 1.53 (s, Me), 3.09 (br s, O-H). δ_F (376 MHz; $CDCl_3$) -50.45 (s). δ_C (101 MHz; $CDCl_3$) 30.4 (s, Me), 64.8 (s, C(2)-OH), 69.4 (q, $^2J_{CF}$ 52.5, C4), 91.8 (q, $^3J_{CF}$ 6.5, C3), 114.3 (q, $^1J_{CF}$ 257.0, C5). HRMS (ESI+) m/z calc. for $[M+H]^+$ $C_{11}H_{10}OF_3$ 153.0527; found 153.1749. Spectroscopic data consistent with literature reports.¹⁷

1,1-Diphenyl-4,4,4-trifluorobut-2-yn-1-ol (**309**).

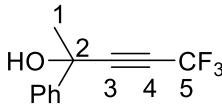

 Following the general procedure, **1** (0.97 g, 8.5 mmol), diisopropylamine (2.4 mL, 17 mmol), *n*-butyl lithium (7.0 mL, 17.5

mmol) and benzophenone (1.314 g, 7.211 mmol) in MTBE (50 mL) gave 1,1-diphenyl-4,4,4-trifluorobut-2-yn-1-ol, **309** (1.23 g, 62%), as a white solid, m.p. 56-57 °C (lit. 54-56 °C).¹⁸ δ_{H} (400 MHz; CDCl_3) 3.02 (1H, s, OH), 7.31-7.44 (4H, m), 7.51-7.58 (6H, m). δ_{F} (376 MHz; CDCl_3) -50.31 (s). δ_{C} (101 MHz; CDCl_3) 74.3 (q, $^4J_{\text{CF}}$ 4.5, C(2)-OH), 89.3 (q, $^2J_{\text{CF}}$ 53.2, C3), 114.3 (q, $^1J_{\text{CF}}$ 257.7, C4), 126.0 (s, Ar, C-H), 128.6 (s, Ar C-C), 128.8 (s, Ar C-H), 142.6 (s, Ar C-C). HRMS (ESI+) m/z calc. for $[\text{M}+\text{H}]^+$ $\text{C}_{16}\text{H}_{12}\text{OF}_3$ 277.0840; found 277.2381. Spectroscopic data consistent with literature reports.¹⁸

1-(3',3',3'-Trifluoroprop-1'-ynyl)-1-cyclohexanol (**310**).

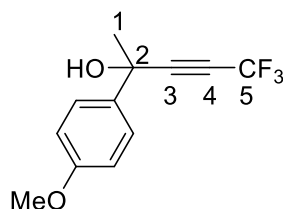
 Following the general procedure, **1** (0.85 g, 7.5 mmol), diisopropylamine (2.1 mL, 15 mmol), *n*-butyl lithium (6.0 mL, 15 mmol) and cyclohexanone (0.66 g, 6.72 mmol) in Et_2O (50 mL) gave 1-(3',3',3'-trifluoroprop-1'-ynyl)-1-cyclohexanol, **310** (0.97 g, 67%), as a yellow oil. δ_{H} (400 MHz; CDCl_3) 1.23-1.35 (1H, m), 1.44-1.59 (2H, m), 1.58-1.69 (1H, m), 1.67-1.79 (1H, m), 1.80-1.91 (2H, m), 1.90-2.00 (1H, m), 2.31-2.35 (1H, m), 2.36-2.54 (1H, m). δ_{F} (376 MHz; CDCl_3) -50.07 (s). δ_{C} (101 MHz; CDCl_3) 22.8 (s, CH_2), 24.9 (s, CH_2), 27.1 (s, CH_2), 38.9 (s, CH_2), 42.0 (s, CH_2), 71.6 (q, $^2J_{\text{CF}}$ 52.4, C2'), 90.8 (q, $^3J_{\text{CF}}$ 6.4, C1'), 114.3 (q, $^1J_{\text{CF}}$ 257.2, C3'), 212.91 (s, C(1)-O). HRMS (ESI+) m/z calc. for $[\text{M}+\text{H}]^+$ $\text{C}_9\text{H}_{12}\text{OF}_3$ 193.0840; found 193.0809. Spectroscopic data consistent with literature reports.¹⁷

1-Phenyl-5,5,5-trifluoropent-3-yn-2-ol (**311**).

 Following the general procedure, diisopropylamine (3.5 mL, 25 mmol), *n*-butyllithium (10 mL, 25 mmol), **1** (1.40 g, 12.3 mmol) and acetophenone (1.03 g, 8.57 mmol) in MTBE (40 mL) after 6 hours gave the crude product as a brown oil, which was purified by flash column chromatography over silica gel (hexane/ethyl acetate 10:1) to give 1-phenyl-5,5,5-trifluoropent-3-yn-2-ol, **311** (1.47 g, 80%), as a yellow oil. δ_{H} (400 MHz; CDCl_3) 1.81 (3H, s, Me), 2.67 (br s, OH), 7.36-7.39 (3H, m, Ar-H), 7.58-7.60 (2H, m, Ar-H). δ_{F} (376 MHz; CDCl_3) -50.35 (s). δ_{C} (101 MHz; CDCl_3) 32.3 (s, Me), 69.8 (q, $^4J_{\text{CF}}$ 1.4, C1), 72.1 (q, $^2J_{\text{CF}}$ 52.9, C3), 90.1 (q, $^3J_{\text{CF}}$ 6.5, C2), 114.3 (q, $^1J_{\text{CF}}$ 257.7, C4), 124.7 (s, C3'/4'), 128.6 (s, C5'), 128.8 (s, C3'/4'), 143.1 (s, C2'). LC-MS (ESI+) m/z 214 (M^+ , 15%), 193 (100, $[\text{M}-\text{HF}]^+$), 115 (34, $[\text{M}-\text{Ph}]^+$), 106 (11, PhMe^+). HRMS (ESI+) m/z calc. for $[\text{M}]^+$

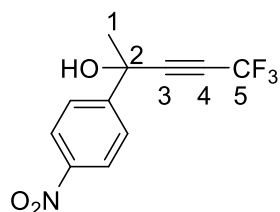
$C_{11}H_9OF_3$ 214.0606; found 214.1357. Spectroscopic data consistent with literature reports.¹⁷

1-(4-Methoxyphenyl)-5,5,5-trifluoropent-3-yn-2-ol (**312**).

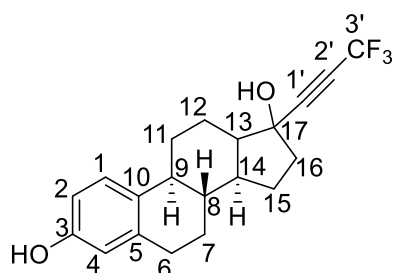


Following the general procedure, **1** (0.274 g, 2.40 mmol), diisopropylamine (0.7 mL, 5.2 mmol), *n*-butyl lithium (1.9 mL, 4.8 mmol) and 4-methoxyacetophenone (0.507 g, 3.40 mmol) in Et₂O (50 mL) gave 1-(4-methoxyphenyl)-5,5,5-trifluoropent-3-yn-2-ol, **312** (0.456 g, 55%), as a yellow oil. δ_H (400 MHz; CDCl₃) 2.52 (3H, s, C-Me), 3.84 (3H, s, O-Me), 7.46-7.53 (2H, m, Ar), 7.87-7.93 (2H, m, Ar). δ_F (376 MHz; CDCl₃) -50.20 (s). δ_C (101 MHz; CDCl₃) 26.1 (s, Me), 32.1 (s, Me), 69.0 (q, $^4J_{CF}$ 1.4, C1), 71.3 (q, $^2J_{CF}$ 52.5, C3), 90.9 (q, $^3J_{CF}$ 6.5, C2), 113.7 (s, Ar C-H), 114.3 (q, $^1J_{CF}$ 257.3, C4), 126.0 (s, Ar C-H), 135.5 (s, Ar C-C), 159.4 (s, Ar C-O). HRMS (ESI+) m/z calc. for [M+H]⁺ C₁₂H₁₂O₂F₃ 245.0789; found 245.0754.

1-(4-Nitrophenyl)-5,5,5-trifluoropent-3-yn-2-ol (**313**).



Following the general procedure, **1** (0.286 g, 2.51 mmol), diisopropylamine (0.7 mL, 5.2 mmol), *n*-butyl lithium (2.1 mL, 5.3 mmol) and 4-nitroacetophenone (0.373 g, 2.23 mmol) in Et₂O (50 mL) gave 1-(4-nitrophenyl)-5,5,5-trifluoropent-3-yn-2-ol, **313** (0.451 g, 78%), as a yellow oil. δ_H (400 MHz; CDCl₃) 1.83 (3H, s, Me), 3.90 (1H, br s, O-H), 7.70-7.79 (2H, m, Ar), 8.15-8.22 (2H, m, Ar). δ_F (376 MHz; CDCl₃) -50.63 (s). δ_C (101 MHz; CDCl₃) 32.56 (s, C1), 72.41 (q, $^2J_{CF}$ 53.1, C4), 88.99 (q, $^3J_{CF}$ 6.4, C3), 114.11 (q, $^1J_{CF}$ 258.1, C5), 123.91 (s, Ar C-H), 125.94 (s, Ar C-H), 129.47 (s, Ar C-C), 147.74 (s, Ar C-N), 197.38 (s, C2). HRMS (ESI+) m/z calc. for [M+H]⁺ C₁₁H₉NO₃F₃ 260.0534; found 259.0456. Spectroscopic data consistent with literature results.¹⁹



17 α -(Trifluoropropynyl)-1,3,5(10)-estratriene-3,17 β -diol (**314**).

1 (0.97 g, 8.5 mmol), diisopropylamine (5.0 mL, 36 mmol), *n*-butyl lithium (14 mL, 35 mmol) and estrone (1.01 g, 3.74 mmol) in MTBE (35 mL) and THF (15 mL) gave 17 α -(trifluoropropynyl)-1,3,5(10)-estratriene-

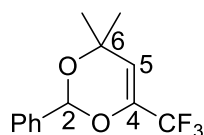
3,17β-diol, **314** (0.42 g, 32%), as a yellow oil. δ_{H} (400 MHz; DMSO- d_6) 1.17-1.18 (1H, m), 1.31-1.33 (2H, m), 1.46-1.47 (1H, m), 1.60-1.62 (1H, m), 1.74-1.77 (2H, m), 1.93-1.94 (1H, m), 1.97-1.99 (1H, s), 2.06-2.07 (1H, m), 2.20-2.21 (1H, m), 2.30-2.32 (1H, m), 2.68-2.71 (2H, m), 4.01-4.03 (2H, m), 6.05-6.06 (1H, s, C(3)H), 6.43 (1H, d, $^4J_{\text{HH}}$ 2.6, Ar C-H), 6.51 (1H, dd, $^3J_{\text{HH}}$ 8.5, $^4J_{\text{HH}}$ 2.6, Ar C-H), 7.04 (1H, d, $^3J_{\text{HH}}$ 8.5, Ar C-H), 8.99 (1H, s, C(17)H). δ_{F} (376 MHz; DMSO- d_6) -48.13 (s). δ_{C} (101 MHz; DMSO- d_6) 14.1 (s, CH), 20.7 (s, CH), 22.5 (s, CH₂), 26.0 (s, CH₂), 26.9 (s, CH₂), 29.1 (s, CH₂), 32.8 (s, CH₂), 38.1 (s, CH₂), 43.2 (s, CH), 49.6 (s, CH), 70.7 (q, $^2J_{\text{CF}}$ 51.1), 94.4 (q, $^3J_{\text{CF}}$ 6.5), 112.8 (s, Ar C-H), 114.2 (q, $^1J_{\text{CF}}$ 256.0), 114.9 (s, Ar, C-H), 126.1 (s, Ar, C-H), 129.9 (s, Ar C-C), 137.0 (s, Ar C-C), 155.0 (s, C10), 170.2 (s, C17). HRMS (ESI+) m/z calc. for $[\text{M}+\text{H}]^+$ C₂₀H₂₂O₂F₃ 351.1572; found 351.3850. Spectroscopic data consistent with literature reports.²⁰

General procedure: deacetonative Sonogashira coupling.

An aryl bromide (1 eq.), Pd(PPh₃)Cl₂ (5 mol-%), CuI (10 mol-%), K₃PO₄ (2.5 eq.) and trifluoropropynyl alcohol (2 eq.) were all dissolved in diisopropylamine (5 mL) in a 10 mL glass vial which was then sealed with a Teflon-lined cap and purged with argon for 10 minutes. The resulting mixture was stirred at 100 °C for 2 hours then allowed to cool to room temperature before being filtered through a silica plug, which was washed with hexane. The resulting solution was concentrated *in vacuo* to give the product without further purification unless otherwise specified.

General procedure: dioxene synthesis.

Alkynol **308** or **310** (1 eq.), aldehyde (1.1 eq.) and KO^tBu (1 eq.) were dissolved in that order in THF (10 mL) then refluxed at 80 °C for one hour before being poured into a saturated aqueous solution of sodium bisulfite at room temperature and stirred for a further 20 minutes. The resulting mixture was extracted twice with dichloromethane, the combined organic extracts were washed with saturated aqueous sodium bicarbonate, dried over MgSO₄ and concentrated *in vacuo* to give the product dioxene without further purification unless otherwise specified.

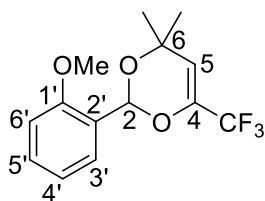


2-Phenyl-4-trifluoromethyl-6,6-dimethyl-1,3-diox-4-ene (**319**).

308 (0.129 g, 0.848 mmol), benzaldehyde (0.1 mL, 0.98 mmol) and KO^tBu (0.09 g, 0.8 mmol) gave 2-phenyl-4-trifluoromethyl-6,6-

dimethyl-1,3-diox-4-ene, **319** (0.127 g, 64%), as a yellow oil. δ_{H} (400 MHz; CDCl_3) 1.52 (3H, s, Me), 1.57 (3H, s, Me), 4.58 (1H, q, $^3J_{\text{HF}}$ 7.6, C(5)H), 6.30 (1H, s, C(2)H), 7.41-7.44 (3H, m, Ar-H), 7.48-7.50 (2H, m, Ar-H). δ_{F} (376 MHz; CDCl_3) -56.78 (d, $^3J_{\text{HF}}$ 7.6). δ_{C} (101 MHz; CDCl_3) 25.0 (s, Me), 26.8 (s, Me), 83.0 (s, C6), 83.9 (q, $^2J_{\text{CF}}$ 36.6, C4), 105.1 (s, C2), 124.0 (q, $^1J_{\text{CF}}$ 268.4, CF_3), 126.9 (s, Ar C-H), 128.7 (s, Ar C-H), 130.3 (s, Ar C-H), 135.4 (s, Ar C-C), 165.6 (q, $^3J_{\text{CF}}$ 5.1, C5). HRMS (ESI+) m/z calc. for $[\text{M}+\text{H}]^+$ $\text{C}_{11}\text{H}_{15}\text{O}_2\text{F}_3$ 235.0946; found 235.0904.

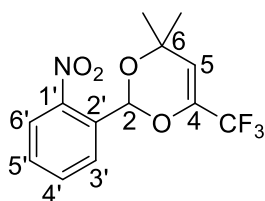
2-(2'-Methoxyphenyl)-4-trifluoromethyl-6,6-dimethyl-1,3-diox-4-ene (320).



308 (0.109 g, 0.717 mmol), 2-methoxybenzaldehyde (0.103 g, 0.757 mmol) and KO^tBu (0.084 g, 0.749 mmol) gave 2-(2'-methoxyphenyl)-4-trifluoromethyl-6,6-dimethyl-1,3-diox-4-ene, **320** (0.074 g, 36%), as a yellow oil. δ_{H} (400 MHz; CDCl_3) 1.36 (3H, s, Me), 1.49 (3H, s, Me), 1.54 (3H, s, Me), 4.54 (1H, q, $^3J_{\text{HF}}$ 7.7, C(2)H), 6.66 (1H, s, C(5)H), 7.28-7.41 (2H, m, Ar-H), 7.43-7.48 (1H, m, Ar-H), 7.55-7.64 (1H, m, Ar-H).

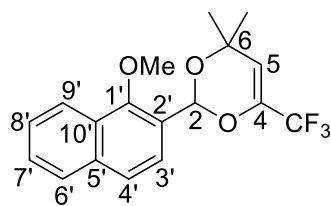
δ_{F} (376 MHz; CDCl_3) -56.69 (d, $^3J_{\text{HF}}$ 7.7). δ_{C} (101 MHz; CDCl_3) 25.0 (s, Me), 26.1 (s, Me), 26.6 (s, Me), 82.74 (s, C6) 83.3 (q, $^2J_{\text{CF}}$ 36.5, C4), 100.8 (s, C2), 124.8 (s, Ar C-H), 126.2 (s, Ar C-H), 127.4 (s, Ar C-H), 130.1 (q, $^1J_{\text{CF}}$ 268.3, CF_3), 131.7 (s, Ar C-C), 138.3 (s, Ar C-H), 157.9 (s, Ar C-O), 165.9 (q, $^3J_{\text{CF}}$ 5.0, C5). HRMS (ESI+) m/z calc. for $[\text{M}+\text{H}]^+$ $\text{C}_{14}\text{H}_{16}\text{O}_3\text{F}_3$ 289.1052; found 289.1042.

2-(2'-Nitrophenyl)-4-trifluoromethyl-6,6-dimethyl-1,3-diox-4-ene (321).

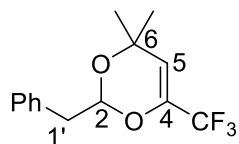


308 (0.102 g, 0.671 mmol), 2-nitrobenzaldehyde (0.101 g, 0.664 mmol) and KO^tBu (0.075 g, 0.669 mmol) gave 2-(2'-nitrophenyl)-4-trifluoromethyl-6,6-dimethyl-1,3-diox-4-ene, **321** (0.159 g, 79%), as a yellow oil. δ_{H} (400 MHz; CDCl_3) 1.46 (3H, s, Me), 1.53 (3H, s, Me), 4.63 (1H, q, $^3J_{\text{HF}}$ 7.6, C(2)H), 6.95 (1H, s, C(5)H), 7.73-7.78 (1H, m, Ar-H), 7.92-7.96 (1H, m, Ar-H), 7.96-8.03 (1H, m, Ar-H), 8.08-8.13 (1H, m, Ar-H).

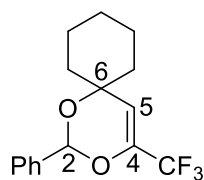
δ_{F} (376 MHz; CDCl_3) -56.87 (d, $^3J_{\text{HF}}$ 7.6). δ_{C} (101 MHz; CDCl_3) 25.3 (s, Me), 26.5 (s, Me), 83.3 (s, C6), 84.8 (q, $^2J_{\text{CF}}$ 36.8, C4), 100.8 (s, C2), 123.5 (s, Ar C-H), 127.8 (s, Ar C-H), 129.2 (q, $^1J_{\text{CF}}$ 264.6, CF_3), 129.4 (s, Ar C-H), 134.2 (s, Ar C-C), 134.7 (s, Ar C-H), 164.8 (q, $^3J_{\text{CF}}$ 5.1, C5), 171.2 (s, Ar C-N). HRMS (ESI+) m/z calc. for $[\text{M}+\text{H}]^+$ $\text{C}_{13}\text{H}_{13}\text{NO}_4\text{F}_3$ 304.0797; found 304.0718.

2-(2'-Naphthyl)-4-trifluoromethyl-6,6-dimethyl-1,3-diox-4-ene (322).

308 (0.181 g, 1.19 mmol), 2-naphthaldehyde (0.187 g, 1.20 mmol) and KO^tBu (0.134 g, 0.120 mmol) gave 2-(2'-naphthyl)-4-trifluoromethyl-6,6-dimethyl-1,3-diox-4-ene, **322** (0.233 g, 63%), as a yellow oil. δ_{H} (400 MHz; CDCl₃) 1.54 (3H, s, Me), 1.59 (3H, s, Me), 4.63 (1H, q, $^3J_{\text{HF}}$ 7.7, C(2)H), 6.43 (1H, s, C(5)H), 7.44-7.66 (2H, m, Ar-H), 7.76-8.00 (4H, m, Ar-H), 8.25-8.28 (1H, m, Ar-H). δ_{F} (376 MHz; CDCl₃) -56.61 (d, $^3J_{\text{HF}}$ 7.7). δ_{C} (101 MHz; CDCl₃) 24.9 (s, Me), 26.7 (s, Me), 83.1 (s, C6), 83.8 (q, $^2J_{\text{CF}}$ 36.5, C4), 105.2 (s, C2), 123.3 (s, Ar), 126.5 (s, Ar), 127.0 (s, Ar), 127.8 (s, Ar), 128.4 (s, Ar), 128.7 (s, Ar), 132.6 (s, Ar), 133.5 (q, $^1J_{\text{CF}}$ 264.7, CF₃), 134.1 (s, Ar), 134.2 (s, Ar), 136.4 (s, Ar), 165.5 (q, $^3J_{\text{CF}}$ 5.1, C5). HRMS (ESI⁺) m/z calc. for [M+H]⁺ C₁₇H₁₆O₂F₃ 309.1102; found 309.1024.

2-(1'-Phenylmethyl)-4-trifluoromethyl-6,6-dimethyl-1,3-diox-4-ene (323).

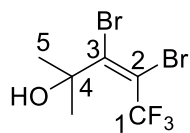
308 (0.180 g, 0.119 mmol), phenylacetaldehyde (0.143 g, 1.19 mmol) and KO^tBu (0.132 g, 1.18 mmol) gave 2-(1'-phenylmethyl)-4-trifluoromethyl-6,6-dimethyl-1,3-diox-4-ene, **323** (0.206 g, 70%), as a yellow oil. δ_{H} (400 MHz; CDCl₃) 2.08 (3H, s, Me), 2.14 (3H, s, Me), 3.12 (2H, q, $^3J_{\text{HH}}$ 4.4, C(1')H₂), 4.47 (1H, q, $^3J_{\text{HF}}$ 7.7, C(2)H), 5.65 (1H, t, $^3J_{\text{HH}}$ 4.4, C(5)H), 7.45-7.56 (2H, m, Ar), 7.57-7.70 (2H, m, Ar), 8.09-8.18 (2H, m, Ar). δ_{F} (376 MHz; CDCl₃) -56.74 (d, $^3J_{\text{HF}}$ 7.7). δ_{C} (101 MHz; CDCl₃) 21.1 (s, Me), 25.2 (s, Me), 50.6 (s, CH₂), 82.6 (s, C6), 83.4 (q, $^2J_{\text{CF}}$ 36.6, C4), 105.9 (s, C2), 127.0 (s, Ar), 127.5 (s, Ar), 129.1 (s, Ar), 129.7 (s, Ar), 133.0 (q, $^1J_{\text{CF}}$ 263.0, CF₃), 165.5 (q, $^3J_{\text{CF}}$ 5.2, C5). HRMS (ESI⁺) m/z calc. for [M+H]⁺ C₁₄H₁₆O₂F₃ 273.1102; found 273.1024.

2-Phenyl-4-trifluoromethyl-6,6-cyclohexyl-1,3-diox-4-ene (324).

310 (0.554 g, 2.87 mmol), benzaldehyde (0.3 mL, 2.9 mmol) and KO^tBu (0.326 g, 2.91 mmol) gave 2-phenyl-4-trifluoromethyl-6,6-cyclohexyl-1,3-diox-4-ene, **324** (0.530 g, 62%), as a yellow oil. δ_{H} (400 MHz; CDCl₃) 1.35-1.50 (1H, m), 1.56-1.67 (1H, m), 1.68-1.84 (4H, m), 1.82-2.01 (2H, m), 2.04-2.20 (2H, m), 4.59 (1H, q, $^3J_{\text{HF}}$ 7.7, C(2)H), 6.31 (1H, s, C(5)H), 7.43-7.48 (3H, m, Ar), 7.52-7.56 (2H, m, Ar). δ_{F} (376 MHz; CDCl₃) -56.51 (d, $^3J_{\text{HF}}$ 7.7). δ_{C} (101 MHz; CDCl₃) 21.91 (s, Cy C-H), 22.20 (s, Cy C-H), 24.97 (s, Cy C-H), 33.15 (s, Cy C-H), 35.72 (s, Cy C-H), 42.05 (s, Cy C-C), 84.16 (q, $^2J_{\text{CF}}$ 36.6, C4), 84.77 (s, C6),

105.26 (s, C2), 124.14 (q, $^1J_{CF}$ 268.2, CF₃), 126.98 (s, Ar C-H), 128.63 (s, Ar C-H), 130.25 (s, Ar C-C), 165.58 (q, $^3J_{CF}$, C5). HRMS (ESI+) m/z calc. for [M+H]⁺ C₁₆H₁₈O₂F₃ 299.1259; found 299.1260.

1,1,1-Trifluoro-2,3-dibromo-4-methylpent-2-yn-4-ol (**325**).



308 (0.552 g, 3.63 mmol) was dissolved in dichloromethane (20 mL) and bromine (0.2 mL, 3.9 mmol) was added. The resulting mixture was stirred at room temperature for 2 hours then saturated aqueous sodium

thiosulfate was added and stirred vigorously for 10 minutes. The aqueous layer was separated and extracted with dichloromethane then the combined organic extracts were washed with thiosulfate solution then sodium bicarbonate solution, dried over MgSO₄ and concentrated *in vacuo* to give 1,1,1-trifluoro-2,3-dibromo-4-methylpent-2-yn-4-ol, **325** (0.967 g, 86%), as a yellow oil. δ_H (400 MHz; CDCl₃) 1.68 (s). δ_F (376 MHz; CDCl₃) -57.79 (s). δ_C (101 MHz; CDCl₃) 28.77 (s, C5), 76.90 (s, C4), 105.56 (q, $^2J_{CF}$ 37.3, C2), 120.33 (q, $^1J_{CF}$ 274.6, C1), 139.09 (q, $^3J_{CF}$ 2.4, C3). HRMS (ESI+) m/z calc. for [M+H]⁺ C₆H₈OF₃(⁷⁹Br)₂ 309.8816; found 309.8894.

Benzylammonium hexafluorosilicate (**329**).

308 (0.273 g, 1.79 mmol) and benzylamine (0.2 mL, 1.8 mmol) were dissolved in ethanol (30 mL) and heated to 80 °C for 24 hours. The resulting white precipitate was filtered and then recrystallised from water to give single crystals of benzylammonium hexafluorosilicate (**329**) suitable for X-ray crystallography. δ_H (400 MHz; DMSO-*d*₆) 3.98 (2H, br s, CH₂), 6.86-7.70 (4H, m, Ar-H), 7.90 (1H, br s, Ar-H). δ_F (376 MHz; DMSO-*d*₆) -123.51 (br s).

9.7 Experimental data for Chapter 7

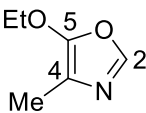
General procedure: *N*-protection of DL-alanine ethyl ester hydrochloride.

Ethyl 2-aminopropanoate hydrochloride (**330**) was dissolved in the appropriate triethyl orthoester and heated to reflux at 145 °C for 2 hours. Excess orthoester and ethanol were removed *in vacuo* to give the *N*-protected aminopropanoate, which was taken forward to the next step without further purification. Spectroscopic data of products were consistent with literature values.²¹

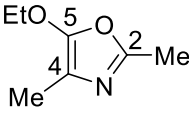
General procedure: Robinson-Gabriel oxazole synthesis.

Phosphorus pentoxide was dissolved in chloroform (150 mL) and stirred vigorously at room temperature until homogenous. Ethyl *N*-protected 2-aminopropanoate was then added dropwise and the resulting mixture was heated to reflux at 65 °C. On cooling to room temperature, the reaction mixture was neutralised with saturated aqueous sodium bicarbonate, added carefully at 0 °C, and then extracted twice with chloroform. The combined organic extracts were washed with brine then dried over MgSO₄ and concentrated *in vacuo* to give the oxazole, which was taken forward to the next step without further purification.

4-Methyl-5-ethoxyoxazole (331).

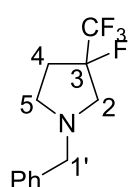
 Ethyl *N*-formyl-2-aminopropanoate (3.82 g, 26.3 mmol) and phosphorus pentoxide (20.3 g, 71.5 mmol) after 1.5 hours gave 4-methyl-5-ethoxyoxazole, **331** (2.29 g, 68%), as a dark orange oil. δ_{H} (400 MHz; CDCl₃) 1.36 (3H, t, $^3J_{\text{HH}}$ 7.1, OEt CH₃), 2.05 (3H, s, Me), 4.15 (2H, q, $^3J_{\text{HH}}$ 7.1, OEt CH₂), 7.38 (1H, s, C(2)H). δ_{C} (101 MHz; CDCl₃) 9.9 (s, Me), 14.9 (s, OEt CH₃), 70.1 (s, OEt CH₂), 112.2 (s, C4), 142.2 (s, C5), 154.2 (s, C2). GC-MS (EI+) m/z 127 (M⁺, 94%), 99 ([M-Et]⁺, 94), 71 ([M-HCOEt]⁺, 96), 42 ([NCMe+H]⁺, 100). HRMS (AI+) m/z calc. for [M+H]⁺ C₆H₁₀NO₂ 128.0712; found 128.0742. Spectroscopic data consistent with literature values.²¹

2,4-Dimethyl-5-ethoxyoxazole (332).

 Ethyl *N*-acetyl-2-aminopropanoate (4.88 g, 30.7 mmol) and phosphorus pentoxide (21.07 g, 74.2 mmol) after 2 hours gave 2,4-dimethyl-5-ethoxyoxazole, **332** (2.25 g, 52%), as a yellow oil. δ_{H} (400 MHz; CDCl₃) 1.17 (3H, t, $^3J_{\text{HH}}$ 7.1, OEt CH₃), 1.82 (3H, s, C(4)Me), 2.13 (3H, s, C(2)Me), 3.93 (2H, q, $^3J_{\text{HH}}$ 7.1, OEt CH₂). δ_{C} (101 MHz; CDCl₃) 9.70 (s, C(2)Me), 13.93 (s, C(4)Me), 14.73 (s, OEt CH₃), 69.97 (s, OEt CH₂), 112.32 (s, C4), 151.85 (s, C5), 153.43 (s, C2). GC-MS (EI+) m/z 141 ([M]⁺, 88%), 113 ([M-Et]⁺, 54), 85 ([M-HCOEt]⁺, 65), 43 ([NCMe+H]⁺, 100), 42 (NCMe⁺, 100). HRMS (AI+) m/z calc. for [M+H]⁺ C₇H₁₂NO₂ 142.0868; found 142.0877. Spectroscopic data consistent with literature values.²¹

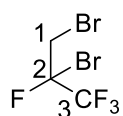
General procedure: Diels-Alder reaction of 2,3,3,3-tetrafluoropropene.

A glass Carius tube was charged with the diene then cooled to $-196\text{ }^{\circ}\text{C}$ and **1** was condensed. The Carius tube was then evacuated and sealed while still cold then heated in a blast-proof furnace overnight. On cooling to room temperature, the Carius tube was again cooled to $-196\text{ }^{\circ}\text{C}$ and opened. On warming to room temperature, the contents were extracted with ethyl acetate and concentrated *in vacuo* to give the crude product.

***N*-Benzyl-3-fluoro-3-(trifluoromethyl)pyrrolidine (98).**

N-Benzyl-*N*-(methoxymethyl)-*N*-(trimethylsilylmethyl)amine (**97**, 10 mL, 39 mmol) was dissolved in anhydrous THF (100 mL) and stirred under an atmosphere of **1** (15 g, 130 mmol) at room temperature for 16 hours. 2,2,2-

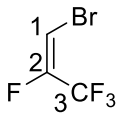
Trifluoroacetic acid (0.3 g, 4 mmol) was separately dissolved in anhydrous THF (5 mL) and added over 20 minutes via syringe pump to the solution of **1** and **97** at $0\text{ }^{\circ}\text{C}$. The resulting mixture was stirred at $0\text{ }^{\circ}\text{C}$ for 2 hours then allowed to warm to room temperature. The reaction was quenched by pouring into saturated aqueous sodium bicarbonate and then extracted twice with MTBE. The combined organic extracts were washed with brine, dried over MgSO_4 and concentrated *in vacuo* to give the crude product as a dark yellow oil, which was then purified by column chromatography (CombiFlash hexane/ethyl acetate 0-100 % over 10 min) then dried *in vacuo* to give *N*-benzyl-3-fluoro-3-(trifluoromethyl)pyrrolidine, **98** (4.34 g, 45%), as a clear, pale yellow oil. δ_{H} (400 MHz; CDCl_3) 2.31-2.35 (2H, m, C(2-5)H), 2.62-2.64 (1H, m, C(2-5)H), 2.91-2.96 (2H, m, C(2-5)H), 3.00-3.02 (1H, m, C(2-5)H), 3.71 (2H, s, C(1')H), 7.29-7.37 (5H, m, Ar-H). δ_{F} (376 MHz; CDCl_3) -81.36 (3F, d, $^3J_{\text{FF}}$ 6.7), -158.02 - -158.08 (1F, m). δ_{C} (101 MHz; CDCl_3) 32.8 (d, $^3J_{\text{CF}}$ 22.7, C2/4), 52.6 (s, C1'), 59.4 (d, $^3J_{\text{CF}}$ 24.3, C2/4), 59.6 (s, C5), 99.7 (dq, $^1J_{\text{CF}}$ 191.4, $^2J_{\text{CF}}$ 32.4, C3), 123.7 (qd, $^1J_{\text{CF}}$ 280.9, $^2J_{\text{CF}}$ 32.0, CF_3), 127.5 (s, Ar C-H), 128.6 (s, Ar C-H), 128.7 (s, Ar C-C), 138.1 (s, Ar C-C). HRMS (ESI+) m/z calc. for $[\text{M}+\text{H}]^+$ $\text{C}_{12}\text{H}_{14}\text{NF}_4$ 248.1062; found 248.1085. Spectroscopic data consistent with literature values.²²

1,2-Dibromo-2,3,3,3-tetrafluoropropane (335).

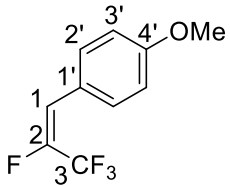
Bromine (5.92 g, 37.1 mmol) was dissolved in CH_2Cl_2 (100 mL) and stirred under an atmosphere of **1** (8.37 g, 73.4 mmol) for 16 hours. The resulting mixture was washed twice with saturated aqueous sodium thiosulfate then sodium bicarbonate and dried over MgSO_4 . The solvent was then removed by distillation

at atmospheric pressure to leave 1,2-dibromo-2,3,3,3-tetrafluoropropane, **335** (7.94 g, 79%), as a clear, pale yellow liquid, b.p. 56 °C. δ_{H} (400 MHz; CDCl_3) 3.92 (1H, dq, $^3J_{\text{HF}}$ 20.9, $^4J_{\text{HF}}$ 0.9), 4.02 (1H, dq, $^3J_{\text{HF}}$ 12.4, $^4J_{\text{HF}}$ 0.6). δ_{F} (376 MHz; CDCl_3) -126.14 (1F, ddq, $^3J_{\text{HF}}$ 20.9, $^4J_{\text{HF}}$ 12.5, $^2J_{\text{FF}}$ 8.3), -78.10 (3F, ddq, $^2J_{\text{FF}}$ 8.3, $^4J_{\text{HF}}$ 0.9, $^4J_{\text{HF}}$ 0.6). δ_{C} (101 MHz; CDCl_3) 32.4 (d, $^2J_{\text{CF}}$ 23.6, CHBr), 97.8 (dq, $^1J_{\text{CF}}$ 265.3, $^2J_{\text{CF}}$ 36.3, CFBr), 120.2 (qd, $^1J_{\text{CF}}$ 284.4, $^2J_{\text{CF}}$ 30.2, CF_3). IR $\nu_{\text{max}}/\text{cm}^{-1}$ 1297, 1208, 1185, 1139, 1009, 670 (s, C-Br). LC-MS (ESI-) m/z 273 (M^- , 100%), 191 ($[\text{M}^{-81}\text{Br}]^-$, 13). HRMS (ESI-) m/z calc. for $[\text{M}-\text{H}]^- \text{C}_3\text{HF}_4(^{79}\text{Br})_2$ 270.8381; found 270.8232.

1-Bromo-2,3,3,3-tetrafluoroprop-1-ene (**336**).

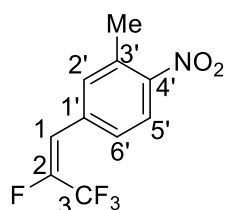
 **2** (14.36 g, 52.58 mmol) was dissolved in DMF (50 mL) and DBU (10 mL, 67 mmol) was added dropwise at 0 °C. The reaction mixture was allowed to warm to room temperature then stirred for 30 minutes. Water was added until all solids dissolved to give a black homogenous solution which was then acidified to pH 1 with 6M HCl. The lower organic layer was collected and dried overnight in a desiccator with P_2O_5 to give 1-bromo-2,3,3,3-tetrafluoroprop-1-ene, **336** (5.05 g, 50%, $E:Z = 3:97$) as a clear yellow liquid. δ_{H} (400 MHz; CDCl_3) 6.56 (1H, d, $^3J_{\text{HF}}$ 24.3). δ_{F} (376 MHz; CDCl_3) Z (98%) -71.96 (3F, d, $^3J_{\text{FF}}$ 12.1), -121.52 (1F, dq, $^3J_{\text{HF}}$ 24.3, $^3J_{\text{FF}}$ 12.1); E (2%) -67.52 (3F, d, $^3J_{\text{FF}}$ 7.7), -116.68 (1F, dq, $^3J_{\text{HF}}$ 15.3, $^3J_{\text{FF}}$ 7.7). δ_{C} (101 MHz; CDCl_3) 94.1 (dq, $^2J_{\text{CF}}$ 15.6, $^3J_{\text{CF}}$ 4.5, CBr), 117.9 (qd, $^1J_{\text{CF}}$ 272.9, $^2J_{\text{CF}}$ 39.8, CF_3), 148.9 (dq, $^1J_{\text{CF}}$ 263.6, $^2J_{\text{CF}}$ 40.0, CF). GC-MS (EI+) 193 ($[\text{M}^{81}\text{Br}]^+$, 1.5%), 191 ($[\text{M}^{79}\text{Br}]^+$, 1.5%).

1-(4'-Methoxyphenyl)-2,3,3,3-tetrafluoroprop-1-ene (**337**).

 **335** (0.128 g, 0.472 mmol), *p*-methoxybenzene boronic acid (0.072 g, 0.472 mmol) and $\text{Pd}(\text{dppf})\text{Cl}_2$ (0.035 g, 0.047 mmol) were dissolved in 1,4-dioxane (5 mL) in a 10 mL glass vial under nitrogen. The resulting solution was cooled to 0 °C and DBU (0.075 g, 0.493 mmol) was added dropwise and the reaction mixture allowed to warm to room temperature stirring for 30 minutes. The vial was then transferred to a Biotage Initiator microwave synthesiser and heated to 120 °C for 90 minutes. The resulting mixture was filtered through a silica plug, eluting with hexane then concentrated in vacuo to give 1-(4'-methoxyphenyl)-2,3,3,3-tetrafluoroprop-1-ene, **337** (0.073 g, 7%), as a yellow oil. δ_{H} (400 MHz; CDCl_3) 3.84 (3H, s, OMe), 6.29 (1H, d, $^3J_{\text{HF}}$ 36.2, vinyl CH), 6.90-6.95 (2H, m, Ar-H), 7.50-7.54 (2H, m, Ar-H). δ_{F} (376 MHz; CDCl_3) -135.28 (1F, dq, $^3J_{\text{HF}}$ 36.3,

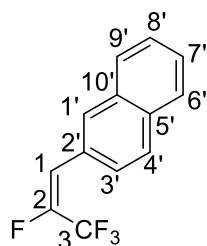
$^3J_{\text{FF}}$ 11.7), -71.79 (3F, d, $^3J_{\text{FF}}$ 11.7). δ_{C} (101 MHz; CDCl_3) 64.0 (s, OMe), 73.4 (q, $^2J_{\text{CF}}$ 52.9), 86.7 (q, $^3J_{\text{CF}}$ 6.5), 114.1 (q, $^1J_{\text{CF}}$ 257.7), 126.7 (s, Ar), 129.1 (s, Ar), 138.1 (s, Ar), 140.7 (s, Ar). GC-MS (EI+) m/z 220 (M^+ , 100%), 205 (28), 157 (15), 127 (56). HRMS (ESI+) m/z calc. for $[\text{M}+3\text{H}]^+$ $\text{C}_{10}\text{H}_8\text{OF}_4$ 223.0746; found 223.0670.

1-(3'-Methyl-4'-nitrophenyl)-2,3,3,3-tetrafluoroprop-1-ene (338).



3-Methyl-4-nitrophenylboronic acid (0.136 g, 0.751 mmol), **336** (0.227 g, 1.18 mmol) and $\text{Pd}(\text{dppf})\text{Cl}_2$ (0.058 g, 0.079 mmol) were dissolved in 1,4 dioxane (4 mL) with saturated aqueous sodium bicarbonate (1 mL) and purged with argon for 5 minutes. The resulting mixture was heated in a sealed glass vial to 100 °C for 2 hours using a silicone oil bath then filtered through a silica plug, washing with ethyl acetate, and concentrated *in vacuo* to give 1-(3'-methyl-4'-nitrophenyl)-2,3,3,3-tetrafluoroprop-1-ene, **338** (0.097 g, 56%, $E:Z = 10:90$), as a yellow solid, m.p. 62-64 °C. δ_{H} (400 MHz; CDCl_3) 2.63 (3H, s, Me), 6.40 (1H, d, $^3J_{\text{HF}}$ 34.4, C(1)H), 7.41 (1H, d, $^3J_{\text{HH}}$ 8.0, C(5')H), 7.70 (1H, dd, $^3J_{\text{HH}}$ 8.0, $^4J_{\text{HH}}$ 1.9, C(6')H), 8.16 (1H, d, $^4J_{\text{HH}}$ 1.9, C(2')H). δ_{F} (376 MHz; CDCl_3) Z (90%) -72.25 (3F, d, $^3J_{\text{FF}}$ 10.9), -128.89 (1F, dq, $^3J_{\text{HF}}$ 34.4, $^3J_{\text{FF}}$ 10.9); E (10%) -66.83 (3F, d, $^3J_{\text{FF}}$ 9.5), -121.72 (1F, q, $^3J_{\text{FF}}$ 9.5). δ_{C} (101 MHz; CDCl_3) 20.6 (s, Me), 109.6 (d, $^4J_{\text{CF}}$ 5.9, C(1')H), 118.6 (qd, $^1J_{\text{CF}}$ 271.8, $^2J_{\text{CF}}$ 40.6, C3), 125.7 (d, $^2J_{\text{CF}}$ 7.3, C1), 128.8 (d, $^4J_{\text{CF}}$ 3.6, C(6')H), 133.6 (s, C(5')H), 133.7 (s, C(4')H), 135.1 (d, $^4J_{\text{CF}}$ 2.3, C(2')H), 146.4 (dq, $^1J_{\text{CF}}$ 270.5, $^2J_{\text{CF}}$ 38.9, C2), 149.6 (s, C(3')H). HRMS (ESI+) m/z calc. for $[\text{M}+\text{H}]^+$ $\text{C}_{10}\text{H}_8\text{NO}_2\text{F}_4$ 250.0491; found 250.0494.

1-(1'-Naphthyl)-2,3,3,3-tetrafluoroprop-1-ene (339).



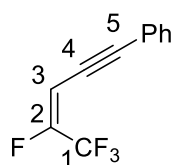
1-Naphthylboronic acid (0.122 g, 0.709 mmol), **336** (0.215 g, 1.12 mmol), Cs_2CO_3 (1.269 g, 3.89 mmol) and $\text{Pd}(\text{dppf})\text{Cl}_2$ (0.047 g, 0.064 mmol) were dissolved in DMF (4 mL) with water (1 mL) and purged with argon for 5 minutes. The resulting mixture was heated in a sealed glass vial to 90 °C for 1 hour using a silicone oil bath then filtered through a silica plug, washing with ethyl acetate, and concentrated *in vacuo* to give 1-(1'-naphthyl)-2,3,3,3-tetrafluoroprop-1-ene, **339** (0.104 g, 61%, $E:Z = 2:98$), as a yellow oil. δ_{H} (400 MHz; CDCl_3) 7.12 (1H, d, $^3J_{\text{HF}}$ 33.4, C(1)H), 7.71-7.79 (4H, m, C(6'-9')H), 7.84-7.88 (1H, m, C(2'-4')H), 7.89-7.93 (2H, m, C(2'-4')H). δ_{F} (376 MHz; CDCl_3) Z (88%) -132.28 (1F, dq, $^3J_{\text{HF}}$ 33.4, $^3J_{\text{FF}}$ 11.4), -71.93 (3F, dd, $^3J_{\text{FF}}$ 11.4, $^4J_{\text{HF}}$ 0.7); E (12%)

-122.93 (1F, dq, $^3J_{\text{HF}}$ 19.4, $^3J_{\text{FF}}$ 9.7), -67.01 (3F d, $^3J_{\text{FF}}$ 9.7). δ_{C} (101 MHz; CDCl_3) 108.5 (p, $^3J_{\text{CF}}$ 3.8, C1), 119.1 (qd, $^1J_{\text{CF}}$ 271.6, $^2J_{\text{CF}}$ 41.5, C3), 123.3 (s, Ar), 125.49 (s, Ar), 126.3 (s, Ar), 127.1 (s, Ar), 128.3 (d, $^2J_{\text{CF}}$ 8.8, C1'), 129.0 (s, Ar), 130.1 (d, $^3J_{\text{CF}}$ 1.4, C2'/C10'), 131.2 (s, Ar), 133.7 (s, Ar), 138.6 (s, Ar), 146.0 (dq, $^1J_{\text{CF}}$ 267.1, $^2J_{\text{CF}}$ 38.3, C2). HRMS (ESI+) m/z calc. for $[\text{M}+\text{H}]^+$ $\text{C}_{13}\text{H}_9\text{F}_4$ 241.0640; found 241.0649.

General procedure for Sonogashira coupling reaction.

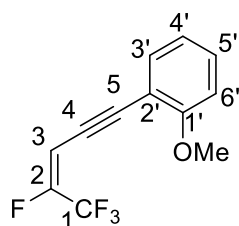
The alkyne (1 eq.) was added to a 10 mL glass vial along with 10 mol-% $\text{Pd}(\text{PPh}_3)_2\text{Cl}_2$ and 20 mol-% CuI . Bromoalkene **336** (1.5 eq.) and Et_3N (~5 mL) were then added and the vial quickly sealed with a crimped Teflon cap. The sealed vial was purged with argon for 5 minutes then heated to 80 °C overnight in an oil bath before being allowed to cool to room temperature. The resulting mixture was then filtered through a short silica plug, which was washed with ethyl acetate, then concentrated *in vacuo* to give the tetrafluoroenyne product without further purification unless otherwise specified.

1,1,1,2-Tetrafluoro-5-phenyl-pent-2-en-4-yne (**341**).



Following the general procedure, phenylacetylene (0.093 g, 0.91 mmol) and **336** (0.353 g, 1.82 mmol) gave 1,1,1,2-tetrafluoro-5-phenyl-pent-2-en-4-yne, **341** (0.093 g, 48%, $E:Z = 7:93$), as a yellow oil. δ_{H} (400 MHz; CDCl_3) 5.94 (1H, dd, $^3J_{\text{HF}}$ 29.0, $^4J_{\text{HF}}$ 1.2, C(3)H), 7.38 (2H, m, Ar-H), 7.53 (2H, m, Ar-H), 7.68 (1H, m, Ar-H). δ_{F} (376 MHz; CDCl_3) Z -72.47 (3F, dd, $^3J_{\text{FF}}$ 11.2, $^4J_{\text{HF}}$ 1.0), -120.34 (1F, dq, $^3J_{\text{HF}}$ 29.0, $^3J_{\text{FF}}$ 11.2); E -69.09 (3F, d, $^3J_{\text{FF}}$ 9.3), -121.30 - -121.36 (1F, m). δ_{C} (101 MHz; CDCl_3) 74.0 (s, C4/5), 81.7 (s, C4/5), 118.4 (dq, $^1J_{\text{CF}}$ 271.8, $^2J_{\text{CF}}$ 39.5, C1), 121.9 (d, $^2J_{\text{CF}}$ 4.3, C3), 129.3 (s, Ar), 129.6 (s, Ar), 132.0 (s, Ar), 132.6 (s, Ar), 152.1 (qd, $^1J_{\text{CF}}$ 273.3, $^2J_{\text{CF}}$ 39.2, C2). HRMS (ASAP) m/z calc. $[\text{M}+\text{H}]^+$ $\text{C}_{11}\text{H}_7\text{F}_4$ for 215.0484; found 215.0451.

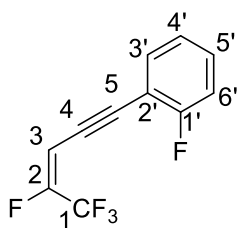
1,1,1,2-Tetrafluoro-5-(2'-methoxyphenyl)-pent-2-en-4-yne (**342**).



Following the general procedure, 2-methoxyphenylacetylene (0.102 g, 0.077 mmol) and **336** (0.296 g, 0.154 mmol) gave 1,1,1,2-tetrafluoro-5-(2'-methoxyphenyl)-pent-2-en-4-yne, **342** (0.133 g, 71%, $E:Z = 3:97$), as a yellow oil. δ_{H} (400 MHz; CDCl_3) 4.00 (3H, s, OMe), 6.10 (1H, dq, $^3J_{\text{HF}}$ 29.1, $^4J_{\text{HF}}$ 1.1, C(3)H), 7.01-7.03 (1H, m, Ar-H), 7.28-7.30 (1H, m, Ar-H), 7.40-7.44 (1H, m, Ar-H), 7.45-7.48 (1H, m, Ar-H).

δ_{F} (376 MHz; CDCl_3) *Z* -72.42 (qd, $^3J_{\text{FF}}$ 11.3, $^4J_{\text{HF}}$ 1.0), -120.77 (dq, $^3J_{\text{HF}}$ 28.8, $^3J_{\text{FF}}$ 11.3), *E* -69.03 (d, $^3J_{\text{FF}}$ 9.3), -122.09 (dq, $^3J_{\text{HF}}$ 14.3, $^3J_{\text{FF}}$ 9.3). δ_{C} (101 MHz; CDCl_3) 55.9 (s, O-CH₃), 78.1 (s, C4/5), 78.8 (s, C4/5), 118.5 (dq, $^1J_{\text{CF}}$ 271.7, $^2J_{\text{CF}}$ 39.4, C1), 128.5 (d, $^3J_{\text{CF}}$ 8.9, C3), 129.1 (s, Ar), 130.6 (s, Ar), 131.2 (s, Ar), 133.9 (s, Ar), 134.5 (s, Ar), 151.7 (qd, $^1J_{\text{CF}}$ 272.8, $^2J_{\text{CF}}$ 39.2, C2), 161.4 (s, C2'). HRMS (ESI+) *m/z* calc. for $[\text{M}+\text{H}]^+$ $\text{C}_{12}\text{H}_9\text{OF}_4$ 245.0590; found 245.1165.

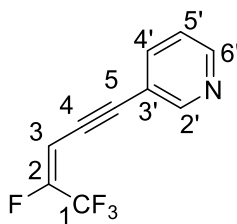
1,1,1,2-Tetrafluoro-5-(2'-fluorophenyl)-pent-2-en-4-yne (343).



Following the general procedure, 2-fluorophenylacetylene (0.106 g, 0.82 mmol) and **336** (0.332 g, 1.71 mmol) gave 1,1,1,2-tetrafluoro-5-(2'-fluorophenyl)-pent-2-en-4-yne, **343** (0.108 g, 57%, *E:Z* = 4:96), as a yellow oil. δ_{H} (400 MHz; CDCl_3) 5.97 (1H, dd, $^3J_{\text{HF}}$ 28.9, $^4J_{\text{HF}}$ 1.2, C(3)H), 7.11-7.15 (1H, m, Ar-H), 7.36-7.39 (1H, m, Ar-H),

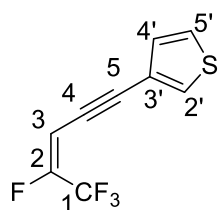
7.50-7.53 (1H, m, Ar-H), 7.67-7.69 (1H, m, Ar-H). δ_{F} (376 MHz; CDCl_3) *Z* -72.55 (3F, dd, $^3J_{\text{FF}}$ 11.1, $^1J_{\text{HF}}$ 1.0), -108.40 (1F, ddd, $^3J_{\text{HF}}$ 9.4, $^4J_{\text{HF}}$ 7.0, $^4J_{\text{HF}}$ 5.3, Ar-F), -119.06 (1F, dq, $^3J_{\text{HF}}$ 28.9, $^3J_{\text{FF}}$ 11.1, C(2)F); *E* -69.20 (3F, dd, $^3J_{\text{FF}}$ 9.1, $^3J_{\text{HF}}$ 1.3), -108.94 - -108.99 (1F, m, Ar-F), -120.01 - -120.10 (1F, m, C(2)F). δ_{C} (101 MHz; CDCl_3) 78.4 (s, C5), 82.3 (d, $^3J_{\text{CF}}$ 3.3, C4), 118.2 (dq, $^1J_{\text{CF}}$ 271.9, $^2J_{\text{CF}}$ 39.3, C1), 124.1 (d, $^4J_{\text{CF}}$ 3.8, C5'), 127.8 (q, $^3J_{\text{CF}}$ 6.7, C3), 128.5 (d, $^2J_{\text{CF}}$ 12.1, C1'/3'), 131.1 (d, $^3J_{\text{CF}}$ 7.9, C4'/6'), 131.4 (d, $^3J_{\text{CF}}$ 8.0, C4'/6'), 132.1 (d, $^2J_{\text{CF}}$ 9.9, C1'/3'), 133.9 (d, $^1J_{\text{CF}}$ 72.0, C2'), 163.2 (qd, $^1J_{\text{CF}}$ 253.6, $^2J_{\text{CF}}$ 39.7, C2). HRMS (ESI+) *m/z* calc. for $[\text{M}+\text{H}]^+$ $\text{C}_{11}\text{H}_6\text{F}_5$ 233.0390; found 239.0392.

1,1,1,2-Tetrafluoro-5-(3'-pyridinyl)-pent-2-en-4-yne (344).

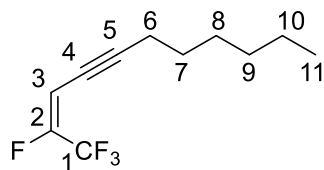


Following the general procedure, 3-ethynylpyridine (0.103 g, 0.988 mmol) and **336** (0.397 g, 2.04 mmol) gave 1,1,1,2-tetrafluoro-5-(3'-pyridinyl)-pent-2-en-4-yne, **344** (0.139 g, 65%, *E:Z* = 11:89), as a yellow oil. δ_{H} (400 MHz; CDCl_3) 5.97 (1H, dd, $^3J_{\text{HF}}$ 28.8, $^4J_{\text{HF}}$ 1.1, C(2)H), 7.35-7.39 (1H, m, Ar-H), 7.86-7.88 (1H, m, Ar-H), 8.65-

8.69 (1H, m, Ar-H), 8.83-8.84 (1H, m, Ar-H). δ_{F} (376 MHz; CDCl_3) *Z* -72.56 (3F, dd, $^3J_{\text{FF}}$ 10.9, $^4J_{\text{HF}}$ 1.1), -118.32 - -118.39 (1F, m); *E* -69.17 (3F, $^3J_{\text{FF}}$ 9.1), -119.05 - -119.15 (1F, m). δ_{C} (101 MHz; CDCl_3) 161.5 (qd, $^1J_{\text{CF}}$ 254.3, $^2J_{\text{CF}}$ 37.9, C2), 154.9 (s, Ar), 151.3 (s, Ar), 141.2 (s, Ar), 127.8 (q, $^3J_{\text{CF}}$ 7.4, C3), 125.1 (s, Ar), 121.4 (s, Ar), 116.9 (dq, $^1J_{\text{CF}}$ 273.4, $^2J_{\text{CF}}$ 39.1, C1), 82.7 (s, C4/5), 82.3 (s, C4/5). HRMS (AI+) *m/z* calc. for $[\text{M}+\text{H}]^+$ $\text{C}_{10}\text{H}_6\text{NF}_4$ 216.0436; found 216.0438.

1,1,1,2-Tetrafluoro-5-(3'-thiophenyl)-pent-2-en-4-yne (345).

Following the general procedure, 3-ethynylthiophene (0.1 mL, 1.02 mmol) and **336** (0.410 g, 2.11 mmol) gave 1,1,1,2-tetrafluoro-5-(3'-thiophenyl)-pent-2-en-4-yne, **345** (0.092 g, 41%, *E:Z* = 5:95), as a yellow oil. δ_{H} (400 MHz; CDCl_3) 5.96 (1H, dd, $^3J_{\text{HF}}$ 29.1, $^4J_{\text{HF}}$ 1.2, C(2)H), 7.25-7.29 (1H, m, Ar-H), 7.39-7.42 (1H, m, Ar-H), 7.63-7.67 (1H, m, Ar-H). δ_{F} (376 MHz; CDCl_3) *Z* -72.40 (dd, $^3J_{\text{FF}}$ 11.3, $^4J_{\text{HF}}$ 1.2), -120.57 (dq, $^3J_{\text{HF}}$ 29.1, $^3J_{\text{FF}}$ 11.3); *E* -69.08 (d, $^3J_{\text{FF}}$ 9.2), -121.58 (dq, $^3J_{\text{HF}}$ 14.1, $^3J_{\text{FF}}$ 9.2). δ_{C} (101 MHz; CDCl_3) 151.9 (dq, $^1J_{\text{CF}}$ 273.2, $^2J_{\text{CF}}$ 39.2, C2), 132.5 (s, Ar), 132.0 (s, Ar), 128.5 (s, C5), 128.1 (q, $^3J_{\text{CF}}$ 5.6, C3), 127.3 (s, Ar), 123.2 (s, Ar), 118.38 (dd, $^1J_{\text{CF}}$ 271.8, $^2J_{\text{CF}}$ 39.4, C1), 95.14 (dq, $^3J_{\text{CF}}$ 8.6, $^4J_{\text{CF}}$ 4.4, C4), 80.8 (s, C5). HRMS (AI+) *m/z* calc. for $[\text{M}+\text{H}]^+$ $\text{C}_9\text{H}_5\text{F}_4\text{S}$ 221.0048; found 221.0094.

1,1,1,2-Tetrafluoroundec-2-en-4-yne (346).

Following the general procedure, 1-octyne (0.1 mL, 0.678 mmol) and **336** (0.264 g, 1.36 mmol) gave 1,1,1,2-tetrafluoroundec-2-en-4-yne, **346** (0.118 g, 78%, *E:Z* = 15:85), as a yellow oil. δ_{H} (400 MHz; CDCl_3) 0.88-0.94 (3H, m, C(11)H), 1.27-1.35 (4H, m, C(9-10)H), 1.38-1.42 (2H, m, C(8)H), 1.52-1.55 (2H, m, C(7)H), 2.20-2.24 (2H, m, C(6)H), 5.70 (1H, dq, $^3J_{\text{HF}}$ 29.3, $^4J_{\text{HF}}$ 2.1, C(2)H). δ_{F} (376 MHz; CDCl_3) *Z* -72.58 (dq, $^3J_{\text{FF}}$ 11.5, $^4J_{\text{HF}}$ 2.1), -123.28 - -123.35 (1F, m); *E* -69.15 (3F, d, $^3J_{\text{FF}}$ 9.1), -124.55 - -123.64 (1F, m). δ_{C} (101 MHz; CDCl_3) 15.9 (s, alkyl), 23.5 (s, alkyl), 30.9 (s, alkyl), 33.4 (s, alkyl), 33.8 (s, alkyl), 36.1 (s, alkyl), 75.0 (s, alkyl), 99.5 (dq, $^3J_{\text{CF}}$ 8.3, $^4J_{\text{CF}}$ 3.9, C4), 117.9 (dq, $^1J_{\text{CF}}$ 272.0, $^2J_{\text{CF}}$ 39.4, C1), 128.2 (d, $^3J_{\text{CF}}$ 8.3, C3), 149.6 (qd, $^1J_{\text{CF}}$ 273.5, $^2J_{\text{CF}}$ 38.8, C2). HRMS (AI+) *m/z* calc. for $[\text{M}+\text{H}]^+$ $\text{C}_{11}\text{H}_{15}\text{F}_4$ 223.1110; found 223.1011.

9.8 References for Chapter 9

- ¹ Y. Hiraoka, T. Kawasaki-Takasuka, Y. Morizawa and T. Yamazaki, *J. Fluorine Chem.*, 2015, **179**, 71.
- ² R. J. Abraham and C. J. Medforth, *Mag. Res. Chem.*, 1988, **26**, 334.
- ³ Z.-C. Chen, L. Tong, Z.-B. Du, Z.-F. Mao, X.-J. Zhang, Y. Zou and M. Yan, *Org. Biomol. Chem.*, 2018, **16**, 2634.

- ⁴ H. Xie, D. Ng, S. N. Savinov, B. Dey, P. D. Kwong, R. Wyatt, A. B. Smith and W. A. Hendrickson, *J. Med. Chem.*, 2007, **50**, 4898.
- ⁵ R. S. Givens, B. Hrinchenko, J. H-S. Liu, B. Matuszewski and J. Tholen-Collison, *J. Am. Chem. Soc.*, 1984, **106**, 1779.
- ⁶ T. Taguchi, G. Tomizawa, A. Kawara, M. Nakajima and Y. Kobayashi, *J. Fluorine Chem.*, 1988, **40**, 171.
- ⁷ S. Tajammal and A. E. Tipping, *J. Fluorine Chem.*, 1990, **47**, 45.
- ⁸ Y.-F. Lin, C. Wang, B.-L. Hu, P.-C. Qian and X.-G. Zhang, *Synlett*, 2017, **28**, 707.
- ⁹ T. Yamazaki, T. Yamamoto and R. Ichihara, *J. Org. Chem.*, 2006, **71**, 6251.
- ¹⁰ A. Miyagawa, M. Naka, T. Yamazaki and T. Kawasaki-Takasuka, *Eur. J. Org. Chem.*, 2009, **26**, 4395.
- ¹¹ A. K. Brisdon and I. R. Crossley, *Chem. Commun.*, 2002, 2420.
- ¹² G. Yang and R. G Rapatis, *J. Heterocyclic Chem.*, 2003, **40**, 659.
- ¹³ P. R. Brodfuehrer, B.-C. Chen, T. R. Sattelberg, Sr., P. R. Smith, J. P. Reddy, D. R. Stark, S. L. Quinlan and J. G. Reid, *J. Org. Chem.*, 1997, **62**, 9196.
- ¹⁴ M. Amarosa, *Farmaco Sci. Tech.*, 1948, **3**, 389.
- ¹⁵ L. S. Pavase, D. V. Mane and K. G. Baheti, *J. Heterocyclic Chem.*, 2018, **55**, 913.
- ¹⁶ V. M. Muzalevskiy, A. Yu. Rulev, A. R. Romanov, E. V. Kondrashov, I. A. Ushakov, V. A. Chertkov and V. G. Nenajdenko, *J. Org. Chem.*, 2017, **82**, 7200.
- ¹⁷ T. Yamazaki, K. Mizutani and T. Kitzaume, *J. Org. Chem.*, 1995, **60**, 6046; (b) A. R. Katritzky, M. Qi and A. P. Wells, *J. Fluorine Chem.*, 1996, **80**, 145.
- ¹⁸ A. R. Katritzky, M. Qi and A. P. Wells, *J. Fluorine Chem.*, 1996, **80**, 145.
- ¹⁹ T. Yamazaki, T. Kawasaki-Takasuka, A. Furuta and S. Sakamoto, *Tetrahedron*, 2009, **65**, 5945.
- ²⁰ C. Burgess, D. Burn, P. Feather, M. Howarth and V. Petrow, *Tetrahedron*, 1966, **22**, 2829.
- ²¹ A. Dean, A. Venzo, M. G. Ferlin, G. G. Bombi, P. Brun, I. Castagliuolo and V. B. Di Marco, *Dalton Trans.*, 2007, 1689.
- ²² D. Meyer and M. El Qacemi, *Org. Lett.*, 2020, **22**, 3479.

Appendix I: X-ray crystallography

Crystals suitable for X-ray diffraction were typically grown by slow evaporation of a solution of the compound in an appropriate solvent from a partially sealed glass vial. All crystallographic data collection and analysis was carried out by Dr. Dmitry S. Yufit (Durham University).

Single crystal X-ray data were collected using λ MoK α radiation ($\lambda = 0.71073 \text{ \AA}$) on a Bruker D8Venture (Photon100 CMOS detector, I μ S-microsource, focusing mirrors) diffractometer equipped with Cryostream (Oxford Cryosystems) open-flow nitrogen cryostats at the temperature 120.0(2) K. All structures were solved by direct method and refined by full-matrix least squares on F^2 for all data using Olex2¹ and SHELXTL² software. All non-disordered non-hydrogen atoms were refined anisotropically, hydrogen atoms in structures **149** and **249** were placed in the calculated positions and refined in riding mode. Coordinates and isotropic temperature factors of hydrogen atoms in all other structures were freely refined. The iodine atom in slightly twinned ([001, 0-10, 100], BASF = 0.0058(4)) structure **249** was found to be disordered and minor components were refined isotropically with fixed SOF = 0.05. Crystal data and parameters of refinement are listed in Tables 10.1, 10.2, and 10.3. Crystallographic data for some structures have been deposited with the Cambridge Crystallographic Data Centre with the supplementary publication CCDC numbers as shown below:

- Naphthyl CF₃-enol ether (**149**): 1947946
- Benzylamino CF₃-enaminone (**232**): 1995120
- Iodinated CF₃-enone (**249**): 1995119
- Naphthyl CF₃-pyrimidine (**252**): 1995123

¹ O. V. Dolomanov, L. J. Bourhis, R. J. Gildea, J. A. K. Howard and H. Puschmann, *J. Appl. Cryst.*, 2009, **42**, 339.

² G.M. Sheldrick, *Acta Cryst.*, 2008, **A64**, 112.

Table 10.1. Crystal data and structure refinement parameters for 149, 249, and 232

Compound	149	249	232
Empirical formula	C ₁₄ H ₁₁ F ₃ O	C ₁₁ H ₇ ClF ₃ IO ₂	C ₂₀ H ₁₄ NOF ₃
Formula weight	252.23	390.52	341.32
Temperature /K	120.0	120.0	120.0
Crystal system	monoclinic	monoclinic	monoclinic
Space group	P2 ₁ /c	P2 ₁ /c	P2 ₁ /n
a /Å	12.8217(8)	11.5447(8)	13.1524(5)
b /Å	9.7652(6)	7.9210(5)	7.0536(3)
c /Å	9.4436(6)	14.6465(10)	17.2367(7)
α /°	91.502(2)	90	90
β /°	90	109.402(2)	99.1175(17)
γ /°	90	90	90
Volume /Å³	1181.99(13)	1263.30(15)	1578.88(11)
Z	4	4	4
ρ_{calc} g /cm³	1.417	2.053	1.436
μ / mm⁻¹	0.120	2.773	0.113
F(000)	520.0	744.0	704.0
Reflections collected	25281	16872	24616
Independent refl., R_{int}	3438 [R _{int} = 0.0356, R _{sigma} = 0.0229]	3629, 0.0404	4581, 0.0361
Data/restraints /parameters	3438/0/207	3629/0/173	4581/0/282
Goodness-of-fit on F²	1.061	1.243	1.022
Final R₁ indexes [I ≥ 2σ (I)]	R ₁ = 0.0372 wR ₂ = 0.0974	0.0537	0.0394
Final wR₂ indexes [all data]	R ₁ = 0.0529 wR ₂ = 0.1055	0.1168	0.1135
Largest diff. peak/hole /e Å⁻³	0.36/-0.28	2.27/-3.90	0.41/-0.31

Table 10.2. Crystal data and structure refinement parameters for 252, 224b, and 323

Compound	252	224b	314
Empirical formula	C ₂₁ H ₁₃ F ₃ N ₂	C ₁₄ H ₇ OF ₃	C ₃₃ H ₄₉ ClCuP
Formula weight	350.33	248.20	575.68
Temperature /K	120.0	120.0	120.0
Crystal system	triclinic	monoclinic	monoclinic
Space group	P-1	P2 ₁	C2/c
a /Å	8.8507(6)	7.1227(15)	40.5727(18)
b /Å	9.9178(7)	29.443(6)	8.7943(4)
c /Å	10.0735(7)	10.657(2)	17.5373(8)
α /°	67.033(3)	90	90
β /°	75.888(3)	90.212(8)	96.195(2)
γ /°	77.276(3)	90	90
Volume /Å³	781.79(10)	2234.8(8)	6220.9(5)
Z	2	8	8
ρ_{calc} g /cm³	1.488	1.475	1.229
μ / mm⁻¹	0.113	0.126	0.859
F(000)	360.0	1008.0	2464.0
Reflections collected	15357	24835	69736
Independent refl., R_{int}	4142, 0.0339	8770 [R _{int} = 0.1200, R _{sigma} = 0.1798]	8666 [R _{int} = 0.0714, R _{sigma} = 0.0415]
Data/restraints /parameters	4142/0/287	8770/433/650	8666/0/331
Goodness-of-fit on F²	1.064	1.016	1.071
Final R₁ indexes [I ≥ 2σ (I)]	0.0415	R ₁ = 0.1073 wR ₂ = 0.2644	R ₁ = 0.0572 wR ₂ = 0.1571
Final wR₂ indexes [all data]	0.1252	R ₁ = 0.1788 wR ₂ = 0.3078	R ₁ = 0.0674 wR ₂ = 0.1635
Largest diff. peak/hole /e Å⁻³	0.43/-0.30	0.53/-0.64	1.64/-1.40

Table 10.3. Crystal data and structure refinement parameters for 329, 98·HCl, and 338

Compound	329	98·HCl	338
Empirical formula	C ₁₄ H ₂₀ F ₆ N ₂ Si	C ₁₂ H ₁₄ ClF ₄ N	C ₁₀ H ₇ F ₄ NO ₂
Formula weight	358.41	283.69	249.17
Temperature /K	120.0	120.0	120.0
Crystal system	monoclinic	orthorhombic	orthorhombic
Space group	P2 ₁	Pna2 ₁	Pbca
a /Å	10.3288(3)	8.8319(3)	11.5532(3)
b /Å	5.7293(2)	13.6609(4)	6.8369(2)
c /Å	14.2005(5)	21.7159(7)	25.5514(7)
α /°	90	90	90
β /°	104.6950(10)	90	90
γ /°	90	90	90
Volume /Å³	812.85(5)	2620.06(14)	2018.26(10)
Z	2	8	8
ρ_{calc} g /cm³	1.464	1.438	1.640
μ / mm⁻¹	0.205	0.321	0.163
F(000)	372.0	1168.0	1008.0
Reflections collected	18608	55357	31746
Independent refl., R_{int}	4721 [R _{int} = 0.0410, R _{sigma} = 0.0412]	6913 [R _{int} = 0.0718, R _{sigma} = 0.0389]	2678 [R _{int} = 0.0450, R _{sigma} = 0.0206]
Data/restraints /parameters	4721/1/288	6913/19/373	2678/0/182
Goodness-of-fit on F²	1.067	1.054	1.066
Final R₁ indexes [I ≥ 2σ (I)]	R ₁ = 0.0405 wR ₂ = 0.0859	R ₁ = 0.0549 wR ₂ = 0.1263	R ₁ = 0.0406 wR ₂ = 0.1023
Final wR₂ indexes [all data]	R ₁ = 0.0457 wR ₂ = 0.0881	R ₁ = 0.0609 wR ₂ = 0.1302	R ₁ = 0.0468 wR ₂ = 0.1064
Largest diff. peak/hole /e Å⁻³	0.31/-0.35	0.52/-0.49	0.36/-0.23

Appendix II: DFT calculations

All DFT calculations were carried out by Dr. Mark A. Fox (Durham University).

The computations shown in Figures 4.10, 4.11, 4.14, and 4.18 were all carried out with the Gaussian 09 package.³ The geometries were fully optimised with the hybrid-DFT B3LYP functional⁴ using the 6-31G(d) basis set⁵ for all atoms. The IEF solvent model⁶ was applied to all calculations with chloroform (CHCl₃) as the solvent. Many minima were located and the conformer with the lowest energy was selected in each case. Frequency calculations on these optimised geometries revealed no imaginary frequencies. As the 6-31G(d) basis set for iodine is not available within the software package, the bromine atom is used in its place for iodinated enone **149**.

The computation shown in Figure 5.1 were carried out with the Gaussian 16 package. The S₀ model geometry of phenyl ynone **204a** with no symmetry constraints was optimised with the B3LYP functional using the 6-31G(d) basis set for all atoms. The geometry was confirmed to be a true minimum with no imaginary frequencies from a frequency calculation at B3LYP/6-31G(d). An electronic structure calculation at B3LYP/6-31G(d) was carried out on **204a** to examine the molecular orbitals visually. The frontier orbitals were generated with the Gabedit package.⁷

³ M. J. Frisch, G. W. Trucks, H. B. Schlegel, G. E. Scuseria, M. A. Robb, J. R. Cheeseman, G. Scalmani, V. Barone, B. Mennucci, G. A. Petersson, H. Nakatsuji, M. Caricato, X. Li, H. P. Hratchian, A. F. Izmaylov, J. Bloino, G. Zheng, J. L. Sonnenberg, M. Hada, M. Ehara, K. Toyota, R. Fukuda, J. Hasegawa, M. Ishida, T. Nakajima, Y. Honda, O. Kitao, H. Nakai, T. Vreven, Jr., J. A. Montgomery, J. E. Peralta, F. Ogliaro, M. Bearpark, J. J. Heyd, E. Brothers, K. N. Kudin, V. N. Staroverov, R. Kobayashi, J. Normand, K. Raghavachari, A. Rendell, J. C. Burant, S. S. Iyengar, J. Tomasi, M. Cossi, N. Rega, J. M. Millam, M. Klene, J. E. Knox, J. B. Cross, V. Bakken, C. Adamo, J. Jaramillo, R. Gomperts, R. E. Stratmann, O. Yazyev, A. J. Austin, R. Cammi, C. Pomelli, J. W. Ochterski, R. L. Martin, K. Morokuma, V. G. Zakrzewski, G. A. Voth, P. Salvador, J. J. Dannenberg, S. Dapprich, A. D. Daniels, O. Farkas, J. B. Foresman, J. V. Ortiz, J. Cioslowski, D. J. Fox, *Gaussian 09*, Revision A.02, Gaussian, Inc., Wallingford CT, 2009.

⁴ (a) A. D. Becke, *J. Chem. Phys.*, 1993, **98**, 5648; (b) C. Lee, W. Yang and R. G. Parr, *Phys. Rev. B*, 1988, **37**, 785.

⁵ (a) G. A. Petersson and M. A. Al-Laham, *J. Chem. Phys.*, 1991, **94**, 6081; (b) G. A. Petersson, A. Bennett, T. G. Tensfeldt, M. A. Al-Laham, W. A. Shirley and J. Mantzaris, *J. Chem. Phys.*, 1988, **89**, 2193.

⁶ E. Cancès, B. Mennucci and J. Tomasi, *J. Chem. Phys.*, 1997, **107**, 3032.

⁷ A. R. Allouche, *J. Comput. Chem.*, 2011, **32**, 174.

Appendix III: Seminars and conferences attended

Departmental seminars and lectures

13.02.20	Dr. Sinead Keaveney Macquarie University	Developing new synthetic methodology: from solvents effects to transition metal catalysis and photocatalysis
05.02.20	Prof. Chris Hunter FRS University of Oxford	Evolution engines
27.01.20	Nessa Carson Pfizer	Twitter and freelancing for chemists
15.01.20	Dr. Alexander Romanov University of East Anglia	Linear coinage metal complexes for the highly efficient solution and vapour-deposited OLEDs
06.11.19	Prof. Scott Cockcroft Edinburgh University	Moving away from equilibrium: from molecular interactions to transmembrane nanodevices
15.10.19	Dr. Matthew Kitching Durham University	Asymmetric Synthesis of Chiral Nitrogen Stereocentres
15.10.19	Prof. Paulo Cezar Vieira University of Sao Paulo	Ginger: pungency and much more
15.10.19	Dr. David Hodgson Durham University	Nucleoside and Nucleotide Chemistry in Durham
12.06.19	Prof. Perdita Barran Manchester University	Adventures with Dynamic and Disordered Systems and Joy
11.06.19	Prof. Mike Ashfold FRS University of Bristol	Synthesis and Applications of Diamond
29.05.19	Prof. Igor Alabugin Florida State University	From Alkyne Origami to Electron Upconversion: Shaping Potential Energy Landscapes in Cyclization Reactions

14.05.19	Prof. Andrew Evans Queen's University Ontario	New Vistas in the Asymmetric Construction of C-C Bonds: Total Synthesis of Complex Bioactive Agents
01.05.19	Prof. Lee Cronin University of Glasgow	Exploring Computation with Chemical Reactions
20.03.19	Prof. Linda Doerrer Boston University	Teflon-coated Molecules: Electronic Structure and Reactivity
12.03.19	Dr. Jason Lynam University of York	Using Time-Resolved Infra-Red Spectroscopy to Probe Transition Metal-Catalysed Reactions
21.02.19	Prof. Pasi Virta University of Turku	¹⁹ F NMR spectroscopy; a valuable tool to monitor secondary structures of nucleic acids
20.02.19	Prof. Duncan Wass University of Bristol	Cooperative Catalysis - From Frustrated Lewis Pairs to Advanced Biofuels
15.02.19	Prof. Guillermo Labadie National University of Rosario	Introducing new chemical entities into the NTDs drug development pipeline
27.11.18	Dr. Ali Huerta-Flores Universidad Autónoma de Nuevo León	Development of new photocatalysts for the production of renewable fuels
27.11.18	Prof. Bryan Koivisto Ryerson University	Bio-inspired dyes for light-harvesting applications
23.10.18	Dr. Rob Law GlaxoSmithKline	Targeted Protein Degradation Using PROTACs: An Emerging Drug Discovery Paradigm

17.10.18	Dr. Jiri Vana University of Pardubice	Palladium Catalysed C–H Activation Reactions; On the Way from Understanding of Basic Principles to Rational Design of Reaction Conditions
17.10.18	Prof. Ian Fairlamb University of York	The importance of Pd speciation in catalytic cross-couplings: solving industrial problems through academic curiosity
17.10.18	Prof. Andy Whiting Durham University	The particular peculiarities of producing polyenic products using palladium
28.09.18	Prof. Guiliano Clososki University of Sao Paulo	Faculty of Pharmaceutical Science at University of Sao Paulo - Ribeirao Preto
28.09.18	Camila Bertallo University of Sao Paulo	Base-controlled regioselective functionalization of aromatic indolizines
28.09.18	Prof. Flavio Emery University of Sao Paulo	Strategies toward the synthesis and application of fragments and fluorescent probes
22.05.18	Prof. Jon Steed Durham University	Gel-Based Approaches to Novel Crystal Forms
22.05.18	Dr. Guillaume de Bo University of Manchester	Molecular tug-of-war: promoting reactions with force
14.05.18	Dr. Ian Ashworth AstraZeneca	Process Understanding: A Tool in Chemical Process Development
14.05.18	Dr. Basile Curchod Durham University	Photochemistry on a Computer

09.05.18	Prof. David Procter University of Manchester	From metal-free cross-couplings to radical cyclization cascades: new methods for synthesis
04.05.18	Prof. Jean-François Soulé University of Rennes	Transition Metal-Catalyzed C–H Bond Functionalization: Application to the Synthesis of Life and Material Molecules
04.05.18	Dr. Na Wu Guangxi Normal University	Transition-metal catalysed enynes domino (cascade) reactions
04.05.18	Jay Wright Durham University	Regioselective Borylation of Heterocycles
04.05.18	Dr. Adam Calow University of Bristol	Medium ring lactams via <i>N</i> -directed carbonylative C–C bond activation
28.02.18	Dr. Allan Watson University of St. Andrews	Asking Questions in Cu catalysis
21.02.18	Dr. Viktor Chechik University of York	Understanding organic free radicals: from highly reactive to very stable
20.02.18	Dr. Uwe Schneider University of Edinburgh	Challenging Catalytic C–H Bond Activation
14.02.18	Dr. Robert Phipps University of Cambridge	Harnessing non-covalent interactions for control of regioselectivity and site selectivity in catalysis
23.01.18	Prof. Graham Sandford Durham University	Synthesis of fluorinated pharmaceuticals
15.12.17	Prof. David Parker FRS Durham University	Who We Are, Where We Come From, Where We're Going... Probe, Excite, Relax
15.12.17	Prof. Andrew Beeby Durham University	Why Things Glow (And What We Can Do With Them)

Conferences attended

19th RSC Fluorine Group Postgraduate Meeting (**Oral Presentation**)

Online, 10-11.06.21

First place prize for best talk

2020 #RSCPoster Twitter Conference (**Poster Presentation**)

Online, 03.03.20

19th European Symposium on Fluorine Chemistry (**Poster & Flash Oral Presentation**)

University of Warsaw, 25.08.19 – 31.08.19

First place poster prize in organic stream and first place 'Fluorine Technology' prize for industrial relevance

2019 Durham Postgraduate Gala Research Symposium (**Poster Presentation**)

Durham University, 20.06.19

18th RSC Fluorine Group Postgraduate Meeting (**Poster Presentation**)

University of Southampton, 11.04.19 – 12.04.19

2019 RSC Organic Division Northeast Postgraduate Meeting

University of York, 27.03.19

22nd International Symposium on Fluorine Chemistry

University of Oxford, 22.07.18 – 27.07.18

2018 Durham Postgraduate Gala Research Symposium

Durham University, 21.06.18

35th SCI Process Development Symposium

Churchill College, Cambridge, 11.04.18 – 13.04.18